Natural Gas
New Perspectives and Future Developments

Edited by Maryam Takht Ravanchi

Natural Gas - New Perspectives and Future Developments

Edited by Maryam Takht Ravanchi

IntechOpen

Supporting open minds since 2005

Natural Gas – New Perspectives and Future Developments
http://dx.doi.org/10.5772/intechopen.94656
Edited by Maryam Takht Ravanchi

Contributors
Tomasz Chrulski, Mohamed Jaouad Malzi, Buthainah Ali Al-Timimi, Zahira Yaakob, Lina Montuori, Manuel Alcázar-Ortega, Ocktaeck Lim, Kyeonghun Jwa, Yanghwa Kim, Fatimata Tall, Akhoury Kumar Sudhir Kumar Sinha, Umaprasana Ojha, Marriyappan Sivagnanam Balathanigaimani, Sanjay Kumar Kar, John Yang, Milind M. Vaidya, Sebastien A. Duval, Feras Hamad, Maximilian Lackner, David Drew, Valentina Bychkova, Ildar Mustakhimov, Mohsen Askaryan

Notice
Statements and opinions expressed in the chapters are these of the individual contributors and not necessarily those of the editors or publisher. No responsibility is accepted for the accuracy of information contained in the published chapters. The publisher assumes no responsibility for any damage or injury to persons or property arising out of the use of any materials, instructions, methods or ideas contained in the book.

We are IntechOpen,
the world's leading publisher of Open Access books
Built by scientists, for scientists

5,800+
Open access books available

144,000+
International authors and editors

180M+
Downloads

156
Countries delivered to

Our authors are among the
Top 1%
most cited scientists

12.2%
Contributors from top 500 universities

Selection of our books indexed in the Book Citation Index (BKCI)
in Web of Science Core Collection™

Interested in publishing with us?
Contact book.department@intechopen.com

Numbers displayed above are based on latest data collected.
For more information visit www.intechopen.com

Meet the editor

Dr. Maryam Takht Ravanchi holds a Ph.D. in Chemical Engineering. She is a researcher for a petrochemical research and technology company. Her research interests are in the fields of natural gas conversion, C1 chemistry, heterogeneous catalyst synthesis, membrane separation technologies, and the environment. She has about twenty years of experience in the petrochemical industry as a process engineer and researcher. She has published seventy journal papers, seventy conference papers, seven national patents, and fifteen books.

Contents

Preface

Natural gas or fossil fuel is a hydrocarbon gas mixture that mainly consists of methane. It also has different amounts of higher alkanes and small amounts of nitrogen, carbon dioxide, helium, or hydrogen sulfide. As it is a colorless and odorless gas, a sulfur odor is usually added to it for its early leakage detection. Over millions of years, under the earth's surface, in the expanse of layers of decomposing plant and animal matter to heat and pressure, natural gas is formed. Plants obtain energy from the sun, which is stored in natural gas in the form of a chemical bond.

Natural gas as a non-renewable hydrocarbon is used as an energy source for cooking, heating, vehicle fuel, and electricity generation. It is also used as a chemical feedstock in the manufacturing of plastics and organic chemicals. Unfortunately, natural gas extraction and consumption is a major cause of climate change. Potentially, natural gas is a greenhouse gas and due to burning, it releases CO_2 into the atmosphere. Before being used as a fuel, natural gas must be processed to eliminate impurities and meet marketable specifications. Ethane, propane, butanes, pentanes (and higher hydrocarbons), H_2S, CO_2, water vapor, helium, and nitrogen are byproducts of this purification step. This book presents new perspectives and future developments regarding natural gas.

In Chapter 1, the authors conduct a life-cycle assessment to evaluate the environmental impact of marine fuel and LNG produced by energy consumption and greenhouse gas emissions. These results are in accordance with the environmental policy of South Korea.

Chapter 2 describes adsorbed natural gas as a cleaner substitute for gasoline to be used as a transportation fuel. Due to specific compression, liquefaction, and adsorption methods required for the storage of natural gas, adsorption-based natural gas is the economic and safe option for its storage.

Chapters 3 and 4 discuss and evaluate fermentation processes for producing value-added products from natural gas. As C–H bonds have high activation energy, extreme separating conditions are required for the chemical conversion of natural gas. Recently, microbiological processes are being investigated.

Chapter 5 reviews various processes used for C_{3+} hydrocarbon separation from natural gas, with a focus on a polymer-based membrane separation process. C_{3+} hydrocarbons are one of the significant natural gas impurities that can be used as valuable chemical feedstocks as well as liquid fuel for power generation.

Chapter 6 discusses natural gas consumption in the United States. Due to the COVID-19 pandemic, the forecast of long-term natural gas consumption was obsoleted.

Chapter 7 examines developments in India's goal of increasing its share of natural gas, which is critical to developing India's green economy.

Chapter 8 uses a smart grid concept to discuss the operation of a natural gas system in the framework of energy systems. It also discusses the worldwide application of demand-response principles for increasing the efficiency and operability of natural gas networks.

Chapter 9 focuses on natural gas dehydration, which is normally performed by absorption process using TEG (tri ethylene glycol). Generally, natural gas and TEG thermodynamic parameters must be optimized for successful glycol regeneration.

Chapter 10 discusses biogas as an interesting source of renewable energy. It has high methane content and its use as an alternative to fossil fuels can help minimize energy dependence. The chapter also discusses different aspects of biogas decomposition processes for the simultaneous production of syngas and carbon nanofilaments.

Chapter 11 evaluates the properties of carbon nanotubes as a new material for storing renewable energy. Due to their exceptional characteristic properties, carbon nanotubes are advantageous for energy storage.

Chapter 12 presents 2005–2016 data from twenty-nine nations to study the effect of price and income on natural gas demand elasticities and addresses how to incorporate these characteristics into natural gas demand modeling.

I wish to express my sincere appreciation to IntechOpen for giving us the opportunity to publish this book. I would like to thank all the authors for their significant contributions and for sharing their high-quality research.

Maryam Takht Ravanchi, Ph.D.
National Petrochemical Company,
Teheran, Iran

Chapter 1

Comparative Life Cycle Assessment of Liquefied Natural Gas and Marine Fuel for Ship from Well to Hull

Kyeonghun Jwa, Yanghwa Kim and Ocktaeck Lim

Abstract

In this study, well-to-hull was obtained by life cycle assessment (LCA) and GREET, which is developed by Argonne National Laboratory to evaluate the environmental impact of marine LNG and marine fuel. This study compared the environmental impact of marine LNG and marine fuels, which were caused by green house gases (GHGs) emissions and energy consumption. The effect resulted from well-to-pump (WTP) process and pump to hull (PTH). Natural gas has the potential to generate more greenhouse gases than liquid fuels due to the amounts of leaks of the gas that were sent out of the air during production and processing. Nevertheless, the results showed that the greenhouse gases produced during transportation were enough to reduce the disadvantages (pump-to-hull process). The research expects that the results will be under the environmental policy of South Korea.

Keywords: liquified natural gas (LNG), GREET 2018, well to hull, life cycle assessment (LCA), marine fuel, greenhouse gas

1. Introduction

Even though having the disadvantages from 2020.01.01, the International Maritime Organization (IMO) will strengthen a regulation to enforce the content of sulfur compounds in ship engine exhaust gas from 3.5% to 0.5%. In response, using liquified natural gas (LNG) as a fuel of transportation has emerged. To respond to IMO's environmental regulations, shipbuilders in each country are ordering eco-friendly ships in consideration of new ship construction, and the order status of ships using LNG as fuel is shown in **Figure 1** below. LNG-fueled ships are rapidly being applied and distributed in northern Europe. Since the first passenger ship 'Glutra' was built in Norway for the first time in 2000, National Steel and Shipbuilding Company (NASSCO) has recently ordered 3, 400TEU (twenty-foot equivalent unit) container ships.

The current market is still hesitant to introduce LNG fueled vessels. However, if LNG fueled vessels are ordered in earnest, the size of the market is not expected. However, the biggest obstacle to ordering LNG fueled vessels is the lack of infrastructure for fueling vessels [2]. Even though the disadvantages, The Korea government plan to introduce the LNG industry. Life Cycle Assessment for vehicles is
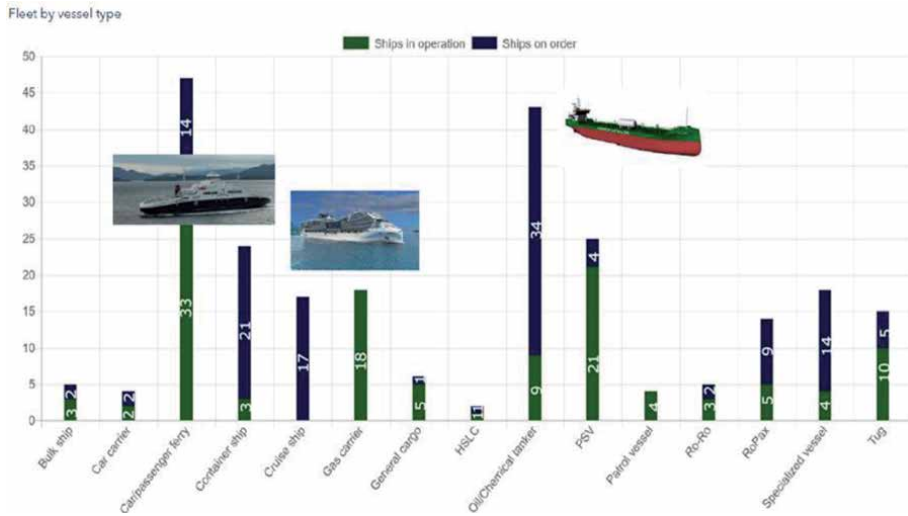
Figure 1.
Order status of ships using LNG as fuel [1].

studied in South Korea [3]. There is little research on ship emissions. Especially, emissions from return gas, boil-off-gas are hard to evaluate

In this study, we evaluated the environmental impact of the whole process for Well-to-Hull. It analyzes and evaluates the environmental problems arising from each process of the product through evaluation, including the production and transportation of fuel used for ships as well as operation and compared fossil fuels with natural gas [4]. Therefore, it is necessary to compare and analyze the WTP (Well to Pump) process using GREET. Generally, natural gas occurs greenhouse gas in the WTP than diesel due to the amounts of leakage generated during the production and treatment process. Nevertheless, the greenhouse gases produced during transportation are expected to be good enough to reduce the shortcomings because of the pump-to-hull process. A more detailed comparison of the operation part is needed through WTP analysis using GREET. The PTH result is obtained from the emission information in operating. There are many limitations to conducting experiments using large marine engines. Therefore, the PTH is calculated from an engine specification that is operated in ships (Ilshin Shipping and Incheon Port Authority).

2. Methods

2.1 LCA

LCA (life cycle Assessment) is developed and utilized by many companies, and research institutes around the world in the 1970s to compare and analyze the environmental friendliness of products [5]. The process in LCA is described in **Figure 2**. It is
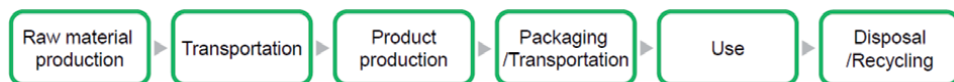
Figure 2.
Process of life cycle assessment [1].

possible to analyze and evaluate the environmental problems caused by the process of the product, and it is possible to perform a comparative analysis of the products.

2.2 GREET

The Greenhouse Gases, Regulated Emissions, and Energy Use in Transportation Model (GREET) was developed by Argonne under the auspices of the US Department of Energy (Energy Efficiency and Renewable Energy) [6]. It is a program that enables LCA of energy usage and emissions that occur during production and transportation of fuel as well as the driving of the vehicle. Also, it can accumulate data on a wide range of data, including moving parts in the picking and transportation production of raw materials. It is calculated based on actual measurement results rather than simulation results. In addition to gasoline and diesel, there are data on full-range fuels used in transportation such as natural gas, electricity, and bio-oil. Not only energy consumption but also exhaust gas and greenhouse gas emissions are investigated, and it is very useful for comparative analysis under the purpose of life cycle assessment. GREET includes more than 100 fuel routes, including petroleum and natural gas fuels, as well as biofuels, hydrogen, and electricity from a variety of energy sources. It is easy to compare and analyze the effects of each stage in the calculation by dividing the process from fuel production to supply. It provides the sources, usage from, contents of the data used in the GREET development process in the public domain.

2.3 LCA method

Well-to-hull processes of marine fuel and LNG are described in **Figures 3** and **4**. To evaluate the environmental impact of diesel compared to natural gas, we use GREET to compare the following WTP processes. In the case of natural gas, it is expected that more greenhouse gases will be generated than diesel due to the amounts of leaks generated during production and processing. However, compared to diesel, the amount of traffic generated during transport is expected to be good enough to reduce the above disadvantages. To compare and analyze this, we want to compare and analyze the operation part using GREET and WTP analysis, PTH data [7].

In the case of the WTP process, it is difficult to obtain reliable data, and there are a lack of extensive data on each process. To solve this problem, we would like to compare and analyze the results using the following GREET results.
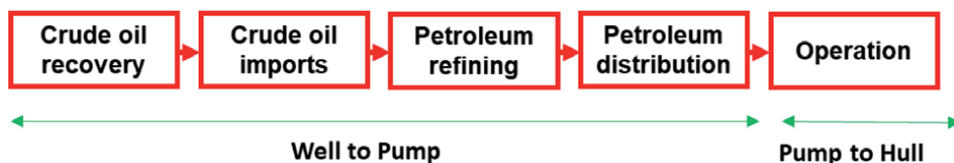
Figure 3.
Well-to-hull process of marine fuel [1].
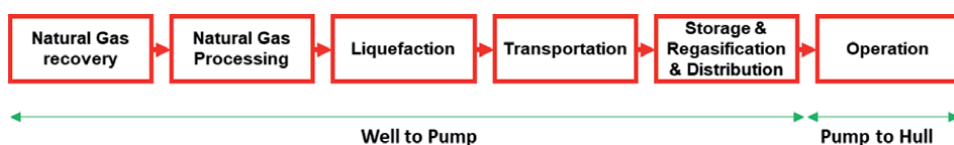
Figure 4.
Well-to-hull process of LNG [1].

2.4 Well to pump

2.4.1 Marine fuel

GREET shows five things related to the WTP process of marine fuels. The values are 1) petroleum-based marine fuels from crude oil, 2) Fisher-Tropsch diesel fuel from natural gas, coal, and cellulosic biomass, 3) hydro-processed esters and fatty acids (HEFA) or hydro-processed renewable diesel (HRD) diesel fuel from bio-oil found in soybeans, palm, rapeseed, jatropha, camelina, and algae, 4) renewable diesel from pyrolysis of cellulosic biomass, and 5) biodiesel or fatty acid methyl esters (FAMEs) from bio-oil found in soybeans, palm, rapeseed, jatropha, camelina, and algae. Among them, crude oil-based marine fuels are chosen. The average distance from oil-importing country to the Korean refinery is 12,135 km based on Korea National Oil Corporation's data, using Voyage calculator. According to the Korea National Oil Corporation, most volume of crude oil is imported from overseas. About 76% of total crude oil imports are from the Middle East (Saudi Arabia, Kuwait, Iraq, Qatar, etc.) in 2018. Domestic data on crude oil import, preparation, and distribution for the diesel life cycle analysis were provided by the Korea Petroleum Association [8].

2.4.2 LNG

The data of LNG required for well-to-pump analysis are as follows. We consider the energy efficiency of raw material extraction and processing and the ratio of process fuel in natural gas production in the NG recovery and NG processing steps. Korea Gas Corporation provides information about natural gas imports. From the information, we calculate the import distance to consider the transportation step. The information is described in **Table 1**. In the case of storage, regasification, and distribution step after importing LNG, the data were used in GREET because there were not enough data accumulated.

2.5 Pump to hull

Although it is necessary to find and compare diesel ships of similar specifications as LNG vessels, it is difficult to obtain information on the number of days of sailing, sailing distance, ship weight (including load weight), fuel consumption, and electricity consumption for a certain period required for calculation. There are three types of marine-fueled vessels that are bulk carriers, oil tankers, and container ships. At the time, GREET only provided specifications of these ships. We average the total energy use and greenhouse gases to calculate data in the operation step. The information related to ships using LNG as fuel is not explained. Therefore, we get data from a company that operates LNG ships in South Korea.

Country	Distance(km)	Import volume(ton)
Qatar	11,297	14,250,000
Australia	6,667	7,870,000
The U.S.	10,556	4,660,000
Oman	10,556	4,280,000
Malaysia	4,598	3,700,000

Table 1.
Import distance to South Korea of natural gas (2018).

3. Results

In the case of marine fuel, shows the well-to-pump result of energy use and greenhouse gas emissions are in **Table 2**. In the pump-to-hull pathway, the GHG emissions are only calculated from the specification of HYUNDAI MAN B & W TYPE: 6G50ME-GI used in Ilshin Shipping LNG propulsion vessel because of the company's secret. The GHG emissions result is 74.4 g/MJ in diesel mode.

Processes of extraction, production processing, and storage before importing LNG to Korea are included. Since NG also uses GREET, it is necessary to analyze additional information by importing the country later. Based on GREET, energy use: 59,287 kJ / GJ. GHGs emission results: 12606 gCO_2 / GJ. In the natural gas processing step, energy use is 4510 kJ/GJ, and GHGs emission result is 34,741gCO_2/ GJ. In the transportation step, GREET only provides a specification of oil tankers that transport crude oil, so we use the same value as well. Because LNG carriers generate electricity and heat from vented gases, they are expected to emit fewer emissions than diesel ships. The results are 19,646 kJ/GJ and 1643.8gCO_2/GJ. In the storage, re-gasification, and distribution step, the data are not accumulated enough to evaluate, so we use the value in GREET. The values are 15,478 kJ/GJ and 1904gCO_2/GJ.

For LNG, the well-to-pump result of energy use is 194.8 kJ/MJ, and GHG emissions are 19.75 g/MJ. In the pump-to-hull step, the GHG emission result is 56.5 g/MJ in gas mode.

In **Figures 5**–**7**, all the results of WTP are organized to be comprehensive. In the case of well to pump (WTP), LNG has higher energy consumption and GHGs emissions due to the addition of processes such as compressed gas and re-liquefaction, as

	Residual oil	**Marine Distillate**	**Low suffer Marine Distillate**
Energy use(kJ/MJ)	152.1	202.8	202.8
GHG emissions(g/MJ)	13.74	16.77	16.78

Table 2.
Well to pump results in marine fuel.
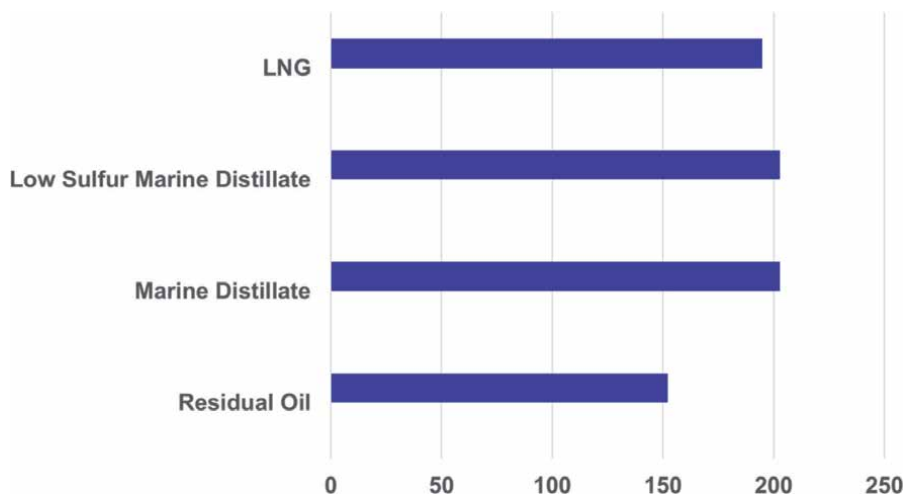
Figure 5.
Marine fuel WTP energy usage results (kJ/MJ).
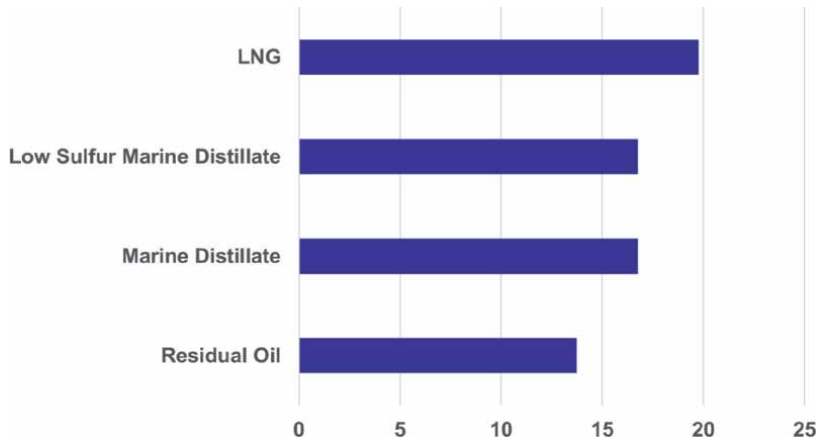
Figure 6.
Marine fuel WTP GHG emissions results (g/MJ).
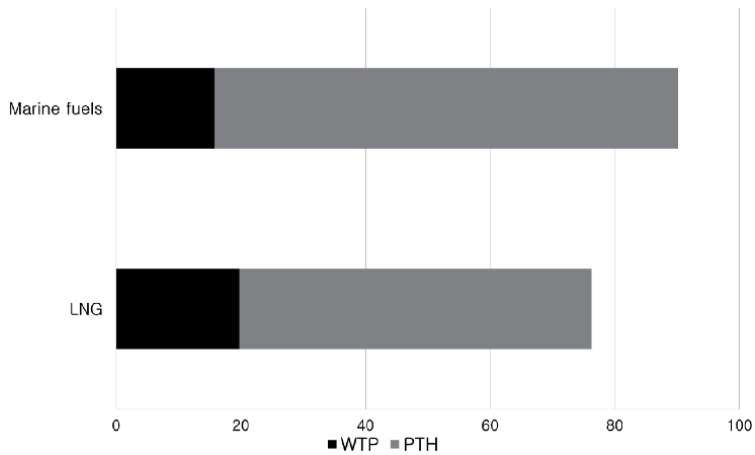
Figure 7.
Marine fuel WTH GHG emissions results (g/MJ).

well as the amount of gas discharged during production compared to marine fuels such as residual oil and marine distillate. Energy consumption data in PTH CANNOT have been obtained from Ilshin. However, it is considered that the energy consumption of LNG is higher because of use to boil-off-gas re-liquefaction. For pump to hull (PTH), GHGs emissions from operations are far above the WTP process.

4. Conclusions

The research was carried out to investigate the environmental impacts of LNG as fuel, comparing marine fuels. LCA analysis shows that natural gas produces more GHGs in WTP compared to liquid fuel for ships, but fewer in PTH. In the case of pump to hull (PTH), the energy consumption and GHG emissions in operation far exceed the WTP process due to the nature of ships that must cross the Pacific. Therefore, LNG, which emits less GHGs than diesel, is thought to be much better than diesel in terms of the environment but may differ from actual operating conditions, so engine experiments and additional data are needed to confirm in the future.

In South Korea, both natural gas and marine fuels depend on imports, so GHG emissions from WTP are relatively low. To satisfy the IMO regulations, the exhaust gas generated during ship operation (PTH) should be managed in a focused manner. Therefore, the amount of exhaust gas generated during operation is less than that of marine fuel, so it is considered to be suitable for satisfying environmental regulations. However, more detailed comparisons are needed between engine efficiency and operating costs (price, storage costs, safety management costs, etc.) compared to diesel. However, the emissions from WTP in LNG, which is higher than marine fuels could not be ignored.

Author details

Kyeonghun Jwa[1], Yanghwa Kim[1] and Ocktaeck Lim[2]*

1 Graduate School of Mechanical Engineering, University of Ulsan, Ulsan, South Korea

2 School of Mechanical Engineering, University of Ulsan, Ulsan, South Korea

*Address all correspondence to: otlim@ulsan.ac.kr

IntechOpen

References

[1] Ole Vidar Nilsen. DNV GL-LNG Fueled Vessels n.d. www.golng.eu%2Ffiles%2FMain%2F20180417%2F2.%2520 Ole%2520Vidar%2520Nilsen% 2520-%2520DNV%2520GL. pdf&usg=AOvVaw1Ln

[2] Ministry of Land, Infrastructure, Transport and T of J. VI. Operation Guidelines for Truck to Ship LNG Transfer [Purpose and Scope of Application] n.d

[3] Choi W, Song HH. Well-to-wheel analysis on greenhouse gas emission and energy use with natural gas in Korea. International Journal of Life Cycle Assessment. 2014;**19**:850-860. DOI: 10.1007/s11367-014-0704-7

[4] Heywood JB. Internal Combustion Engine Fundamentals. New York: McGraw-Hill Education; 1988

[5] NETL. Development of Baseline Data and Analysis of Life Cycle Greenhouse Gas Emissions of Petroleum-Based Fuels. Pittsburgh: National Energy Technology Laboratory; 2008. https:// doi.org/DOE/NETL-2009/1346

[6] Laboratory AN. Argonne National Laboratory, GREET1 (Greenhouse gases, Regulated Emissions, and Energy use in transportation) transportation fuel cycle analysis model Version 2018 - Google Search n.d. https://www. google.com/search?safe=strict&biw=19 20&bih=880&sxsrf=ALeKk02-6QVL0g eYlLoZG0Glz3znnhQAhA%3A16158976 16677&ei=EKRQYKXxKIf70gSf- qfQBA&q=Argonne+National+Laborat ory%2C+GREET1+%28Greenhouse+gas es%2C+Regulated+Emissions%2C+and +Energy+use+in+transport (accessed March 17, 2021)

[7] Jwa K, Lim O. Comparative life cycle assessment of lithium-ion battery electric bus and Diesel bus from well to wheel. Energy Procedia. 2018;**145**: 223-227. DOI: 10.1016/j.egypro. 2018.04.039

[8] KEMCO. No Title n.d. http://www. petronet.co.kr/main2.j.

Adsorbed Natural Gas Storage for Vehicular Applications

Akhoury Sudhir Kumar Sinha, Umaprasana Ojha,
Marriyappan Sivagnanam Balathanigaimani and Sanjay Kar

Abstract

The use of adsorbed natural gas (ANG) as a transportation fuel is a relatively cleaner alternative compared to that of gasoline and is important from the perspective of environmental safety. However, unlike gasoline and diesel, natural gas requires compression, liquefaction, and adsorption techniques for its storage, as it has a very low volumetric energy density. Among all storage techniques, adsorption-based natural gas (ANG) storage is considered as more economical and relatively safe technology due to its mild temperature and pressure conditions for the storage. This chapter will summarize the recent advances in the area of ANG with reference to various synthetic storage materials recently developed for the purpose and their efficiency towards storage and deliverability of natural gas. Particular emphasis will be given to adsorbents based on porous carbon materials, metal organic frameworks, and covalent organic frameworks for the said application. The synthetic procedure for the above adsorbents, followed by their efficiency to store and deliver natural gas, will be discussed. Finally, in the conclusion, the future scope of the technology will be summarized.

Keywords: adsorbed natural gas storage, metal organic framework, covalent organic framework, vehicular application, porous carbon materials

1. Introduction

The well-known alternative fuels for crude oil-based liquid products are natural gas and hydrogen. Nevertheless, these gaseous fuels require a special storage technique for effective utilization due to their lower volumetric energy density values. Natural gas with wide availability and improved production technology is considered to be an important energy source for the future and a cleaner form of energy compared to that of the higher hydrocarbon-based fuels such as gasoline and diesel due to its low C/H ratio. This consists of mainly methane (55–98 vol%) as the primary component along with other gases such as ethane (2–4 vol%), propane (0.5–2 vol%), and butane (0.25–0.5 vol%) in minor amounts along with few acid gases in trace amounts [1]. An estimate has shown that natural gas produces 55.9 kg CO_2/GJ of energy, which is lower than that of anthracite coal (91.3 CO_2/GJ), gasoline (78.5 CO_2/GJ), and diesel (73.3 CO_2/GJ) [2]. Therefore, among the several areas of attention for further technological advances in the natural gas domain, storage, utilization, and supply chain are prominent in the downstream sector. The concept of natural gas storage is old and typically produced and, in some cases,

the processed gas is stored in an underground facility in the vicinity of the supply center. The stored gas is regularly monitored for potential loss and emission reliability of the supply chain to meet the customer demand is an important parameter for this form of energy [3]. The current issues related to the environment has led to adopting effective measures to handle major pollution sources and the transportation sector is considered as one of the important one among these. The use of natural gas owing to wide availability and its lower carbon emission compared to that of the higher hydrocarbons as fuel for vehicular application is projected to control the pollution level to a certain extent. Natural gas in two forms are utilized as vehicle fuel, i.e. compressed natural gas (CNG) and liquefied natural gas (LNG). The CNG is especially important for light vehicle transport such as cars and other cargo transporting vehicles, whereas the LNG form is utilized in industries and manufacturing along with domestic applications. However, these systems suffer from the limitations of high cost, low storage efficiency, and safety issues.

To improve the efficiency of the process, the concept of adsorbed natural gas (ANG) originated, in which the natural gas was stored in a comparatively high amount in a porous adsorbent system under ambient temperature conditions. In this process, the methane is believed to be adsorbed in molecular form in the nano-sized pores of the adsorbent network and the density in the adsorbed form exceeds the bulk density. The adsorption process being exothermic typically depended on the thermodynamic conditions. The amount of adsorption increased with a decrease in temperature and an increase in pressure. The ANG is considered to be a cost-effective alternative compared to that of liquefaction and energy-intensive compression. The storage pressure in this scenario can be decreased to ~35 bar compared to that of the utilized in CNG technology (200 bar) [4]. The target set by the Department of Energy (DOE) is 263 cm^3/cm^3 working capacity under standard conditions for the adsorbent material to be commercially viable. The value is gravimetrically equivalent to 0.5 g/g of adsorbent and amount of CNG at 200 bar and 25°C pressure and temperature respectively. Furthermore, the low energy density value of the natural gas also requires improvement which may be achieved by high-density packing so that it mimics the energy density value of LNG, i.e. ~22.2 MJ/L. Therefore, efficient adsorbents with high adsorption and desorption efficiency are desirable to utilize this ANG technology in an affordable manner for commercial implementation.

2. Materials for ANG storage

The selection of a suitable adsorbent is one of the most important criteria for the utilization of the technology for successful commercial application. An adsorbent with high surface area, large pore volume, narrow micropore distribution, the pore size of 1–1.2 nm, and high density is required to achieve the ambitious ANG storage target for vehicular application set by the US DOE. The porous materials studied in recent literature for adsorption based natural gas storage at relatively low pressure compared to that of the CNG and ambient temperature conditions are resins, zeolites [5], xerogels [6], aerogels, carbon-based materials [7] such as carbon nanotubes and fibers, metal organic frameworks (MOF) and covalent organic frameworks (COF). The methane adsorption efficiency is known to be linearly dependent on the surface area of the adsorbent (**Figure 1**) [8]. Earlier studies have revealed that Zeolites exhibiting adsorption capacity up to 100 V/V storage capacity are not suitable to reach the target set by the DOE and the interest has shifted to the carbon-based materials and 3D frameworks [4].
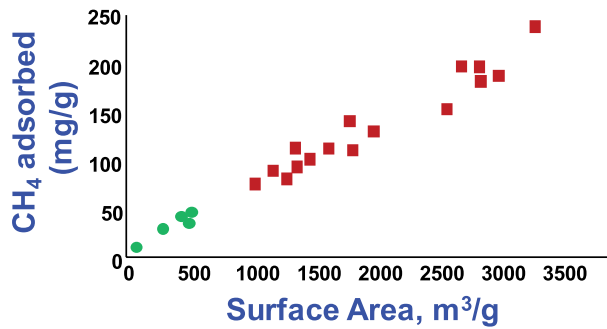
Figure 1.
Schematics showing the effect of the surface of the carbon-based adsorbents on the methane uptake capacity, the red squares represent the carbon in granular powder form and the green circles represent the coal samples.

The volumetric storage capacity of the adsorbed natural gas may be calculated in a simple manner by following the equation given below;

$$n_{stg} = n_{exc} + \rho_{gas}\left[1 - \left(\rho_{pack} / \rho_{He}\right)\right] \tag{1}$$

where, n_{stg} is the volumetric storage capacity, n_{exc} is the excess amount of adsorbate per volume of adsorbent, ρ_{gas}, $\rho_{pack,}$ and ρ_{He} is the gas, packing and helium density respectively.

2.1 Porous carbon materials

Porous carbon materials are one of the widely studied systems for said application. In general carbon-based materials have exhibited higher adsorption capacity compared to that of the other studied porous materials possessing similar surface area due to their slit-shaped pore structure [9]. The packing density of activated carbon-based materials is also known to exhibit a linear dependence on the applied pressure and the value reaches up to 0.8 g/cm^3 on applying pressure till 980 MPa [10]. Furthermore, the activated carbon-based materials can be easily synthesized from readily available low-cost starting materials such as wooden materials, corns, different fossil fuels, and polymer and are cost-effective. These materials can be easily physically activated using steam or CO_2 and chemically activated in an industrial scale using acids and bases under high-temperature conditions [11]. Earlier studies on carbon-based adsorbent for the natural gas storage application was based on the single-walled carbon nanotubes (SWCNT). The Monte Carlo simulation-based theoretical studies predicted that the SWCNT bundles may be suitable for methane storage under moderate pressure conditions [12]. However, experimental studies afterward suggested that the adsorption capacity is limited to 0.11 g/g in these systems at 60 bar and 30°C [13]. The activated carbon-based materials have been successful in achieving excess gravimetric methane uptake till 0.2 g/g at 35 bar and ambient temperature conditions and in this case the delivery capacity was 170 V/V at 65 bar pressure [14]. Further increase in pressure to 100 bar improved the adsorption capacity to 263 V/V, which surpassed the target set by DOE. However, the deliverable capacity of carbon-based materials is reported to be inferior, which limits the utilization of these materials for storage applications. The carbon nanotube (CNT) though has shown promise to achieve high adsorption capacity, the experimental value is limited to 160 V/V at 35 bar and 25°C [15].

One of the advantages of these carbon-based materials is that these can be synthesized from renewable, polymeric, and cost-effective sources and activated via multiple routes. For example, olive stones were utilized to prepare carbon-based materials, which on carbonization at 500°C under inert atmosphere produced the carbon material. The sample was activated using KOH at a high temperature of 800°C [16]. The sample exhibited 3551 m^2/g BET surface area and 215 V/V methane uptake capacity at 100 bar with a working capacity of 135 V/V. In another instance, polyacrylonitrile beads were pyrolyzed at 600°C to synthesize carbon flowers. The carbon flowers were then activated with KOH by heating the mixture at 800°C. The flowers were also activated by heating these under CO_2 flow at 850°C. The resulting carbon materials exhibited a BET surface area of 1077 m^2/g and methane adsorption capacity of 196 V/V at 65 bar [17]. Other biomass precursors for the synthesis of porous carbon materials include coconut shells [18], corn straws [19], banana peels [20], and soya [21]. Xiao and coworkers published a summary on the use of various biomass for the synthesis of porous carbon materials and the surface area of the resulting materials [22]. The review also summarized the different activation methods utilized to activate the carbon materials such as strong inorganic bases [23], lewis acid [24], and H_3PO_4 [25] based procedures to optimize the pore structure further and enhance their adsorption performance. Templating is another useful technique utilized in literature to achieve highly ordered and large surface area carbon materials. Both soft and hard templating can be used for this purpose. Hard templates could be a various nanoparticles, silica, and molecular sieves. For example, mesoporous silica sieve hard templates in presence of 1,10-phenanthroline ligand were utilized to synthesize Co immobilized nitrogen-doped porous carbon materials for catalytic applications. The calcination for the material synthesis was carried out at 800°C [26]. Typically, in the case of the soft templating method, the polymers or surfactant self-assemble into a particular ordered shape, which is then immobilized into the mesoporous material to be synthesized. Subsequently, the templates are removed to expose the pores and obtain the porous material. Ionic liquid and self-assembled block polymers have been utilized as the soft templates for this purpose [27, 28]. Direct carbonization of ordered nanostructures is also becoming another attractive option to generate porous carbon materials. For example, the MOF can be utilized as precursors to directly synthesize porous carbon materials via pyrolysis under an inert environment [29]. The presence of various organic ligands may also serve as the carbon source for the above synthesis, whereas the metal nodes often help to control the pore structure and control the physical properties of the carbon material. For example, Yamaguchi and coworkers utilized a Zn and Co-based bimetallic MOF to synthesize nanoporous carbon by pyrolyzing the precursor under an inert atmosphere at 900°C [30]. The shape of the precursor was replicated in the carbon material produced as can be shown in **Figure 2** below. Metal such as Zn evaporates at a high temperature allowing the formation of pores in the resulting carbon product. In some cases, the metal ions convert to the corresponding nanoparticles and serve as a catalytic site for further applications. The type of metal, the metal content, and ligand type play important role in developing nanoporous carbon structures.

2.2 Metal organic frameworks

In this regard, the MOFs have gained strong interest in their ability to reversibly store natural gas for vehicular application. MOFs are a wide family of reticular and highly porous coordination polymers formed by the coordination self-assembly of the metal center with multidentate organic building blocks [32, 33]. The MOFs are reported to exhibit ultra-high surface area up to 10,000 m^2/g, and tunable pore sizes
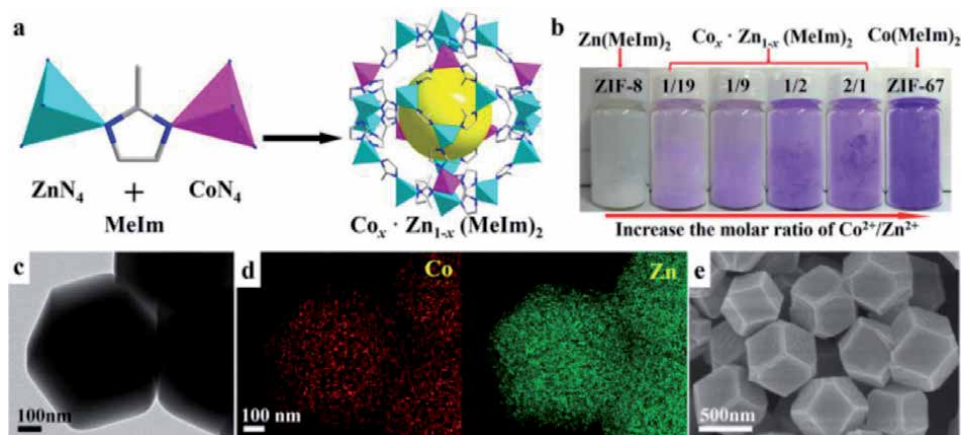
Figure 2.
(a) The crystal structure of Zn and Co-based bimetallic MOF, (b) the photographs of solutions possessing different molar ratios of Co^{2+} to Zn^{2+}, (c and d) the TEM and (e) SEM images of the MOF and produced nanoporous carbon., Reproduced with permission from 30. Copyright 2016 Nature Publishing Group. The elemental mapping images show the presence of Co and Zn in the parent system.

MIL-47 $Zn_6(H_2O)_3(BTP)_4$ CAU-8

Zn-MOF-74   3W-ROD-1
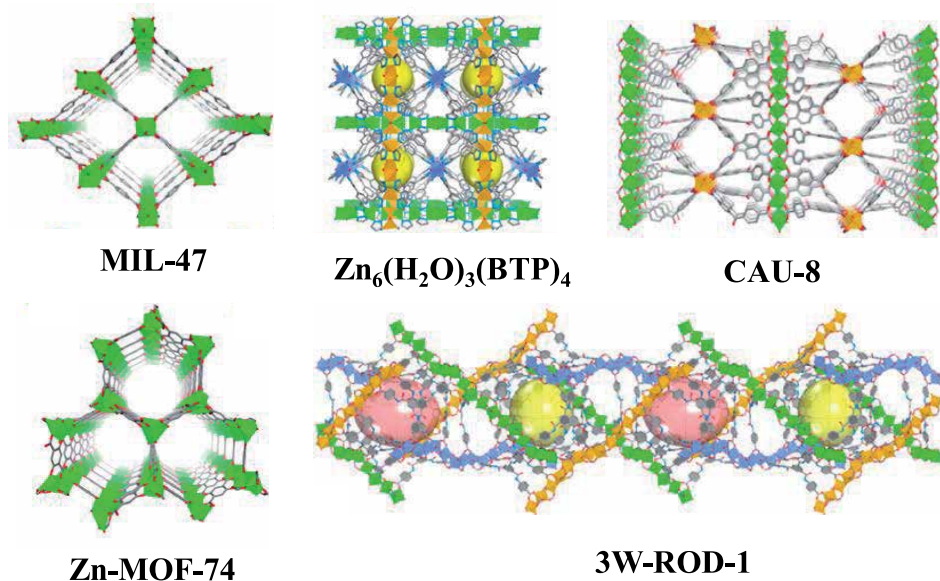
Figure 3.
Structure of some of the rod MOFs synthesized in recent literature. Reproduced with permission from [31], Copyright 2021, American Chemical Society.

with the possibility to functionalize them [34]. A number of MOF materials such as MIL-74, CAU-8, $Zn_6(H_2O)_3(BTP)_4$, Zn-MOF-74, 3W-ROD-1, and Ni-MOF-74 are studied towards their ability to store natural gas (**Figure 3**) [31]. Similarly, Pore size optimization is one of the important targets in the field of MOF materials. The effective way to address the same is by gradually changing the length of the organic linker and introducing functionality into the linker. For example, the introduction of sulfone and carbonyl groups notably improved the CO_2 absorption capacity compared to that of the un-functionalized one (**Figure 4**) [35].

For an adsorbent to exhibit adequate adsorption ability, the system should maintain a balance between gravimetric (SA_G) and volumetric surface area (SA_V)
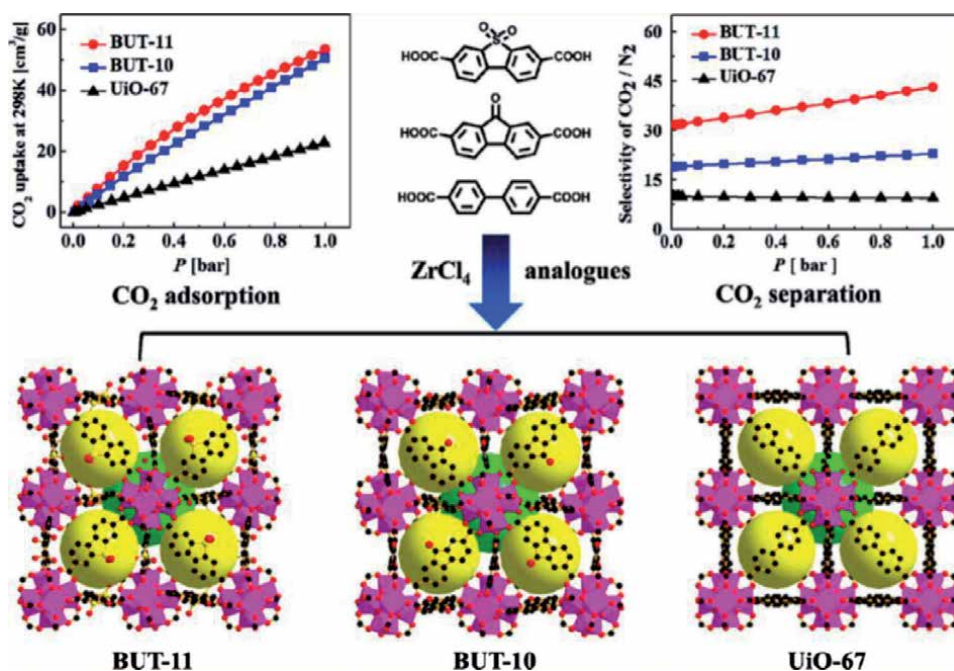
Figure 4.
Effect of ligand size on the pore structure of the resulting MOFs. Reproduced with permission from [35], Copyright 2014, American Chemical Society.

along with high porosity. Often the normalized value of the product of SA_G and SA_V is utilized to suggest the above. It is known that the helium void fraction displays a volcano relationship with the largest pore diameter. The NU-1500; Al and PET-based MOF systems exhibit void fraction and largest pore diameter values of 0.76 and 12.7 Å respectively and display high CH_4 storage capacity. A similar system with Fe at the coordinating center, the NU-1501 series displayed increased VF values of 0.87 and an LPD value of 18.8 Å [36]. The MOF series based on extended PET system and Al metal displayed SA_G and SA_V of 7310 m^2/g and 2060 m^2/cm^3 respectively. The corresponding Fe-based system showed a somewhat lower SA_G value (7140 m^2/g) and comparable SA_V value (2130 m^2/cm^3). The study showed that the SA_G and SA_V values can be controlled further to significantly improve the gravimetric uptake capacity while retaining the volumetric storage capacity.

The gas adsorption capacity and separation performance of the MOFs may be optimized further by suitably modifying the organic building blocks with functional groups using simple organic transformation. The presence of polar functional groups in the mainframe of MOFs effectively improves the CO_2 capture and separation abilities. For example, MOF is based on flexible hexadentate ligands containing amide groups, N-tris-isophthalic acid-1,3,5-benzenetricarboxamide (TPBTM) such as $[Cu_{24}(TPBTM^{6-})_8(H_2O)_{24}]$ (Cu-TPBTM) with high surface area [37]. The pore structure of the resulting MOFs depended on the size, structure, and functionality of the organic building blocks as shown in **Figure 5** for representative purposes.

These class of materials are reported to exhibit adsorption capacity up to 180 V/V. For example, the HKUST-1 based on Cu metal and 1,3,5-benzenetricarboxylate organic linker exhibits surface area up to 1800 m^2/g with adequate stability [37]. Similarly, a MOF system based on Cu and a hexadentate linker 3,3′,3″,5,5′,5″-benzene-1,3,5-triyl-hexabenzoic acid exhibited BET surface area up to 6240 m^2/g [39]. The open metal site in these MOFs serves as the site to bind to the methane molecule. At 100 bar pressure and 25°C, these MOFs display
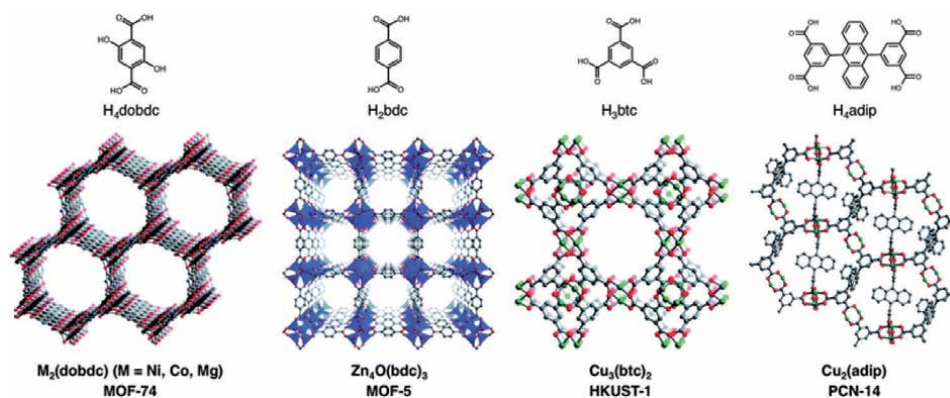
Figure 5.
The Cu-TPNTM MOFs and their pore structure is depicted above. Reproduced with permission from [38].
Copyright 2014, Royal Society of Chemistry.

storage capacity up to 330 V/V. The issue with this MOF system towards practical applications is that higher hydrocarbons, such as ethane and propane adsorb more strongly compared to that of the methane and tend to block the pore site [40]. Seki reported a MOF system, based on copper and triethylenediamine (TED), $[Cu-(O_2CRCO_2)\cdot 1/2TED\}_n]$ $[R = 4,4'-C_6H_4C_6H_4$ (1)] which recorded a volumetric storage capacity for methane up to 225 V/V [41]. For the synthesis of MOFs for said application, key factors such as the number of coordinating sites, size, shape, and geometric configuration of organic linkers require careful attention, which determines the self-assembled structure and gas adsorption performance of MOFs. Typically, the coordinating sites of the organic building blocks consist of electron-donating elements such as O, S, and N. Among the corresponding coordinating functionalities, the carboxylic acid groups tend to form stable MOFs. A set of crystalline MOFs based on 4,4',4''-[benzene-1,3,5-triyl-tris(ethyne-2,1-diyl)] tribenzoate organic linker and $Zn_4O(CO_2)_6$ was synthesized that exhibited non-interpenetrating 3D crystal structures with pores of ~48 Å sizes [42]. The MOF displayed an extremely high BET surface area of 6240 m^2/g. A table summarizing the adsorption capacity under given temperature and pressure conditions for various MOFs is included for reference (**Table 1**) [43].

Considering the gas density in the pores of the adsorbent to be considerably higher compared to that of the bulk density, the optimization of void space becomes important to maximize the adsorption capacity. Therefore, monoliths of MOFs are prepared using compression, binder, and polymeric additives [45]. However, the use of additives though known to improve the mechanical strength has their drawback as these tend to block the pore space and decrease the uptake capacity [46]. Therefore, preparation of pure monolith of MOF using compression has been pursued in literature. Even mechanical compression notably decreased the uptake capacity possibly due to the collapse of the pore structure. For example, the uptake capacity of Ni_2(1,4-dioxido-2,5-benzenedicarboxylate) based MOF decreased from 230 to 100 V/V at 34 bar and 30°C after palletization [47]. Another way to handle the issue is to use a sol-gel technology in which gradual evaporation of solvent from the monoliths without destroying the pore structure. Recently, HKUST-1 monolith prepared using sol-gel technique exhibited uptake capacity of 259 V/V at 65 bar and 25°C [48].

The methane binding sites were studied in the literature on Zn-based MOF samples using low-temperature synchrotron analysis. The data revealed two primary adsorption sites and one secondary adsorption site. The primary adsorption sites

MOFs	BET (m²/g)	Pressure (bar)	Capacity (cm³/g)	Reference
NU-1500-Al	3650	100	549.1	[43]
MOF-177	4500	65	475	[38]
NU-1501-Al	7310	100	929.7	[43]
PCN-46	2500	65	310.7	[43]
PCN-61	3000	65	366.8	[43]
PCN-66	4000	65	397.9	[43]
PCN-68	5109	65	465.2	[43]
UTSA-61	2171	65	337	[43]
UTSA-20	1620	65	252.7	[43]
NOTT-119	4118	65	426.6	[43]
NU-111	4930	65	503	[43]
NU-125	3286	65	395	[43]
NU-140	4300	65	451.5	[43]
NOTT-100	1661	35	210	[43]
NOTT-102	3342	35	308	[38]
UTSA-110	3241	65	402	[44]
UTSA-76	2820	65	363	[44]
NJU-Bai-43	3090	65	396	[44]
LIFM-82	1624	65	267	[44]
MFM-38	2022	65	346	[44]
MFM-115a	3394	65	389	[44]
MIL-53 (Cr)	1500 (Langmuir)	35	159	[38]
SNU-77	3670	35	250	[38]
PCN-68	5109	35	332	[38]
IRMOF	1102	35	163	[38]
DUT-4	1308	35	158	[38]
FJI-1	4043	35	273	[38]
DUT-13	5570 (Langmuir)	35	250	[38]
MOF-210	6240	35	331	[38]
DUT-8 (Co)	1400	35	78	[38]

Table 1.
The methane gas adsorption capacity of various MOFs under different pressures conditions [38, 43, 44].

were located near the Zn complex paddlewheel and the center of the small windows was recognized as the second primary adsorption site. At these sites, the methane interacted with the phenyl units and paddlewheel units. The secondary adsorption site was recognized as the center of the cavity [49]. However, still, the interaction of functional groups with methane is not very clear. More studies with support from spectroscopic tools may be necessary for future to completely ascertain the mechanism of methane storage. Using flexible MOFs is attractive to improve desorption capacity and minimize the loss during desorption. Considering the desorption pressure of the working engine is fixed at 4.8 bar by DoE, the reported flexible

MOFs are known to absorb ANG at between 35 and 65 bar and release most of the gas at ~5 bar pressure [50, 51]. The type of metal center in the MOF also controls the uptake capacity and thermal management of the system. For example, Co(bdp) and Fe(bdp) based MOFs through exhibit comparable methane uptake capacity, Fe-based system has desorption steps at higher pressures of 10 bar compared to that of the Co-based system [52]. Similarly, in terms of intrinsic thermal management, the amount of heat released by Fe(bdp) based system (64.3 kJ/L) is 12% compared to that of the Co(bdp) (73.4 kJ/L) based system. Overall, the challenge with these systems lies with the fact that the 3D structure to be produced in such a way that the aromatic rings are exposed for the CH_4 interaction. However, expansion of the organic linkers leads to fragile materials and allows for the self-interpenetration of lattices. Furthermore, the thermal stability of the coordination linkage, low heat of adsorption, and high packing density are also important from the perspective of commercial viability. Keeping in view of the above, suitable MOFs with high surface area and porosity may be designed and synthesized for the ANG storage application.

2.3 Covalent organic frameworks

Another exciting avenue for reversible storage of CH_4 is the covalent organic frameworks (COFs). The COFs are nanoporous materials formed by the covalent crosslinking of organic functional groups. These are lightweight materials with large pore volume, low density, and presence of hydrocarbon frames that enhances the interaction towards CH_4 and improve the uptake capacity. Importantly, these possess high thermal stability and low molecular weight. For example, the COFs based on boronic acid linkage exhibited high thermal stability till 500°C and surface area up to 1590 cm^2/g [53]. The surface area of boronic acid-based COFs increased further by restructuring the pore structure through the incorporation of two nodes, i.e. triangular (ctn) and tetrahedral (bor). The surface area of the COFs was measured to be 4210 cm^2/g [54]. Earlier studies have proposed to minimize the methane COF interaction and increase the heat of adsorption to enhance the delivery efficiency of methane. These studies have further proposed that substitution on the phenyl ring does not alter the binding ability in the samples [55].

A study based on aromatic imine networks revealed that sub-stoichiometric construction of COFs hexagonal building blocks with four connecting sites, where the two unreacted sites can be used to enhance the selectivity of hydrocarbon adsorption [56]. The COF displayed a high BET surface area up to 3478 m^2/g and methane adsorption capacity of 11.2 cm^3/g. Similarly, another sub-stoichiometric COFs based on imines displaying bex net topology synthesized using tri- and tetratopic linkers are reported in the literature [57]. Topology control in COF is another important aspect to control the uptake capacity. For example, recently an N,N-dimethyl acetamide and 1,3,5-trimethylbenzene based imine-COF was synthesized that displayed two different types of triangular micropores of different pore dimensions. The diameter of the pores was 11.3 and 15.2 Å respectively [58]. The COFs with tbo topology have been reported in the literature by using planar porphyrin with four coordinating sites and 3 coordinating trigonal aldehydes of a triphenylamine. The COFs are arranged into a $Pm\bar{3}$ space group and constitute a non-interpenetrating framework [59].

COFs possessing pcu topology have been synthesized using distorted aromatic compounds serving as triangular antiprismatic nodes [60]. Imine-based COFs possessing fjh topology was synthesized by coupling a triangular linker with a square building block [61]. Triptycene-based COFs displaying a non-interpenetrated ceq or acs topology was synthesized using a combination of a triangular prism and

planar triangle nodes [44]. The sample displayed methane adsorption capacity up to 48 cm^3/g at 0°C and 1 bar. The COF exhibited a BET surface area value of 2650 m^2/g. Overall, studies have shown that the organic building block structure and functionality can be utilized as a control to develop COFs with controlled pore size, pore structure, and topology. The functionality in the COF system may be introduced to enhance the selectivity of such systems towards methane adsorption compared to that of the polar gases. The stoichiometry also serves as one of the handles to control the topology of the COFs. Several studies have shown that these materials possessing adequate thermal stability and binding ability towards methane may be a useful option for methane storage applications.

3. Conclusion

To summarize, ANG holds strong promise in the area of fuel for transportation and other consumer sectors. The affordability depends on the availability of cost-effective adsorbents with high storage capacity with optimized deliverability. Though porous carbon, metal-organic framework, and covalent organic framework have shown promise, the target set by the DOE is yet to be complied with optimum deliverability. Selective compositions have been successful in achieving the storage capacity limits, the cost-effective and large scale production of such materials is under ways to materialize a commercializable product. These porous nanostructures are predicted to reach a high surface area up to 4000 m^2/g and beyond. A greater understanding of the pore structure, synthetic process, and mechanism of formation, pore controlling factors during synthesis and factors contributing towards the pore uniformity and stability would notably help towards the development of nonporous materials with high surface area and controlled pore structure. Therefore, the development of new cost-effective, thermally stable adsorbents with high uptake capacity and material strength is still desirable to further fulfill the commercial viability aspect of the technology.

Author details

Akhoury Sudhir Kumar Sinha*, Umaprasana Ojha,
Marriyappan Sivagnanam Balathanigaimani and Sanjay Kar
Rajiv Gandhi Institute of Petroleum Technology, Jais, Uttar Pradesh, India

*Address all correspondence to: asksinha@rgipt.ac.in

IntechOpen

References

[1] Saha D, Grappe HA, Chakraborty A, Orkoulas G. Postextraction separation, on-board storage, and catalytic conversion of methane in natural gas: A review. Chemical Reviews. 2016;**116**(19):11436-11499

[2] Sapag K, Vallone A, Garca A, Solar C. Adsorption of methane in porous materials as the basis for the storage of natural gas. In: Natural Gas. IntechOpen; 2010. DOI: 10.5772/9846

[3] Alden CB, Wright RJ, Coburn SC, Caputi D, Wendland G, Rybchuk A, et al. Temporal variability of emissions revealed by continuous, long-term monitoring of an underground natural gas storage facility. Environmental Science and Technology. 2020;**54**(22):14589-14597

[4] Wegrzyn J, Gurevich M. Adsorbent storage of natural gas. Applied Energy. 1996;**55**:71-83

[5] Zhang SY, Talu O, Hayhurst DT. High-pressure adsorption of methane in zeolites NaX, MgX, CaX, SrX and BaX. The Journal of Physical Chemistry. 1991;**95**:1722-1726

[6] MaCgibbon R, Badheka R, Sermon P. Organically-modified silica xerogels for adsorption of CH_4 at 298 K. Journal of Sol-Gel Science and Technology. 2004;**32**:53-56

[7] Rodríguez-Reinoso F, Almansa C, Molina-Sabio M. Contribution to the evaluation of density of methane adsorbed on activated carbon. Journal of Physical Chemistry B. 2005;**109**(43):20227-20231

[8] Menon VC, Komarneni S. Porous adsorbents for vehicular natural gas storage: A review. Journal of Porous Materials. 1998;**5**:43-58

[9] Pfeifer P, Ehrburger-Dolle F, Rieker T, González M, Hoffman W, Molina-Sabio M, et al. Nearly space-filling fractal networks of carbon nanopores. Physical Review Letters. 2002;**88**:115502

[10] Im JS, Jung MJ, Lee YS. Effects of fluorination modification on pore size controlled electrospun activated carbon fibers for high capacity methane storage. Journal of Colloid and Interface Science. 2009;**339**(1):31-35

[11] Tsivadze AY, Aksyutin OE, Ishkov AG, Men'shchikov IE, Fomkin AA, Shkolin AV, et al. Porous carbon-based adsorption systems for natural gas (methane) storage. Russian Chemical Reviews. 2018;**87**(10):950-983

[12] Kowalczyk P, Solarz L, Do DD, Samborski A, MacElroy JMD. Nanoscale tubular vessels for storage of methane at ambient temperatures. Langmuir. 2006;**22**(21):9035-9040

[13] Yang CM, Noguchi H, Murata K, Yudasaka M, Hashimoto A, Iijima S, et al. Highly ultramicroporous single-walled carbon nanohorn assemblies. Advanced Materials. 2005;**17**(7):866-870

[14] Kaneko K, Rodríguez-Reinoso F. Nanoporous Materials for Gas Storage. Berlin, Germany: Springer; 2019

[15] Kumar KV, Preuss K, Titirici MM, Rodríguez-Reinoso F. Nanoporous materials for the onboard storage of natural gas. Chemical Reviews. 2017;**117**(3):1796-1825

[16] Casco ME, Martínez-Escandell M, Gadea-Ramos E, Kaneko K, Silvestre-Albero J, Rodríguez-Reinoso F. High-pressure methane storage in porous materials: Are carbon materials in the pole position? Chemistry of Materials. 2015;**27**(3):959-964

[17] Chen S, Gong H, Dindoruk B, He J, Bao Z. Dense carbon nanoflower pellets for methane storage. ACS Applied Nano Materials. 2020;**3**(8):8278-8285

[18] Yue L, Xia Q, Wang L, Wang L, DaCosta H, Yang J, et al. CO_2 adsorption at nitrogen-doped carbons prepared by K_2CO_3 activation of urea-modified coconut shell. Journal of Colloid and Interface Science. 2018;**511**:259-267

[19] Qiu Z, Wang Y, Bi X, Zhou T, Zhou J, Zhao J, et al. Biochar-based carbons with hierarchical micro-meso-macro porosity for high rate and long cycle life supercapacitors. Journal of Power Sources. 2018;**376**:82-90

[20] Fasakin O, Dangbegnon JK, Momodu DY, Madito MJ, Oyedotun KO, Eleruja MA, et al. Synthesis and characterization of porous carbon derived from activated banana peels with hierarchical porosity for improved electrochemical performance. Electrochimica Acta. 2018;**262**:187-196

[21] Rana M, Subramani K, Sathish M, Gautam UK. Soya derived heteroatom doped carbon as a promising platform for oxygen reduction, supercapacitor and CO_2 capture. Carbon. 2017;**114**:679-689

[22] Li B, Xiong H, Xiao Y. Progress on synthesis and applications of porous carbon materials. International Journal of Electrochemical Science. 2020;**15**(2):1363-1377

[23] Liang C, Bao J, Li C, Huang H, Chen C, Lou Y, et al. One-dimensional hierarchically porous carbon from biomass with high capacitance as supercapacitor materials. Microporous and Mesoporous Materials. 2017;**251**:77-82

[24] Wu Z, Wee V, Ma X, Zhao D. Adsorbed natural gas storage for onboard applications. Advanced Sustainable Systems. 2021;**5**(4):1-16

[25] Yorgun S, Yildiz D. Preparation and characterization of activated carbons from Paulownia wood by chemical activation with H_3PO_4. Journal of the Taiwan Institute of Chemical Engineers. 2015;**53**:122-131

[26] Zhang L, Wang J, Shang N, Gao S, Gao Y, Wang C. Ultra dispersed cobalt anchored on nitrogen-doping ordered porous carbon as an efficient transfer hydrogenation catalyst. Applied Surface Science. 2019;**491**:544-552

[27] Du J, Liu L, Yu Y, Zhang Y, Chen A. N-doping carbon sheet and core–shell mesoporous carbon sphere composite for high-performance supercapacitor. Journal of Industrial and Engineering Chemistry. 2019;**76**:450-456

[28] Libbrecht W, Verberckmoes A, Thybaut JW, Van Der Voort P, De Clercq J. Tunable large pore mesoporous carbons for the enhanced adsorption of humic acid. Langmuir. 2017;**33**(27):6769-6777

[29] Chu X, Meng F, Deng T, Zhang W. Metal organic framework derived porous carbon materials excel as an excellent platform for high-performance packaged supercapacitors. Nanoscale. 2021;**13**(11):5570-5593

[30] Tang J, Salunkhe RR, Zhang H, Malgras V, Ahamad T, Alshehri SM, et al. Bimetallic metal-organic frameworks for controlled catalytic graphitization of nanoporous carbons. Scientific Reports. 2016;**6**:3-4

[31] Zhang Y-F, Zhang Z-H, Ritter L, Fang H, Wang Q, Space B, et al. New reticular chemistry of the rod secondary building unit: Synthesis, structure, and natural gas storage of a series of three-way rod amide-functionalized metal–organic frameworks. Journal of the American Chemical Society. 2021;**143**:12202-12211

[32] Yan Y, Kolokolov DI, Da Silva I, Stepanov AG, Blake AJ, Dailly A, et al.

Porous metal-organic polyhedral frameworks with optimal molecular dynamics and pore geometry for methane storage. Journal of the American Chemical Society. 2017;**139**(38):13349-13360

[33] Kirchon A, Feng L, Drake HF, Joseph EA, Zhou HC. From fundamentals to applications: A toolbox for robust and multifunctional MOF materials. Chemical Society Reviews. 2018;**47**(23):8611-8638

[34] Choi PS, Jeong JM, Choi YK, Kim MS, Shin GJ, Park SJ. A review: Methane capture by nanoporous carbon materials for automobiles. Carbon Letters. 2016;**17**(1):18-28

[35] Wang B, Huang H, Lv XL, Xie Y, Li M, Li JR. Tuning CO_2 selective adsorption over N_2 and CH_4 in UiO-67 analogues through ligand function-alization. Inorganic Chemistry. 2014;**53**(17):9254-9259

[36] Chen Z, Li P, Anderson R, Wang X, Zhang X, Robison L, et al. Balancing volumetric and gravimetric uptake in highly porous materials for clean energy. Science. 2020;**368**(6488):297-303

[37] Zheng B, Bai J, Duan J, Wojtas L, Zaworotko MJ. Enhanced CO_2 binding affinity of a high-uptake rht-type. Journal of the American Chemical Society. 2011;**133**:748-751

[38] Mason JA, Veenstra M, Long JR. Evaluating metal-organic framework for natural gas storage. Chemical Science. 2014;**5**:32-35

[39] Guo Z, Wu H, Srinivas G, Zhou Y, Xiang S, Chen Z, et al. A metal-organic framework with optimized open metal sites and pore spaces for high methane storage at room temperature. Angewandte Chemie. International Edition. 2011;**50**(14):3178-3181

[40] Hang H, Deria P, Farha OK, Hupp JT, Snurr RQ. A thermodynamic tank model for studying the effect of higher hydrocarbons on natural gas storage in metal-organic frameworks. Energy and Environmental Science. 2015;**8**(5):1501-1510

[41] Seki K. Design of an adsorbent with an ideal pore structure for methane adsorption using metal complexes. Chemical Communications. 2001;**1**(16):1496-1497

[42] Furukawa H, Ko N, Go YB, Aratani N, Choi SB, Choi E, et al. Ultrahigh porosity in metal-organic frameworks. Science. 2010;**329**(5990): 424-428

[43] Fan W, Zhang X, Kang Z, Liu X, Sun D. Isoreticular chemistry within metal–organic frameworks for gas storage and separation. Coordination Chemistry Reviews. 2021;**443**:213968

[44] Li H, Chen F, Guan X, Li J, Li C, Tang B, et al. Three-dimensional triptycene-based covalent organic frameworks with ceq or acs topology. Journal of the American Chemical Society. 2021;**143**(7):2654-2659

[45] Rubio-Martinez M, Avci-Camur C, Thornton AW, Imaz I, Maspoch D, Hill MR. New synthetic routes towards MOF production at scale. Chemical Society Reviews. 2017;**46**(11):3453-3480

[46] Zhu H, Yang X, Cranston ED, Zhu S. Flexible and porous nanocellulose aerogels with high loadings of metal–organic-framework particles for separations applications. Advanced Materials. 2016;**28**(35):7652-7657

[47] Tagliabue M, Rizzo C, Millini R, Dietzel PDC, Blom R, Zanardi S. Methane storage on CPO-27-Ni pellets. Journal of Porous Materials. 2011;**18**(3):289-296

[48] Bueken B, Van Velthoven N, Willhammar T, Stassin T, Stassen I,

Keen DA, et al. Gel-based morphological design of zirconium metal-organic frameworks. Chemical Science. 2017;**8**(5):3939-3948

[49] Kim H, Samsonenko DG, Das S, Kim GH, Lee HS, Dybtsev DN, et al. Methane sorption and structural characterization of the sorption sites in $Zn_2(bdc)_2(dabco)$ by single crystal x-ray crystallography. Chemistry—An Asian Journal. 2009;**4**(6):886-891

[50] Li H, Wang K, Sun Y, Lollar CT, Li J, Zhou HC. Recent advances in gas storage and separation using metal–organic frameworks. Materials Today. 2018;**21**(2):108-121

[51] Bolinois L, Kundu T, Wang X, Wang Y, Hu Z, Koh K, et al. Breathing-induced new phase transition in an MIL-53(Al)-NH_2 metal-organic framework under high methane pressures. Chemical Communications. 2017;**53**(58):8118-8121

[52] He Y, Chen F, Li B, Qian G, Zhou W, Chen B. Porous metal–organic frameworks for fuel storage. Coordination Chemistry Reviews. 2018;**373**:167-198

[53] Côté AP, Benin AI, Ockwig NW, O'Keeffe M, Matzger AJ, Yaghi OM. Chemistry: Porous, crystalline, covalent organic frameworks. Science. 2005;**310**(5751):1166-1170

[54] El-Kaderi HM, Hunt JR, Mendoza-Cortés JL, Côté AP, Taylor RE, O'Keeffe M, et al. Designed synthesis of 3D covalent organic frameworks. Science. 2007;**316**(5822):268-272

[55] Mendoza-Cortes JL, Pascal TA, Goddard WA. Design of covalent organic frameworks for methane storage. Journal of Physical Chemistry A. 2011;**115**(47):13852-13857

[56] Chen L, Gong C, Wang X, Dai F, Huang M, Wu X, et al. Substoichiometric 3D covalent organic frameworks based on hexagonal linkers. Journal of the American Chemical Society. 2021;**143**(27):10243-10249

[57] Banerjee T, Haase F, Trenker S, Biswal BP, Savasci G, Duppel V, et al. Sub-stoichiometric 2D covalent organic frameworks from tri- and tetratopic linkers. Nature Communications. 2019;**10**(1):1-10

[58] Xu SQ, Zhan TG, Wen Q, Pang ZF, Zhao X. Diversity of covalent organic frameworks (COFs): A 2D COF containing two kinds of triangular micropores of different sizes. ACS Macro Letters. 2016;**5**(1):99-102

[59] Kang X, Han X, Yuan C, Cheng C, Liu Y, Cui Y. Reticular synthesis of tbo topology covalent organic frameworks. Journal of the American Chemical Society. 2020;**142**(38):16346-16356

[60] Martínez-Abadía M, Strutyński K, Lerma-Berlanga B, Stoppiello CT, Khlobystov AN, Martí-Gastaldo C, et al. π-Interpenetrated 3D covalent organic frameworks from distorted polycyclic aromatic hydrocarbons. Angewandte Chemie. 2021;**133**(18):10029-10034

[61] Nguyen HL, Gropp C, Ma Y, Zhu C, Yaghi OM. 3D covalent organic frameworks selectively crystallized through conformational design. Journal of the American Chemical Society. 2020;**142**(48):20335-20339

Value-Added Products from Natural Gas Using Fermentation Processes: Fermentation of Natural Gas as Valorization Route, Part 1

Maximilian Lackner, David Drew, Valentina Bychkova and Ildar Mustakhimov

Abstract

Methanotrophic bacteria can use methane as their only energy and carbon source, and they can be deployed to manufacture a broad range of value-added materials, from single cell protein (SCP) for feed and food applications over biopolymers such as polyhydroxybutyrate (PHB) to value-added building blocks and chemicals. SCP can replace fish meal and soy for fish (aquacultures), chicken and other feed applications, and also become a replacement of meat after suitable treatment, as a sustainable alternative protein. Polyhydroxyalkanoates (PHA) like PHB are a possible alternative to fossil-based thermoplastics. With ongoing and increasing pressure towards decarbonization in many industries, one can assume that natural gas consumption for combustion will decline. Methanotrophic upgrading of natural gas to valuable products is poised to become a very attractive option for owners of natural gas resources, regardless of whether they are connected to the gas grids. If all required protein, (bio)plastics and chemicals were made from natural gas, only 7, 12, 16–32%, and in total only 35–51%, respectively, of the annual production volume would be required. Also, that volume of methane could be sourced from renewable resources. Scalability will be the decisive factor in the circular and biobased economy transition, and it is methanotrophic fermentation that can close that gap.

Keywords: methanotroph, biopolymers, polyhydroxyalkanoates (PHA), polyhydroxybutyrate (PHB), single cell protein (SCP), value-added chemicals, feed, food, scalability

1. Introduction

While most petrochemicals are made from crude oil, they are also accessible through natural gas or coal. For instance, synthesis gas can be converted to various hydrocarbons through Fischer Tropsch synthesis [1], which was performed on a large scale in economies without access to oil in times of war (Germany) or

Apartheid (South Africa). Over the last 50 years, petrochemicals have seen stronger growth than other materials such as steel or aluminum, because of cheap crude oil and the versatility of the products. It was particularly the plastics that have experienced a tremendous increase in use. The importance of oil and gas for various industries is depicted in **Figure 1**.

As one can see from **Figure 1**, approx. 14% of crude oil (left) and 8% of natural gas (right) are deployed to produce petrochemicals. These are first some standard "base chemicals" or building blocks, from which a huge variety of materials can be derived at low-cost in large quantities.

From natural gas, today chiefly hydrogen, methanol and ammonia are made. Ammonia is used for urea and fertilizer production, for instance. The importance of natural gas as feedstock [3] varies with geography and is shown in **Figure 2**.

The key question, in times of an impending huge energy transition towards renewables, is which trajectory petrochemicals will take in the two or three decades to come, whether crude oil will continue to dominate or whether, e.g., coal or natural gas will be brought in as main feedstocks, or possibly even biomass, in the medium turn. In the long run, i.e., 2050 and beyond, it can be assumed that biomass will have become the dominant feedstock.
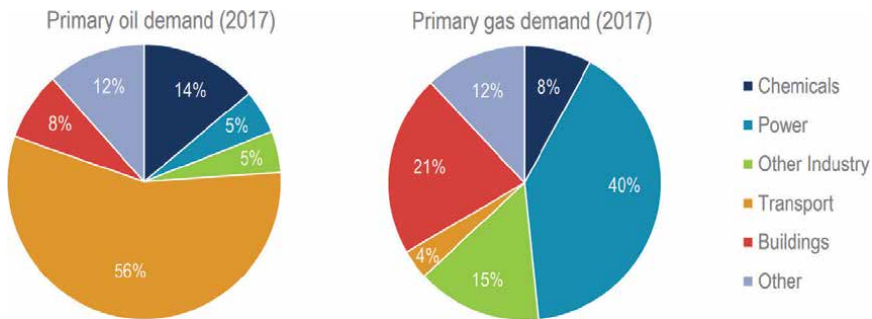
Figure 1.
How crude oil (left) and natural gas (right) are used. Source: [2].
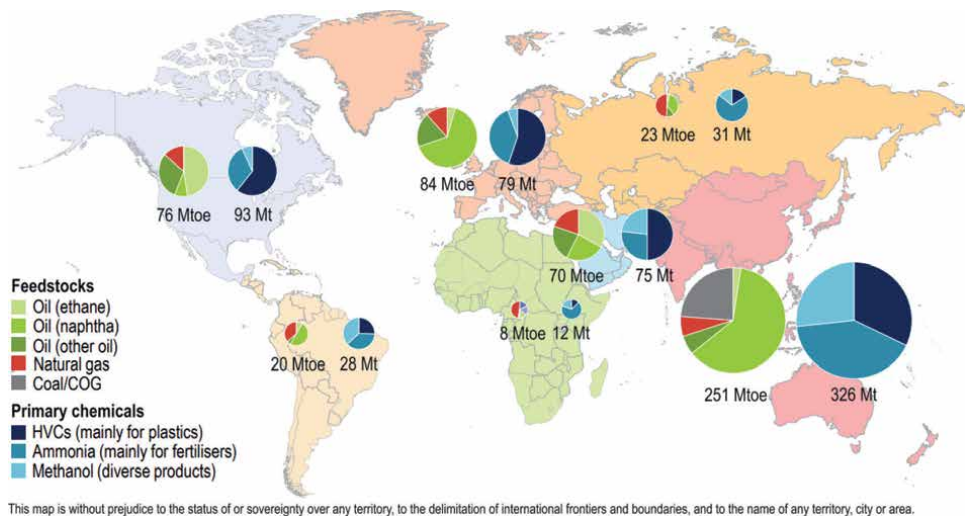
Figure 2.
Feedstocks and primary products. COG = coke oven gas; HVC = high value chemicals; Mtoe = million tons of oil equivalent. Source: [2].
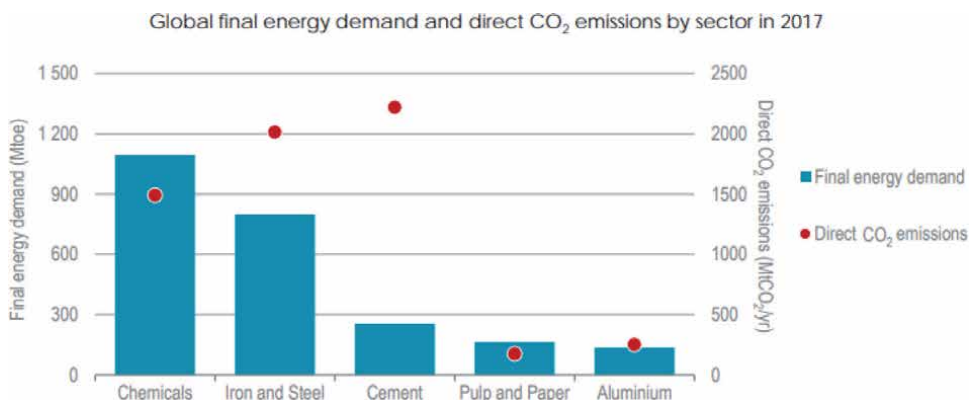
Figure 3.
Source: CO_2 emissions and energy demand for materials in 2017. The final energy demand is given in Mtoe (million tons of oil equivalent). Source: [2].

The world population is growing [4], and industrialization and economic development are moving ahead. Hence, the demand for petrochemicals is bound to further increase. For plastics (thermoplastics), it can be expected that the historic growth rate of ~6%/year will go down significantly, and that more recycling will be implemented. Other products, such as fertilizers, cannot be turned into a circular economy concept as easily as for instance polymers, so with them, demand most probably will continue to rise.

The energy consumption and its source in different industries is another important aspect. Let us take a look at **Figure 3**, the energy demand and the CO_2 emissions (footprint) of 5 vital sectors.

Iron and steel, as well as cement, today are very carbon-intense industries, due to the processes which are being used. Global cement production consumes on the order of 6% of global primary energy demand, mainly by combustion of fossil fuels in the rotary kiln reactors and due to the large production volumes on the order of
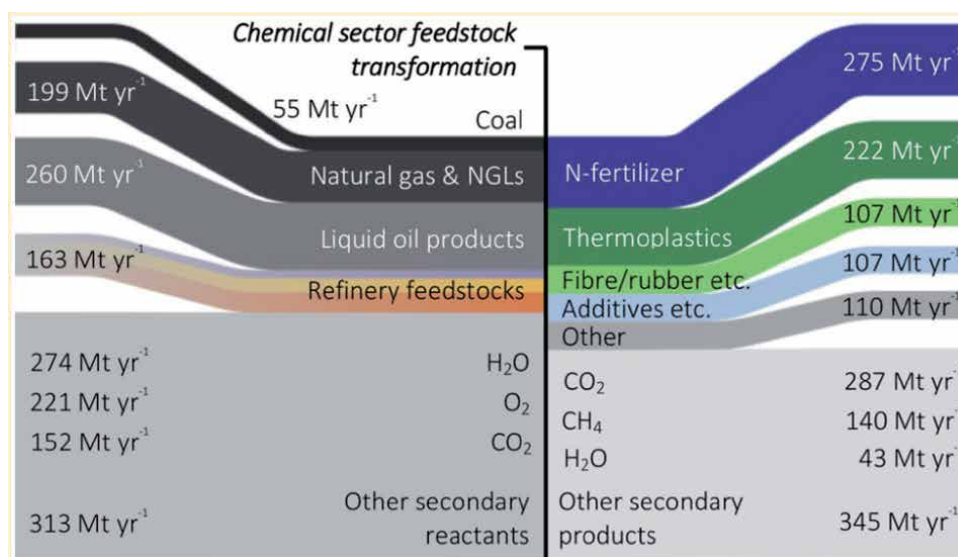
Figure 4.
Part of a Sankey diagram in the chemical sector: Approx. 200 million tons/year of natural gas and NGL (natural gas liquids) are converted into NH_3 (which is then processed to fertilizer) and other products. Source: [6].

4.1 billion tons/year [5]. Iron and steel still rely to a large extent of the blast furnace, being fuelled by coke, but less carbon-emitting reducing agents are being tested and implemented, such as CH_4 or H_2, as well as more electric arc furnaces particularly for the increasing share of recycled steel (scrap smelting). Chemicals account for significant energy demand, too, from various processes. **Figure 4** looks at the mass flow in the chemical sector.

As **Figure 4** shows, coal plays a minor role today, and crude oil dominates. Natural gas has a significant share, though. Decarbonization by moving to a less carbon-intense feedstock such as CH_4 will be a key driver in the industry in the decades to come. Natural gas is less carbon-intense than crude oil and coal, so one might see more natural gas conversion to chemicals.

1.1 Natural gas today

Natural gas is an established fossil fuel, with existing infrastructure in many parts of the world. It is considered as a "clean" fuel, which burns without ash or significant soot production, and releases less CO_2 per unit of energy delivered than do oil-derived fuels or particularly coal-based heating materials. The main constituent of natural gas, methane (CH_4), can also be sourced and be distributed through the grid from alternative sources such as landfills ("landfill gas") or anaerobic digestion facilities ("biogas"). There is also a strong link towards renewables, though the option of storing (excess) wind energy or (excess) photovoltaic energy in the huge natural gas network under the P2G (power2gas) [7] concept, as hydrogen or as methane (which can be made from H_2 in the Sabatier process). The market size of natural gas is on the order of 1000 billion USD per year, and it amounts to approx. 4000 billion m^3/year [8]. 24% of the global energy mix comes from natural gas, which is double the contribution from renewables today. For electricity, the share of natural gas is even higher, where it lies at 55.7% (and at 38.1% for renewables, for comparison). Almost all countries rely on natural gas to some extent. It is the UAE, Russia, Iran, Qatar, Oman and Algeria that are gas-based economies [9]. Methane emissions from industrial operations (production, distribution and use) have lately been identified as a significant and previously underestimated contribution to climate change, and can be addressed by organizational and technological means, see later.

Pipeline transport offers the lowest unit cost for short distances for natural gas. Other methods exist, too, e.g., LNG (liquefied natural gas) [10], particularly for economic long-haul transportation.

1.2 Projection on natural gas utilization

The IEA World Energy Outlook [9] is an authoritative reference work, updated annually to provide trustful projections of global energy developments. According to the latest 2021 report by IEA (WEO-2021), the natural gas demand is believed to increase over the next 5 years, which is the case for all scenarios considered. After that period, one can see sharp divergences in the different scenarios. The report states that *"Today, natural gas is the largest source of electricity in advanced economies and its level of use remains broadly stable in those economies over the next decade, while it increases by about one-third in the emerging market and developing economies, helping to moderate the use of coal"*, according to IEA [9]. **Figure 5** shows the scenarios.

For their latest report WEO-2021, IEA has modeled four scenarios:

• Announced Pledges Scenario (APS)

• Net Zero Emissions by 2050 Scenario (NZE)
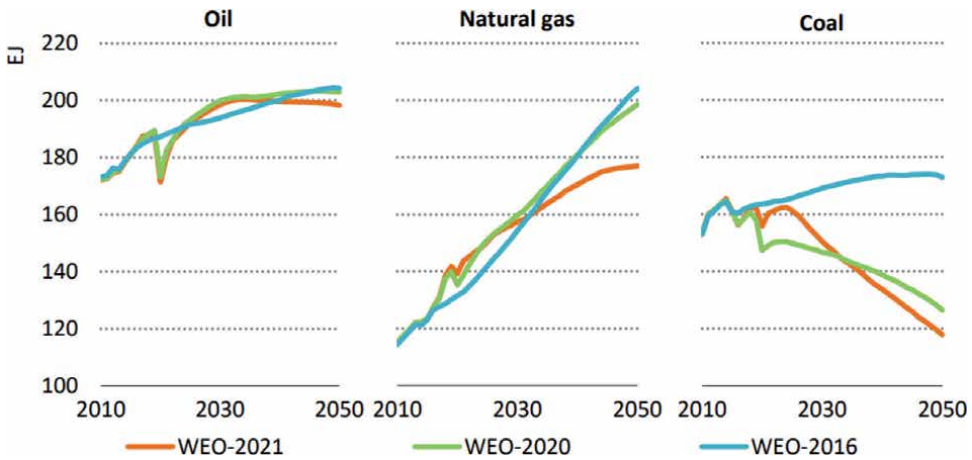
Figure 5.
Demand for oil, natural gas and coal according to IEA, in the STEPS (stated policies scenario) in the reports of 2016 (blue), 2020 (green) and 2021 (red). One can see that the new report is much less in favor of fossil fuels than previous projections. Source: [9].

• Stated Policies Scenario (STEPS)

• Sustainable Development Scenario (SDS)

"The NZE is normative, in that it is designed to achieve specific outcomes – an emissions trajectory consistent with limiting the global temperature rise to 1.5 °C without a temperature overshoot (with a 50% probability), universal access to modern energy services and major improvements in air quality – and shows a pathway to reach it. APS and STEPS are exploratory, in that they define a set of starting conditions, such as policies and targets, and then see where they lead based on model representations of energy systems, including market dynamics and technological progress. The SDS is also normative, mapping out a pathway consistent with the "well below 2 °C" goal of the Paris Agreement, while achieving universal access and improving air quality" [11].

The historic price development of the fossil fuels natural gas, coal and oil is depicted in **Figure 6** [9].
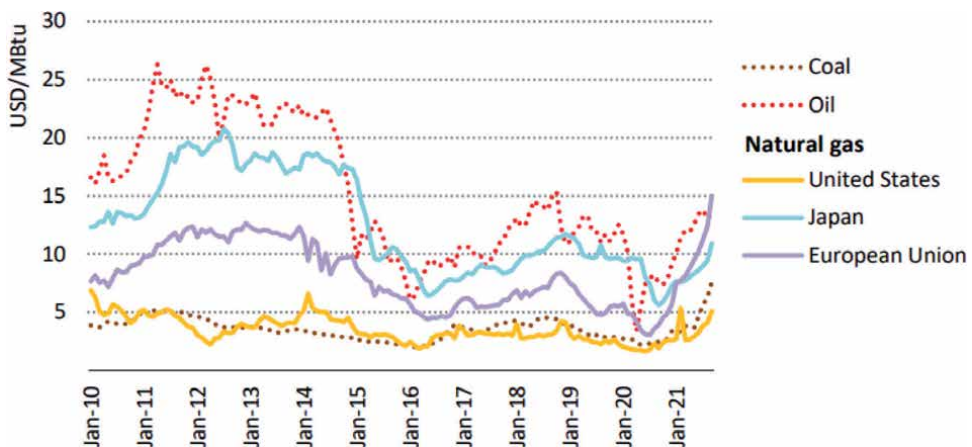
Figure 6.
Regional oil, coal and natural gas prices from 2010 to 2021. MBtu = million British thermal units. Source: [9].

One can infer from **Figure 6** that natural gas is less volatile than oil, and can be on the lowest unit costs level.

In the STEPS scenario, the demand for natural gas will increase to approx. 4500 billion m^3 by 2030 (which is 15% higher than in 2020) and to 5100 billion m^3 in 2050. According to IEA, there will be a rise in natural gas utilization both in industry and in the power sector, and it will remain the standard for space heating.

By contrast, the APS scenario predicts a peak of natural gas use shortly after 2025, followed by a decrease to 3850 billion m^3 by 2050. *"Countries with net zero pledges move away from the use of gas in buildings, and see a near 25% decrease in consumption in the power sector to 2030".*

In the NZE scenario, the demand for natural gas is forecast to drop even more sharply from 2025 onwards and will fall to 1750 billion m^3 in 2050. *"By 2050, more than 50% of natural gas consumed is used to produce low-carbon hydrogen, and 70% of gas use is in facilities equipped with CCUS".* (CCUS = carbon capture, utilisation and storage). Likewise, we can expect more natural gas being deployed for the production of additional materials.

Figure 7 offers a visual depiction of the scenario projections.

An interesting aspect worth noting from **Figure 7** is that biogas is forecast to have a relevant role in all scenarios, on the order of 5% of natural gas volumes, being at ~double the level of 2020 production. It is complemented by hydrogen to various degrees. Natural gas demand changes per scenario are detailed in **Figure 8**.

Only emerging markets and developing economies are expected to use more natural gas, as do industry and hydrogen production. Details on the projected natural gas consumption per region are shown in **Figure 9**.

One can observe from **Figure 9** that in all 3 scenarios, up to 2050, natural gas use in Europe will decline.

Table 1 shows the remaining natural gas resources in terms of "technically recoverable natural gas".

As **Table 1** demonstrates, it is in the Middle East and Eurasia where most of the proven reserves of natural gas are sitting. All regions have significant proven reserves and even more resources, so that availability is not the determining factor for natural gas use but rather other factors such as climate change considerations.
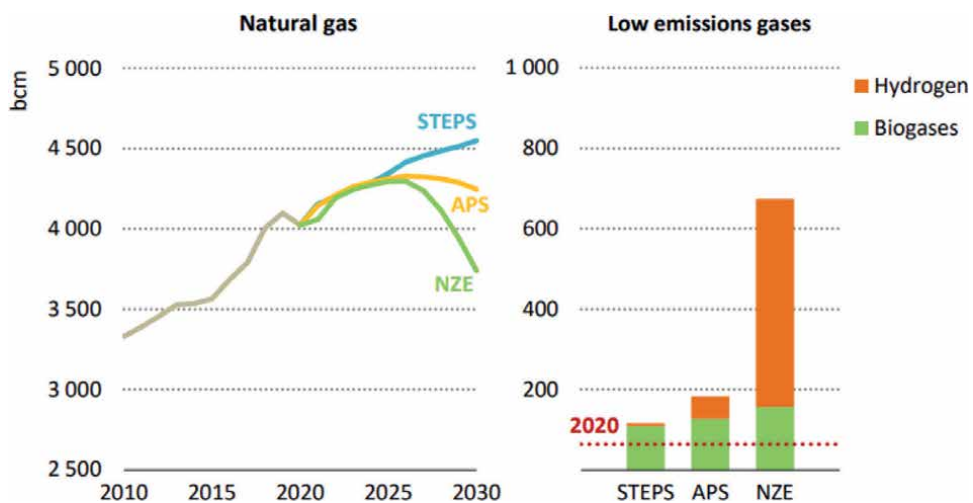
Figure 7.
Left: Timeline of natural gas use; right: Supply of low emissions gasses in 2030. Bcm = billion m³. Note: Hydrogen gases are inclusive of low-carbon gaseous hydrogen and synthetic methane with 1 EJ = 29 bcm. Source: [9].
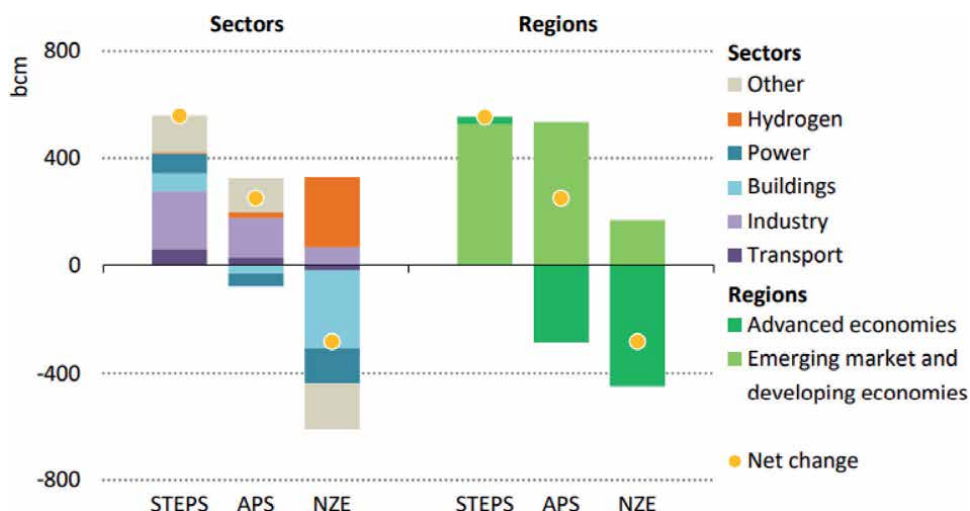
Figure 8.
Development of natural gas demand from 2020 to 2030. Bcm = billion m³. Source: [9].
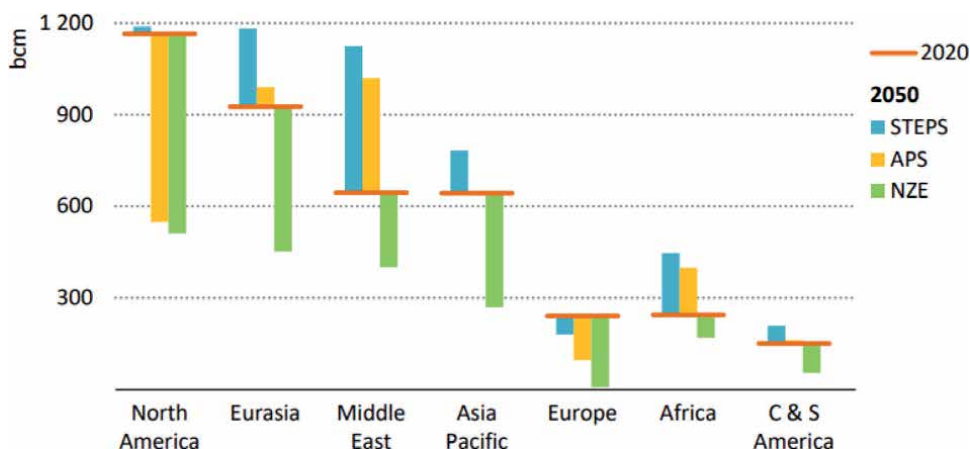
Figure 9.
How natural gas production is expected to change by region and scenario from 2020 to 2050. Bcm = billion m³; C & S America = central and South America. Source: [9].

Natural gas (trillion m³)	Proven reserves	Resources	Conventional gas	Tight gas	Shale gas	Coalbed methane
North America	17	149	50	10	81	7
Central and South America	8	84	28	15	41	—
Europe	5	46	18	5	18	5
Africa	19	101	51	10	40	0
Middle East	81	121	101	9	11	—
Eurasia	70	169	131	10	10	17
Asia Pacific	21	139	45	21	53	2ß
World	**221**	**809**	**425**	**80**	**253**	**49**

Table 1.
The remaining "technically recoverable" resources of natural gas. Source: [9].

1.3 Methane emissions from the gas industry

The debate of climate change has shifted from merely considering CO_2 to also methane, where a significant fraction of the emissions is associated with oil and gas production. These methane emissions can reduce or even completely offset the greenhouse gas benefits of using gas instead of the more carbon-intense fuels coal and **oil.** The "2021 Oil & Gas Benchmarking Report "[12] with a focus on the USA reads: *"EPA-estimated methane emissions from crude oil and refined oil product systems decreased 28% from 1990 to 2015. However, emissions estimates remain uncertain"* [13], see also **Figure 10**.
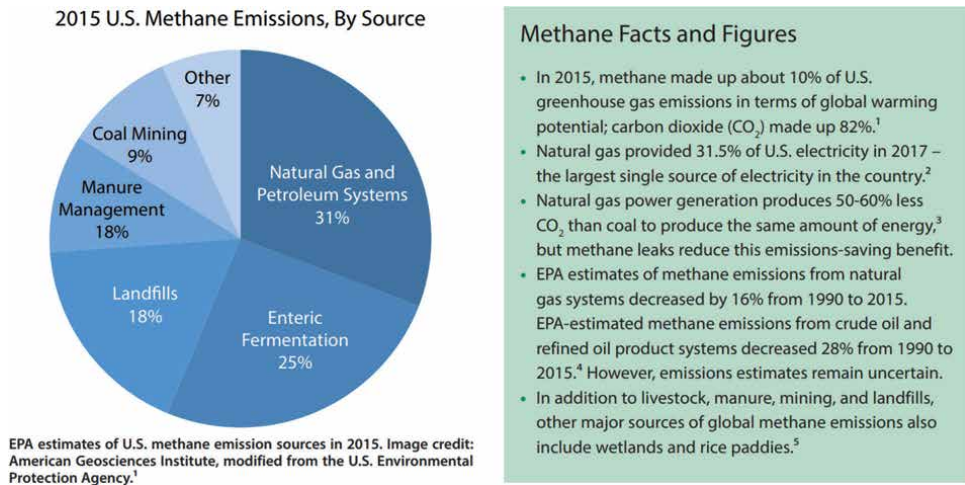
Figure 10.
Sources of methane emissions in the USA in 2015, as estimated by the Environmental Protection Agency (EPA). Source: [13].
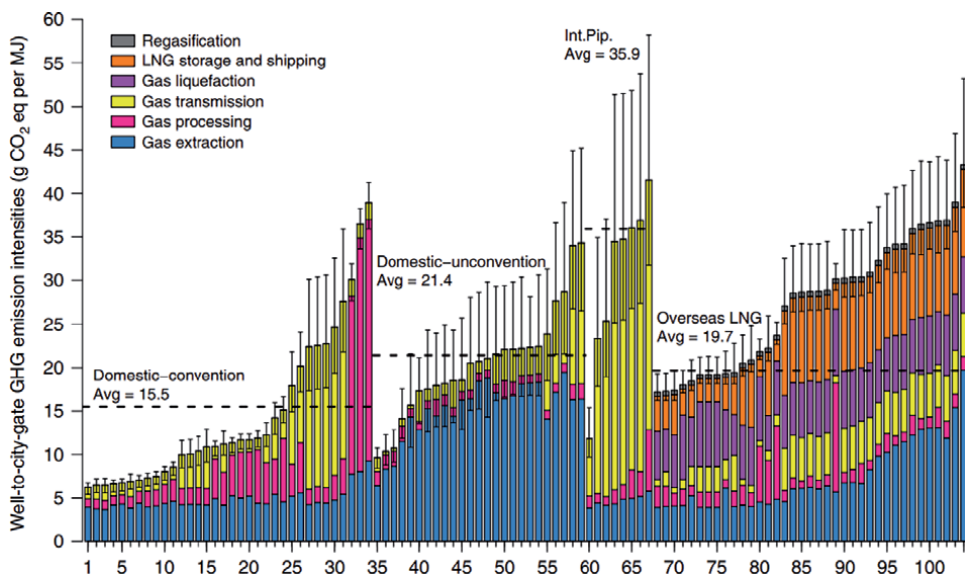
Figure 11.
"Well-to-city-gate" greenhouse gas intensities of natural gas supplies to China from >100 different fields. In the depiction, the colors represent emissions by individual processes. The confidence intervals are 90% (error bars). X-axis: Number of gas field; Y-axis: kg of CO_2 equivalent per MJ [14].

In the US, it is estimated that enteric fermentation, e.g., from cattle, accounts for ¼ of anthropogenic methane emissions. Landfills are responsible for 1/5 of the emissions, on the same level as manure. Approx. 1/3 of man-made methane emissions are attributed to natural gas and petroleum systems, with high uncertainty (and recent evidence that this fraction will be higher).

Recent work has assessed the well-to-city-gate greenhouse gas intensities of natural gas in a Chinese setting, see **Figure 11**.

We can see from that study that there are huge differences in the negative climate effects of natural gas. Domestic natural gas from domestic sources is slightly better, on average, than overseas LNG, but can be a factor of 10 better than international pipeline-derived natural gas. Natural gas can be lost in pumping stations or at the end user, e.g., as unburnt fuel, which all adds up to the radiative forcing.

1.4 The future of natural gas

The world is hungry for energy. On the one hand, there is a need for cheap and increasing energy, on the other hand, fossil fuels are seeing more and more resistance, and the energy sector has started its transformation.

"Industry discussions about the future of gas in North America are polarizing. On [the] one hand, the shale revolution keeps delivering, displacing liquefied natural gas (LNG) imports since the late 2000s, as abundant gas resources and technological innovation drove costs down... On the other hand, as state-level decarbonization policies ramp up, the demand for natural gas in key segments such as power generation and local distribution companies (LDC) is expected to decline" [15].

Natural gas can bring supply and demand of electricity into balance, by fuelling dispatchable on-demand power generation (as huge energy storage devices are lacking). There will probably be more volatility in demand for that natural gas with an increasing share of wind power and photovoltaics, which are difficult to predict in their actual production and which cannot be tuned to demand. Also, it is not yet clear how fast and how effectively the gas industry can curb its fugitive methane emissions, and which policies different countries will enact.

In any case, we are on a path of decarbonization, and times have become unsecure for natural gas owners and industry incumbents. This is not a convenient situation, and energy-related investments are typically characterized by very long (several decades) investment times.

In the near future, we might see

- natural gas to replace the carbon-intense coal

- more co-generation and possibly polygeneration

- more use of methane as feedstock for chemicals

- more coal gasification and biomass gasification to produce chemicals (due to the price volatility of natural gas)

- SNG (synthetic natural gas) [16], where coal, waste or biomass is the feedstock

- more combinations with carbon capture and storage [17]

What can be taken for granted, owners of natural gas will be more inclined to produce value-added materials from natural gas, rather than betting on their resource being continuously used as fuel in the next decades.

Also, owners of natural gas resources that have not yet been connected to the grid might turn towards materials production, as the corresponding production plants can be economic also at smaller scale than mere natural gas extraction for energy. Depending on the value of the products, units of 10,000 tons/year of materials or less can be viable. In the transition to the bioeconomy, biorefineries face the challenge of scalability. Larger scale translates into lower unit costs, however, at the same time, raw material transport over longer distances will increase the costs, so the optimum scale is narrower than with a natural-gas operated plant.

What's more, there has been a strong technology push for gas fermentation technology from biogas gasification (to synthesis gas), which generates technology spill-over potential for natural gas fermentation. Biogas production by anaerobic digestion of various substrates [18] is an established technology.

These 3 aspects make natural gas fermentation a highly attractive route for methane valorization.

2. Natural gas fermentation to value-added products

Fermentation processes are ubiquitous in nature. They can be aerobic (see e.g. [19, 20] for methane) or anaerobic (see e.g. [21–24] for methane) and they have been used by mankind for thousands of years [25–27]. Methane is produced by anerobic fermentation, as it is well known from and deployed in biogas plants [28] or happening in landfills [29]. Also, methane is released from waste-water treatment plants, manure storage pits, ruminants (e.g., cattle) or natural soil such as wetlands. It is in these habitats where also methane-consuming microorganisms, so-called methanotrophic bacteria [30–33] can be found. They can be isolated [34] and be deployed for various target products. The methanome contains methanogenic and methanotrophic bacteria. Basically, methanotrophs are found in all habitats where methane is available [30, 35]. However, methane-oxidizing bacteria only constitute a fraction of the microbial community in most soils, in general <4% of all bacteria [36]. Anaerobic methane fermentation constitutes an important process in the deep subsurface, e.g., in marine sediments [37], as a biogeochemical process that limits the release of methane into the atmosphere. For industrial use, aerobic methanotrophs are more relevant. There are also other bacteria which feed on (higher) hydrocarbons, e.g., as they are found in contaminated land [38].

Methanotrophic bacteria (methanotrophs, methane-oxidizing bacteria (MOB)) [39] belong to the wider "methylotrophic" group that subsumes microorganisms which can use C_1 substrates like methane or methanol [32, 40, 41]. Methane is found in nature; In the atmosphere, its concentration is slightly below 2 ppm. Biogenic methane is emitted from rice fields, various wetlands, termites and herbivores. Also, methanogenic archaea liberate methane from organic matter decomposition [42]. Aerobic methanotrophs are estimated to consume 10–90% of the methane that comes out of the deep anoxic layers of wetlands before it reaches the atmosphere [43], hence they have a strong impact on the climate, as methane is a very potent greenhouse gas with a greenhouse warming potential (GWP) of 24 relative to CO_2 [44].

Said methanotrophs are gram-negative bacteria that use methane as their only source of carbon and energy [31], making them unique and interesting for biotechnological applications. Apart from being hosts for biotechnological production with native and engineered microorganisms in industry, they could be used for geoengineering purposes to fight global warming by methane, e.g., from thawing permafrost soil, fugitive anthropogenic emissions or direct air capturing of methane. Methanotrophs have also been described to co-metabolize toxic compounds [31]. **Table 2** lists several methane-utilizing bacteria.

Methylomonas methanica	*Methylococcus capsulatus*	*Methylococcus vinelandii*
Methylomonas carbonatophila	*Methylococcus capsulatus strain Bath*	*Methylosinus sporium*
Methylomonas rubrum	*Methylococcus ucrainicus*	*Methylosinus trichosporium*
Methylomonas rosaceus	*Methylococcus fulvus*	*Methylosinus trichosporium TG*
Methylomonas agile	*Methylococcus thermophilus*	*Methylocystis parvus*
Methylomonas albus	*Methylococcus albus*	*Methylobacterium organophilum*
Methylomonas streptobacterium	*Methylococcus minimus*	*Mycobacterium methanicum*
Methylomonas methanooxidans	*Methylococcus luteus*	*Mycobacterium cuneatum*
Methylomonas methanitrificans	*Methylococcus bovis*	*Nocardia rhodochrous*
Pseudomonas strain L-8	*Methylococcus chroococcus*	*Nocardia ucrainica*
Pseudomonas strain L-47	*Methylococcus whittenburii*	*Rhodopseudomonas gelatinosa*
Pseudomonas strain L-49		*Strain TM-10*

Table 2.
Selection of methane-oxidizing bacteria. Source: [45].

Methanotrophs are an important biological sink for methane, and thereby are very relevant for the global carbon cycle [46]. The very first methanotrophic bacterium, *bacillus methanicum*, was discovered in the year 1906. To date, more than 100 different methanotrophs are known. Aerobic methanotrophs comprise >20 [47] recognized genera that belong to three major phylogenetic groups (type I, type II and type X). That classification is done on the microorganisms' characteristics such as morphology or carbon assimilation pathways [31]. Apart from the described bacteria, also some yeasts were found to feed on methane [48–50].

2.1 Motivation for microbial methane fermentation

Biocatalytic conversion of methane [51] is a promising route for both commodities and for specialty materials. There is consensus on the need for alternative proteins other than meat. Projections say that alternatives for meat can account for up to 60% of the market in 2040 [52]. Also, there is significant consumer interest in such alternatives [53].

Agriculturally-produced alt protein, e.g., from peas or soy, is one option, non-crop-based proteins are another one. However, there are significant cost hurdles when non-agricultural protein is to be made. For insect protein [54], the price (2021 level) is between 4250 and 6066 USD/ton [55]. Single cell protein (SCP) from side streams of lignocellulose was estimated at requiring a minimum selling price of 5160–9007 €/ton to be economically viable [56]. A ubiquitous raw material is methane, but its use is not straightforward either; one of the most invidious molecules for the organic chemist is CO_2. Almost next in line comes CH_4. One requires 438.8 kJ/mol [30] to activate the C━H bond. As a result, thermochemical processes with methane are energy-intensive, requiring high temperatures and pressures, and/or costly catalysts, see **Table 3**.

By contrast, biocatalysts operate at mild conditions. Also, their carbon conversion efficiency tends to be higher. Therefore, biotechnological methane oxidation using methanotrophic bacteria offers an interesting route.

2.2 Methanotroph product range and cultivation

When we look at the products accessible through methanotrophic bacteria, wild types can be used to obtain compounds from the natural microorganisms' metabolic pathways. Generic engineering allows to expand that range, see **Figure 12**.

	Catalyst	Pressure [atm]	Temperature [°C]	Oxidant	Methane conversion [%]
Chemical conversion	Hg(II)	—	180	O_2	50
	Au + additives (H_2SeO_4/ SeO_4/O_2)	27 bar	180	SO_3	3–28
	$PMo_{11}V$	1 atm	700–750	O_2	3–13
	$PMo_{11}Fe$				4–23
	$SiMo_{11}Fe$				4–32
	ZSM-5	30.5 bar	50	H_2O_2	0.3
Bioconversion	*M. trichosporium OB3b*	1	30	O_2	64
	Methanotrophic consortium	1	30	O_2	43–80
	M. trichosporium OB3b	1	30	O_2	73.8–75.2

Table 3.
Comparison of process conditions and carbon conversion efficiencies of chemical and biochemical catalysts. Source: [30].
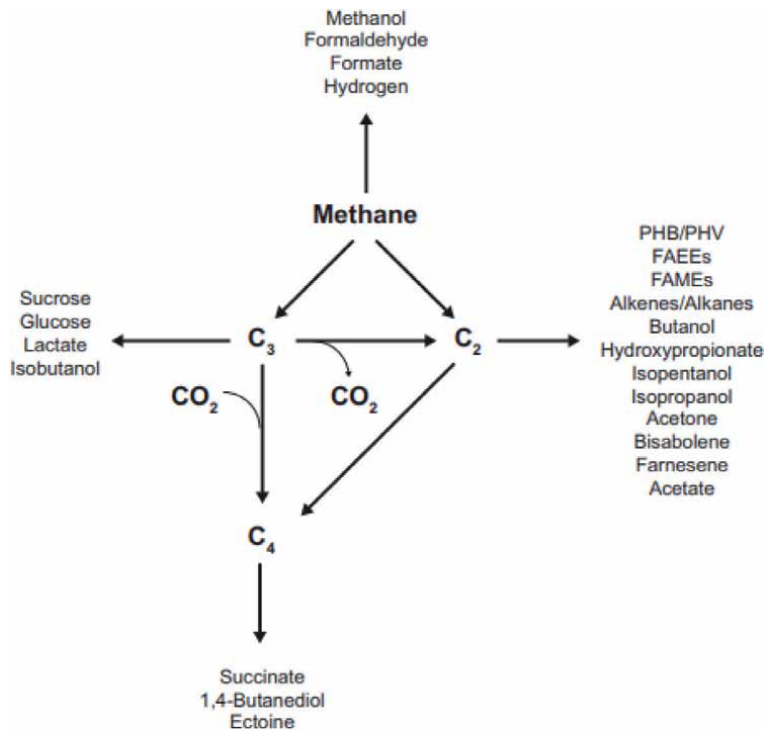
Figure 12.
Potential fuels and chemicals accessible through methane fermentation. Methanotrophic bacteria can generate all relevant 1-, 2- and 3-carbon intermediate compounds. "Virtually all biosynthetic modules for the production of advanced fuels or chemicals, developed for glucose-based fermentation in E. coli, could potentially be implemented in methane-utilizing strains". PHB = polyhydroxybutyrate; PHV = polyhydroxyvalerate; FAEEs = fatty acid ethyl esters; FAMEs = fatty acid methyl esters; source: [57].

Genetic engineering is useful when the target products are chemicals. Obtaining approval for feed and food made with GMO (genetically modified organisms) will be significantly harder and is therefore discouraged. To date, most metabolic engineering was achieved with type I methanotrophs [58]. Synthetic methanotrophs [59, 60] offer

the potential for improved product range, yields and productivities [61]. Recently, the engineering of type II methanotrophs to produce 3-hydroxypropionic acid (3-HP), cadaverine and lysine [62–64] was reported. They are of particularly interest, because type II methanotrophs (e.g., *M. trichosporium OB3b*) can co-metabolize methane and CO_2 [58]. Also, they were described to consume C_1, C_2 and C_3 compounds and to be able to fix nitrogen [58]. Whilst most methanotrophs are mesophiles, extremophile methanotrophs are known, e.g., alkaliphiles, acidophiles, thermophiles [65], psychrophiles (cryophiles) and halophiles [31]. Obligate methanotrophs (most known methanotrophs) can only use methane as their carbon source, whereas the limited facultative ones (*Methylocapsa aurea*, *Methylocystis spp.*) can also grow on acetate and ethanol. Facultative methanotrophs (*Methylocella silvestris*) are also able to utilize higher hydrocarbons. *Methylocella silvestris* was found to consume acetone, acetol, 2-propanol, 1,2-propanediol, methylacetate, glycerol, gluconate, propionate, tetrahydrofurane, ethane and propane [66].

Methanotrophs were shown to produce methanol, ectoine [67], polyhydroxy butyrate (PHB, more specifically P3HB), 2,3-butanediol, single cell protein (SCP) [68], carotenoids, vitamin B12 [69] and lactic acid [47, 70]. Basically, production can be intracellularly or extracellularly, where the latter offers advantages in downstream processing through avoided need for cell lysis, provided that no cell inhibition [71] occurs by the excreted compounds as was shown e.g., for methanol.

For methane-utilizing *Pseudomoms sp.*, it was found that *Hyphomicrobium sp.*, when added to a mixed culture fermentation regime, could eliminate any inhibitory methanol [72].

Methanol may be used as biofuel [73]. It can be burnt directly, be used in fuel cells or utilized for transesterification of various plant oils to fatty acid methyl esters (FAME, aka biodiesel).

The methanotrophs, when deployed in a bioreactor, are typically grown as free cells. Using immobilized cells was found to increase productivity [74, 75] for methanol.

Production can be carried out with pure cultures or with mixed cultures [76–78] with the latter being more robust for industrial production, e.g., of single cell protein (SCP) [72, 79, 80].

In [81] a mixed culture of type I methanotrophs that had been obtained from waste activated sludge was tested. The key genera were *Methylococcus, Methylobacter, Methaylocaldum, Methylomicrobium, Methylomonas, Methylosarcina and Methylosphaera*. The maximum specific growth rate (μ_{max}) was determined as 0.358 h^{-1} (8.59 per day), and the maximum specific methane biodegradation rate (q_{max}) was 14.52 g CH_4 per total g(DCW) and per hour reported in mixed cultures (DCW = dry cell weight).

In [72], a culture of *Pseudomonas sp.* and *Hyphomicrobium sp.* could be stabilized by the addition of *Acinetobacter sp.* and/or *Flavobacterium sp*.

Co-cultures of methanotrophs have been described, too, e.g., the syntrophic co-culturing of a methanotroph and heterotroph to obtain mevalonate from methane [82]. Syntrophy (symbiosis) describes a system where one species lives off the products of another one. *M. capsulatus bath* was combined with *E. coli SBA01* in that study. Mevalonic acid (MVA) is a precursor molecule for terpenes and steroids. In another study, co-culturing methanotrophs with microalgae was suggested [83, 84], or with hydrogen-oxidizing bacteria [85].

Many industrial fermentation processes rely on (sterile) monocultures. However, one has to bear in mind that in nature, mixed cultures are the norm. For traditional fermentation processes such as cheese, yoghurt, soy sauce and sauerkraut, it has also been mixed cultures that have been used.

Harrison [78] coined the term of "structured mixed cultures" to describe cultures which were obtained by a combination of well-defined microorganisms

Raw material	Organisms	Benefits of culture
Methane	A methane oxidizer + a methanol-utilizer + a citrate-utilizing bacterium	High stability
Methane	*Pseudomonas sp.* + *Hyphomicrobium sp.* + *Flavobacterium sp.* + *Acinetobacter sp.*	Removal of the toxic methanol-inhibiting growth of *Pseudomonas sp.* and removal of organic byproducts resulting in high stability
Methane	*Methylococcus sp.* NCIB 11083 + *Flavobacterium sp.* NCIB 11282 + *Pseudomonas sp.* NCIB 11309 + *Pseudomonas sp.* NCIB 11310 + *Moraxella sp.* NCIB 11308 + *Nocardia sp.* NCIB 11307	Culture was stable under methane limitation and high concentration of ethane
Methane	*Methylococcus sp,* + *Pseudomonas sp.* NCIB 11310 + *Mycobacterium rhodochrous* NCIB 11307 + *Moraxella sp.* NCIB 11038 + *Pseudomonas sp.* NCIB 11309	High stability, lack of foaming and growth at 45°C
Methane	*Methylococcus ucrainicus* + *Rhodopseudomonas glutinis* + *Methylomonas methanica* + *Pseudomonas fluorescens*	Less inhibition by added amino acids

Table 4.
"structured mixed cultures" and their benefits exemplified. Source: [45].

instead of enriched undefined natural and thus "uncontrolled" mixtures [45]. **Table 4** gives some examples.

The advantages of these "structured" mixed cultures, compared to monocultures, are summarized as follows [45]:

• Improved utilization of a mixture of carbon sources or a complex carbon source.

• Targeted protein composition can be obtained.

Organic carbon that is secreted by one microorganism of the consortium is removed by another one:

a. removal of toxic substances (which can affect the microbiome)

b. Higher total biomass yield from the primary carbon source

c. Elimination of foam

d. Higher growth rate

e. Possibility for water recycling

f. Better tolerance of perturbations

g. Resistance against contamination by fungi, yeasts, bacteria and phages [45].

Picking up the point of extracellular products, these two disadvantages might arise next to inhibition:

Risk for contamination with other microorganisms feeding on these compounds and being unable to utilize the primary substrate. That risk can be alleviated by sterile operation, which however is difficult to maintain over several weeks of

production [45]. Secondly, more effort to purify the fermentation medium for reuse. Therefore, mixed cultures were proposed to avoid the need for aseptic operation with the minor partner removing unwanted compounds from the fermentation broth. Hamer et al. [86] reported an excellent mixed culture. It contained 4 bacteria:

1. *Pseudomonas* sp.—a methane-utilizing Gram-negative bacterium.

2. *Hyphomicrobium* sp.—a bacterium that can grow on methanol, but not on methane.

3. two Gram-negative bacteria, incapable of growth on either methane or methanol, but growing on a broad variety of organic molecules (*Acinetobacter* sp., *Flavobacterium* sp.)

In the EU feed catalog EU No. 68/2013 [87], this mixed culture is listed for protein production from methane:

1. *Methylococcus capsulatus (Bath)* (NCIMB strain 11,132).

2. *Alcaligenes acidovorans* (NCIMB strain 12,387).

3. *Bacillus brevis* (NCIMB strain 13,288).

4. *Bacillus firmus* (NCIMB strain 13,280).

Methylococcus capsulatus [88–90] is the most-studied host for SCP. Other strains are *Pseudomonas methanica* [91]*, Methylosinus trichosporium (OB3B)* [92] and methanotroph *Methylomicrobium buryatense5GB1* [93].

As a feedstock for the fermentation process, pure methane, pure [94] or mixed C_1 feedstock [95], natural gas, biogas or hythane (a mixture of CH_4 and H_2) can be used [96, 97].

While methanotrophs favor CH_4 as their source of carbon and energy, some of them can also use methanol in its absence. *Methylocella tundrae* was found to prefer methanol over methane [98]. Methanol has a better solubility in the growth medium than methane, but is more costly. The Pruteen™ [99] process was based on methanol, and the strain *Methylophilus methylotrophus***.**

All type II methanotrophs, some type I methanotrophs (*Methylococcus, Methylosoma, Methyloglobulus, Methyloprofundus,* and selected strains within *Methyomonas* and *Methylobacter*) can fix atmospheric nitrogen [98]. Therefore, type II methanotrophs are generally dominant under N-limiting conditions or high carbon to nitrogen (C/N) ratios, while type I methanotrophs generally need a high nitrogen content, i.e., lower value of the C/N ratio [98].

Nitrogen addition was found to decrease methane uptake in a natural environment containing methanotrophs and methanogens [100]. For the effect of ammonia on methanotrophs growth, see [101].

Author details

Maximilian Lackner[1]*, David Drew[1], Valentina Bychkova[1] and Ildar Mustakhimov[2]

1 Circe Biotechnologie GmbH, Vienna, Austria

2 Federal Research Center "Pushchino Scientific Center for Biological Research of the Russian Academy of Sciences", G.K. Skryabin Institute of Biochemistry and Physiology of Microorganisms, Russian Academy of Sciences, Moscow Region, Russian Federation

*Address all correspondence to: m.lackner@circe.at

IntechOpen

References

[1] Davis BH, Occelli ML. Fischer-Tropsch Synthesis, Catalysts and Catalysis: Advances and Applications. Boca Raton, Florida, USA: CRC Press LLC; 2016

[2] The Future of Petrochemicals Mechthild Wörsdörfer, Director of Sustainability, Technology and Outlooks IEA 7 December 2018, Brussels—EU Refining Forum, PowerPoint Presentation (europa.eu)

[3] Ren T, Patel MK. Basic petrochemicals from natural gas, coal and biomass: Energy use and CO_2, emissions. Resources, Conservation and Recycling. 2009;**53**:513-528

[4] Available from: https://population.un.org/wpp/

[5] Available from: https://www.statista.com/statistics/1087115/global-cement-production-volume/

[6] Levi PG, Cullen JM. Mapping global flows of chemicals: From fossil fuel feedstocks to chemical products. Environmental Science & Technology. 2018;**52**:1725-1734

[7] Bailera M, Lisbona P, Peña B, Romeo LM, Storage E. Hybridization of Power-to-Gas Technology and Carbon Capture. New York, USA: Springer; 2020. ISBN: 978-303046526

[8] Natural Gas Information—Data product—IEA. Available from: https://www.iea.org/data-and-statistics/data-product/natural-gas-information

[9] World Energy Outlook. 2021. Available from: https://iea.blob.core.windows.net/assets/4ed140c1-c3f3-4fd9-acae-789a4e14a23c/WorldEnergyOutlook2021.pdf

[10] Speight JG. Handbook of Industrial Hydrocarbon Processes. 2nd ed. Houston, Texas, USA: Gulf Professional Publishing; 2019. ISBN: 978-0128099230

[11] Understanding WEO Scenarios. Available from: https://www.iea.org/reports/world-energy-model/understanding-weo-scenarios

[12] Benchmarking Methane and Other GHG Emissions | Ceres. Available from: https://www.ceres.org/resources/reports/benchmarking-methane-and-other-ghg-emissions

[13] Allison E, Mandler B. Methane Emissions in the Oil and Gas Industry, Petroleum and the Environment, Part 19/24. Available from: https://www.americangeosciences.org/sites/default/files/AGI_PE_MethaneEmissions_web_final.pdf

[14] Gan Y, El-Houjeiri HM, Badahdah A, Zifeng L, Cai H, Przesmitzki S, et al. Carbon footprint of global natural gas supplies to China. Nature Communications. 2020;**11**:824. DOI: 10.1038/s41467-020-14606-4

[15] Barth A, Brick J, Dediu D, Tai H. The Future of Natural Gas in North America. McKinsey; 2019. Available from: https://www.mckinsey.com/~/media/mckinsey/industries/electric%20power%20and%20natural%20gas/our%20insights/the%20future%20of%20natural%20gas%20in%20north%20america/the-future-of-natural-gas-in-north-america-final.pdf

[16] Schildhauer TJ, Biollaz SMA. Synthetic Natural Gas: From Coal, Dry Biomass, and Power-to-Gas Applications. Weinheim, Germany: Wiley; 2016. ISBN: 978-1118541814

[17] Siirola JJ. Natural Gas as a Chemical Industry Fuel, and Feedstock: Past, Present, Future, (and Far Future). Kingsport, TN 37662: Eastman

Chemical Company; 2013. Available from: http://egon.cheme.cmu.edu/esi/docs/pdf/SiirolaNaturalGas.pdf

[18] Schulze KL, Naga Raju B. Studies on sludge digestion and methane fermentation: II. Methane Fermentation of Organic Acids, Sewage and Industrial Wastes. 1958;**30**:164-184. DOI: 10.2307/25033539

[19] Stadtman TC. Methane fermentation. Annual Reviews in Microbiology. 1967;**21**(1):121-142

[20] Timmis KN. Handbook of Hydrocarbon and Lipid Microbiology, The Aerobic Methane Oxidizing Bacteria (Methanotrophs). Vol. 363. Heidelberg: Springer; 2010

[21] Switzenbaum MS, Giraldo-Gomez E, Hickey RF. Monitoring of the anaerobic methane fermentation process. Enzyme and Microbial Technology. 1990;**12**(10): 722-730. DOI: 10.1016/0141-0229(90) 90142-D

[22] Ziemiński K, Frąc M. Methane fermentation process as anaerobic digestion of biomass: Transformations, stages and microorganisms. African Journal of Biotechnology. Mar 2012;**11**(18):4127-4139. DOI: 10.5897/AJBX11.054. Available from: http://www.academicjournals.org/AJB

[23] Anaerobic oxidation of methane (AOM) is a crucial bioprocess in global methane mitigation. Adoption of AOM in an engineered system provides an opportunity for the development of methane-based biotechnologies. Energy & Environmental Science. 2021;**14**:4803-4830. DOI: 10.1039/D1EE00708D

[24] Cai C, Zhang X, Mengxiong W, Liu T, Lai C-Y, Frank J, et al. Roles and opportunities for microbial anaerobic oxidation of methane in natural and engineered systems. Energy &

Environmental Science. 2021;**09**:4803-4830. DOI: 10.1039/D1EE00708D

[25] Ray RC, Didier M. Microorganisms and Fermentation of Traditional Foods. Boca Raton, Florida, USA: CRC Press; 2014. ISBN: 9781482223088

[26] McNeil B, Harvey L. Practical Fermentation Technology. Weinheim, Germany: Wiley; 2008. ISBN: 9780470725283

[27] Berenjian A. Essentials in Fermentation Technology. New York, USA: Springer; 2019. ISBN: 978-3-030-16230-6

[28] Balagurusamy N, Chandel AK. Biogas Production: From Anaerobic Digestion to a Sustainable Bioenergy Industry. New York, USA: Springer; 2022. ISBN: 978-3030588298

[29] Rajaram V, Siddiqui FZ, Emran Khan M. From Landfill Gas to Energy: Technologies and Challenges. London, UK: Taylor & Francis Ltd; 2011. ISBN: 978-0415664745

[30] Lee EY. Methanotrophs: Microbiology Fundamentals and Biotechnological Applications, Methanotrophs: Multifunctional Bacteria with Promising Applications in Environmental Bioengineering. New York, USA: Springer; 2020. ISBN: 978-3030232634

[31] Jiang H, Chen Y, Jiang P, Zhang C, Smith TJ, Murrell JC, et al. Biochemical Engineering Journal. 2010;**49**(3): 277-288

[32] Hanson RS, Hanson TE. Methanotrophic bacteria. Microbiological Reviews. 1996;**60**: 439-471. DOI: 10.1128/mmbr.60.2. 439-471.1996

[33] Hanson RS. Murrell JC, Dalton H. Methane and Methanol Utilizers. New York, USA: Springer US; 1992

[34] Meruvu H, Wu H, Fei Q. From nature to nurture: Essence and methods to isolate robust methanotrophic bacteria. Synthetic and Systems Biotechnology. 2020;**5**(3):173-178

[35] Øverland M, Tauson A-H, Shearer K, Skrede A. Evaluation of methane-utilising bacteria products as feed ingredients for monogastric animals. Archives of Animal Nutrition. 2010;**64**(3):171-189. DOI: 10.1080/17450391003691534

[36] Lau E, Ahmad A, Steudler PA, Cavanaugh CM. Molecular characterization of methanotrophic communities in forest soils that consume atmospheric methane. FEMS Microbiology Ecology. 2007;**60**(3):490-500. DOI: 10.1111/j.1574-6941.2007.00308.x

[37] Kotelnikova S. Microbial production and oxidation of methane in deep subsurface. Earth-Science Reviews. 2002;**58**:367-395

[38] Geetha SJ, Joshi SJ, Kathrotiya S. Isolation and characterization of hydrocarbon degrading bacterial isolate from oil contaminated sites. APCBEE Procedia. 2013;**5**:237-241

[39] Higgins IJ, Best DJ, Hammond RC, Scott D. Methane-oxidizing microorganisms. Microbiological Reviews. 1981;**45**(40146-0749/81/040556-35):556-590

[40] Quayle JR. In: van Verseveld HW, Duine JA, editors. Microbial Growth on C1 Compounds: Proceedings of the 5th International Symposium. Dordrecht, Netherlands: Springer Netherlands; 1987

[41] Quayle JR. In: Lidstrom ME, Tabita FR, editors. Microbial Growth on C1 Compounds: Proceedings of the 8th International Symposium on Microbial Growth on C1 Compounds, 27 August–1 September 1995; San Diego, USA. Netherlands: Springer; 1996

[42] Kizilova AK, Sukhacheva MV, Pimenov NV, Yurkov AM, Kravchenko IK. Methane Oxidation Activity and Diversity of Aerobic Methanotrophs in pH-Neutral and Semi-neutral Thermal Springs of the Kunashir Island, Russian Far East, Extremophiles. New York, USA: Springer; 2013. DOI: 10.1007/s00792-013-0603-z

[43] Tikhonova EN, Kravchenko IK. Activity and Diversity of Aerobic Methanotrophs in Thermal Springs of the Russian Far East New and Future Developments in Microbial Biotechnology and Bioengineering. Amsterdam, Netherlands: Elsevier; 2019. DOI: 10.1016/B978-0-444-64191-5.00001-8

[44] Lackner M, Sajjadi B, Chen W-Y. Handbook of Climate Change Mitigation and Adaptation. 3rd ed. New York, USA: Springer; 2022. Available from: https://link.springer.com/book/9783030725785

[45] Goldberg I. Single Cell Protein. New York, USA: Springer; 1985. DOl: 10.1007/978-3-642-46540-6. ISBN: 978-3-642-46542-0

[46] Russell M, Nitschke W. Methane: Fuel or exhaust at the emergence of life? In: Liebert MA, editor. Astrobiology. Vol. 17(10). 2017. pp. 1053-1066. DOI: 10.1089/ast.2016.1599

[47] Kulkarni PP, Khonde VK, Deshpande MS, Sabale TR, Kumbhar PS, Ghosalkar AR. Selection of methanotrophic platform for methanol production using methane and biogas. Journal of Bioscience and Bioengineering. 2021;**132**(5):460-468

[48] Wolf HJ, Hanson RS. Identification of methane-utilizing yeasts. FEMS Microbiology Letters. Feb 1980;**7**(2):

177-179. DOI: 10.1111/j.1574-6941.1980.tb01602.x

[49] Vergara-Fernández A, Morales P, Scott F, Guerrero S, Yañez L, Mau S, et al. Methane biodegradation and enhanced methane solubilization by the filamentous fungi Fusarium solani. Chemosphere. Jul 2019;**226**:24-35

[50] García-Garibay M, Gómez-Ruiz L, Bárzana E. Single cell protein | yeasts and bacteria. In: Batt CA, Tortorello ML, editors. Encyclopedia of Food Microbiology. 2nd ed. Cambridge, Massachusetts, USA: Academic Press; 2014. pp. 431-438

[51] Kasprzycka A, Lalak-Kańczugowska J, Stępień Ł. Biocatalytic conversion of methane—Selected aspects. Current Opinion in Chemical Engineering. 2019;**26**:28-32

[52] AT Kearney expects alternative meats to make up 60% market in 2040. Available from: https://www.thefuturescentre.org/signal/at-kearney-expects-alternative-meats-to-make-up-60-market-in-2040/

[53] Van Loo EJ, Caputo V, Lusk JL. Consumer preferences for farm-raised meat, lab-grown meat, and plant-based meat alternatives: Does information or brand matter? Food Policy. 2020;**95**:101931

[54] van Huis A. Insects as food and feed, a new emerging agricultural sector: A review. Journal of Insects as Food and Feed. 2020;**6**(1):27-44. DOI: 10.3920/JIFF2019.0017 [Published Online: August 27, 2019]

[55] Available from: https://www.feednavigator.com/Article/2021/02/24/Demand-for-insect-protein-could-hit-500-000-tons-by-2030

[56] Voutilainen E, Pihlajaniemi V, Parviainen T. Economic comparison of food protein production with single-cell organisms from lignocellulose side-streams. Bioresource Technology Reports. 2021;**14**(6):100683. DOI: 10.1016/j.biteb.2021.100683

[57] Kalyuzhnaya MG, Puri AW, Lidstrom ME. Metabolic engineering in methanotrophic bacteria. Metabolic Engineering. 2015;**29**:142-152. DOI: 10.1016/j. ymben.2015.03.010

[58] Nguyen DTN, Lee OK, Lee EY. Type II methanotrophs: A promising microbial cell-factory platform for bioconversion of methane to chemicals. Biotechnology Advances. 2021;**47**:107700

[59] Gregory GJ, Bennett RK, Papoutsakis ET. Recent advances toward the bioconversion of methane and methanol in synthetic methylotrophs. Metabolic Engineering. 2022;**71**:99-116

[60] Chen Y-Y, Soma Y, Hori K. Metabolic alteration of *Methylococcus capsulatus* str. Bath during a microbial gas-phase reaction. Bioresource Technology. 2021;**330**:125002

[61] Nguyen AD, Lee EY. Engineered methanotrophy: A sustainable solution for methane-based industrial biomanufacturing, Trends in Biotechnology. 2020;**39**(4):381-396

[62] Nguyen DTN, Lee OK, Lim C, Lee J, Na J-G, Lee EY. Metabolic engineering of type II methanotroph, Methylosinus trichosporium OB3b, for production of 3-hydroxypropionic acid from methane via a malonyl-CoA reductase-dependent pathway. Metabolic Engineering. 2020;**59**:142-150

[63] Nguyen TT, Lee OK, Sanzhar N, Lee EY. Bioconversion of methane to cadaverine and lysine by engineered type II methanotroph, Methylosinus trichosporium OB3b. Green Chemistry. 2020;**22**:7803-7811

[64] Nguyen TT, Lee OK, Naizabekov S, Lee EY. Bioconversion of methane to

cadaverine and lysine using an engineered type II methanotroph, Methylosinus trichosporium OB3b. Green Chemistry. 2020;**22**:7803-7811. DOI: 10.1039/D0GC02232B

[65] McFarland MJ, Jewell WJ. The effect of sulfate reduction on the thermophilic (55°C) methane fermentation process. Journal of Industrial Microbiology & Biotechnology. 1 Jun 1990;**5**(4):247-257. DOI: 10.1007/BF01569682

[66] Dunfield PF, Dedysh SN. Methylocella: A gourmand among methanotrophs. Trends in Microbiology. 2014;**22**(7):368-369

[67] Cantera S, Lebrero R, Muñoz R. Ectoine bio-milking in methanotrophs: A step further towards methane-based bio-refineries into high added-value products. Chemical Engineering Journal. 2017;**328**:44-48

[68] Bewersdorff M, Dostálek M. The use of methane for production of bacterial protein. Biotechnology and Bioengineering. 1971;**13**(1):49-62. DOI: 10.1002/bit.260130104

[69] Yang Y, Zhang Z, Jun L, Maekawa T. Continuous methane fermentation and the production of vitamin B12 in a fixed-bed reactor packed with loofah. Bioresource Technology. 2004;**92**(3):285-290

[70] Gęsicka A, Oleskowicz-Popiel P, Łężyk M. Recent trends in methane to bioproduct conversion by methanotrophs. Biotechnology Advances. 2021;**53**:107861

[71] Czatzkowska M, Harnisz M. Inhibitors of the methane fermentation process with particular emphasis on the microbiological aspect: A review. Energy Science & Engineering. 2020;**8**(5):1880-1897. DOI: 10.1002/ese3.609

[72] Wilkinson TG, Topiwala HH, Hamer G. Interactions in a mixed bacterial population growing on methane in continuous culture. Biotechnology and Bioengineering. 1974;**16**(1):41-59

[73] Agarwal AK, Gautam A, Sharma N, Singh AP, editors. Methanol and the Alternate Fuel Economy. Singapore: Springer Nature; 2019. ISBN: 978-981-13-3286-9. DOI: 10.1007/978-981-13-3287-6

[74] Patel SKS, Gupta RK, Lee J-K. Conversion of biogas to methanol by methanotrophs immobilized on chemically modified chitosan. Bioresource Technology. 2020;**315**:123791

[75] Patel SKS, Kondaveeti S, Lee J-K. Repeated batch methanol production from a simulated biogas mixture using immobilized *Methylocystis bryophila*. Energy. 2017;**145**:477-485

[76] Harrison DEF, Harrison DEF. Proceedings of the Sixth International Fermentation Symposium Held in London, Canada, July 20-25, 1980. Oxford, UK: Pergamon; 1981. pp. 15-21. DOI: 10.1016/B978-0-08-025383-1.50010-2

[77] Harrison DEF. Mixed cultures in industrial fermentation processes. Advances in Applied Microbiology. 1978;**24**:129-164

[78] Harrison DEF. Mixed cultures in industrial fermentation processes. In: Perlman D, editor. Advances in Applied Microbiology. Vol. 24. Dordrecht, Netherlands: Elsevier, Academic Press; 1978. ISBN: 9780120026241

[79] Nunes JJ, Aufderheide B, Ramjattan DM, Dass R. Enhanced production of single cell protein from *M. capsulatus* (Bath) growing in mixed culture. Journal of Microbiology, Biotechnology and Food Sciences. Jan 2016;**6**(3):894-899

[80] Bothe H, Jensen KM, Mergel A, Larsen J, Jørgensen C, Bothe H, et al.

Heterotrophic bacteria growing in association with Methylococcus capsulatus (Bath) in a single cell protein production process. Applied Microbiology and Biotechnology. 2002;**59**:33-39. DOI: 10.1007/s00253-002-0964-1

[81] AlSayed A, Fergala A, Khattab S, Eldyasti A. Kinetics of type I methanotrophs mixed culture enriched from waste activated sludge. Biochemical Engineering Journal. 2018;**132**:60-67

[82] Lee H, In Baek J, Lee S-G. Syntrophic co-culture of a methanotroph and heterotroph for the efficient conversion of methane to mevalonate. Metabolic Engineering. 2021;**67**:285-292

[83] Rasouli Z, Valverde-Perez B, D'Este M, De Francisci D, Angelidaki I. Nutrient recovery from industrial wastewater as single cell protein by a co-culture of green microalgae and methanotrophs. Biochemical Engineering Journal. 2018;**134**: 129-135

[84] Badr K, Hilliard M, Roberts N, He QP, Wang J. Photoautotroph-methanotroph coculture—A flexible platform for efficient biological CO_2-CH_4-Co-utilization. IFAC PapersOnLine. 2019;**52-1**:916-921

[85] Salehi R, Chaiprapat S. Conversion of biogas from anaerobic digestion to single cell protein and bio-methanol: Mechanism, microorganisms and key factors—A review. Environmental Engineering Research. 2022;**27**(4): 210109. DOI: 10.4491/eer.2021.109. ISSN 1226-1025

[86] Hamer G, Heden CG, Carenberg CO. Methane as a carbon substrate for the production of microbial cells. Biotechnology and Bioengineering. 1967;**9**:499. DOI: 10.1002/bit.260090406

[87] Handan U, Nuri Aydogan M, Algur OF. Effect of single cell protein as a protein source in Drosophila culture. Environmental and Soil Microbiology Brazilian Journal of Microbiology. 2002;**33**(4):314-317. DOI: 10.1590/S1517-83822002000400007

[88] Harwood JH, Pirt SJ. Quantitative aspects of growth of the methane oxidizing bacterium *Methylococcus capsulatus* on methane in shake flask and continuous chemostat culture. Journal of Applied Bacteriology. 1972;**35**: 697-607

[89] Nunes JJ, Aufderheide B, Dass R. Enhanced production of single cell protein from *M. capsulatus* (bath) growing in mixed culture. The Journal of Microbiology, Biotechnology and Food Sciences. 2016;**6**(3):894-899. DOI: 10.15414/JMBFS.2016/17.6.3.894-899Corpus ID: 56392478

[90] Eccleston M, Kelly DP. Assimilation and toxicity of some exogenous C1 compounds, alcohols, sugars and acetate in the methane-oxidizing bacterium Methylococcus capsulatus. Journal of General Microbiology. 1973;**75**:211-221

[91] Ferenci T, Strom T, Quayle JR. Oxidation of carbon monoxide and methane by Pseudomonas methanica. Journal of General Microbiology. 1975;**91**:751-791

[92] Str0m T, Ferenci T, Rodneyquayle J. The carbon assimilation pathways of *Methylococcus capsulatus*, *Pseudomonas methanica* and *Methylosinus trichosporium* (OB3B) during growth on methane. Biochemical Journal. 1974;**144**:465

[93] Gilman A, Laurens LM, Puri AW, Chu F, Pienkos PT, Lidstrom ME. Bioreactor performance parameters for an industrially-promising methanotroph Methylomicrobium buryatense5GB1. Microbial Cell Factories. 2015

[94] Papoutsakis E, Lim HC. Single cell protein production on C1 compounds. The bioefficiency. Industrial & Engineering Chemistry Fundamentals. 1981;**20**(4):307-314

[95] Papoutsakis E, Hirt W, Lim HC. Utilization of pure and mixed C1 compounds for single cell protein production. Biotechnology and Bioengineering. 1981;**23**(1):235-242. DOI: 10.1002/bit.260230118

[96] Bolzonella D, Battista F, Pavan P. Recent developments in biohythane production from household food wastes: A review. Bioresource Technology. 2018;**257**:311-319

[97] Patel SKS, Singh RK, Kumar A, Jeong JH, Jeong SH, Kalia VC, et al. Biological methanol production by immobilized Methylocella tundrae using simulated biohythane as feed. Bioresource Technology. 2017;**241**:922-927

[98] AlSayed A, Fergala A, Eldyasti A. Sustainable biogas mitigation and value-added resources recovery using methanotrophs integrated into wastewater treatment plants. Reviews in Environmental Science and Biotechnology. 2018;**17**:351-393. DOI: 10.1007/s11157-018-9464-3

[99] Braude R, Hosking ZD, Mitchell KG, Plonka S, Sambrook IE. Pruteen, a new source of protein for growing pigs. I. Metabolic experiment: Utilization of nitrogen. Livestock Production Science. Mar 1977;**4**(1):79-89

[100] Li Q, Peng C, Zhang J, Li Y, Song X. Nitrogen addition decreases methane uptake caused by methanotroph and methanogen imbalances in a Moso bamboo forest. Scientific Reports. 2021;**11**:5578

[101] Available from: https://www.heise.de/tp/features/Zur-Geschichte-einer-ehemaligen-Zukunftstechnologie-die-noch-nicht-abgehakt-ist-4221160.html?seite=all

Chapter 4

Value-Added Products from Natural Gas Using Fermentation Processes: Products from Natural Gas Using Fermentation Processes, Part 2

Maximilian Lackner, David Drew, Valentina Bychkova and Ildar Mustakhimov

Abstract

Methanotrophic bacteria can use methane as their only energy and carbon source, and they can be deployed to manufacture a broad range of value-added materials, from single-cell protein (SCP) for feed and food applications over biopolymers, such as polyhydroxybutyrate (PHB), to value-added building blocks and chemicals. SCP can replace fish meal and soy for fish (aquacultures), chicken, and other feed applications, and also become a replacement for meat after suitable treatment, as a sustainable alternative protein. Polyhydroxyalkanoates (PHA) like PHB are a possible alternative to fossil-based thermoplastics. With ongoing and increasing pressure toward decarbonization in many industries, one can assume that natural gas consumption for combustion will decline. Methanotrophic upgrading of natural gas to valuable products is poised to become a very attractive option for owners of natural gas resources, regardless of whether they are connected to the gas grids. If all required protein, (bio) plastics, and chemicals were made from natural gas, only 7, 12, 16–32%, and in total only 35–51%, respectively, of the annual production volume would be required. Also, that volume of methane could be sourced from renewable resources. Scalability will be the decisive factor in the circular and biobased economy transition, and it is methanotrophic fermentation that can close that gap.

Keywords: methanotroph, biopolymers, polyhydroxyalkanoates (PHA), polyhydroxybutyrate (PHB), single-cell protein (SCP), value-added chemicals, feed, food, scalability

1. Introduction

1.1 Methanol

Today, methanol is mainly produced from synthesis gas. It is a very versatile basic chemical. Processes to further process methanol include the following ones:

- methanol to gasoline (MtG)

- methanol-to-hydrocarbons (MtH)

- methanol to olefins (MtO), and

- methanol to propylene (MtP).

The most used strain to obtain methanol from methane by biochemical conversion is *Methylosinus trichosporium. M. trichosporium* was found to produce up to 4101 mg methanol/L/day [1]. Methanol is of interest, for example, for fuel cells and combustion, apart from being a basic chemical for synthesis.

In Ref. [2] immobilized *Methylocystis bryophila* were used to produce methanol by repeated batch fermentation from a simulated biogas mixture.

1.2 Biopolymers

Biopolymers are defined as either being biobased and/or biodegradable according to certain standards. They are used as thermoplastics, elastomers, and thermosets, to replace conventional polymers. Methanotrophs have been described to produce, for instance, PHB [1].

1.2.1 Polyhydroxyalkanoates (PHA) including PHB

The common energy storage compound in microorganisms is glycogen. When a shortage of essential nutrients occurs, particularly nitrogen or phosphorus, several microorganisms are able to store their energic carbon in a different compound, which is polyhydroxybutyrate (PHB). That PHB, which is accumulated intracellularly in granules up to 50% dry cell weight and above, can be extracted and used as a thermoplastic material. PHB is a biopolymer that is both biobased and biodegradable. The biodegradability can occur aerobically or anaerobically, in different environments. This property, together with the property set that is comparable to the commodity polyolefin PP (polypropylene), makes PHB an interesting bioplastics material. PHB belongs to the class of PHA (polyhydroxyalkanoates), which are polyesters and as such are naturally occurring compounds [3]. In plants, only PHB can be found [4], whereas microorganisms can produce a wide variety of PHA copolymers depending on available comonomers.

PHB formation was seen with type II methanotrophs. For instance, *Methylocystis parvus OBBP* was found to accumulate 60% of PHB on nitrogen limitation (ammonium), as opposed to only 36% accumulation with nitrate limitation. The strain *Methylosinus trichosporium IMV3011* could accumulate 47% PHB with both nitrogen sources, nitrate and ammonium. *Methylocystis hirsute* could accumulate up to 51% PHB on ammonium (again after N-limitation). A total of 51% of PHB accumulation were found with a mixed culture dominated by *Methylocystis GB25* on ammonium [1], see **Table 1**.

The yield that was obtained varied between 0.22 and 0.67 g of PHB per gram of methane.

EPS production can limit the yield. There were no extracellular products (EPS) under methane-limited growth conditions [5].

In **Table 2**, several bioreactor configurations to produce PHB were compared.

While PHB generally resembles PP in its property set, the material has a low elongation at break and due to its high crystallinity is brittle. Adding a few percent of valeric acid as a comonomer to PHB, yielding PHBV, makes the material softer and thereby more versatile. PHBV can be synthesized by methanotrophs, too.

Strain	PHB yield [g PHB/g CH$_4$]	Accumulation condition
Methylocystis GB25	0.4	Sulfur deficiency
	0.45	Potassium deficiency
	0.22	Iron deficiency
	0.52	Ammonium deficiency
	0.55	Phosphorus deficiency
	0.37	Magnesium deficiency
Methylocystis parvus OBBP	0.34	Nitrogen limitation
Methylobacterium Organophilum CZ-2	0.43	Nitrogen limitation
Mixed culture dominated by type II	0.4	Nitrogen limitation
Methylocystis sp. *WRRC1*	0.67	Nitrogen and copper limitation

Source: [1].

Table 1.
Yield of PHB found for selected strains of methanotrophs (type II).

Bioreactor configuration	pH	Temp. [°C]	CH$_4$:O$_2$ or air	Nitrogen source
5 L batch fermenter	6.8–7.2	30	1:3	Nitrate
2 L batch fermenter	7	30	1:3	Ammonium and nitrate
5 L fed-batch fermenter	7	34	1:1	Ammonium and nitrate
70 L pressure bioreactors	5.7	38	pCH$_4$ = 30%, pO$_2$ = 15%	Ammonium
1 L bubble column bioreactor	7	30	1:1	Ammonium
2.5 L bubble column bioreactor with internal gas recirculation	7.3	25	Polluted air emission (4% CH$_4$) EBRT = 30 min GRR = 0.5 m^3/ (m^3 min)	Nitrate
1.4 L vertical loop bioreactor	7	30	1:1	Ammonium
0.5 L jacketed stirred tank reactor	7.2	25	Gas flow 0.4 L/min CH$_4$ conc. 2 g/m^3	Nitrate
4 L completely mixed batch reactor	–	–	1:1	Cyclic between ammonium and nitrate
4 L sequencing batch reactor	–	30–32	1:4 (8 h) 1:1 (16h)	Nitrate
15.2 L fluidized bed reactor	6.5–6.9	20–23	1:2.3	Nitrogen gas

EBRT = empty bed residence time; GRR = gas recycling rate; Source: [1].

Table 2.
How different fermenters fare in PHB accumulation studies.

Another important PHA copolymer is PHBH, with a certain content of hexanoic acid being incorporated in the polymer.

Biopolymers can be an environmentally benign material class. For a life cycle assessment (LCA) for biopolymers made from biogas, see Ref. [6].

In Ref. [7], the yields were found to be 1.13 g of PHB per gram of methane for *Methylosinus trichosporium OB3b* and 0.88 g of PHB per gram of methane for *Methylocystis parvus OBBP* [7], which is significantly above the figures reported in **Table 2**, see **Table 3**.

Methanotrophic strains producing PHB are listed in **Table 4**.

Yield figures have a broad spread. PHB will form copolymers when comonomers, such as valeric acid, are supplied in the medium.

	Parameter	Units	Model value in LCA study [6]	Observed for strain OB3b	Observed for strain OBBP
(1)	Percent PHB	% [g PHB/g dry weight]	50	29	60
(2)	Non-PHB biomass = [100/(1)] − 1	g biomass	1.00	2.45	0.66
(3)	Methanotrophic growth yield	g biomass/ g methane	0.345	0.63	0.73
(4)	Methane requirement for the production of non-PHB biomass = (2)/(3)	g methane	2.90	3.89	0.92
(5)	Yield of PHB on methane	g PHB/g methane	0.55	1.13	0.88
(6)	Methane requirement for the production of 1 g of PHB during PHB production phase = 1/(5)	g methane	1.82	0.88	1.13
(7)	Total methane requirement for both phases = (4) + (6)	g methane	4.72	4.77	2.05

The numbers are based on 1.0 g of PHB. Source: [8].

Table 3.
Production of PHB from methane.

Strain	Carbon source	PHA structure	PHA yield	Molecular weight
Methylocystis parvus OBBP	Methane	PHB	0.34 g/g methane	–
Methylocystis parvus OBBP	Methane	PHB	0.88 g/g methane	–
Methylosinus trichosporium OB3b	Methane	PHB	18.1 mg/mg dry cell weight	–
Methylosinus trichosporium OB3b	Methane	PHB	901.8 mg/L	–
Methylosinus trichosporium OB3b	Methane	PHB	1.13 g/g methane	–
Methylosinus trichosporium IMV3011	Methane	PHB	0.6 g/L	1500 kDa
Methylocystis sp. GB 25 DSMZ 7674	Methane	PHB	0.55 g/g methane	Up to 2500 kDa
Methylobacterium organophilum CZ-2	Methane	PHB	233.3 mg/L	–
Methylocystis hirsuta	Methane	PHB and PHV	0.63 g/g methane	–

Source: [1].

Table 4.
PHB production by methanotrophs.

1.2.2 PHBV and other PHA

As stated above, polyhydroxyalkanoates (PHAs) are (bio)polyesters of hydroxy acids. They can be naturally synthesized by bacteria with the purpose of hoarding carbon under N- and P-limitation [9]. PHA consists of 3-, 4-, 5-, and 6-hydroxycarboxylic acids [10]. Lactic acid, citric acid, glycolic acid, malic acid, mandelic acid, and tartaric acid, by contrast, are alpha hydroxy acids (1-hydroxycarboxylic acids). Thereby, their polymers are no PHA. An example of a 2-hydroxycarboxylic acid (beta hydroxy acids, where the acid and hydroxy functional groups are separated by two carbon atoms) is salicylic acid. For hydroxybutyric acid, there are three isomers—alpha, beta, and gamma. When we talk about PHB, we typically mean poly(3-hydroxybutyric acid). Valeric acid (petanoic acid) has four isomers. It is found in some foods.

Polyhydroxyalkanoates (PHA) are established biopolymers. Some well-known brands and producers are given below in alphabetic order:

- AirCarbon®/Newlight Technologies

- EnMat/TianAn

- Minerv-PHA™/Bio-On

- Nodax™/Danimer Scientific

- PHBH™/Kaneka

- TephaFlex®/Tepha [11].

The organization Go!PHA [12] is promoting PHA.

To synthesize the copolymer PHBV, valeric acid is supplied as a comonomer to the fermentation broth.

It was found that above valerate concentrations of 0.7% (by volume), the PHBV accumulation in *Methylocystis sp. WRRC1* was inhibited [1]. While the standard content of PHB, without any valerate present, was found to be 30%, it reached 15% only with high valeric acid concentrations. At 0.34% (by volume) of valerate, the PHBV content in the cells reached 60%, with 50% comonomer content [1]. *Methylocystis parvus OBBP* could be used to make different PHA from various supplied comonomers. 3-hydroxy-butyrate (3HB), butyrate, valerate, hexanoate, and octanoate were added and nitrogen limitation was applied [13]. The products included P(3HB-co-4HB), P(3HB-co-5HV-co-3HV), and P(3HB-co-6HHx-co-4HB). **Table 5** shows PHBV production by methanotrophs.

Figure 1 shows how various PHA can be obtained by methanotrophs through suitable comonomer addition.

In **Table 6**, details on PHA yields from *M. parvus OBBP* with different comonomers are given.

Table 7 lists the physical properties of the obtained PHA.

As **Table 7** shows, the elongation at break is strongly increased by the comonomers, improving the biopolymer properties compared to heat PHB. Applications of PHA are described in Ref. [14].

1.2.3 Other biopolymers

Several microorganisms, also methanotrophs, produce EPS (extracellular polymeric substances, exopolysaccharides) [15, 16], which might be used potentially for

Methanotrophs	Substrate	Co-substrate	PHBV content [%]	HV content [%]	Biomass density [g/L]
Mixed culture dominated by *Methylocystis sp.*	Methane	Valerate 100 mg/L	44	20	1.2
	Methane	Valerate 400 mg/L	30	39	1
Methylocystis parvus OBBP	Methane	Propionate 100 mg/L	32	8	1.25
	Methane	Valerate 100 mg/L	54	22	1.82
	Methanol	Valerate 100 mg/L	52	22	–
	Formate	Valerate 100 mg/L	58	15	–
Methylosinus trichosporium OB3b	Methane	Valerate 100 mg/L	50	20	1.72
Methylocystis hirsuta	Biogas	Valeric acid 130 mg/L	54	25	1.7
Methylocystis sp. WRRC1	Methane	Valerate 0.34%	60	50	3
	Methane	Valerate 0.34%, and biopolymer accumulation in a copper-free medium	78	58	3
Source: [1].					

Table 5.
PHBV accumulation from various substrates.
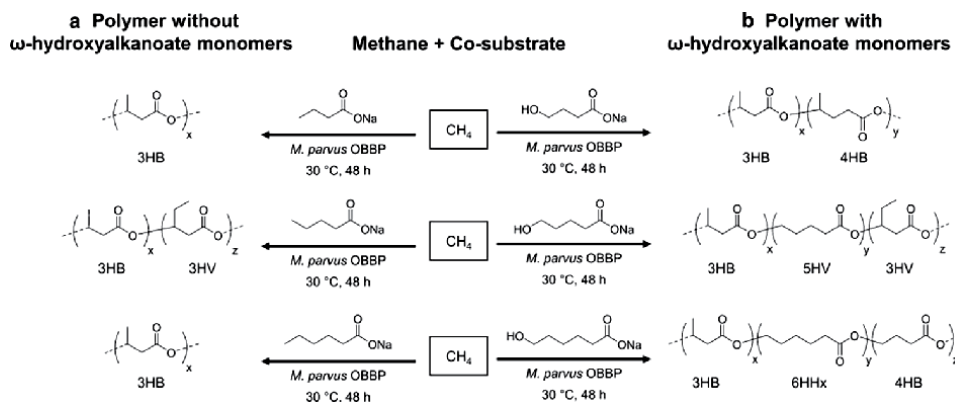
Figure 1.
Production of different PHA by comonomer choice. (a) Shows co-substrates without the hydroxy group and (b) With the hydroxyl group. Source: [13].

biopolymer applications. A higher oxygen concentration increases the excretion of EPS by methanotrophs [8]. *Methylobacter luteus, Methylomonas rubra, Methylococcus thermophilus*, and *Methylobacter ucrainicus* were found to produce EPS from methane in the range of 0.5–0.8 g/L. In general, it is extreme conditions that promote EPS production. *M. alcaliphilum* 20Z, under moderately saline conditions, gave 1.8 g EPS/g of biomass when grown in a bubble column bioreactor for the treatment of dilute methane emissions [8].

A well-known biopolymer is PLA (polylactic acid). Its monomer, lactic acid, has been obtained from methanotrophs, too, see **Table 8**.

Co-substrates	wt% PHA polymer	PHA monomer ratio [mol%]					TSS [mg/L]
		3HB	3 HV	4HB	5HB	6HHx	
None	42 ± 3	100	0	0	0	0	1600 ± 180
Butyrate (1.2 mM)	55 ± 3	100	0	0	0	0	1660 ± 200
3-Hydroxybutyrate (1.2 mM)	59 ± 5	100	0	0	0	0	1820 ± 220
4-Hydroxybutyrate (1.2 mM)	50 ± 4	91.5	0	9.5	0	0	1720 ± 240
Valerate (1.2 mM)	54 ± 4	75.0	25.0	0	0	0	1760 ± 160
5-Hydroxyvalerate (1.2 mM)	48 ± 4	95.0	1.4	0	3.6	0	1640 ± 180
Hexanoate (1.2 mM)	56 ± 4	100	0	0	0	0	1740 ± 200
6-Hydroxyhexanoate (1.2 mM)	48 ± 3	97.6	0	1.0	0	1.4	1680 ± 220
Octanoate (1.2 mM)	54 ± 3	100	0	0	0	0	1720 ± 180

TSS = total suspended solids. Source: [13].

Table 6.
Synthesis of different PHA through a variation of fatty acid co-substrates with the strain M. parvus *OBBP.*

PHA products	Molecular weights		Thermal properties			Mechanical properties		
	M_n	M_w/M_n	T_m [°C]	ΔH_m [J/g]	T_g [°C]	E [GPa]	σ_t [MPa]	ε_b [%]
P3HB	1.48E+06	1.82	178	83	3	3.0	43.2	5.2
P(3HB-co-24 mol% 3HV)	1.32E+06	2.24	147	45	−1	1.0	22.0	50.5
P(3HB-co-3.0 mol% 4HB)	1.33E+06	2.12	148	65	−2	1.2	35.6	176
P(3HB-co-9.5 mol% 4HB)	1.22E+06	2.01	135	47	−5	0.8	31.2	284
P(3HB-co-3.6 mol% 5HV-co-1.4 mol% 3HV)	1.26E+06	2.17	144	44	−2	0.8	29.9	106
P(3HB-co-1.4 mol% 6HHx-co-1.0 mol% 4HB)	1.27E+06	2.11	150	40	−1	0.7	27.6	134
Commercial P3HB	7.38E+05	2.02						
Commercial PHBV	4.48E+05	2.18						

M_n = number average molecular weight; M_w = weight average molecular weight; T_m = melting temperature; ΔH_m = apparent heat of fusion; T_g = glass transition temperature; E = Young's modulus; σ_t = tensile strength; ε_b = elongation at break; Source: [13].

Table 7.
Properties of the PHA materials derived by methanotrophic fermentation.

PLA is biobased and degradable (however, it requires 70°C for disintegration, so "home compost" standards are not met by PLA-based bioplastics products; The material is only "industrially compostable," see EN 13432 standard). PLA is suitable for food packaging (FDA rating as gras = generally recognized as safe). Today, PLA is made from sugar-derived LA, which requires agricultural starch or sugar production with the associated food/feed competition over land, fertilizer and water consumption, etc. Significant efforts are undertaken to make the enzymatic hydrolysis of lignocellulosic biomass economically viable, however, no breakthrough has been achieved in that field yet (compare 2nd generation biofuel production attempts). Methane-derived PLA can offer a lower environmental footprint and be produced with less price volatility than agriculture-based material. Of PLA, several

Product	Strain	Methane	Temperature	Cultivation type	Process details	Titer (productivity)
Lactic acid	*Methylomicrobium buryatense 5GB1S pLhldh mutant strain*	20% CH$_4$	30°C	Batch	Increased nitrate, phosphate, and trace elements in the medium	0.808 g/L
Lactic acid	*Methylomicrobium alcaliphilum 20Z mutant strain*	20% CH$_4$ (33% mock biogas in air)	30°C	Continuous	Bubble column bioreactor	0.027 g/g DCW/ h
Lactic acid	*M. buryatense 5GB1 mutant strain pAMR4*	21% CH$_4$	30°C	Batch	Ammonium as N source	0.50 g/L
Crotonic acid	*M. buryatense 5GB1C mutant strain pCA09*	25% CH$_4$	30°C	Batch	–	0.06 g/L
Butyric acid						0.08 g/L
D-Lactic acid	*Methylomonas sp. DH-1, LA-tolerant strain JHM80*	20% CH$_4$	30°C	Batch	Increased nitrate	1.19 g/L
Acetic acid	Mixed culture dominated by *Candidatus* "*Methanoperedens nitroreducens*"	90% CH$_4$	Room temperature	Batch	Nitrogen limitation	0.097 g/L (1620 µmol/L)
Muconic acid	*M. buryatense 5GB1 mutant strain pMUC*	20% CH$_4$	30°C	Semi-continuous	CSTR continuous gas supply	0.012 g/L
Succinic acid	*Methylomonas sp. DH-1 mutant DS-GL strain*	30% CH$_4$	30°C	Batch	pH 6.9	0.195 g/L
3-HP acid (hydroxypropionic)	*Methylosinus trichosporium OB3b mutant MCRMP strain*	30% CH$_4$	30°C	Batch	pH 7.0	0.061 g/L
4-HB acid (hydroxybutyric)	*M. trichosporium OB3b 4HB-SY4 mutant strain*	40% CH$_4$	30°C	Batch	–	0.011 g/L (10.5 mg/L)

The table gives the titer (g/L). Source: [17].

Table 8.
Organic acids from methanotrophs.

copolymers and blends exist, e.g. with glycolic acid (PLA + GLA, PLGA), as well as compounds. For LA production by methanotrophs, see [17, 18].

1.3 Other value-added products accessible through methane fermentation

Using natural and engineered strains, not only protein and biopolymers can be obtained from methane, but also several other compounds, for example

- Isoprene [19]

- Squalene [20]

- Succinic acid [21]

- Methanobactin [22]

- Ectoine [23, 24]

- Muconic acid [25]

- Astaxanthin [26]

For a recent review on bioproducts from methane using methanotrophs, see Ref. [17]. A methanotroph-based 2nd generation biorefinery, that is, single-input, multiple-output configuration is treated in Refs. [23, 27]. In general, multi-product biorefineries are better from an economical point of view for methane-based industrial biomanufacturing. For biorefinery downstream processes, see Refs. [28–30].

1.4 Protein from methane: Single-cell protein (SCP)

Protein is a vital part of our diet. It can be found in plants and meat. For several decades, there has been interest in single-cell protein (SCP), that is, protein derived from yeasts, algae, and bacteria [31, 32]. Yeast cells have been used to make beverages and bread for over 4500 years [33], and also algae have a long history of food. Bacterial SCP is of particularly high interest for commercial production as will be outlined below.

There exit proteinaceous methanotrophs, which contain high amounts of protein made from methane. Bacterial SCP, also called BPM (bacterial protein meal), can be obtained from methane with methanotrophs, in pure and mixed cultures, see Refs. [34]. Continuous aerobic fermentation [35, 36] is generally preferred for higher yield.

A mixed culture with *Methylococcus capsulatus (Bath)*, complemented by *Ralstonia sp, Brevibacillus agri*, and *Aneurinibacillus sp.* [37] was described to yield SCP. Also, SCP production from methanol has been reported [38], using methylotrophs.

Applications of SCP are mainly in the feed and food sector. In 1997, the United Nations "Protein-Calorie Advisory Group" discussed the safety of SCP for Animal and Human Feeding [39], apart from other commissions and panels [40–42].

Twenty-three years earlier, in November 1974, the European Association of Single-Cell Protein Producers (Association européenne des producteurs de protéines unicellulaires) UNICELPE had been founded [43].

SCP produced on a commercial scale has been reported to be deployed in these areas:

- As animal feed, for example, for poultry, calves, mink, and pigs.

- As food additives, for example, vitamin carrier, aroma carrier, and emulsifying agent.

- In industrial processes, for example, as foam-stabilizing agents and in the processing of leather and paper [33, 44, 45].

For food, another application is to boost the nutritional value, for example, of baked food items, ready-made meals, and soups. Single cells have also been used in the food industry as starter cultures (e.g., in bread, beer, and wine making by various yeasts) [33, 44, 45].

SCP has been described as antiobesity food [46]. A patent [47], EP 79.1641475, discloses the use of lipids from methanotrophs for cholesterol reduction. The use of biogas as feedstock for methanotrophs is detailed in Refs. [48, 49]. In Ref. [50], the simultaneous production and use of SCP and PHB bioplastics are discussed.

1.4.1 History of SCP

In Germany during World War I and II, yeast was used to produce food for soldiers, prisoners, and the civilian population [51, 52]. Also, Russia and Japan used similar single-cell proteins for food [51]. Different feedstocks had been tested and used, also fossil-based ones, which gave a negative touch to the products in some peoples' eyes. Hence, in the year 1966, the term "single-cell protein" (SCP) was introduced by Carl L. Wilson, building upon prior successful productions of protein from fossil sources, to provide a more positive term than "petroprotein." In fact, in the Soviet Union, early attempts were made to obtain cost-effective protein from oil. "BVK" (belkovo-vitaminny kontsentrat = protein-vitamin concentrate) plants close to oil refineries in Kstovo (year 1973) and Kirishi (year 1974) were built [33]. Till 1989, eight such factories had been constructed by the Soviet Ministry of Microbiological Industry [33].

In Russia, the single-cell protein variants were called "Gaprin" (SCP from methane) [53], "Paprin" (SCP from paraffins), [54, 55] "Meprin" (SCP from methanol), and Eprin (SCP from ethanol). The total capacity was estimated at 1.5 million tons of SCP per year [56].

Work was pioneered by Alfred Champagnat [57, 58].

For petroleum-derived SCP, see [59–62].

Also in Western Europe, similar attempts were made. British ICI (Imperial Chemical Industries Ltd) succeeded in commercializing Pruteen™ single-cell protein. As feedstock, methanol was used, deploying *Methylophilus methylotrophus* in a 1500 m^3 airlift fermenter [63, 64]. That production was a major milestone in biotechnology [65]. It can be considered the foundation for mycoprotein Quorn™ [66, 67], which is made from a fungus (*Fusarium venenatum*) from sugar and sold on the order of several 10,000 tons/year today as a meat replacement.

The historic Pruteen™ plant was designed for an output of 50,000–75,000 metric tons/year. The investment was $70 million (1979), and development costs had been $20 million [68].

Scientific American [69] wrote in 1981: *"Beer, Wine, bread, and cheese have been made by microorganisms since Neolithic times. To them have been added spirits, yogurt, pickles, sauerkraut, Oriental fermented foods, and today single-cell protein."*

The BP (British Petrol) SCP process for "Toprina" is described in Ref. [70].

French activities from SCP from methane are reviewed in Ref. [71].

German Hoechst/Uhde had developed Probion™ as a single-cell protein from *Methylomonas clarae* with 70% protein content [56]. A purified version, with 90% protein content with the nucleic acids and fats being removed, was intended for human consumption under the name Probion-S [56].

Liquipron™ (by Liquichimica from Italy) production is detailed in Ref. [72].

Another early, large single-cell protein project was Bioprotein™, which company Norferm (owned 50–50 by Statoil and Anglo-Norwegian pharmaceuticals group Nycomed Amersham [73], later DuPont) developed. Out of Norferm, the companies Calysta and UniBio developed. The Norferm SCP plant can be seen in **Figure 2**. Bioprotein™ was made from methane.

In the Norferm process, methane (from natural gas), oxygen, ammonia, and minerals were fermented. The concentration of the biomass was 20 g/L, and the temperature was 45°C in a continuous process. By centrifugation, the biomass was concentrated to 80–90 g/L in centrifuges and then further to 220 g/L by ultrafiltration. By a *"short intensive heat process, the cells are partially opened to improve the digestibility of the protein."* Spray drying is used to dry the biomass. The specific growth rate was 0.2/h, corresponding to biomass productivity of 4 kg/h/m^3 [74].

These numbers are confirmed from additional sources; industrial production of SCP is feasible at an output of 4.0 kg biomass/m^3 reactor/h with an expected yield of 0.8 g biomass/g CH$_4$ [75]. The process is shown in **Figure 3**.

The cooling requirement amounted to 62.3 MJ/kg of biomass, and the total volume of the loop reactor measured 300 m^3. As a strain, *M. capsulatus* was used to yield the following product composition:

- Crude protein: 70%

- Fat: 10%

- Fiber: 1%

- Carbohydrates: 12%

- Minerals: 1%

Figure 2.
The historic Norferm single-cell protein production facility at Tjeldbergodden, Norway. Source: [74].
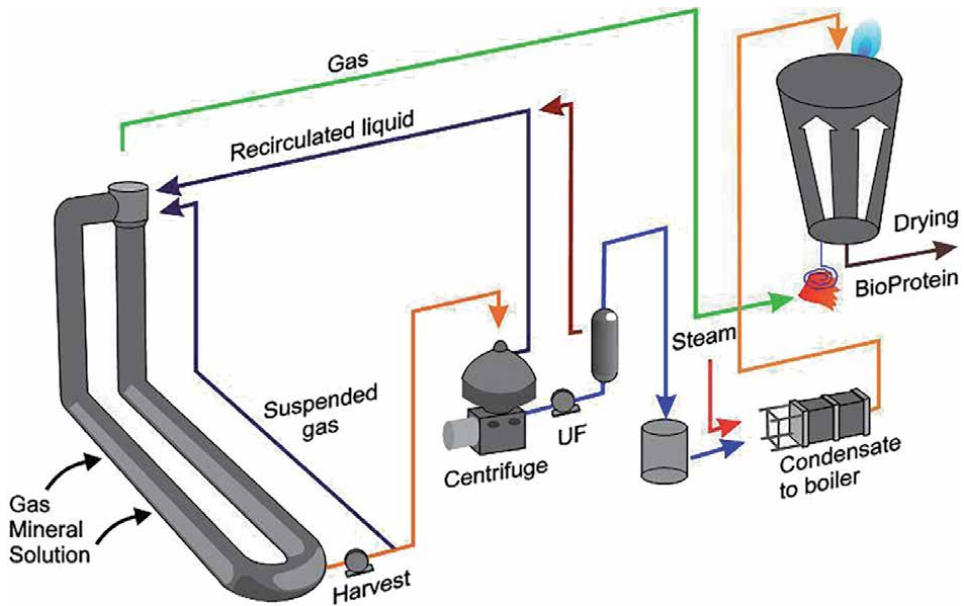
Figure 3.
Process diagram of the single-cell protein process at Norferm. Source: [74].

Norferm's BioProtein® (BP) SCP had been approved in the EU *"as a protein source in animal feeds since 1995, for fattening pigs (8%), calves (8%) and salmon (19-33%)"* [76].

Table 9 provides an overview of several other commercially implemented SCP processes from the "golden age" of the industry around the year 1977 when also licensing options were available [78, 79]. An interesting retrospective view is provided by [80].

Another well-known SCP derived from n-alkanes (paraffins) was Fermosin™ [61].

Table 10 gives additional projects (status 1977).

The overview above gives testimony of a fairly developed industry, which then disappeared again from the market. Fifty years ago, SCP succeeded technologically, but then failed economically, mainly due to cheap soy prices and increasing fossil fuel costs, as this quotation for the pertinent literature exemplifies:

> *"By 1974, Shell announced plans for enlarged pilot plant facilities at Sittingbourne, and a development program in Amsterdam, with the ultimate goal of constructing a 100,000 ton/year plant. In the spring of 1976, however, Shell announced that it had stopped work on commercialization, and the expansion and development plans were "indefinitely postponed." The decision was said to be based on three factors— the low price of soybeans and maize; the potential in large areas of the world for expanding existing sources of protein; and the difficulty of applying Shell's sophisticated process in* "underdeveloped countries" *[77].*

So Shell bailed out of SCP within a short period of time, after prior heavy investments. That step cannot be considered unusual, compare to the press release from Dow in 2005 [81], when Dow stepped out of the bioplastics business *"due to slow sector maturation"* after having invested an estimated 750 million USD.

Four seminal books on SCP are [51, 82–84].

1.4.2 Use of SCP: Feed and food

SCP has multiple possible applications, both in the feed sector and in the food sector [33, 48, 85], see **Table 11**:

Organization	Location	Substrate	Organism	Product name	Capacity [tons/ year]	Status
British Petroleum (BP)	Lavéra, France	Gas oil	*Candida tropicalis*	Toprina	16,000	Shut down
British Petroleum (BP)	Grangemouth, Scotland	n-Paraffins	*Candida lipolytica*	Toprina	4000	Operating
BP-ANIC	Sarroch, Sardinia	n-Paraffins	*Candida lipolytica*	Toprina	100,000	Constructed, awaiting government approvals
Liquichimica (with Kanegafuchi)	Saline di Montebello, Italy	n-Paraffins	*Candida maltosa*	Liquipron	100,000	Constructed, awaiting government approvals
USSR	Several sites	n-Paraffins	*Candida spp.*	BVK	300,000 or more	Operating
Imperial Chemical Industries (ICI)	Teesside, UK	Methanol	*Methylophilus methylotropha*	Pruteen	50–75,000	Construction approved, start-up late 1979
Amoco	Hutchinson, Minnesota, USA	Ethanol	*Tortula yeast* (*Candida utilis*)	Torutein	5–7000	Operating

Source: [77].

Table 9.
Commercial-scale SCP processes with hydrocarbons and alcohols and feedstocks.

Kuzniar et al. have suggested the use of methanotrophic bacterial biomass as a mineral feed ingredient for animals [87].

Also, applications in paper processing, leather processing, and foam stabilization are mentioned in the literature [33, 48].

In Ref. [88], SCP is discussed as a basis for microbial growth media, and in Ref. [89] for wood adhesives.

For (animal) *feed* applications, the dried bacterial biomass, which typically contains 70% of protein, can be fed directly. In SCP for (human) *food* applications, the content of nucleic acids (NA) has to be reduced from 10–15 to approximately 1–2%, which can be done thermally or enzymatically. Nucleic acid reduction by heat shocks is described in Ref. [90].

1.4.3 Properties of bacterial SCP

Table 12 summarizes the properties of different SCPs:
Bacteria are very well suited to make SCP, see **Table 5**. They exhibit the highest growth rates. On the other hand, the nucleic acid content is elevated compared to SCP by other microorganisms. The extraordinary growth performance of bacteria is also visible in **Table 13**.

With doubling times of the mass on the order of 10–100 minutes, bacteria and yeasts grow incomparably faster than plants or animals. This translates into unsurpassed productivity, as **Table 14** illustrates.

Organization	Location	Substrate	Organism	Status and capacity [tons/year]	
Societé Nationale Sempac: Engineering by Process Engineering Co. (PEC; Member of Chemap, Switzerland)	Algeria	Molasses	*Yeast*	20,000	Project start December 1977 (Algiers)
	Bulgaria	Methane, methanol, n-paraffins	*Depends upon the process chosen*	100,000	Discussions with ICI, BP, Shell, USSR, location will depend on the process chosen
Alberta Gas Chemicals with Alberta Research Council, Celanese Canada, with Mitsubishi Gas Chemical	Canada	Methanol, n-paraffins	*Yeast*	100,000	Study, for a plant in Medicine Hat (Alberta/Canada)
	Czechoslovakia	Ethanol	*Yeast*	4000 (pilot plant); in planning: 100,000 t/a in Kojetin/Northern Moravia; pilot plant in operation	
Joint East Germany/ Polish project using USSR/East German-developed process	East Germany	Gas oil	*Yeast*	60,000 t/a in Schwedt	
Groupement Francais des Proteines (50% owned by Institute Francais du Petrole; other 50% shared by Elf-Erap and Cie-Francaise des Petroles)	France	*n-Paraffins*	*Yeast*	Pilot plant (Soleize); earlier plans for 100,000 tons/year plant canceled	
Institute of Petroleum	India	"crude oil"	*Yeast*	Pilot plant (Gujarat, near Baroda)	
Hebrew University (Yissium Research Devel. Co.) with Dor Chemicals (Haifa)	Israel	Methanol	*Bacteria*	50 tons/year pilot plant to be scaled up to 1000 and then to 25–100,000 tons/ year	
Montedison	Italy	Ethanol; carbohydrate	*Depends upon the process chosen*	Two small pilot plants. Ethanol jointly with Czechoslovakia, carbohydrate jointly with PEC, Switzerland; joint marketing study with Amoco	
Societa Italiana Resine S.p.A., Milan (SIR)		Methanol	*Candida boidini*	Pilot plant (Milan)	
Dainippon Ink and Chemicals (with Koa Oil)	Japan	n-Paraffins	*Yeast*	Foundation laid for 60–120,000 tons/year plant; canceled	
Kanegafuchi (with Maruzen)		n-Paraffins	*Yeast*	60,000 tons/year plant; canceled	
Mitsubishi Ga Chemical Co.		Methanol	*Yeast, bacteria*	4000–5000 semicommercial (Niigata)	

Organization	Location	Substrate	Organism	Status and capacity [tons/year]
Mitsubishi Petrochemical		Ethanol	*Yeast*	
Kyowa Hakko Kogyo		n-Paraffins	*Yeast*	100,000 tons/year; canceled
Mitsui Toatsu Chemical		n-Paraffins	*Yeast*	50–60,000 tons/year; canceled
Asahi Chemical		n-Paraffins	*Yeast*	50–60,000 tons/year; canceled
Sosa Texcoco SA	Mexico	CO_2	*Spirulina maxima*	1 ton/day (Mexico City)
Roniprot L.L.A.; Technology from Japan (reports of negotiations with Ron, Dainippan, Sumito Shoji Kaisha)	Romania	n-Paraffins	*Yeast*	60,000 tons/year (Arges; Jassyon) said to have started construction in 1973
Petromin (state-owned Saudi Arabian Oil Co.) with British Petroleum	Saudi Arabia	n-Paraffins	*Yeast*	Study for 100,000 tons/year (Al Jubail)
Instituto de Fermentaciones Industriales, Centro Superior de Investigaciones Cientificas (government sponsored, but autonomous)	Spain	Ethanol	*Hansenula anomala*	Pilot plant, 100 kg/day (Madrid)
Norsk Hydro and AB Marabou formed "Norprotein" (financial support from Nordic Industrial Fund and Swedish Council for Technical Development)	Sweden	Methanol		Pilot plant planned (Sundbyberg)
Chi Yee Solvent Works, Chinese Petroleum Corp.	Taiwan	Kerosene, fuel oil, gas oil	*Pseudomonas*	
Phillips Petroleum	United States	Methanol	*Bacteria*	Pilot plant, Bartlesville, Oklahoma
Bio Proteinas de Venezuela (Venproteinas) (with BP), Stone and Webster, contractor	Venezuela	n-Paraffins	*Yeast*	100,000 tons/year (early 1979) (Puerto la Cruz)
Schick-Chemie-Technik GmbH (Cologne), with technology licensed from the Institute of Industrial Fermentation, Spain (see above)	West Germany	Ethanol	*Hansenula anomala*	100,000 tons/year (several 50 m³ fermenters) planned for 1978

Organization	Location	Substrate	Organism	Status and capacity [tons/year]
Society for Biotechnological Research (Braunschweig Stoeckheim) with Wintershall AG (subsidiary of BASF)		"Oil"	*Aerobic mycobacteria*	Effluent to be used for secondary oil recovery in a field test in Lower Saxony
Friedrick Uhde GmbH; Hoechst AG (Gelsenberg has withdrawn), with government support		Methanol (also n-paraffins)	*Methylomonas sp., Candida lipolytica*	Pilot plant planned (earlier plans for demonstration plant (100 tons/year) at Gelsenkirchen-Horst canceled), ultimate plans for 100,000 tons/year
Kohlenstoffbiologische Forschungsstation, E. V., Dortmund		CO_2	*Scenedesmus acutus*	200 tons/year

Source: [77].

Table 10.
Additional SCP projects as of 1977.

Potential application for SCP in animal diets (feed)	Potential application for SCP in foodstuff
• *"Calves having fattening ability.* • *Poultry having fattening ability.* • *Pigs having fattening ability.* • *Fish breeding.* • *Laying hens feed.* • *Feeding of household animal"* [65, 86]	• *"As carriers of vitamin.* • *As emulsifying agent.* • *As carriers of scent.* • *In soups.* • *Improving the nutritional worth of baked items.* • *In readymade meals.* • *Within food recipes"* [65, 86]

Source: [33, 48].

Table 11.
Where SCP could be used.

Within 24 h, a starting mass of bacteria of 1000 kg can yield, theoretically, 10^{12} kg of protein, whereas beef would only produce 0.1 kg and soy in the order of 10 kg. An analysis of bacterial meal (BM) derived from methane is given in **Table 15**.

As one can infer from **Table 15**, the protein content approaches and exceeds 70%. **Table 16** shows the protein content of SCP from selected microorganisms.

Another important aspect of SCP is its quality, which can be expressed by the amino acid profile. In **Table 17**, the composition of amino acids of bacterial SCP compared to other proteins is shown.

Bacterial SCP is approved as a feed ingredient in the EU feed catalog (EU 68/ 2013) [63]. SCP for feed has been tested extensively, see **Table 18** for an overview.

SCP feed trials were made with Drosophila [87] several monogastric species [98], including rats [99, 100], pigs [61, 100–102], dogs [45, 103], (lactating) cows [104], veal calves [105], chickens (broilers) [72], mink (*Mustela vison*), fox (*Alopex lagopus*), Atlantic salmon (*Salmo salar*), rainbow trout (*Oncorhynchus mykiss*) [106], Pacific White Shrimp (*Penaeus vannamei*) [107, 108], Atlantic halibut (*Hippoglossus hippoglossus*), tilapia (*Oreochromis niloticus, Oreochromis mossambicus*) [109, 110],

Feature	Bacteria	Yeast	Filamentous fungi	Algae
Growth rate	Highest	Quite high	Lower than bacteria and yeast	Low
Substrate	A wide range of substrates	Most substrates except hydrocarbons and CO_2	Limited substrates (mostly starchy and cellulosic materials)	Light, inorganic carbon sources, for example, CO_2 (preferably)
pH range	5–7	5–7	3–8	up to 2
Cultivation system	Bioreactors	Bioreactors	Bioreactors	Open ponds, tanks in sunlight
Risk of contamination	High; precautions are necessary	Low	Low if grown below pH 5	High
Biomass recovery	Sometimes problematic; new improved methods are needed	Easy by centrifugation	Easy for filamentous or pellet forms	Difficult and costly with unicellular algae
Protein content (crude)	80% or more	55–60%	50–55%	Up to 60%
Amino acid profile	Generally good, a small deficit in S-containing acids	Generally good, deficit in S-containing amino-acids	Low in S-containing amino acids	Generally good; low in S-containing amino acids
Nucleic acid content	High (8–14%)	High (5–12%)	High (3–10%)	Low (4–6%)
Removal of nucleic acids	Necessary			
Toxins	Gram-negative bacteria may produce endotoxins	–	Many species produce mycotoxins	Three types of toxins: endotoxin, neurotoxins, heptotoxins
Other features	–	High vitamin B content	Chitin may contain a significant proportion of N content, which is unavailable	Low yield (1–2 g dry wt/L). High chlorophyll content is unsuitable for humans

Source: [91].

Table 12.
Comparison of some cultural and biochemical characteristics of various microbe groups to make SCP.

Japanese yellowtail (*Seriola quinqueradiata*) [111], zebrafish (*Danio rerio*) [112] and other aquaculture species [113, 114]. In feed, SCP can replace fish meal and soy. It was found in Ref. [65] that *"bacterial meal (BM) derived from natural gas fermentation, utilizing a bacteria culture containing mainly the methanotroph Methylococcus capsulatus (Bath), is a promising source of protein based on criteria, such as amino acid composition, digestibility, and animal performance and health."* [65].

The oral immunogenicity of bacterial SCP was tested by [115].

The use of SCP for feed and food was also proposed by John H. Litchfield in 1979 [116].

An example from Germany (1943–1949) is the "wood sausage," a spread made in Wildshausen from paper production waste (sugars) using the fungus *Oidium laktis*. The process was licensed from Biosyn GmbH [117]. Other yeast spreads on

Organism	Mass doubling time
Bacteria	10–120 min
Algae/molds	2–6 h
Yeasts	10–120 min
Plants	1–2 weeks
Chickens	2–4 weeks
Pigs	4–6 weeks

Source: [91].

Table 13.
Mass doubling time of different organisms.

Organism (1000 kg)	Amount of protein produced in 24 h [kg]
Beef cattle	10^{-1}
Soybeans	10^{1}
Yeast	10^{2}
Bacteria	10^{12}

Source: [91].

Table 14.
Comparison of protein production efficiency of selected organisms over 24 h.

Feedstock	Bacterial culture	Crude protein	Lipids	Ash	Nucleic acids
Methanol	*Methylophilus methylotrophus*	81.3	7.2	9.1	15.9
Methane	*Methylococcus capsulatus, Ralstonia sp., Brevibacillus agri, Aneurinibacillus sp.*	73.2	10.7	8.5	9.9
		68.1	10.4	8.0	Not determined
		68.7	8.0	8.0	Not determined
		73.4	8.4	7.7	Not determined
		71.9	8.3	6.7	Not determined
		69.5	8.1	6.2	11.1
		67.0	9.9	6.4	Not determined

Source: [65].

Table 15.
Properties of BM (bacterial meal) made from methane and methanol, based on g/100g of dry mass.

the market are Marmite, Cenovis, and Vegemite: *"Spent brewer's yeast (Saccharomyces cerevisiae) have been sold for more than a century in yeast extracts such as Marmite® (Unilever and Sanitarium Health Food), Vegemite® (Bega Cheese Ltd.), Cenovis® (Gustav Gerig AG), and Vitam-R® (VITAM Hefe-Produkt GmbH)."* [117]

"Another commercially available yeast, Torula (*Candida utilis*, renamed as *Pichia jadinii*), a widely used flavoring agent, is also high in protein. Torula was used in Provesteen® T, produced by the Provesta Corporation in the 1980s, along with similar products using *Pichia* and *Kluyveromyces* yeast)" [118].

Bacteria	Substrate	SCP (%)	Reference
Haloarcula sp. IRU1	Petrochemical wastewater	76	[92]
Methylococcus capsulatus, Ralstonia sp., Brevibacillus agri	Methane (natural gas)	67–73	[65]
Aneurinibacillus sp., Methylomonas and Methylophilus spp., Metilococ capsulatus	Gas and liquid products of sewage	< 41	[93]
Methylococcus capsulatus (bath)	Methane	53	[94]
Methylophilus sp	Supernatant and biogas	24	[93]
Methylocapsa acidiphila	Methane	59	[95]
Methilomonas sp.	Natural gas	69.3	[96]
Methilomonas sp.	Biogas and supernatant of sewage sludge	56	[93]

Source: Excerpt from [44].

Table 16.
Protein content of bacteria expressed as SCP (single-cell protein) grown on different substrates.

Amino acids		BM	Soybean meal	Fishmeal	Methanol-grown bacterial protein (Pruteen™)
Indispensible amino acids	Arginine	6.3	7.4	6.2	4.6
	Histidine	2.2	2.7	2.5	1.9
	Isoleucine	4.4	4.7	4.7	4.3
	Leucine	7.5	7.5	7.9	7.0
	Lysine	5.6	6.1	8.2	6.0
	Methionine	2.6	1.3	3.0	2.4
	Phenylalanine	4.2	5.0	4.1	4.1
	Threonine	4.3	3.9	4.0	4.6
	Tryptophan	2.2	1.4	0.9	0.9
	Valine	5.8	4.8	5.3	5.6
Dispensible amino acids	Alanine	7.1	4.2	6.1	7.1
	Apartic acid	8.5	11.2	9.9	8.8
	Cysteine + cystine	0.7	1.5	0.9	0.7
	Glutamic acid	10.6	18.2	12.6	10.6
	Glycine	4.9	4.2	6.0	5.7
	Proline	3.8	5.0	4.3	2.9
	Serine	3.6	5.2	4.1	3.3
	Tyrosine	3.6	3.8	3.2	3.4

For reference, the data for soybean meal and fishmeal are provided. The rightmost SCP was obtained from methanol, Pruteen™, by Methylophilus methylotrophus *[g/16 g N ± standard deviation of free, hydrated amino acids].*
Source: [65].

Table 17.
Amino acid profile of SCP made from natural gas (BM = bacterial meal).

SCP-protein evaluations by animal tests			
Organism	**Digestability**	**Protein efficiency ratio**	**Biological value**
Algae	65–86	0.7–2.6	48–81
Bacteria	80–90		73–82
Fungi			10–75
Yeast	81–96	0.9–1.7	32–69
Yeast and methionine	96	2.0–2.3	91–96
FAO/WHO reference protein	100		100
Source: [97].			

Table 18.
As early as 1981, SCP was tested for feed.

1.4.4 Aquatic species

Approximately half of the global fish and aquatic species production comes from aquaculture operations, with an increasing share. Fish meal is volatile in price and, due to overfishing, is not a sustainable feed material. The same holds true for soy; while soy is cheap, its immense monoculture production has resulted in rainforest destruction on a global level. It was shown that soybean meal-induced enteritis in Atlantic salmon (*Salmo salar*) can be prevented by cell wall fractions obtained from *Methylococcus capsulatus* [119].

1.4.5 Chicken

Various tests were carried out to feed chickens with bacterial SCP. SCP could maintain chicken growth performance and increase the feed to gain (feed conversion) and reduce the fat content in chicken [120]. *"Replacing soybean meal and small amounts of rendered fat with BPM caused less intensity of odor and less rancid flavor of chicken meat"* [120].

Processed animal protein (PAP) from poultry/pig for poultry/pig [121] is currently being investigated, too, but brings back memories about BSE [122]. Also, potential quantities are limited.

1.4.6 Mink

Another species where SCP was tested successfully is mink (*Mustela vison*). SCP digestibility tests were carried out in 2009 by the Department of Animal and Aquacultural Sciences at The Norwegian University of Life Sciences, Ås [123]. Mink are of importance for the fur industry.

1.5 Status of single-cell protein as food

Oral delivery of bacteria is not novel [124]; for an overview of beneficial microorganisms in food and nutraceuticals, see Ref. [125]. Microorganisms in food are covered in Refs. [126–128].

In the literature, there is ample coverage of food trials of SCP in the last 50 years.

One example is a trial from 1979 to include SCP "Pekilo" in sausages and meat balls [129].

SCP has a peculiar taste. Some variants, which have a high content of glutamic acid, have been proposed and used instead of monosodium glutamate (MSG) [118] as the flavor enhancer in food.

Pekilo is a microfungus-derived SCP from *Paecilomyces varioti* based on pulp and paper waste streams. It is now being revived by Enifer [130]. Another work with SCP from waste is discussed in Ref. [131], SCP with the fungus *P. chrysosporium* in [132].

As early as 1971, single-cell protein had been subjected to clinical testing in tolerance trials in adults [133]. For immunogenicity testing of food proteins, see Ref. [134].

For humans, it is recommended that the daily nucleic acid (NA) intake does not exceed 2 g, as higher quantities (particularly RNA and, to a lesser extent, DNA) have been reported to increase the content of uric acid in blood plasma to an unhealthy level [135], leading to gout [136]. As SCP contains a comparatively large amount of nucleic acids, it needs special processing for food applications. For feed, by contrast, the nucleic acid species do not harm. In **Table 19**, approaches for RNA reduction in SCP are summarized.

Tables 20–23 compare different treatments of SCP to reduce nucleic acids [137].

There is currently a strong movement toward alternative protein (alt protein), as concerns over the healthiness and sustainability of meat, first and foremost imported beef, are increasing all over the world. Hence there is good potential for SCP for food applications. By the end of 2021, Solein™ submitted its dossier for SCP food approval in the EU [138].

Occupational health aspects of SCP are discussed in Ref. [139], where it was found that inhalable dust needs to be avoided.

Method	Protocol	Organism	Initial and final % RNA (of dry wt)
Base-catalyzed hydrolysis	0.12 N NaOH for 30 min at 50°C	*P. variotii*	9%→3%
Chemical extraction	5% NaCl at 120°C	*Baker's yeast*	Complete removal
Cell disruption; physical separation:	Disintegration-glass beads	*Different microorganisms*	Final % RNA = 2
(a) Enzymatic treatment	Malt sprout nuclease	*Yeast*	Final % RNA < 3
(b) Chemical	Succinic anhydride, pH 4.2–4.4	*S. carlsbergensis*	6–8%→1.8%
(c) Chromatography	Cellex E-Ecteola cellulose	*C. utilis, S. cerevisiae, S. carlsbergensis, Z. mobilis*	Less than 3% of initial content
Exogenous RNAase	Bovine pancreatic ribonuclease, 55–56°C, pH 6.7–8.0	*S. utilis, C. intermedia*	Final % RNA = 1.5
Endogenous RNAase	90°C, pH 2, 20 min	*R. glutinis*	6.5%→1.2%
-heat shock	45°C, pH 5.8–6.9, 2 h	*C. utilis*	6–8%→2%
	68°C for a few sec, 50°C, 1 h, 55°C, 1 h	*C. utilis*	7–8%→1–2%
	50–60°C + NaCl	*S. cerevisiae*	7–8%→1.4%

Source: [51].

Table 19.
RNA reduction in SCP.

Amino acids	Yeast cells [mg/g]	Protein extracted with NaOH [mg/g]
Cystine + cysteine	8.15	11.88
Lysine + histidine	10.81	16.55
Aspargagine	7.58	15.5
Aspartic acid	1.89	3.54
Serine + glycine	7.82	8.86
Glutamic acid	4.11	5.72
Threonine	26.11	33.1
Alanine	29.94	32.79
Tyrosine	11.89	14.77
Methionine + tryptophan	6.94	11.96
Phenylalanine	7.14	9.45
Leucine + isoleucine	22.85	37.28
Source: [137].		

Table 20.
Change of the amino acid composition of yeast cells by NaOH extraction.

NaCl [%]	RNA	Reduction [%]
1	4.54	6.4
2	4.05	16.5
3	3.68	24.1
4	3.19	34.2
5	4.05	16.5
Control	4.85	0.0
Source: [137].		

Table 21.
*Reduction of RNA in yeast cells (*Candida lipolytica *YB-423) by NaCl treatment, incubation at 50°C for 20 min.*

Type of protein	Total nitrogen [%]	Total protein [%]	RNA [%]	DNA [%]
Yeast cells	6.72	42.00	4.90	2.13
Protein extract	10.80	67.50	1.22	0.399
Source: [137].				

Table 22.
Nucleic acid and protein content of yeast cells by extraction with NaOH.

2. Operational aspects of methane fermentation

Methane fermentation occurs naturally and is carried out in bioreactors. Medium optimization and mineral requirement are treated in Refs. [140–142].

The reactions can be described as follows for methane limitation 4.9 g is for bacteria and products together [5]:

$$\underset{\underset{16\ \text{g}}{}}{CH_4} + \underset{\underset{56\,g}{}}{1.8O_2} \rightarrow \underset{\underset{16.1\ \text{g dry wt.}}{}}{\text{Bacteria}} + \underset{\underset{15.8\ \text{g}}{}}{0.34CO_2} \tag{1}$$
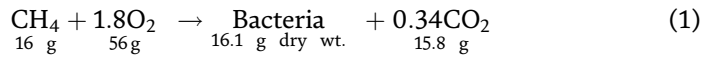
Under oxygen limitation, it was found [5]:

$$\underset{\underset{16\ \text{g}}{}}{CH_4} + \underset{\underset{9.6\,g}{}}{0.3O_2} \rightarrow \underset{\underset{4.9\ \text{g dry wt.}}{}}{\text{Bacteria}} + \text{Products} + \underset{\underset{2.2\ \text{g}}{}}{0.05CO_2} \tag{2}$$
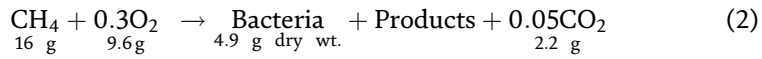
By contrast, [96] found for methane limitation:

$$4.25\ \text{g}\ O_2 + 1.245\ \text{g}\ CH_4 \rightarrow 1\ \text{g cells} + 2.0\ \text{g}\ CO_2 \tag{3}$$
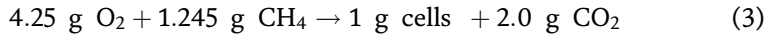
For oxygen limitation, this formula could be determined [72]:

$$2.5\ \text{g}\ O_2 + 1.01\ \text{g}\ CH_4 \rightarrow 1\ \text{g cells} + 1.216\ \text{g}\ CO_2 \tag{4}$$
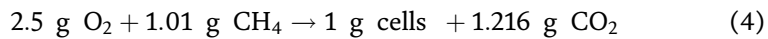
Temperature [°C]	Time [s]	RNA [%]	DNA [%]	Reduction of nucleic acids [%]
60	5	3.325	1.460	31.93
	10	3-150	1.375	35.63
	20	2.712	1.350	42.22
	40	2.625	1.320	43.88
	80	2.450	1.300	50.92
70	5	2.187	1.250	51.11
	10	1.662	1.240	58.72
	20	1.575	1.230	60.10
	40	1.400	1.200	63.02
	80	1.000	1.150	69.42
Untreated cells		4.900	2.130	0.0

Source: [137].

Table 23.
RNA and DNA in yeast cells (C. lipolytica YB-423) treated by heat shock.

For fermentation technology in general, see Refs. [143–146], for its economics [147].

2.1 SCP production process

As SCP has already been produced at a large scale some 50 years ago, see above, there is ample experience with gas fermentation. SCP production is summarized in **Table 24**.

As **Table 24** shows, different approaches are being followed. For a review on SCP, see Refs. [85, 151].

A major difficulty with methane is its low solubility in water, resulting in low productivity. Paraffin oil as a "methane vector" for improved mass transfer and higher cell densities was suggested in the literature [64]. Koutinas et al. have proposed to use of γ-alumina pellets to improve methane fermentation [152]. Emulsion-based fermentation to enhance the mass transfer of methane is presented in Ref. [153].

For the bioprocess, **Table 25** contrasts two reactor configurations, the "classic" CSTR (continuously stirred tank reactor) and the loop reactor.

Cultivation operation	Growth modality	Capital and operational considerations	Emerging commercial examples
Aerobic bioreactor	Heterotrophs Mixotrophs	High cell mass yield High capital costs High energy consumption Sterile operation Significant installed industrial capacity	Methanol, glycerol, or ethanol—KnipBio Glucose—Veramis Cellulose—Arbiom, Menon, EniferBio
Anaerobic bioreactor	Heterotrophs Mixotrophs	Low cell mass yield Low capital costs Low energy consumption Requires metabolite production and valorization Non-sterile operation Most installed industrial capacity	Glucose or glycerol—White Dog Labs Yeast separation—Fluid Quip Technologies & ICM
Gas bioreactor	Methylotrophs Chemoautotrophs Mixotrophs	Variable cell mass yield High capital costs High energy consumption Could require metabolite production and valorization Sterile & non-sterile operation Limited installed industrial capacity	Methane—Calysta, Unibio, String Bio & Circe Biotechnologie CO_2, H_2, and O_2—Kiverdi, Novo Nutrients, Deep Branch Biotechnology, Solar Foods, Avecom & LanzaTech Glucose & syngas—White Dog Labs
Photosynthetic bioreactor	Photoautotrophs Mixotrophs	High cell mass yield Low capital costs High energy consumption Sterile operation No known installed capacity	CO_2 and light—Bioprocess Algae & Pond Technologies
Open cultivation systems	Photoautotrophs Heterotrophs Mixotrophs	Variable cell mass yield Low capital costs Low energy consumption Non-sterile operation Limited installed industrial capacity	Brewing by-products—iCell Sustainable Nutrition Open photosynthetic system—Cellana

Source: [148], extended from Refs. [149, 150].

Table 24.
Production of SCP.

For methane fermentation in a sequencing batch bioreactor, see Ref. [154], for batch fermentation, see Ref. [155], and for a cascade of fermenters, see Ref. [156].

The historic Norferm process (see above) used a loop reactor, which can be seen as a PFR (plug flow reactor) comparable to an airlift fermenter only with a different agitation mode of the fluid, using a pump instead of the injected gasses to circulate the medium. **Table 26** assesses the relative production costs of different SCP processes.

It is estimated that methane fermentation comes with the highest investment costs (CAPEX), but will allow the lowest operational costs (OPEX), making that feedstock attractive for large-scale operations. When we look at the relative cots for substrate and utilities, there are also marked differences in the various processes. A waste stream has the advantage of low costs, but stable quality and quantity have to be ensured. Utility costs will depend on the geographic location of the site, apart from the unit operations chosen. Cooling costs are determined by the process temperature, and labor costs can be controlled by the degree of plant automation and the complexity of the process. Costs in SCP production are further discussed in Ref. [157].

Conventional stirred vessels	Modern loop reactors
High energy costs	Low energy costs
10 kW/m^3 (approx.)	2 kW/m^3 (approx.)
Less defined fluid flow pattern	Quantified fluid flow pattern
Intrafermentor cooling (jacket)	Extrafermentor cooling (plate exchanger)
Complicated heat removal	Easy removal of the fermentation heat load
Limited scale-up	Less limited scale-up
Indefinite mixing—irregular residence times	More definite mixing—regular residence times
Cell yield on oxygen of 10–20%, hence requiring a high aeration rate	Cell yield on oxygen of 40–50%, hence requiring less aeration
Batch and continuous operation	Continuous operation
Low yield and productivity	High yield and productivity
Limited control	Efficient control
Moving parts (easily contaminated)	No moving parts
Expensive capital and running costs	Cheaper to install and run

Source: [51].

Table 25.
Fermenter comparison for SCP production.

Capital and manufacturing cost [%] for several SCP processes

Relative costs (units) for:				
	Methanol	Ethanol	Methane	n-Paraffins
Total capital cost	100	97.6	150.8	107.7
Total manufacturing cost	100	229.6	75.2	129.7

Comparative production costs of SCP

Process	Relative production costs [%] for:					
	Raw materials					
	Substrate	Other chemicals	Utilities	Labor	Miscellaneous	Total
Yeast—paraffin	29.4	33.9	23.8	8.4	14.5	100
Bacterium—methanol	47.4	26.4	14.2	6.2	5.8	100
Yeast—ethanol	63.9	9.9	12.0	5.1	9.1	100
Fungus—sulfite liquor	17.0	33.7	24.8	11.0	13.5	100
Bacterium—bagasse	25.7	13.5	36.6	8.3	15.9	100
Algae—CO_2	?	16.5	13.8	15.3	54.4	-
Fungus—lignocellulosic wastes	?	14.5	11.3	22.9	51.3	-

Source: [51].

Table 26.
Comparative costs of various SCP processes.

For engineering factors in the production of SCP, see Refs. [158, 159]. For process development, see Refs. [160].

Downstream processing depends on the exact target product(s). The "classic" separation of cells from the fermentation medium is centrifugation, followed by spray drying. Imasaka et al. have suggested cross-flow filtration of the fermentation broth with ceramic membranes [161], and Yang et al. the continuous methane fermentation in a fixed-bed reactor packed with loofah [69]. Heat treatment or enzymatic treatment [132, 162] can be used for nucleic acid reduction and digestability improvements.

2.2 PHB production process

In Ref. [163], the authors carried out a techno-economic assessment of methanotrophic PHB manufacturing, compare **Figure 4**.

The key findings from Ref. [163] for a PHB production on the order of 100,000 t/a by methanotrophic fermentation were:

- Downstream process: acetone–water solvent extraction

- Production costs: $4.1–$6.8/kg PHA

- Raw material costs reduction compared to sugar feedstock: 22% instead of 30–50%

- Cooling costs: 28% of the operational costs

- Strong advantages of using thermophilic methanotrophs—production costs go down to $3.2–5.4/kg PHA [163], because of cheaper cooling (cooling water instead of a refrigerant)
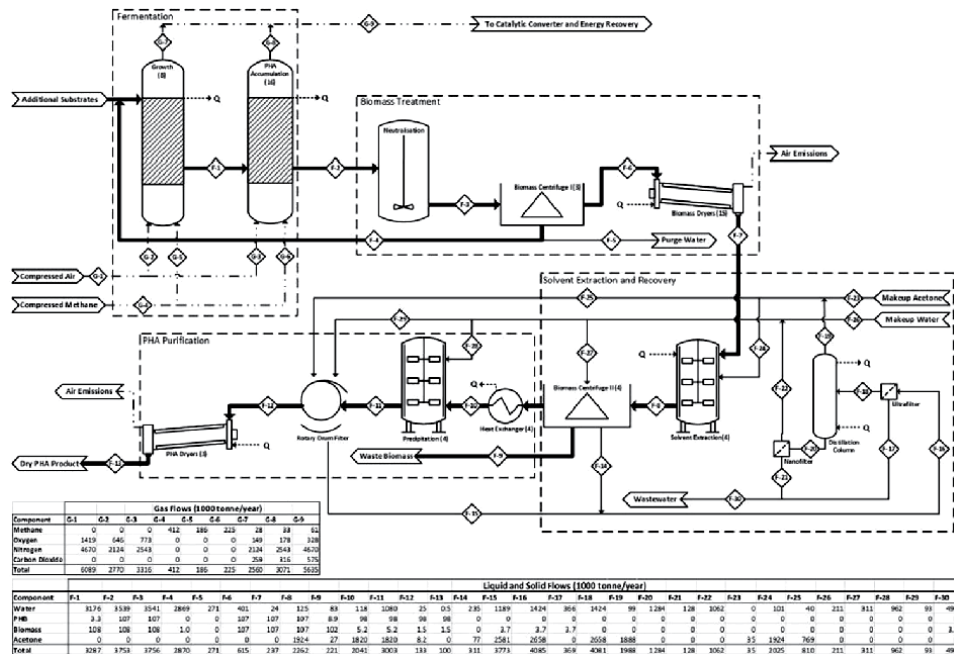

Figure 4.
PFD (process flow diagram) to convert methane into PHB, with mass balance. Source: [163].

These figures of 3.2–6.8$/kg of PHB are very promising, as today PHA suffers from high production costs and hence a limited market.

3. Discussion

Today, we are in an "oil economy," as crude oil is the basis for a major share of energy and materials production. With an accelerating shift toward a circular economy and renewable resources, a paradigm change is about to happen. Biorefineries and biobased products are seeing strong interest from various stakeholders, as do renewable energies, such as wind and solar.

However, when a realistic view is applied, one will quickly see that decarbonization is not that simple. Biomass and hydrogen will play an important role, for sure; the major issue with stepping out of oil is the sheer size of the industry. When one wants to replace the feedstock for 400 million tons of polymers per year, and for hundreds of millions of tons of base chemicals, agricultural resources are simply not sufficiently available, at least not without creating serious disruptions in feed and food production. There is not only a distribution problem of feed and food but a more fundamental land scarcity issue. We are simply not able to convert all "unmanaged" land into fields and pastures to cater to the world population not only for food but also for materials. Neither can be the productivity of the existing land be pushed upwards indefinitely; for fast, secure, and reliable scale-up of SCP, biopolymer, and other materials produced from non-agricultural and non-oil sources, methane from natural gas seems to be the one option.

Based on the circular economy concept, deriving nutrients from (bio)waste is a sustainable approach. For an analysis of SCP made from biowaste as a feed additive using, see Refs. [164, 165].

3.1 SCP

In **Table 27**, the market of alternative protein sources is summarized.

As **Table 27** exemplifies, the "farm gate" price of vegetable protein is rather low. Production volumes of alternative protein from microbes are tabulated (**Table 28**).

Today, yeast is undoubtedly the largest volume SCP source, also for food applications.

In Ref. [167], SCP production by the yeast *Kluyveromyces marxianus var marxianus* is described.

Protein source		Production volume [Mton DM/y]	Farm gate price [$/kg DM)	Average protein content [% DW]	Price per unit protein [$/kg protein DM]
Animal	Fish	66.7	2.07	15–20	10–14
	Pork	108.5	1.54	20	7.7
	Chicken	92.7	1.43	31	4.6
	Beef	62.7	2.70	25	10.8
Vegetable	Soybean	320.2	0.37	35	1.1
	Wheat	712.7	0.19	12	1.6
DM = dry matter. Reproduced from [166].					

Table 27.
Different animal and vegetable protein sources compared by their production volumes and prices.

Organisms	Production volume [ton DM/y]	Production costs [€/ kg DM]	Global market value [Billion €]	Yearly growth [% per year]	Remarks
Yeast	3,000,000	–	9.2	7.9	Mostly commercialized as baker's yeast and for ethanol fermentation. Global market value projected to 2019
Algae (microalgae)	9000	4–25	2.4	10	Besides feed and food, derivatives are also used
Mycoprotein (Quorn™)	25,000	–	0.214	–	Investments for a plant of 22,000 tons per year were done in 2015
Bacteria (Profloc™)	5000	1–1.1	–	–	No commercial production yet
Bacteria (FeedKind™)	80,000	–	–	–	No commercial production yet
Valpromic	5000	–	–	–	No commercial production yet

Source: [166].

Table 28.
Current status of different microbial proteins based on their market size and production volumes.

The FeedKind™ plant is currently under construction [168], Profloc™ went out of business.

When we assume a protein demand per person of 70 g per day of SCP, with a world population of 7.9 billion people, the theoretical market potential for bacterial SCP would be 0.5 million tons per day or 200 million tons per year. At a conversion ratio of 1 g CH_4 to 1 g of SCP, we arrive at ∼288 million m^3 of methane, which is approximately 7% of today's natural gas consumption. So if we were to provide all protein for humanity by bacterial SCP, only a fraction of the natural gas stream would be required.

Bacterial single-cell protein has also been envisioned as a possible protein source in a global food catastrophe, where agricultural protein production is suddenly impaired, as elaborated by Juan B. Garcia Martinez [169, 170].

3.2 Bioplastics

Today, bioplastics have a market share of 1–2% of conventional plastics materials. It is estimated that bioplastics could replace 90% of petrochemical plastics, particularly in standard application like packaging (only for high-performance materials, such as PEEK or PFTE, no suitable bioplastics counterparts is yet known to exist). **Table 29** takes a look at which bioplastics could replace the most common petrochemical plastics. For instance, LDPE could be replaced to some extent by a "drop in" material of similar property set (bio-PE), and by biopolymers with different characteristics, such as PBAT, PBS, and PHA, to the other part.

As **Table 29** shows, a handful of "drop-in" and degradable bioplastics can replace the most common petrochemical plastics. Overall, it is estimated that up to 90% of conventional polymers can be replaced by biopolymers. The benefits of such a replacement are depicted in **Figure 5**.

For simplification, the land use of petroplastics is set to zero, as it is negligible. Also, as **Figure 7** shows, the water use of petroplastics is low. The error bars indicate

Non-biodegradable			Biodegradable						
Petrochemical Plastics	Bioplastics (drop-in, partly biobased)		Petrochemical Plastics			Bioplastics			
		Bio-PTT	PBAT (can be partly biobased)	PBS	PHA	PLA	TPS	Cellulose-based	
LDPE	bio-PE	55		10		15	10	5	5
PP	bio-PP	10	5		10	20	20	15	20
HDPE	bio-PE	50		10		15	10	10	5
PET	bio-PET	60	10			5	20		5
PS						20	30	25	25
PVC	bio-PVC	50				20			30
EPS								70	30
PA	bio-PA	80							
PUR	bio-PUR	80	20			10		10	
Other thermo-plastics				10	10	20	20	20	20
Other plastics				10	10	20	20	20	20

 Numbers are in %. Source: [86].

Table 29.
Overview of the technical substitution potential of regular plastics (left columns) by bioplastics.
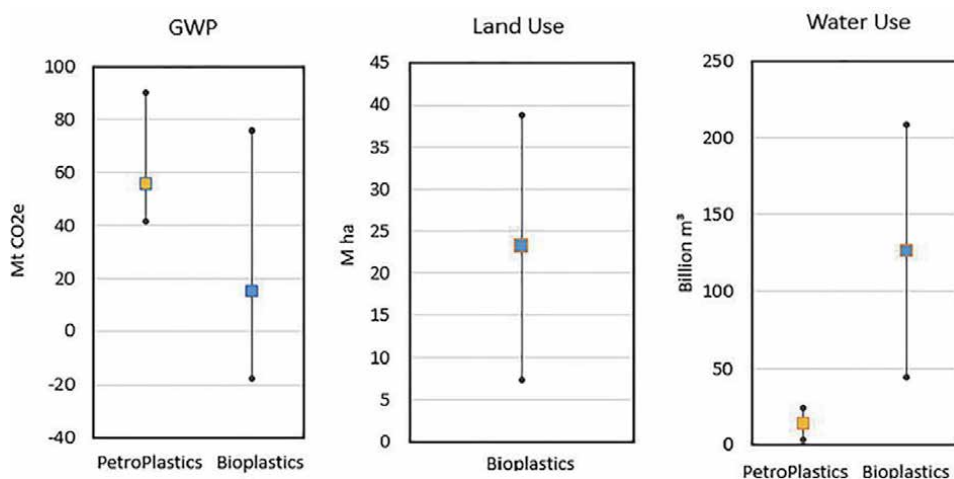
Figure 5.
GWP (global warming potential), land use, and water use of petrochemical and bioplastics packaging materials. Source: [86].

the possible range of the figures. According to IfBB [171], the footprint of bioplastics is considerable. For instance, 1 ton of PHB requires 2.86 tons of sugar (glucose) or 3.24 tons of starch for its production. One ton of PLA requires 1.47 tons of sugar or 1.67 tons of starch. Yields of crops differ, for example, 10.03 tons of sugar/ha for sugar beet and 0.83 tons of starch/ha for wheat, resulting in specific land requirements for the materials' feedstocks, see **Figure 6**.
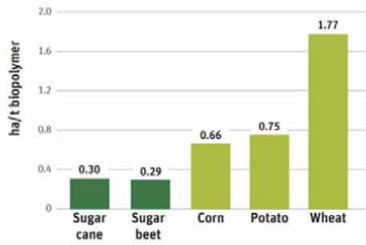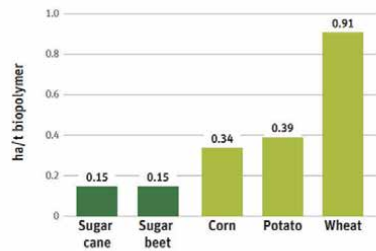
Figure 6.
The footprint of the two bioplastics PHB and PLA. Source: [171].

PLA today is the most important bioplastics material, and there is a shortage of supply in the market, leading to a surge in prices. The strong growth is expected to continue. Major producers of PLA are Total/Corbion (Purac™) and Cargill/Natureworks (Ingeo™). The PHB market cannot be considered mature, as the volume is still minute, but there are several established players, see **Table 30**.

Taking an existing biopolymer and devising a more cost-effective production technology is more likely to bring success than trying to synthesize and/or isolate a totally novel bioplastics material. Hence PLA and PHB are promising materials for methanotrophic fermentation.

Taking 90% of 400 million tons of polymers and a conversion ratio of 1 g of polymer per g of methane, we see that roughly 13% of the global natural gas production would be required to provide the feedstock for the plastics. When we further assume that in the future, a significant share of polymer materials will be recycled, the demand for virgin polymers will be lower, also reducing the fraction of natural gas needed to cater to it.

Current industrial production of polyhydroxyalkanoates (PHA)			
Company name	**Carbon substrate**	**Product name**	**Production [t/a]**
Danimer Scientific (formerly Meredian Holdings Group Inc./MHG)	Canola oil	Seluma™	15,000
Metabolix/Antibioticos	Witchgrass, camelina, sugar cane	Mirel, Mvera™	10,000
TianAn Biologic Material Co	Corn/cassava starch	ENMAT™	10,000
Tianjin GreenBio	Corn starch	SoGreen™	10,000
Bio-on	Beet or sugar cane	Bio-on™	10,000
Shenzhen Ecomann Biotech. Co	Corn starch		5000
PHB Industrial	Sugar cane	Biocycle™	2000
Kaneka	Vegetable oil	Aonilex™	1000
Biomer	Sugar (sucrose)	Biomer P™	–
Newlight Technologies	Waste methane	AirCarbon™	>500
Source: [163].			

Table 30.
Players in the PHB market today (status 2016).

Scale-up of PHB production by methanotrophic fermentation is discussed in Refs. [172–175].

3.3 Value-added materials

Likewise for the above-mentioned and further chemicals that can be obtained from methane by fermentation, there is a sound market. Like SCP and biopolymers, they can be produced virtually without requiring (agricultural) land. Decoupling manufacturing from both crude oil and farming activities is attractive as it relieves pressure on existing feed and food value chains. When we estimate that between 500 and 1000 million tons of chemicals are to be made from other sources than oil, at again a rough value of 1 g methane per g of product, we end up with 16–32% of natural gas consumption per year.
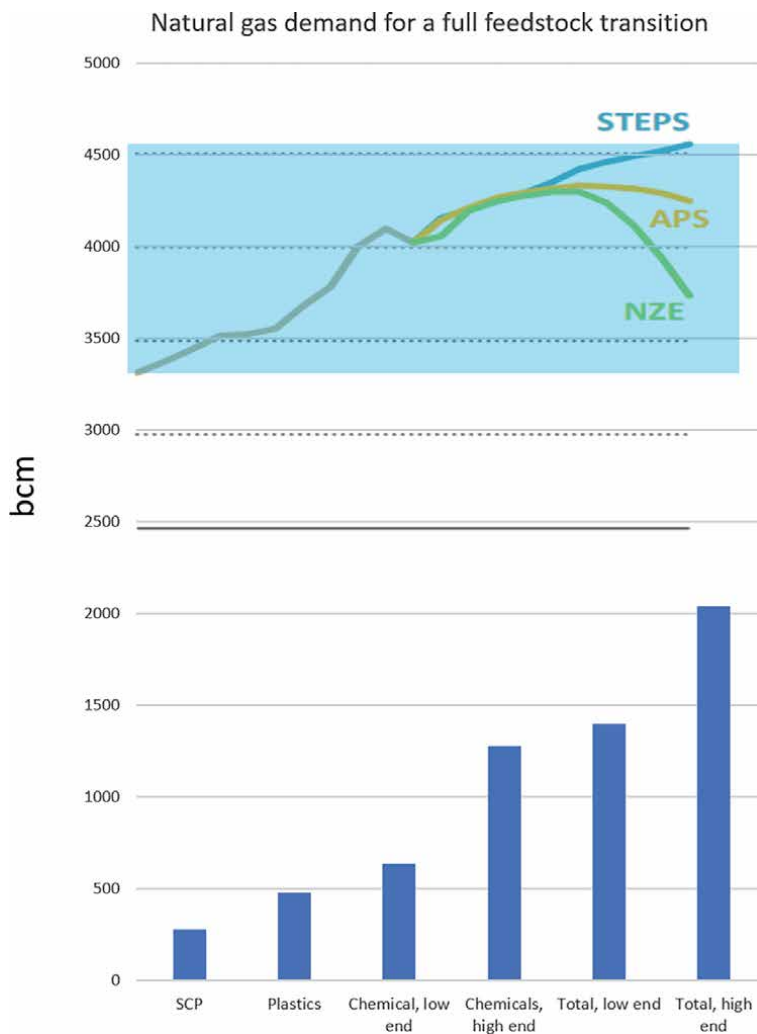

Figure 7.
Graphical depiction of annual natural gas demand for theoretically meeting the entire feedstock demand for SCP, plastics, and chemicals, compared to the natural gas production figures in IEA's scenarios STEPS, APS, and NZE, which span 3300–4500 billion m³/year annual demand between 2010 and 2030 (compare **Figure 7**).

3.4 Scenario of methane as sole feedstock

So if we were to produce "all" global demand for protein, plastics, and chemicals from natural gas, which for sure is an exaggerated assumption, we would require approximately 1/3 to 1/2 of the annual natural gas production of today. Let us revisit briefly **Figure 7** and add the above estimations to it:

Also, biogas could cater to that raw material need. Production volumes are not yet close to 2000 billion m^3 per year, but several studies suggest that that potential is within reach.

The authors are firmly convinced that methanotrophic gas fermentation is the key enabling technology to succeed in abandoning crude oil as universal feedstock, by allowing cost-effective and scaleable production of protein, plastics, and chemicals, in a sustainable way, by avoiding the need for immense agricultural and associated production factors, such as water, fertilizer, and pesticides. As Liew et al. have started in their review article [49]—gas fermentation offers a flexible platform for large, industrial-scale production of low-carbon-fuels and chemicals from various feedstocks. This view is shared by other researchers, see Ref. [176].

4. Summary and outlook

The world faces serious challenges from climate change, growing population, and increasing industrialization. The demand for food skyrockets, as does the desire for energy and various products. The capacity of the world's oceans to supply fish and of the world's fields to provide feed and food is limited, and measures to boost productivity have partly been exhausted. Prominent footprint calculations show clearly that the rate with which resources are consumed surpasses the regeneration by a factor of more than 2. Earth exhaustion day is advancing from year to year.

It is well-understood that the current meat production is not sustainable. Cultured meat obviously still needs significant development time to become cost-competitive [177]. Aquaculture can provide fish to the world's plate despite overfishing, but it needs fodder, which today is often taken from oceans—fish meal and fish oil, or soy, which has its own sustainability issues. Plant-based protein for food is not necessarily sustainable either, considering the large land areas that are required, besides fertilizers, pesticides, etc.

There is an urgent need for large-scale and cheap protein sources that are independent of land use. This has re-sparked interest in microbial protein production, which does not need but very little land and water—feeding microbes sugar or starch virtually perverts any attempts for sustainability: Methane can be a very valid option here. Øverland et al. argued: *"In recent years, the increasing global demand for sustainable protein sources, independent of marine origin, agricultural land use, and climatic changes, has led to renewed attention on the potential of microbial protein for use in animal production. Focus has been on methane, the main component of natural gas, which is found widely in nature [28] as an attractive substrate for bacterial protein production. The abundant supply, cheap transportation, and reasonable cost of natural gas indicate that protein production from natural gas could be realistic on a large scale. Using methane-oxidising bacteria as an amino acid source in animal nutrition may* spare over-exploited sources of protein suitable for direct human consumption" [65].

Protein from natural gas might, in the unfortunate event of a global food catastrophe, be a vital protein source for several years. As Allfed states: *"Human civilization's food production system is unprepared for global catastrophic risks (GCRs). Catastrophes capable of abruptly transforming global climate, such as supervolcanic eruption, asteroid/comet impact, or nuclear winter, which could completely collapse the*

agricultural system. Responding by producing resilient foods requiring little to no sunlight is more cost-effective than increasing food stockpiles, given the long duration of these scenarios (6–10 years)" [169]. The preliminary techno-economic analysis revealed that bacterial SCP can be ramped up fast for global food production when needed [169]. Also, bacterial SCP might play a pivotal role in the energy transition, by providing suitable storage capacity for excess renewable energy in a Power2protein setup [178].

We see strong market dynamics in natural gas fermentation these days. This can be inferred from trends in scientific publications, patent applications, and commercial activities, such as pilot or manufacturing plant establishments by several market incumbents. It can be expected that the interest in this set of technologies will be even more in the near and medium-term future, as the key enabling technology for scaling up bioplastics production, protein manufacturing, and chemicals synthesis in a sustainable way, decoupled from agricultural operations.

Conflict of interest

The authors declare that they have no conflict of interest.

Author details

Maximilian Lackner[1]*, David Drew[1], Valentina Bychkova[1] and Ildar Mustakhimov[2]

1 Circe Biotechnologie GmbH, Vienna, Austria

2 Federal Research Center "Pushchino Scientific Center for Biological Research of the Russian Academy of Sciences", G.K. Skryabin Institute of Biochemistry and Physiology of Microorganisms, Russian Academy of Sciences, Moscow Region, Russian Federation

*Address all correspondence to: m.lackner@circe.at

IntechOpen

References

[1] AlSayed A, Fergala A, Eldyasti A. Sustainable biogas mitigation and value-added resources recovery using methanotrophs integrated into wastewater treatment plants. Reviews in Environmental Science and Biotechnology. 2018;**17**:351-393. DOI: 10.1007/s11157-018-9464-3

[2] Patel SKS, Kondaveeti S, Lee J-K. Repeated batch methanol production from a simulated biogas mixture using immobilized *Methylocystis bryophila*. Energy. 2017;**145**:477-485

[3] Spring F. Naturally occurring polyesters. Nature. 1945;**155**:272. DOI: 10.1038/155272b0

[4] Nawrath C, Poirier Y. Pathways for the synthesis of polyesters in plants: Cutin, suberin, and polyhydroxy alkanoates, Chapter 8. In: Advances in Plant Biochemistry and Molecular Biology. Vol. 1. 2008. pp. 201-239

[5] Harwood JH, Pirt SJ. Quantitative aspects of growth of the methane oxidizing bacterium *Methylococcus capsulatus* on methane in shake flask and continuous chemostat culture. Journal of Applied Bacteriology. 1972;**35**:697-607

[6] Rostkowski KH, Criddle CS, Lepech MD. Cradle-to-gate life cycle assessment for a cradle-to-cradle cycle: Biogas-to-bioplastic (and back). Environmental Science and Technology. 2012;**46**:9822-9829. DOI: 10.1021/es204541w

[7] Rostkowski KH, Pfluger AR, Criddle CS. Stoichiometry and kinetics of the PHB-producing Type II methanotrophs, *Methylosinus trichosporium* OB3b and *Methylocystis parvus* OBBP. Bioresource Technology. 2013;**132**:71-77

[8] Wang J, Salem DR, Sani RK. Microbial polymers produced from methane: Overview of recent progress and new perspectives. Microbial and Natural Macromolecules. 2021. DOI: 10.1016/B978-0-12-820084-1.00006-5

[9] Poirier Y. Polyhydroxyalknoate synthesis in plants as a tool for biotechnology and basic studies of lipid metabolism. Progress in Lipid Research. 2002;**41**(2):131-155

[10] Park SJ, Kim TW, Lim S-C. Advanced bacterial polyhydroxyalkanoates: Towards a versatile and sustainable platform for unnatural tailor-made polyesters. Biotechnology Advances. 2012;**30**(6): 1196-1206

[11] Babu RP, O'Connor K, Seeram R. Current progress on bio-based polymers and their future trends. Progress in Biomaterials. 2013;**2**(8):1-16. DOI: 10.1186/2194-0517-2-8

[12] go!PHA. Available from: http://www.gopha.org [Accessed: 13 January 2022]

[13] Myung J, Flanagan JCA, Waymouth RM, Criddle CS. Expanding the range of polyhydroxyalkanoates synthesized by methanotrophic bacteria through the utilization of omega-hydroxyalkanoate co-substrates. AMB Express. 2017;**7**:118. DOI: 10.1186/s13568-017-0417-y

[14] Yadav B, Pandey A, Rajeshwar BT, Tyagi D, Drogui P. 17—Polyhydroxyalkanoate production from feedstocks: Technological advancements and techno-economic analysis in reference to circular bioeconomy. In: Biomass, Biofuels, Biochemicals, Circular Bioeconomy—Current Status and Future Outlook. Amsterdam, Netherlands: Elsevier. 2021. pp. 477-513

[15] Wingender J, Neu TR, Wingender J, Neu TR, Flemming H-C. Microbial Extracellular Polymeric Substances: Characterization, Structure and

Function. Berlin Heidelberg: Springer-Verlag; 1999

[16] Sandford PA, Laskin AI. Extracellular Microbial Polysaccharides. Washington, USA: American Chemical Society. 1978. ISBN: 978-0841203723

[17] Gęsicka A, Oleskowicz-Popiel P, Łężyk M. Recent trends in methane to bioproduct conversion by methanotrophs. Biotechnology Advances. 2021;**53** Article 107861

[18] Production of lactic acid from organic waste or biogas or methane using recombinant methanotrophic bacteria. EP 9.3129513. 15.02.2017

[19] Method for producing isoprene using recombinant halophilic methanotroph. SK Innovation Co.; June 12, 2018. US 9994869

[20] Methanotrophic mutant strain for producing squalene. KR 1020180124189. 21.11.2018

[21] Production of succinic acid from organic waste or biogas or methane using recombinant methanotrophic bacterium. WO/2015/155791. 15.10.2015

[22] Methanobactin: A copper binding compound having antibiotic and antioxidant activity isolated from methanotrophic bacteria. US 75.20040171519. 02.09.2004

[23] Cantera S, Lebrero R, Muñoz R. Ectoine bio-milking in methanotrophs: A step further towards methane-based bio-refineries into high added-value products. Chemical Engineering Journal. 2017;**328**:44-48

[24] Cantera S, Lebrero R, Rodríguez E, García-Encina PA, Munoz R. Continuous abatement of methane coupled with ectoine production by *Methylomicrobium alcaliphilum* 20Z in stirred tank reactors: A step further towards greenhouse gas biorefineries.

Journal of Cleaner Production. 2017;**152**: 134-141

[25] Henard CA, Akberdin IR, Kalyuzhnaya MG, Guarnieri MT. Muconic acid production from methane using rationally-engineered methanotrophic biocatalysts. Green Chemistry. 2019;**21**:6731-6737. DOI: 10.1039/C9GC03722E

[26] Ye RW, Yao H, Stead K, Wang T, Tao L, Cheng Q, et al. Construction of the astaxanthin biosynthetic pathway in a methanotrophic bacterium *Methylomonas* sp. strain 16a. Journal of Industrial Microbiology and Biotechnology. 2007;**34**(4):289. DOI: 10.1007/s10295-006-0197-x

[27] Strong PJ, Kalyuzhnaya M, Clarke WP. A methanotroph-based biorefinery: Potential scenarios for generating multiple products from a single fermentation. Bioresource Technology. 2016;**215**:314-323

[28] Lee SY, Cho JM, Chang YK, Oh Y-K. Cell disruption and lipid extraction for microalgal biorefineries: A review. Bioresource Technology. 2017;**244**:1317-1328

[29] Nitsos C, Filali R, Taidi B, Lemaire J. Current and novel approaches to downstream processing of microalgae: A review. Biotechnology Advances. 2020; **45**:107650

[30] DaSilva EJ, Ratledge C, Sasson A. Biotechnology: Economic and social aspects (issues for developing countries). The Economic Viability of Single Cell Protein (SCP) Production in the Twenty-First Century; Cambridge, UK: Cambridge University Press. 1992

[31] Babel W. Ullmann's Encyclopedia of Industrial Chemistry. Single Cell Proteins; Weinheim, Germany: Wiley VCH. 2000

[32] SRL S, Beveridge EG, Elton C, Danielli JF, Booth IR, Herbert HB. New horizons in industrial microbiology. Single cell protein [and discussion]. Philosophical Transactions of the Royal Society of London Series B Biological Sciences (1934–1990). 1980

[33] Ali S, Mushtaq J, Nazir F, Sarfraz H. Production and processing of single cell protein (SCP)—A review. European Journal of Pharmaceutical and Medical Research. 2017;**4**:86-94

[34] Bewersdorff M, Dostálek M. The use of methane for production of bacterial protein. Biotechnology and Bioengineering. 1971. DOI: 10.1002/bit.260130104

[35] Calcott PH. Continuous Cultures Of Cells. Boca Raton, Florida, USA: CRC Press; 1981 ISBN: 9781000694574

[36] Koo CW, Rosenzweig AC. Biochemistry of aerobic biological methane oxidation. Chemical Society Reviews. 2021;**50**:3424-3436. DOI: 10.1039/D0CS01291B

[37] Schøyen HF, Svihus B, Storebakken T, Skrede A. Bacterial protein meal produced on natural gas replacing soybean meal or fish meal in broiler chicken diets. Archives of Animal Nutrition. 2007;**61**(4):276-291. DOI: 10.1080/17450390701431953

[38] Production of single cell protein by methanol-using bacteria. Journal of Fermentation Technology. 1986;**64**(2):97-186

[39] Single-cell protein. Safety for Animal and Human Feeding. Proceedings of the Protein-Calorie Advisory Group of the United Nations System Symposium "Investigations on Single-Cell Protein" held at the Istituto di Ricerche Farmacologiche 'Mario Negri' Milan, Italy, March 31–April 1, 1977. ISBN: 0-08-023764-9

[40] Liquid protein diets. Hearing Before The Subcommittee on Health and The Environment of The Committee on Interstate and Foreign Commerce Ninety-Fifth Congress. First Session To Provide Consumers With Better Information On The Most Popular Diet In America Today. Liquid. Serial No. 95-83. December 28, 1977

[41] Opinion of the Scientific Panel on additives and products or substances used in animal feed (FEEDAP) on the safety of BioProtein: Product of fermentation from natural gas. 4 July 2005. Available from: https://www.efsa.europa.eu/en/efsajournal/pub/230. doi: 10.2903/j.efsa.2005.230

[42] Giec A, Skupin J. Single cell protein as food and feed. Molecular Nutrition & Food Research. 1988;**32**(3):219–229

[43] Sherwood M. Single-cell protein comes of age. New Scientist. 1974;**28** (11):634-639

[44] Bratosin BC, Darjan S, Vodnar DC. Single cell protein: A potential substitute in human and animal nutrition. Sustainability. 2021;**13**:9284. DOI: 10.3390/su13169284

[45] Ravindra AP. Value-added food: Single cell protein. Biotechnology Advances. 2000;**18**:459-479

[46] Patias LD, Maroneze MM, Siqueira SF, de Menezes CR, Zepka LQ, Jacob-Lopes E. Single-cell protein as a source of biologically active ingredients for the formulation of antiobesity foods. Alternative and Replacement Foods. DOI: 10.1016/B978-0-12-811446-9.00011-3

[47] Lipids from methanotrophic bacteria for cholesterol reduction. 05.04.2006. EP 79.1641475

[48] Vahidi H, Mojab F, Taghavi N. Effects of carbon sources on growth and production of antifungal agents by

Gymnopilus spectabilis. Iranian Journal of Pharmaceutical Research. 2006;**3**:219-222

[49] Liew FM, Martin ME, Tappel RC, Heijstra BD, Mihalcea C, Köpke M. Gas fermentation—A flexible platform for commercial scale production of low-carbon-fuels and chemicals from waste and renewable feedstocks. Frontiers in Microbiology. 2016;**7**:694. doi: 10.3389/fmicb.2016.00694

[50] Kunasundari B, Murugaiyah V, Kaur G, Maurer FHJ, Sudesh K. Revisiting the single cell protein application of *Cupriavidus necator* H16 and recovering bioplastic granules simultaneously. PLoS ONE. 2013;**8**(10):e78528. Available from: www.plosone.org

[51] Goldberg I. Single Cell Protein. New York, USA: Springer; 1985. ISBN: 978-3-642-46542-0. DOI: 10.1007/978-3-642-46540-6

[52] Available from: https://www.heise.de/tp/features/Zur-Geschichte-einer-ehemaligen-Zukunftstechnologie-die-noch-nicht-abgehakt-ist-4221160.html?seite=all

[53] Egorov I, Kupina L, Aksyuk I, Murtazaeva R. Gaprin—A protein source. Ptitsevodstvo. 1990;**8**:25-27

[54] Chirikov S, Shkirin A, Savchenko I, Bunkin N, Diuldin M. Assessment of the possibility of identifying aqueous suspensions of protein-containing particles by the light scattering matrix. In: ECOBALTICA 2019, IOP Conf. Series: Earth and Environmental Science. 2019;390:012030. doi:10.1088/1755-1315/390/1/012030

[55] Chirikov SN, Shkirin AV, Konnova AS. Study of light-scattering properties of protein-containing microparticles with a small difference in refractive indices. Journal of Physics. 2020

[56] Kent JA. Riegel's Handbook of Industrial Chemistry. Springer; 1992 ISBN: 9781475764338

[57] Champagnat A, Vernet C, Lainé B, Filosa J. Biosynthesis of protein–vitamin concentrates from petroleum, Nature, 1963;**197**:13–14

[58] Champagnat A. Protein from petroleum. Scientific American. 1965; **213**(4):13-17

[59] Alani DI, Moo-Young M. Single cell protein production from petroleum derivatives and its utilization as food and feed. Perspectives in Biotechnology and Applied Microbiology. 1986;1-6. DOI: 10.1007/978-94-009-4321-6_1

[60] Ismail WA, Van Hamme, Jonathan D, Kilbane JJ, Gu J-D. Editorial: Petroleum Microbial Biotechnology: Challenges and Prospects

[61] Henk G, Heinz T. Hydrocarbon content in the fat of meat pigs after feeding "Fermosin". Arch Tierernahr. 1993;**45**(1):35-47. DOI: 10.1080/17450399309386086

[62] Alani DI, Moo-Young M. The economical aspects of single cell protein production from petroleum derivatives. Perspectives in Biotechnology and Applied Microbiology. 1986

[63] Regulations Commission Regulation (EU) No. 68/2013 of 16 January 2013 on the Catalogue of feed materials (text with EEA relevance)

[64] Han B, Tao S, Hao W, Gou Z, Xing X-H, Jiang H, et al. Paraffin oil as a "methane vector" for rapid and high cell density cultivation of *Methylosinus trichosporium* OB3b. Applied Microbiology and Biotechnology. 2009; **83**:669-677. DOI: 10.1007/s00253-009-1866-2

[65] Øverland M, Tauson A-H, Shearer K, Skrede A. Evaluation of methane-utilising bacteria products as feed ingredients for monogastric animals. Archives of Animal Nutrition. 2010;**64**

(3):171-189. DOI: 10.1080/ 17450391003691534

[66] Nevalainen H, editor. Grand Challenges in Fungal Biotechnology. New York, USA: Springer ISBN: 978-3-030-29540-0; 2020. DOI: 10.1007/978-3-030-29541-7

[67] Knight N, Roberts G, Shelton D. The thermal stability of Quorn™ pieces. International Journal of Food Science & Technology. 2001;**36**(1):47-52

[68] ICI to scale up single cell protein process, Chemical & Engineering News, 1976;**54**(42):25. DOI: 10.1021/cen-v054n042.p025

[69] Rose AH. The microbiological production of food and drink. Scientific American. 1981;**245**(3):126-134. DOI: 10.1038/scientificamerican0981-126

[70] Jenkins G. SCP—The BP protein process. In: Greenshields R, editor. Resources and Applications of Biotechnology. 1988

[71] Verrier D, Morfaux JN, Albagnac G, Touzel JP. The French programme on methane fermentation. Biomass. 1982

[72] Damron BL, Simpson CF, Eldred AR, Harms RH. Liquipron as a protein source for broilers. Poultry Science. 1979;**58**:247-249

[73] Available from: https://www. equinor.com/en/news/archive/1999/02/ 17/BioproteinBegins.html

[74] Olsen DF, Jørgensen JB, Villadsen J, Jørgensen SB. Modeling and simulation of single cell protein production. In: Banga JR, Bogaerts P, Van Impe J, Dochain D, Smets I, editors. Proceedings of the 11th International Symposium on Computer Applications in Biotechnology (CAB 2010), Vol. 43 (6); July 7–9, 2010; Leuven, Belgium; IFAC Proceedings Volumes. 2010. pp. 502-507

[75] Nunes JJ. Theoretical energy requirements of single cell protein production from methanol and methane using metabolic flux analysis. In: Proceedings of the Tobago Gas Technology Conference (TGTC) 2008, Conference Paper. 2008

[76] Opinion on the safety of BioProtein® by the Scientific Panel on Animal Feed of the Norwegian Scientific Committee for Food Safety, Revised version. Adopted on the 5th of October 2006, VKM Report 2006: 43

[77] Perlman D. Annual reports on fermentation processes. Annual Reports on Fermentation Processes. Cambridge, Massachusetts, USA: Academic Press. 1977. pp. 1. ISBN: 0-12-040301-3

[78] James K. Single cell protein process targeted for licensing. Chemical & Engineering News. 1983;**61**. DOI: 10.1021/cen-v061n031.p021

[79] Single Cell Protein Process Targeted for Licensing. August 1, 1983 C&EN, 21

[80] Israelidis CJ. Nutrition-single cell protein, twenty years later. Available from: https://www.semanticscholar.org/ paper/NUTRITION-SINGLE-CELL-PROTEIN-%2C-TWENTY-YEARS-LATER-Israelidis/cd52ecd95eb39b199b 3fc33893fda2b0cc77ac07

[81] Katsnelson A. Dow pulls out of bioplastics due to slow sector maturation. Nature Biotechnology. 2005;**23**:638

[82] Tannenbaum SR, Wang DIC, editors. Single-Cell Protein II. MIT Press; 1975. ISBN: 0-262-20030-9

[83] Hamer G, Harrison DEF. Single cell protein: The technology, economics and future potential. In: Harrison DEF, Higgins IJ, Watkinson R, editors. Hydrocarbons in Biotechnology.

London: Heyden & Son, Ltd.; 1980. pp. 59-73

[84] Mateles RI, Tannenbaum SR, editors. Single-Cell Protein. Cambridge, Massachusetts: MIT Press; 1968

[85] Cooney CL, Rha C, Tannenbaum SR. Single-cell protein: Engineering, economics, and utilization in foods. Advances in Food Research. 1980; **26**:1-52

[86] Brizga J, Hubacek K, Feng K. The unintended side effects of bioplastics: Carbon, land, and water footprints. One Earth. 2020;**3**(1):45-53

[87] Kuzniar A, Furtak K, Włodarczyk K, Stepniewska Z, Wolinska A. Methanotrophic bacterial biomass as potential mineral feed ingredients for animals. International Journal of Environmental Research and Public Health. 2019;**16**:2674. DOI: 10.3390/ijerph16152674

[88] Gerth K, Trowitzsch W, Piehl G, Schultze R, Lehmann J. Inexpensive media for mass cultivation of myxobacteria. Applied Microbiology and Biotechnology. 1984;**19**:23-28

[89] Núñez Decap M, Ballerini Arroyo A, Alarcón Énos J. Evaluation of single cell protein from yeast for the development of wood adhesives. European Journal of Wood and Wood Products. 2016;**74**:821-828. DOI: 10.1007/s00107-016-1063-9

[90] Yazdian F, Hajizadeh S, Shojaosadati SA, Khalilzadeh R, Jahanshahi M, Nosrati M. Production of single cell protein from natural gas: Parameter optimization and RNA evaluation. Iranian Journal of Biotechnology. 2005;**3**(4):235

[91] Bhalla TC, Mehta PK, Bhatia SK, Pratush A. Microorganisms for food and feed. In: Fundamentals of Food

Biotechnology. New Delhi, India: Anne Publisher; 2009. Available from: https://www.researchgate.net/publication/303941522_Microorganism_for_food_and_Feed

[92] Taran M, Asadi N. A novel approach for environmentally friendly production of single cell protein from petrochemical wastewater using a halophilic microorganism in different conditions. Petroleum Science and Technology. 2014;**32**:625-630

[93] Zha X, Tsapekos P, Zhu X, Khoshnevisan B, Lu X, Angelidaki I. Bioconversion of wastewater to single cell protein by methanotrophic bacteria. Bioresource Technology. 2021;**320**: 124351

[94] Rasouli Z, Valverde-Pérez B, D'Este M, De Francisci D, Angelidaki I. Nutrient recovery from industrial wastewater as single cell protein by a co-culture of green microalgae and methanotrophs. Biochemical Engineering Journal. 2018;**134**:129-135

[95] Xu M, Zhou H, Yang X, Angelidaki I, Zhang Y. Sulfide restrains the growth of *Methylocapsa acidiphila* converting renewable biogas to single cell protein. Water Research. 2020;**184**:116138

[96] Yazdian F, Hajizadeh S, Shojaosadati SA, Khalilzadeh R, Jahanshahi M, Nosrati M. Production of single cell protein from natural gas: Parameter optimization and RNA evaluation. Iranian Journal of Biotechnology. 2005;**3**:235-242

[97] Marstrand PK. Production of microbial protein: A study of the development and introduction of a new technology. Research Policy. 1981;**10**(2): 148-171

[98] Frydendahl Hellwing AL. Bacterial protein meal as protein source for monogastric animals—Comparative studies on protein and energy,

metabolism [PhD thesis]. Frederiksberg, Denmark: Samfundslitteratur Grafik; 2005. ISBN: 87-7611-110-5

[99] Volesky B, Zajic JE, Carroll KK. Author notes: Feeding studies in rats with high protein fungus grown on natural gas. The Journal of Nutrition. 1975;**105**(3):311-316. DOI: 10.1093/jn/105.3.311

[100] Walz OP, Brune H. Zeitschrift für Tierphysiologie Tierernährung und Futtermittelkunde. Proteinverwertung und Wirkung von Methioninergänzung bei Einzellerbiomasse aus Methylomonas clara gemessen mit Ratten und Absetzferkeln. January–August 1984. doi:10.1111/j.1439-0396.1984.tb01428.x

[101] Hanssen JT. Bioproteins in the feeding of growing–finishing pigs in Norway: I. Chemical composition, nutrient digestibility and protein quality of "Pruteen", "Toprina", "Pekilo" and a methanol-based yeast product (*Pichia aganobii*). Journal of Animal Physiology and Animal Nutrition. 1981;**46**(1-5): 182-196

[102] Becker PM. Single cell proteins in diets for weanling pigs. Report 03/0016848. Animal Sciences Group-Nutrition & Food

[103] Stiglmair-Herb MT, Pospischil A. Enzymhistochemische Untersuchungen am Darmepithel von Hunden nach Kasein-Diät, Single Cell Protein-Diät und konventioneller Fütterung. Transboundary and Emerging Diseases. 1985;**32**(1-10):764-771

[104] Teller E, Godeau J-M. Evaluation of the nutritive value of single-cell protein (Pruteen) for lactating dairy cows. The Journal of Agricultural Science. 1986;**106**(3):593-599. DOI: 10.1017/S0021859600063462

[105] Van Weerden EJ, Huisman J. Digestibility of protein and amino acids

of a fermentation single-cell protein for veal calves. Animal Feed Science and Technology. 1977;**1**(4):377-383

[106] Zamani A, Khajavi M, Nazarpak MH, Gisbert E. Evaluation of a bacterial single-cell protein in compound diets for rainbow trout (*Oncorhynchus mykiss*) fry as an alternative protein source. Animals. 2020;**10**:1676. DOI: 10.3390/ani10091676

[107] Jintasataporn O, Chumkam S, Triwutanon S, LeBlanc A, Sawanboonchun J. Effects of a single cell protein (*Methylococcus capsulatus*, Bath) in Pacific White Shrimp (*Penaeus vannamei*) diet on growth performance, survival rate and resistance to *Vibrio parahaemolyticus*, the causative agent of acute hepatopancreatic necrosis disease. Frontiers in Marine Science. 2021;**8**: 764042. DOI: 10.3389/fmars.2021.764042

[108] Chen Y, Chi S, Zhang S, Dong X, Yang Q, Liu H, et al. Replacement of fish meal with Methanotroph (*Methylococcus capsulatus*, Bath) bacteria meal in the diets of Pacific white shrimp (*Litopenaeus vannamei*). Aquaculture. 2021;**541**:736801

[109] Kabwe M, Chama H, Liang H, Ke J. Methanotroph (*Methylococcus capsulatus*, Bath) as an alternative protein source for genetically improved farmed tilapia (GIFT: *Oreochromis niloticus*) and its effect on antioxidants and immune response. Aquaculture Reports. 2021;**21**. Article 100872

[110] Davies SJ, Wareham H. A preliminary evaluation of an industrial single cell protein in practical diets for tilapia (*Oreochromis mossambicus* Peters). Aquaculture. 1988

[111] Biswas A, Takakuwa F, Tanaka H. Methanotroph (*Methylococcus capsulatus,* Bath) bacteria meal as an alternative protein source for Japanese

yellowtail, *Seriola quinqueradiata*. Aquaculture. 2020;**529**. Article 735700

[112] Sisman T, Gur O, Dogan N, Ozdal M, Algur OF, Ergon T. Single-cell protein as an alternative food for zebrafish, *Danio rerio*: A toxicological assessment. Toxicology and Industrial Health. 2013

[113] Glencross BD, Huyben D, Schrama JW. The application of single-cell ingredients in aquaculture feeds—A review. Fishes. 2020;**5**:22. DOI: 10.3390/ fishes5030022

[114] Tlusty M, Rhyne A, Szczebak JT, Bourque B, Bowen JL, Burr G, et al. A transdisciplinary approach to the initial validation of a single cell protein as an alternative protein source for use in aquafeeds. PeerJ. 2017;**5**:e3170. DOI: 10.7717/peerj.3170

[115] Christensen HR, Larsen LC, Frøkiær H. The oral immunogenicity of BioProtein, a bacterial single-cell protein, is affected by its particulate nature. British Journal of Nutrition. 2003;**90**(1):169-178. DOI: 10.1079/ BJN2003863

[116] Litchfield JH. Production of single-cell protein for use in food or feed. In: Microbial Technology. 2nd ed. Academic Press, Inc.; 1979. ISBN: 0-12-551501-4

[117] Available from: http://www.freie nohler.de/index.php/freienohl/geschich te/16-geschichte/481-die-wildshauser-holz-bzw-leberwurst-1943-1949.html

[118] Ritala A, Häkkinen ST, Toivari M, Wiebe MG. Single cell protein—State-of-the-art, industrial landscape and patents 2001–2016. Frontiers in Microbiology. 2017

[119] Romarheim OH, Landsverk T, Mydland LT, Skrede A, Øverland M. Cell wall fractions from *Methylococcus capsulatus* prevent soybean meal-induced enteritis in Atlantic salmon (*Salmo salar*). Aquaculture. 2013; **402–403**:13-18

[120] Skrede A, Faaland Schøyen H, Svihus B, Storebakken T. The effect of bacterial protein grown on natural gas on growth performance and sensory quality of broiler chickens. Canadian Journal of Animal Science. 2013

[121] EU is one step closer to the use of PAPs in animal feed—All about feed. Available from: https://www.allab outfeed.net/animal-feed/raw-materials/ eu-is-one-step-closer-to-the-use-of-paps-in-animal-feed/

[122] Bovine spongiform encephalopathy (BSE). EFSA (europa.eu). Available from: https://www.efsa.europa.eu/en/ topics/topic/bovine-spongiform-encephalopathy-bse

[123] Skrede A, Mydland LT, Øverland M. Effects of growth substrate and partial removal of nucleic acids in the production of bacterial protein meal on amino acid profile and digestibility in mink. Journal of Animal and Feed Sciences. 2009;**18**:689-698

[124] Li S, Jiang W, Li M. Oral delivery of bacteria: Basic principles and biomedical applications. Journal of Controlled Release. 2020;**327**: 801-833

[125] Liong M-T, editor. Beneficial Microorganisms in Food and Nutraceuticals. Basel, Switzerland: Springer International Publishing; 2015

[126] Microorganisms in Foods 6: Microbial Ecology of Food Commodities (Microorganisms in Foods). 2nd ed. International Commission on Microbiological Specifications of Foods (ICMSF); 2005 ISBN: 97803872 88017

[127] Microorganisms in Foods 7: Microbiological Testing in Food Safety Management. 2nd ed, ISBN: 9783319684604. International Commission on Microbiological Specifications for Foods (ICMSF); 2018

[128] International Commission on Microbiological Specifications for Foods. Microorganisms in Foods 8: Use of Data for Assessing Process Control and Product Acceptance. USA, ISBN: 9781441993748: Springer; 2011

[129] Koivurinta J, Kurkela R, Koivistoinen P. Uses of Pekilo, a microfungus biomass from *Paecilomyces varioti* in sausage and meat balls. Journal of Food Science and Technology. 1979; **14**:561-570

[130] Available from: https://www.eniferbio.fi/eniferbio-received-a-e1-2m-blueinvest-grant-by-the-european-maritime-and-fisheries-fund-emff/

[131] LaTurner ZW, Bennett GN, San K-Y, Stadler Lauren B. Single cell protein production from food waste using purple non-sulfur bacteria shows economically viable protein products have higher environmental impacts. Journal of Cleaner Production. 2020

[132] Vogel A, May O. Industrial Enzyme Applications. Wiley–VCH, ISBN: 9783527813780; 2019

[133] Abrahamsson L, Hambraeus L, Hofvander Y, Vahlquist B. Single cell protein in clinical testing, a tolerance test in healthy adult subjects comprising biochemical, clinical and dietary evaluation. Nutrition Metabolism. 1971; **13**:186-199

[134] Steinmann J, Wottge H-U, Müller-Ruchholtz W. Immunogenicity testing of food proteins: In vitro and in vivo trials in rats. International Archives of Allergy & Applied Immunology. 1990; **91**:62-65

[135] Hedenskog G, Ebbinghaus L. Reduction of the nucleic acid content of single-cell protein concentrates. Biotechnology and Bioengineering. 1972;**XIV**:447-457

[136] Jonas DA, Elmadfa I, Engel K-H, Heller KJ, Kozianowski G, König A, et al. Safety considerations of DNA in food. Annals of Nutrition & Metabolism. 2001;**45**:235-254

[137] Abou-Zeid A-ZA, Khan JA, Abulnaja KO. On methods for reduction of nucleic acids content in a single-cell protein from gas oil. Bioresource Technology. 1995;**52**:21-24

[138] Available from: https://solarfoods.fi/our-news/solein-submitted-to-the-european-commission-for-novel-food-approval/

[139] Ekenvall L, Dölling B, Göthe C-J, Ebbinghaus L, Von Stedingk L-V, Wasserman J. Single cell protein as an occupational hazard. British Journal of Industrial Medicine. 1983

[140] Kundiyana DK, Huhnke RL, Maddipati P, Atiyeh HK, Wilkins MR. Feasibility of incorporating cotton seed extract in *Clostridium* strain P11 fermentation medium during synthesis gas fermentation. Bioresource Technology. 2010;**101**(24):9673-9680

[141] Takashima M, Speece RE. Mineral nutrient requirements for high-rate methane fermentation of acetate at low SRT. Research Journal of the Water Pollution Control Federation. 1989;**61** (11/12):1645-1650

[142] Takashima M, Speece RE, Parkin GF. Mineral requirements for methane fermentation. Critical Reviews in Environmental Control. 1990:465-479. DOI: 10.1080/10643389009388378

[143] Paek K-Y, Murthy HN, Zhong J-J, editors. Production of Biomass and Bioactive Compounds using Bioreactor

Technology. Netherlands: Springer; 2014

[144] Ye Q, Bao J, Zhong J-J. Bioreactor Engineering Research and Industrial Applications. I: Cell Factories. Berlin Heidelberg: Springer-Verlag; 2016 ISBN: 9783662491614

[145] Kadic E, Heindel TJ. An Introduction to Bioreactor Hydrodynamics and Gas-Liquid Mass Transfer. Weinheim, Germany: Wiley, ISBN: 9781118104019; 2014

[146] Liao Q, Chang J-s, Herrmann C, Xia A. Bioreactors for Microbial Biomass and Energy Conversion. Singapore, ISBN: 9789811076770: Springer; 2018

[147] Reisman HB. Economic Analysis of Fermentation Processes. Boca Raton, Florida, USA: CRC Press LLC, ISBN: 9780429553165; 2019

[148] Jones SW, Karpol A, Friedman S, Maru BT, Tracy BP. Recent advances in single cell protein use as a feed ingredient in aquaculture. Current Opinion in Biotechnology. 2020;**61**: 189-197

[149] Available from: Strategies for success in single-cell protein production (luxresearchinc.com), https://www. luxresearchinc.com/blog/strategies-for-success-in-single-cell-protein-production

[150] F3 FIN: Feed Innovation Network. Available from: https://f3fin.org/

[151] Nasseri AT, Rasoul-Amini S, Morowvat MH, Ghasemi Y. Single cell protein: Production and process. American Journal of Food Technology. 2011;**6**(2):103-116

[152] Koutinas AA, Toutoutzidakis G, Kana K, Kouinis I. Methane fermentation promoted by γ-alumina pellets. Journal of Fermentation and Bioengineering. 1991;**72**(1):64-67

[153] Myung J, Kim M, Tang SKY. Low energy emulsion-based fermentation enabling accelerated methane mass transfer and growth of poly(3-hydroxybutyrate)-accumulating methanotrophs. Bioresource Technology. 2016;**207**:302-307

[154] Buczkowska A, Witkowska E, Górski Ł, Zamojska A, Szewczyk KW, Wróblewski W, et al. The monitoring of methane fermentation in sequencing batch bioreactor with flow-through array of miniaturized solid state electrodes. Talanta. 2010;**81**(4-5): 1387-1392

[155] Ahmad MN, Holland CR. Growth kinetics of single-cell protein in batch fermenters. Journal of Food Engineering. 1995;**26**(4):443-452

[156] Kianoush K-D, Fatemeh Y, Hamid R, Neda MB, Mohsen M, Soheil RM, et al. Simulation of bioreactors for poly(3-hydroxybutyrate) production from natural gas. Iranian Journal of Chemistry and Chemical Engineering. 2020;**39**(1):313-336

[157] Moo-Young M. Economics of single cell protein production. Process Biochemistry. 1977;**12**:6

[158] Labuza TP, Le Roux JP, Fan TS, Tannenbaum SR. Engineering factors in single-cell protein production. II. Spray drying and cell viability. Biotechnology and Bioengineering. 1970;**12**(1):135-140

[159] Labuza TP, Santos DB, Roop RN. Engineering factors in single-cell protein production. I. Fluid properties and concentration of yeast by evaporation. Biotechnology and Bioengineering. 1970;**12**(1):123-134

[160] Abbott BJ, Clamen A. The relationship of substrate, growth rate, and maintenance coefficient to single cell protein production. Biotechnology and Bioengineering. 1973;**15**:117.

Available from: https://onlinelibrary. wiley.com/doi/abs/10.1002/b it.260150109

[161] Imasaka T, Kanekuni N, So H, Yoshino S. Cross-flow filtration of methane fermentation broth by ceramic membranes. Journal of Fermentation and Bioengineering. 1989;**68**(3):200-206

[162] Kuddus M. Enzymes in Food Biotechnology: Production, Applications, and Future Prospects. Cambridge, Massachusetts, USA: Academic Press. 2019. ISBN: 9780128132807

[163] Levett I, Birkett G, Davies N, Bell A, Langford A, Laycock B, et al. Techno-economic assessment of poly-3-hydroxybutyrate (PHB) production from methane—The case for thermophilic bioprocessing. Journal of Environmental Chemical Engineering. 2016;**4**:3724-3733

[164] Tsapekos P, Angelidaki XZI. Proteinaceous methanotrophs for feed additive using biowaste as carbon and nutrients source. Bioresource Technology. 2020;**313** Article 123646

[165] Tomlinson EJ. The production of single-cell protein from strong organic waste waters from the food and drink processing industries—2. The practical and economic feasibility of a non-aseptic batch culture. Water Research. 1976;**10**(5):367-371

[166] Matassa S, Boon N, Pikaar I, Verstraete W. Microbial protein: Future sustainable food supply route with low environmental footprint. Microbial Biotechnology. 2016;**9**(5):568-575

[167] Anderson PJ, McNeil KE, Watson K. Thermotolerant single cell protein production by *Kluyveromyces marxianusvar. marxianus*. Journal of Industrial Microbiology & Biotechnology. 1988;**3**:9-14

[168] Digital signing ceremony unveils location of Calysseo's world-first commercial FeedKind® plant—FeedKind®. Available from: http://www.feedkind.com/digital-signing-cere mony-unveils-location-calysseos-world-first-commercial-feedkind-plant/

[169] Garcia Martinez JB, Alvarado KA, Denkenberger DC. Synthetic fat from petroleum as a resilient food for global catastrophes: Preliminary techno-economic assessment and technology roadmap. Chemical Engineering Research and Design. 2022;**177**:255-272. DOI: 10.1016/j.cherd.2021.10.017. PII: S0263-8762(21)00427-5

[170] Throup J, Garcia Martinez JB, Bals B, Cates J, Pearce JM, Denkenberger DC. Rapid repurposing of pulp and paper mills, biorefineries, and breweries for lignocellulosic sugar production in global food catastrophes. Food and Bioproducts Processing. 2022;**131**:22-39. DOI: 10.1016/j.fbp.2021.10.012. PII: S0960-3085(21)00162-0

[171] Biopolymers—Facts and statistics. Ausgabe 2021. Available from: https://www.ifbb-hannover.de/files/IfBB/d ownloads/faltblaetter_broschueren/f+s/ Biopolymers-Facts-Statistics-einseitig-2021.pdf

[172] Lackner M. Methane as emerging raw material for biopolymers biobased polymers. In: 4th World Congress on Bio-Polymers and Polymer Chemistry, Webinar, Keynote Speech; 30 March. 2021

[173] Lackner M. Methane as sustainable biopolymer feedstock—Bioprocess engineering using methanotrophic bacteria. In: Renewable Resources and Biorefineries Conference, RRB2021; Aveiro, Portugal; September. 2021. Available from: https://www.rrbconference.com/%20RRB

[174] Morais AMMB, Morais RMSC, Drew D, Mustakhimov I, Lackner M. Biodegradable Bio-based Plastics

Toward Climate Change Mitigation. New York, USA: Springer. 2021. pp. 1-43. DOI: 10.1007/978-1-4614-6431-0_91-2

[175] Lackner M, Mustakhimov I, Drew D. Feedstock considerations for world-scale PHA production: Methane as viable option. In: 2nd PHA platform World Congress; September 23. 2021 14: 15–14:40. Available from: https://www.bioplasticsmagazine.com/en/event-calendar/termine/2nd-pha-world-congress-2020/#anchor_95c7b84a_Accordion-Programme

[176] Pieja AJ, Morse MC, Cal AJ. Methane to bioproducts: The future of the bioeconomy? Current Opinion in Chemical Biology. 2017;**41**:123-131

[177] Available from: https://www.foodnavigator-usa.com/Article/2021/03/15/When-will-cell-cultured-meat-reach-price-parity-with-conventional-meat

[178] Daneels R. Protein at farm scale from feed compatible components. In: Power to Gas to Protein. Utrecht: Innovation Network; 2016. ISBN: 978-90-5059-524-7. Report no. 15.2.334, May

Chapter 5

Polymer-Based Membranes for C_{3+} Hydrocarbon Removal from Natural Gas

John Yang, Milind M. Vaidya, Sebastien A. Duval and Feras Hamad

Abstract

Natural gas can contain significant amounts of impurifies, including CO_2, H_2S, N_2, He, and C_{3+} hydrocarbons. These C_{3+} hydrocarbons are valuable chemical feedstocks and can be used as a liquid fuel for power generation. Membrane-based separation technologies have recently emerged as an economically favorable alternative due to reduced capital and operating cost. Polymeric membranes for the separation and removal of C_{3+} hydrocarbons from natural gas have been practiced in chemical and petrochemical industries. Therefore, these industries can benefit from membranes with improved C_{3+} hydrocarbon separation. This chapter overviews the different gas processing technologies for C_{3+} hydrocarbon separation and recovery from natural gas, highlighting the advantages, research and industrial needs, and challenges in developing highly efficient polymer-based membranes. More specifically, this chapter summarizes the removal of C_3H_8 and C_4H_{10} from CH_4 by prospective polymer architectures based on reverse-selective glassy polymers, rubbery polymers, and its hybrid mixed matrix membranes. In addition, the effect of testing conditions and gas compositions on the membrane permeation properties (permeability and selectivity) is reviewed.

Keywords: glassy polymers, rubbery polymers, membrane separation, C_{3+} hydrocarbons, permeation property, C_{3+}/CH_4 separation

1. Introduction

Natural gas is one of the important and primary sources of global energy. In addition to its primary importance as a fuel, natural gas is also a raw material and source of hydrocarbons for petrochemical feed stocks. According to 2021 BP statistics, there were an estimated 6,642 trillion cubic feet (Tcf) of total world proved reserves of natural gas [1]. The worldwide natural gas production and consumption have been rising over the past 20 years. In 2020, natural gas production and consumption worldwide amounted to roughly 3.85 and 3.82 trillion cubic meters [1].

Raw natural gas contains primarily of methane (CH_4) as the prevailing element but also comprises significant amounts of impurities such as nitrogen (N_2), helium (He), acid gases (carbon dioxide (CO_2) and hydrogen sulfide (H_2S)), heavy hydrocarbons (C_{3+}), mercaptans, water vapor, BTEX (benzene, toluene, ethylbenzene and xylene) etc. These impurities must be removed to meet the pipeline quality
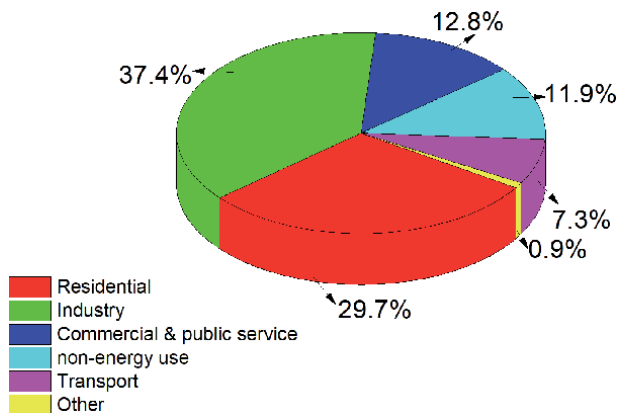
Figure 1.
World natural gas final consumption by sector in 2019 [2].

standard specifications for transport and processing and avoid pipelines corrosion. The operational natural gas plant delivers pipeline-quality dry natural gas that can be used as fuel by residential, commercial, and industrial consumers, or as a feed stocks for downstream chemical synthesis (**Figure 1**) [2].

Membrane-based separation technology has been pointed out as a key technology in the chemical industry [3–5]. It has benefits for small-to-medium scale separation where it exhibits higher energy efficiency, simplicity in operation, compact process design compared to other separation technologies. The global market for gas separation membrane estimated at US$822.1 MM in the year 2020 and is projected to reach a revised size of US$1.1 Billion by 2027, growing at the compound annual growth rate (CAGR) of 5.6% over the analysis period 2020–2027 [6]. Polymeric membrane-based separation technology for natural gas processing was first commercialized in the 1980s [7], and today it is widely used in variety of gas separation applications. Representative gas pairs needing separation in these applications is shown in **Table 1** [8–10], some of the leading industrial membrane producers and their principal glassy and/or rubbery membrane materials used in gas separation is listed in **Table 2** [7, 11–15].

Application	Common gas separation	Producer
• Nitrogen generation/ oxygen enrichment	• N_2/O_2	• Air Products, Praxair, Air Liquide, MTR
• Hydrogen recovery	• H_2/CH_4	• Air Products, Ube, Air Liquide, Praxair, MTR
• Ammonia purge gas	• H_2/N_2	• Air Products, Ube, Air Liquide, Praxair, MTR
• Syngas ratio adjustment	• H_2/CO	• Air Products, Ube, Air Liquide, Praxair, MTR
• Acidic gas separation	• CO_2/CH_4	• NATCO, Air Products, UOP, Uber, Air Liquide, MTR
• Natural gas dehydration	• H_2O/CH_4	• Kvaerner, Air Products, MTR
• Sour gas treatment	• H_2S/CH_4	• NATCO, Air Products, Uber, Kvaerner, MTR
• Helium separation	• He/CH_4	• Air Products, Air Liquide, MTR
• Helium recovery	• He/N_2	• Air Products, Air Liquide, MTR
• Heavy hydrocarbon recovery	• C_{3+}/CH_4	• MTR, ABB
• Air dehydration	• H_2O/Air	• Air Products, Parker Balston, Praxair, Ube, MTR

Table 1.
Primary current industrial gas separation for polymer membranes [8–10].

Polymer type	Typical polymer used	Membrane module type	Company
Glassy	Polysulfone	Hollow fiber	Air Products
	Polyimide/polyaramid	Hollow fiber	Air Liquide
	Polyimide	Hollow fiber	Ube
	Polyimide	Hollow fiber	Parker-Hannifin
	Polyimide	Hollow fiber	Evonik
	Polyimide	Hollow fiber	Praxair
	Polyimide/polysulfone	Hollow fiber	Grasys
	Cellulose acetate	Spiral wound	UOP, Kvaerner
	Cellulose acetate	Spiral wound	W. R. Grace
	Cellulose acetate	Spiral wound	MTR
	Cellulose acetate	Spiral wound	Fuji Film
	Cellulose acetate	Hollow fiber	Schlumberger (Natco)
	Ethyl cellulose	Hollow fiber	Air Liquide
	Poly (phenylene oxide)	Hollow fiber	Aquila
	Perfluoro polymer	Spiral wound	ABB/MTR
	Tetrabromo polycarbonate	Hollow fiber	Generon (MG)
Rubbery	Poly(ether-*b*-amide) copolymer	Spiral wound	MTR
	Poly(ether-*b*-amide) copolymer	Plate and frame	MTR
	Poly(ether-*b*-amide) copolymer	Hollow fiber	Air Liquide
	Polysiloxane	Plate and frame	GKSS
	Polysiloxane	Spiral wound	MTR
	Polysiloxane	Hollow fiber	Air Liquide

Table 2.
Principal polymer membrane materials, modules, and producers [7, 11–15].

Separation of C$_{3+}$ hydrocarbons (e.g. propane (C$_3$H$_8$), butane (C$_4$H$_{10}$)) and their removal from natural gas not only is necessary to prevent condensation during transportation by reducing the dew point and heating value to pipeline specifications, but also it is economically attractive to recover C$_{3+}$ hydrocarbons since they are often of greater value when used as chemical feedstocks, or as a liquid fuel for power generation. In general, both glassy and rubbery polymers are used for this application. Glassy polymeric membranes are in general diffusivity selective and traditional glassy polymer membrane based upon cellulose acetate, polyimide, Tetra Bromo polycarbonate, polysulfone have been widely utilized for a few decades for CO$_2$ removal from natural gas. Only few glassy polymers (e.g. perfluoro-based polymers) have demonstrated remarkable abilities to separate hydrocarbons from natural gas but their application has been limited due to highly aging and plasticization [16–21]. On the other hand, rubbery polymeric membranes are solubility selective and are mainly used in gas/vapor separation processes for separating hydrocarbons from their mixtures based on gas condensability. Commercially, poly (dimethylsiloxane) (PDMS) based rubbery siloxane membranes have been applied to separate C$_3$H$_8$ and C$_4$H$_{10}$ from CH$_4$ [14, 22–25] and other gas pairs (e.g. O$_2$/N$_2$, CO$_2$/CH$_4$, H$_2$/N$_2$, He/N$_2$, He/H$_2$, CO$_2$/N$_2$, N$_2$/CH$_4$, H$_2$/CO$_2$, He/CO$_2$) [26–32] from natural gas; however, development of more selective, higher-flux and cost-effective

rubbery membrane materials can further help improve economics of the C_{3+} hydrocarbon recovery.

In this chapter, the application of synthetic polymeric membranes for C_{3+} hydrocarbon separation and removal (C_{3+}/CH_4) from natural gas is reviewed. The review covers available glassy and rubbery polymer membrane materials, as well as its hybrid mixed matrix membranes. Their transport properties (permeability and selectivity) as well as the effect of testing conditions and feed compositions on the membrane separation performance are reviewed.

2. Outline of C_{3+} hydrocarbon separation membrane techniques

The processing of both associated gas (AG) and non-associated gas (NAG) from oil and natural gas wellheads into pipeline-quality dry natural gas can be quite complex. Generally, the Master Gas System (MGS) in the gas plants consists of three main units: (1) gas-oil separating plants (GOSPs), (2) gas plants and (3) fractionation plants as shown in **Figure 2** (top). A typical natural gas treatment and separation processing plant whose simplified schematic representation shown in **Figure 2** (bottom) consists five main processes to remove various impurities from raw natural gas. C_{3+} hydrocarbons are extracted as byproducts in the production of natural gas and oil, and natural gas processing is by far the most significant, contributing 90%+ production of C_{3+} hydrocarbons. There are three conventional technologies to separate C_{3+} hydrocarbons from natural gas: refrigeration, lean oil absorption and cryogenic [13]. These common processes are costly and energy intensive, which is reflected in the price and available capability of the finished gas (**Table 3**).
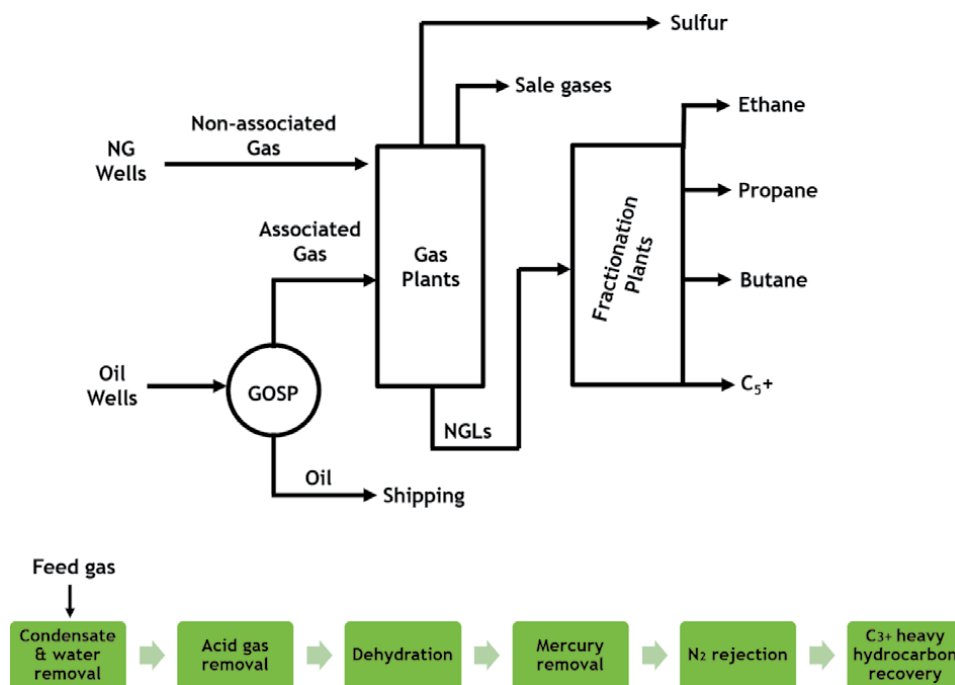

Figure 2.
Top: block diagram showing key process steps in gas treatments and separation plants; bottom: simplified sketch of natural gas separation processes consisting five main processes.

Processing technology	Technology Vintage	Available capacity	C$_{3+}$ hydrocarbons extraction	Fuel consumption
Refrigeration	1940–1960	10%	large C$_3$, most of C$_4$	Least
Lean Oil Absorption	1960–1975	20%	90%+ of C$_3$ and 30% C$_2$	Higher
Cryogenic	1975 on	50%	70–99% C$_2$	Higher

Table 3.
Available gas processing technology for C$_{3+}$ heavy hydrocarbons recovery [12].

The refrigerated condensation process is a conventional way to separate C$_{3+}$ hydrocarbon components from the gas stream through a sequence of conventional distillation columns operating down to $-40°C$ [33]. The refrigeration process is pricey and energy intensive but can extract a large percentage of C$_3$H$_8$ and most of the C$_{4+}$ gases. There was no major improvement of heavy hydrocarbon recovery process since 1910s until the lean oil absorption process was developed.

Lean oil absorption plants were the type of processing plant built in the late of 1960s. These plants were the next evolution from the refrigeration plants and can extract 90%+ of the C$_{3+}$ in the gas stream and about 30% of the ethane by bubbling the gas through a chilled absorption oil operating at approximately 0°C. The fuel consumption of this type of plant is higher than that of the refrigeration plant [34].

Cryogenic plants became prevalent in the 1970s with the development of Turbo-expander technology with great economic advantages for natural gas liquid (NGL) recovery [35]. The 1st generation of this technology could extract 70%+ of ethane (C$_2$) from the gas. Today, ~99% extraction of ethane can be recovered with modified cryogenic process due to the increased pressure reduction involved in the process [34]. Highly energy intensive for regeneration, tendency for block of process of equipment and the use of flammable cryogenic fluids are one the main disadvantages of cryogenic separation.

Membrane-based separation technology can be competitive in the processing of hydrocarbon recovery from natural gas. Inorganic membranes, such as MFI-type zeolite [36–38] and MOF [39], can be appealing due to their unique properties with well-define pore structure and high chemical and mechanical stabilities. These MFI membranes exhibit high C$_{3+}$/CH$_4$ selectivity, but rather low overall permeance, high capital cost and difficulty of scaling up, hence has hardly found industrial usage. Polymeric membranes have been used for the separation and removal of C$_{3+}$ hydrocarbons from natural gas, usually with moderate selectivity [14]. The recovery of C$_{3+}$ hydrocarbons is currently the second biggest market for membranes in natural gas processing, after acidic gas separation [11]. Compared to conventional separation methods, membrane-based separation technologies entail low capital costs, high energy efficiency and constitute a reliable option for separating hydrocarbon mixtures.

Glassy polymeric membrane-based separation process is a separation process shown in **Figure 3A** where gas mixtures consisting of two or more components are separated by a membrane into a "C$_{3+}$ enriched" retentate stream and a "C$_{3+}$ lean" permeate stream. The glassy polymer membrane separates gas mixtures by providing a permeable barrier that allows compounds to move through at specific rates, it separates gas mixtures principally by size or diffusivity. On the other hand, the feed gas mixtures are separated by a rubbery polymer membrane into a "C$_{3+}$ lean" retentate stream and a "C$_{3+}$ enriched" permeate stream (**Figure 3B**). The permeation of gas molecules across the rubbery membrane depends mainly on their solubilities or condensabilities. For example, Membrane Technology and Research (MTR) developed VaporSep® process using rubbery polymer composite
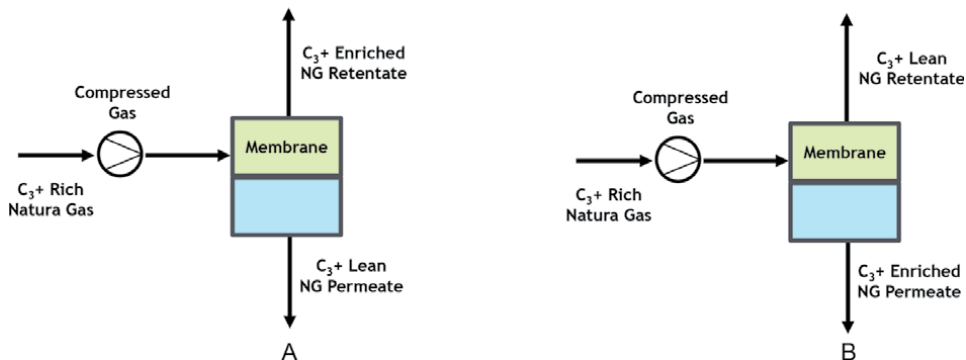
Figure 3.
Schematic of (A) glassy and (B) rubbery polymer membrane-based separation process from natural gas.
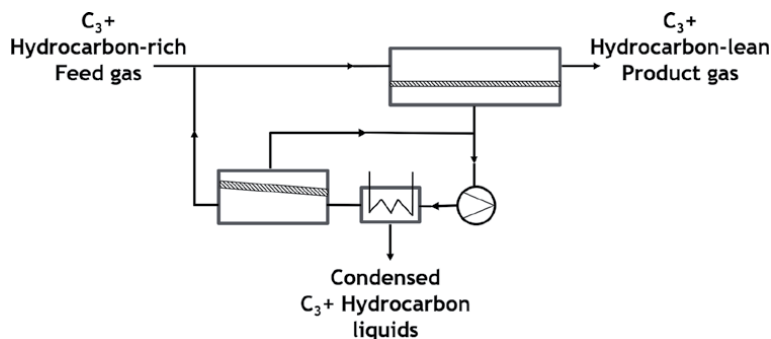
Figure 4.
Flow scheme of a membrane C_{3+} hydrocarbon recovery by means of dew point control unit (MTR/polysiloxane membranes/spiral-wound modules) [13].

membranes to treat high pressure hydrocarbon-rich feed gas mixtures (**Figure 4**) [11, 13]. C_{3+} hydrocarbons and the BTEX aromatics all permeate preferentially and are recompressed and cooled by a fan-cooled heat exchanger to condense higher hydrocarbons, while CH_4 is then recirculated to the feed. The size and cost of the compressor system is often larger than membrane unit, so the selection of higher selectivity of novel rubbery membrane in this processing application can reduce capital expenditures (CAPEX) and operating expenses (OPEX) to the gas processing business.

Commercially available rubbery polymer membranes have been applied to enhance natural gas liquid (NGL) production under C_{3+} rich gas feed stream [24]. Following example illustrates how nitrogen rejective (hydrocarbon selective) rubbery membranes can be utilized for enhancement of the C_{2+} hydrocarbons recovery via a NGL process in a gas plant. The NGL recovery process is cascaded-refrigeration process with and/or without membrane units, as shown in **Figure 5**. The gas plant is processing both AG stream (e.g. 450 psi) and NAG stream (e.g. 800 psi), to produce sales gas (SC) and C_{2+} NGL products.

The core of the NGL process is the Liquid Recovery Unit (LRU), which is a cascaded refrigeration process. **Figure 6** details further the cascaded-refrigeration unit. Dry natural gas feed is cooled down to $-68°C$ ($-90°F$) in three cooling stages; C_3 refrigeration loop is used in the first and second stages, while C_2 refrigeration loop is used in the third stage.

As noted in **Figure 6**, the C_2 refrigeration loop is cascaded in the C_3 refrigeration loop, hence referred to as cascaded-refrigeration NGL recovery process. The residue
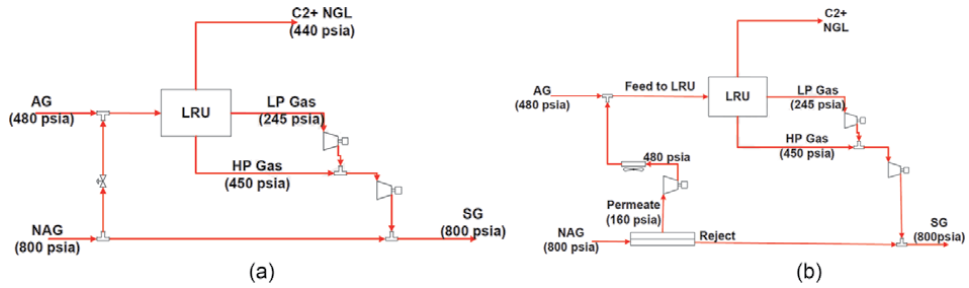
Figure 5.
Schematic of the NGL recovery process: (A) without membrane; (B) utilizing rubbery membrane to divert NAG stream to feed LRU.
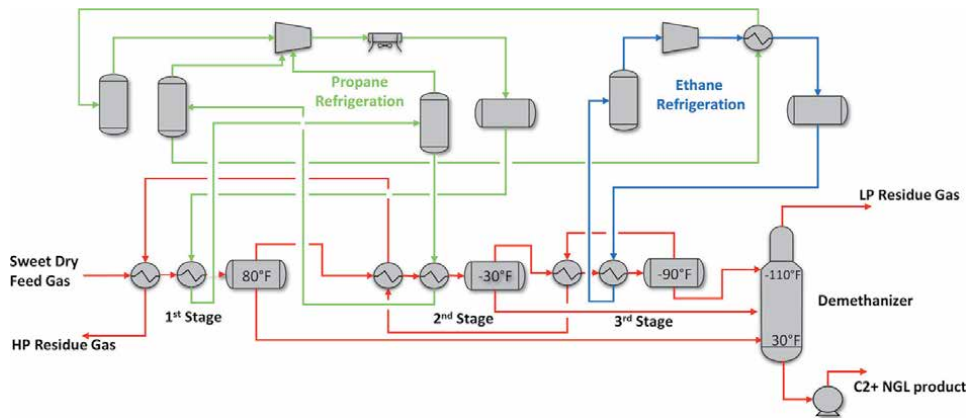
Figure 6.
Schematic of the cascaded-refrigeration process to recover C$_{2+}$ NGL from natural gas.

gas leaving the third cooling stage is recycled back to exchange heat with gas feeding each stage and leaving the first stage at around 450 psi (referred to as high pressure (HP) residue gas). The liquids collected in the three stages are fed to the demethanizer, which is operating at lower pressure. The C$_{2+}$ NGL product is obtained as the bottom product, while the top gas product from the demethanizer (low pressure (LP) residue gas) is consolidated with HP residue stream and sent to SG network. This LRU process is ideally designed to process AG stream, which is C$_{2+}$ rich and free of or very lean in nitrogen. However, under certain situations of higher demand for C$_{2+}$ NGL, the LRU is designed or operated with feed that is composed partially of NAG. As noted in **Table 4**, the N$_2$ content of NAG stream is higher, and the C$_{2+}$ content is considerably lower, than in AG stream.

  Table 5 compares the performance of the NGL process when 140 MMSCFD of the NAG stream is diverted to mix with the 500 MMSCFD AG stream. In reference (base case), **Table 5** provides the performance of the NGL process when only AG stream is fed to the LRU. When portion of NAG is let down directly to mix with AG, the condensability of the feed stream to LRU is reduced, as indicated by the increase in N$_2$ content and reduction in the C$_{2+}$ content. Nevertheless, the C$_{3+}$ NGL liquids production has increased as a direct result of the increase in feed to LRU, while liquid C$_2$ production has decreased in almost similar rate rendering the cascaded-refrigeration NGL recovery process not sensitive to the increase in the flow of C$_{2+}$ to LRU. On the other hand, diverting part of the NAG selectively through membrane has resulted in increasing the condensability of the feed to LRU. As a result of enhancing the

	Flow (MMSCFD)	Pressure (psi)	%N_2	%C_1	%C_2	%C_3	%C_4	%C_{5+}
AG	500	480	0.5	65.5	17.9	10.9	3.98	1.25
NAG	400	800	14	80.2	3.56	1.28	0.67	0.25

Table 4.
Conditions of AG and NAG streams.

	No mixing	Direct let down	Membrane[1]
AG to LRU	500	500	500
NAG diverted to LRU (MMSCFD)	0	140	140
%NAG in feed to LRU	0	21.9	21.9
Feed to LRU (MMSCFD)	500	640	640
%N_2	0.5	3.5	2.6
%C_1	65.5	68.7	68.8
%C_2	17.9	14.7	15.1
%C_{3+}	16.1	13.1	13.5
C_{2+} NGL production (Barrell/day)	92,100	91,900	95,200
C_2 (Barrel/day)	36,900	35,100	36,600
C_{3+} (Barrel/day)	55,200	56,800	58,600
Extra C_{2+} (Barrel/day) Vs let down	Reference[2]	−1800	+3300
Extra C_{3+} (Barrel/day) Vs let down	Reference[2]	+1600	+1800
Sales gas:			
High Heating Value (Btu/SCF)	988.1	985.7	975.6
Sales Gas Shrinkage (MMSCFD)	Reference[2]	0.7	14.0

[1]*Membrane performance: $C_1/N_2 \sim 1.6$, $C_2/N_2 \sim 3.2$, $C_3/N_2 \sim 4.8$, $C_4/N_2 \sim 5.2$, $C_{5+}/N_2 \sim 9$.*
[2]*Base case (only AG stream is fed to the LRU).*

Table 5.
Impact of incorporating part of NAG in the feed to LRU of the cascaded-refrigeration NGL recovery process.

condensability and flow of the feed to LRU, the NGL production has increased, especially valuable C_{3+} productivity. The impact of increasing the flow to LRU, as noted in **Table 5**, is to reduce the heating value of the sales gas. This is mainly the result of separating more condensable valuable C_{3+} hydrocarbons from the sales gas stream. This impact is exacerbated when the diversion of NAG is conducted selectively through the membrane, therefore increasing the shrinkage in produced sales gas.

3. Gas transport mechanism in polymer membranes

Polymeric membranes are generally non-porous and gas permeation through dense polymer membranes is typically described by the solution-diffusion model. Gas permeation occurs by sorption of gas on the feed side of membranes, then molecular diffusion through the membrane matrix, and evaporation of the gas from permeate side of membrane surface. Based on the solution-diffusion model, the membrane permeability, P_i (Barrer), is defined as the product of diffusivity coefficient and solubility coefficient (given by Eq. (1)) at high fugacity differences across the membrane [40]:

$$P_i = D_i \times S_i \qquad (1)$$

where P_i is the permeability coefficient measured in Barrer (1 Barrer = 1×10^{-10} cm^3 (STP) cm/cm^2 s cmHg), S_i is the solubility coefficient (cm^3 gas/cm^3 polymer cmHg), and D_i is the diffusion coefficient of the penetrant (cm^2/s). The solubility coefficient is a thermodynamic parameter and is mainly influenced by the condensability of the penetrant gases [41], and it is inversely proportional to gas boiling point or critical temperature [42]. In contrast to gas sorption, the gas diffusion coefficients vary widely depending on the polymer materials, it is a kinetic parameter that measures the overall mobility of the penetrant molecules in the membrane, depending on various factors such as the size and shape of the gas molecules, the cohesive energy density of the polymer, the mobility of the polymer chains and the free volume size and distribution of the polymer [43]. Accordingly, the membrane selectivity α, the best measure of a membrane's ability to separate gases i and j is defined as the ratio of the permeabilities of penetrant, P_i and P_j (given by Eq. (2)) [44].

$$\alpha_{ij} = P_i/P_j = (D_i/D_j) \times (S_i/S_j) \qquad (2)$$

As shown by Eq. (2), membrane selectivity (also known as permselectivity) can be separated into diffusivity selectivity, D_i/D_j, taken as the ratio of diffusivity coefficients of the two gases and solubility selectivity, S_i/S_j, taken as the ratio of solubility coefficients. Diffusivity selectivity depends primarily on the size-sieving ability of the membrane, the permeation of the smaller molecule is faster as compared to their larger counterparts. While solubility selectivity is largely driven by gas condensability and affinity with the membrane.

In general, glassy polymeric membranes generally tend to permeate smaller molecules, the diffusion coefficients decrease as the molecular size increases; whereas rubbery polymeric membranes permeate more condensable gases, the sorption coefficients generally increase as the condensability increases. Such trends are schematically illustrated in **Figure 7** for glassy and for rubbery polymeric membranes, which shows the gas permeabilities for principal gas components in natural gas with different molecular size (kinetic diameter, d_k, Å) [13] and condensability (critical temperature, T_c, K) [45]. The molecular sizes and relative condensabilities of C$_3$H$_8$ and C$_4$H$_{10}$, relative to CH$_4$, are highlighted in **Figure 7**. CH$_4$ can be separated from C$_{3+}$ hydrocarbons by glassy polymers by size-selectivity; however, interaction of heavier hydrocarbons with the polymers chains tends to increase the flux resulting in decrement in C$_{3+}$/CH$_4$ selectivity in case of rich hydrocarbon natural gas. On the other hand, rubbery polymers (sorption selectivity membranes) are used to separate C$_{3+}$ hydrocarbons from CH$_4$, because of their condensabilities. For example, the selectivity of hydrocarbon vapors in PDMS membranes is dominated by the sorption component, the C$_3$H$_8$/CH$_4$ and C$_3$H$_8$/N$_2$ sorption selectivities (K_i/K_{CH_4} and K_i/K) are 50-fold and 370-fold greater than that of their diffusion selectivities (D_i/D_{CH_4} and D_i/D_{N_2}) (**Table 6**) [16, 46–48].

4. Research and industry needs

The separation and recovery of C$_{3+}$ hydrocarbons from natural gas using polymeric membrane-based technology have gained increasing attentions in chemical, petrochemical and oil and gas companies compared to conventional separation technologies. The choice of polymeric membrane materials is crucial for separation, and the key membrane performance variables are selectivity, permeability, and long-term durability. Research regarding the development of polymer materials and fabrication processes has been reported in the literature mostly with single or binary
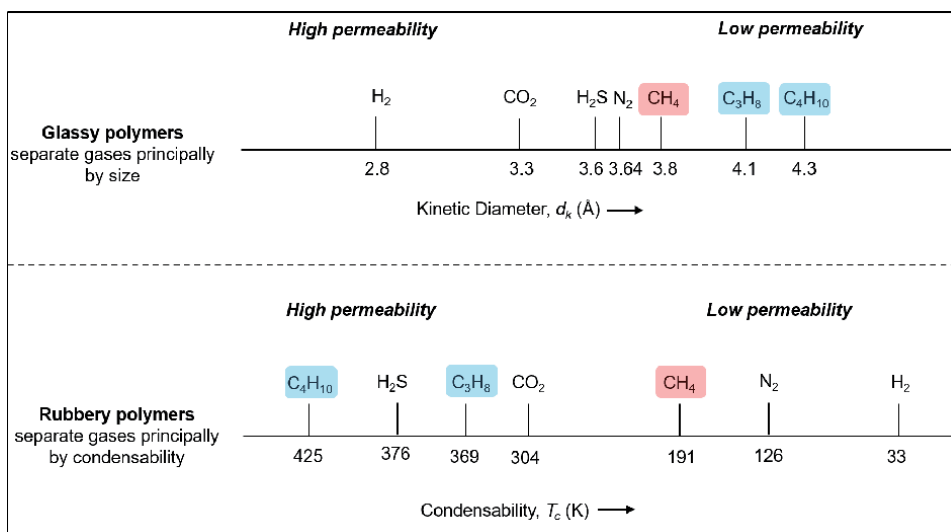
Figure 7.
The relative size (kinetic diameter, d_k, Å) and condensability (critical temperature, T_c, K) of the principal components of natural gas.

gas mixtures short duration gas permeation data; however, their industrial implementation is often hindered due to effects of multicomponent natural gas mixture permeation behavior on membrane physical aging.

Glassy polymer membranes have excellent scalability and continuously increasing being considered for more challenging hydrocarbon separations. The use of glassy polymer membranes with stiff chains, such as polyphenylene oxide (PPO), ethyl cellulose (EC), cellulose acetate (CA), polysulfone (PSF), aromatic polyimides, polymers of intrinsic microporosity (PIMs), disubstituted polyacetylenes and Si-distributed polynorbornenes etc., for separation of olefins and paraffins as well as C_2-C_4, aromatic, alicyclic and aliphatic hydrocarbons have been described in previous reviews [23, 49]. Unique challenges exist for these glassy polymer membranes for C_{3+} hydrocarbon separation and removal, most notably selectivity loss and some cases permeability loss due to physical aging and loss of separation efficiency in ultrathin membranes due to faster physical aging. For example, aging-induced permeability loss in glassy polymers is expected to be significant, especially for those condensable gases with larger molecular sizes (**Figure 8**) [49]. The membrane with ultrathin selective-layers could be the solution to provide economically higher hydrocarbon permeance, however, forming large-scale and defect-free membranes becomes increasing challenging in actual membrane fabrication process. In this regard, a high-flux and a good selectivity for gas separation processes are both required for a reasonable plant size and energy demand [7].

Further, other challenges that these polymer membrane materials need to withstand their C_{3+} hydrocarbon separation performances under natural gas feed streams and testing conditions, including a challenging high feed pressure (800+ psi), C_{3+} rich multicomponent hydrocarbon mixtures along with minor impurities such as CO_2, N_2, a trace amount of BTEX. PDMS based rubbery siloxane membranes are often used for separating C_{3+} hydrocarbons from natural gas. Although, many studies have investigated the permeation properties of PDMS membranes under pure gas, binary or ternary gas mixtures in the literature [44, 50–56], it is important to evaluate them under industrially relevant feed streams and varying operating conditions. Yang et al. [25]. investigated the permeation properties of conventional PDMS and modified siloxane terpolymer (Ter-PDMS) membranes

Gas	Condensability (k)	permeability P_i (Barrer)[1]	total selectivity α_i/α_{N2}	diffusion selectivity D_i/D_{N_2}	sorption selectivity K_i/K_{N_2}	total selectivity α_i/α_{CH4}	diffusion selectivity D_i/D_{CH_4}	sorption selectivity K_i/K_{CH_4}
H$_2$	33	890	2.23	4.12	0.56	0.74	6.36	0.12
O$_2$	155	800	2	1.00	2.00	0.67	1.55	0.43
N$_2$	126	400	1	1.00	1.00	0.33	1.55	0.21
CH$_4$	191	1200	3	0.65	4.67	1	1	1
CO$_2$	304	3800	9.5	0.65	14.33	3.17	1	3.07
C$_2$H$_6$	305	3300	8.25	0.33	24.44	2.75	0.51	5.24
C$_3$H$_8$	369	4100	10.25	0.15	55.56	3.42	0.23	11.90
C$_4$H$_{10}$[2]	425	4350	–	–	–	7.90	0.22	32.40

[1]Barrer = 10^{-10} cm^3(STP).cm/cm^2. S.cm Hg.
[2]Tested at 25°C

Table 6.
Summary of permeability, solubility, and diffusivity parameters in PDMS at 35°C [16, 46–48].
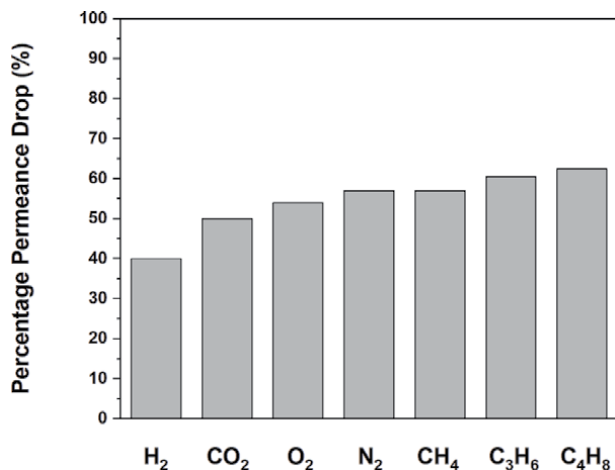
Figure 8.
Aging-induced permeance drop of penetrants in polyimide (6FDA-BPDA-DDBT) membrane aged for 18 months [49].
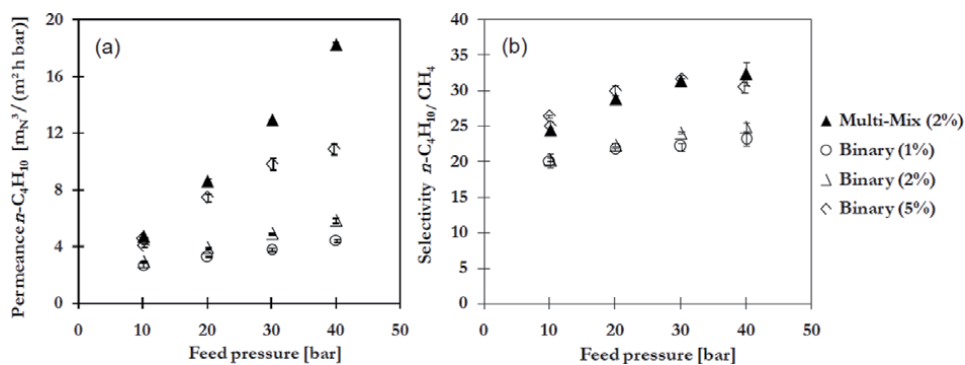
Figure 9.
Comparison of (a) C_4H_{10} permeance and (b) C_4H_{10}/CH_4 selectivity of POMS/AC MMMs in multi-component gas mixture (2 vol% C_4H_{10}) and C_4H_{10}-CH_4 binary mixtures (1, 2 or 5 vol% C_4H_{10}) at 20°C [57].

under simulated typical field gas streams. Results shows that C_4H_{10} vol% had significant influence on membrane separation performances due to the C_4H_{10}-induced swelling of PDMS based rubbery siloxane membranes. Similarly, Mushardt et al. [57] reported the permeation properties of poly(octylmethylsiloxane) (POMS)/ active carbon (AC) mixed matrix membranes (MMMs) under binary and multi-component gas mixtures (**Figure 9**). The best separation performance was achieved under multicomponent gas mixture at highest average fugacity of C_4H_{10} caused by increasing feed pressure and high concentration of C_4H_{10} in feed gas mixture. These outcomes carry the message that membrane separation performance is strongly related to feed gas compositions and testing conditions. Thus, to fully exploit the use of membranes for actual C_{3+} hydrocarbons separation and removal, not only higher-flux and cost-effective new membranes are needed, but also it is worthy to pay more attention to the influence of gas compositions and testing conditions.

5. Design of C_{3+} hydrocarbon separation polymeric membrane materials

The design and selection of polymeric membrane materials with high permeability and selectivity for gas separation is crucial. The following sections

describes the potential research and development activities in the literature of designing C$_{3+}$ hydrocarbon separation membrane materials. There are two types of polymeric membrane materials reported, which allow to selectively separate and remove C$_{3+}$ hydrocarbons from natural gas: (1) reverse-selective glassy polymers with high free volume [58], including polyacetylene-based polymers, polymers of intrinsic microporosity (PIMs), polynorbornene-based polymers; (2) rubbery polymers, including PDMS, POMS, modified rubbery siloxanes, polyurethanes, and poly(ether-*b*-amide) copolymers. Summary of C$_{3+}$ hydrocarbon permeation properties for these selected high free volume glassy polymers, rubbery polymers and their MMMs under pure and mixed gases can be found in **Tables 7–9**.

5.1 Reverse-selective glassy polymers

5.1.1 Polyacetylene-based polymers

Exceptional gas transport properties of polyacetylene-based polymers have led to considerable interest for membrane-based gas separation applications (**Figure 10**). These highly rigid, amorphous glassy polymers exhibit high T_g (>200°C) and high free volumes, providing ultrahigh permeabilities for C$_{3+}$ hydrocarbons and attractive selectivities of C$_{3+}$/CH$_4$ (**Table 7**).

Poly(1-trimethylsilyl-1-propyne) (PTMSP) was synthesized for the first time in 1983 [96]. Unlike conventional glassy polymers, PTMSP is the most permeable glassy polymer known for C$_{3+}$ hydrocarbon separation and removal with a pure gas C$_4$H$_{10}$ permeability >160,000 Barrer, but a low pure gas C$_4$H$_{10}$/CH$_4$ selectivity (<6) (**Table 7**). However, C$_4$H$_{10}$/CH$_4$ selectivity was found to be higher under mixed gas permeation testing, indicating PTMSP may be an alternative to siloxane rubbery polymers for C$_{3+}$ hydrocarbon separation. For example, Pinnau et al. [59] reported that mixed gas selectivities of C$_4$H$_{10}$ over permanent gases (CH$_4$ and H$_2$) are as high as 27 for C$_4$H$_{10}$/CH$_4$ and 39 for C$_4$H$_{10}$/H$_2$ because CH$_4$ and H$_2$ permeabilities in gas mixtures containing 2 vol% C$_4$H$_{10}$ are much lower than the pure CH$_4$ and H$_2$ permeabilities. Raharjo et al. [63] reported the mixed gas C$_4$H$_{10}$/CH$_4$ selectivity was >8 times higher than that of pure gas measurement, ultrahigh mixed gas C$_4$H$_{10}$ permeability (127,000 Barrer) and C$_4$H$_{10}$/CH$_4$ mixed gas selectivity (>50) were obtained under binary gas mixtures containing 6 vol% C$_4$H$_{10}$. Similar trends were observed for other polyacetylene-based polymers, such as poly(4-methyl-2-pentyne) (PMP) [64], poly(1-trimethylgermyl-1-propyne) (PTMGP) [64] and poly[1-phenyl-2-(p-trimethylsilylphenyl) acetylene] (PTMSDPA) [66]. Unlike branched polyacetylenes (i.e. PTMSP and PMP) with bulky side substitutes and higher fractional free volume (FFV = 0.28–0.29), linear-based poly(2-alkylacetylenes) with longer alkyl side chains, i.e., poly(2-hexyne), poly(2-octyne), poly(2-nonyne), poly(2-decyne), and poly- (2-undecyne), have relatively lower fractional free volume (FFV = 0.19–0.22) and permeabilities due to increased polymer chain mobility and interchain interactions [49, 67], and these linear poly(2-alkylacetylenes) membranes exhibit rather inferior performance for C$_4$H$_{10}$/CH$_4$ mixed gas separation (**Figure 11**) under mixed gas testing conditions. However, the use of PTMSP as a potential membrane polymer for C$_{3+}$ hydrocarbon recovery is not feasible due to fast physical aging (nonequilibrium excess free-volume relaxation of PTMSP chains) and solubility (e.g. interactions of PTMSP chains with many compounds), which can result in potential membrane destruction in the gas process streams.

Polymers	Pure gas						Mixed gas							Ref #
	Pressure/Temp	C_3H_8 (Barrer)	C_4H_{10} (Barrer)	CH_4 (Barrer)	α C_3H_8/CH_4	α C_4H_{10}/CH_4	Pressure/Temp	C_4H_{10} mol %	C_3H_8 (Barrer)	C_4H_{10} (Barrer)	CH_4 (Barrer)	α C_3H_8/CH_4	α C_4H_{10}/CH_4	
Polyacetylene-based polymers														
PTMSP	250 psi/23°C		78,000	15,400		5	150 psi/25°C	2		53,500	1800		30	[59]
		38,000					250 psi/25°C	2	28,000	85,300	3100	9	27	[60]
	1 bar/25°C		15,000	15,000	2.5									[16]
							150 psi/25°C	2		39,249	1891		21	[61]
	2.4 atm/35°C	3300												[62]
	4.4 atm/25°C		167,400	31,000		5.4	4.4 atm/25°C	6		127,500	2500		51	[63]
	4.4 atm/35°C		156,800	28,000		5.6	4.4 atm/35°C	6		83,600	2200		38	[63]
	1 atm/23°C	1740	17,500	900	1.9	19	6 atm/23°C	3.7		2600	230		11.3	[64]
								7.5		5900	280		21.1	[12]
PTMSP (L), Toluene	1.4 atm/30°C	8760	12,320	4460	2	2.7	1.4 atm/30°C	2		28,422	2140		13	[65]
PTMSP (L), THF	1.4 atm/30°C	3870	4670	1720	2.3	2.7		2		6120	750		8	[65]
PTMSP(2), THF								2		41,569	1609		26	[65]
PMP	1.3 atm/35°C		11,700	850		14	11.3 atm/35°C	8		6000	450		13	[66]
	1 bar/25°C	7300	26,000	2900	2.5	9								[66]
PTMGP (85% trans content)	3.5 psi/30°C		15,000	8450		1.8	3.5 psi/30°C	1.6		66,190	2130		31.1	[67]
	3.5 psi/30°C		17,000	6300		2.7	3.5 psi/30°C	1.6		70,900	1980		35.8	[67]
PTMSDPA	1.4 atm/25°C		49,600	23,100		2.1	1.4 atm/25°C	2		221,000	14,700		15	[68]
Poly(2-hexyne)	50 psi/35°C	35	440	21	1.7	21.0	50 psi/35°C	2		15	9		0.6	[69]
Poly(2-octyne)	50 psi/35°C	420	2100	51	8.2	41.2	50 psi/35°C	2		150	56		2.7	[69]
Poly(2-nonyne)	50 psi/35°C	450	1850	64	7.0	28.9	50 psi/35°C	2		250	55		4.5	[69]
Poly(2-decyne)	50 psi/35°C	740	4600	84	8.8	54.8	50 psi/35°C	2		500	77		6.5	[69]

Polymers	Pure gas						Mixed gas							Ref #
	Pressure/ Temp	C$_3$H$_8$ (Barrer)	C$_4$H$_{10}$ (Barrer)	CH$_4$ (Barrer)	α C$_3$H$_8$/CH$_4$	α C$_4$H$_{10}$/CH$_4$	Pressure/ Temp	C$_4$H$_{10}$ mol %	C$_3$H$_8$ (Barrer)	C$_4$H$_{10}$ (Barrer)	CH$_4$ (Barrer)	α C$_3$H$_8$/CH$_4$	α C$_4$H$_{10}$/CH$_4$	
Poly(2-undecyne)	50 psi/35°C	840	3900	83	10.1	47.0	50 psi/35°C	2		600	86		7	[69]
Polymers of intrinsic microporosity														
PIM-1	65 psi/35°C	5500	25,100	430	12.8	58.4	150 psi/25°C	2		4200	175		24	[17]
							120 psi/25°C	2	4600		320	14.4		[18]
Polynorbornene-based polymers														
APN-SiMe$_3$	1 atm/23°C	1740	17,500	790	2.2	22.2								[70–72]
PBTCN-Si	6 atm/23°C		26,900	3300	8.1		6 atm/23°C	5.2		10,300	910		11.3	[64]
PTTCN-Si	1 atm/23°C	3490	22,200	1250	2.8	17.8								[73]
MPTTCN-Si	1 atm/23°C	290	1940	180	1.6	10.8								[73]
PTCN-Si	1 atm/23°C	1470	13,030	1010	1.5	12.9								[74]
PBTCN-Si	1 atm/23°C	7530	26,910	3320	2.3	8.1								[74]
ROMP-SiMe$_2$OEt	1 bar/25°C	1	10.2	1.4	0.7	7.4								[75]
ROMP-SiMe(OEt)$_2$	1 bar/25°C	12.8	75.1	13.3	1	5.7								[75]
ROMP-Si(OEt)$_3$	1 bar/25°C	241.8	2100	97.7	2.5	21.5								[75]
APN-SiMe$_3$	1 bar/25°C	856.4	7041	678.9	1.3	10.4								[75]
APN-SiMe$_2$OEt	1 bar/25°C	112.7	1621	57.7	2	28.1								[75]
APN-SiMe(OEt)$_2$	1 bar/25°C	100.1	1104	49	2	22.6								[75]
APN-Si(OEt)$_3$	1 bar/25°C	499.1	3838	176	2.8	21.8								[75]
Polynorbornene-based polymers														
ROMP Si(OEt)$_3$							500 psi/25°C	3	547	1092	138	2	7.9	[21]
							800 psi/25°C	3	945	1976	198	2.1	10	[21]
							500 psi/25°C	4	826	1519	188	4.3	8.1	[21]

Polymers	Pure gas						Mixed gas							Ref #
	Pressure/ Temp	C_3H_8 (Barrer)	C_4H_{10} (Barrer)	CH_4 (Barrer)	α C_3H_8/CH_4	α C_4H_{10}/CH_4	Pressure/ Temp	C_4H_{10} mol %	C_3H_8 (Barrer)	C_4H_{10} (Barrer)	CH_4 (Barrer)	α C_3H_8/CH_4	α C_4H_{10}/CH_4	
APN-Si(OEt)$_3$							800 psi/25°C	4	1213	2160	292	4.2	7.4	[21]
							500 psi/25°C	3	3163	7148	545	5.8	13.1	[21]
							800 psi/25°C	3	4315	9914	682	6.3	14.5	[21]
							500 psi/25°C	4	4467	10,022	615	7.3	16.3	[21]
							800 psi/25°C	4	6448	15,258	811	8	18.8	[21]
ROMP TCN-Si(OMe)$_3$	1 bar/22°C	10	27	11	0.9	2.5								[76]
ROMP TCN-Si(OEt)$_3$	1 bar/22 °C	122	1260	50	2.4	25.2								[76]
ROMP XL TCN-Si(OEt)$_3$	1 bar/22 °C	116	1100	51	2.3	21.6								[76]
ROMP XL TCN-Si(OPr)$_3$	1 bar/22 °C	615	4100	170	3.6	24.1								[76]
ROMP XL TCN-Si(OBu)$_3$	1 bar/22 °C	1300	8100	250	5.2	32.4								[76]
APTCN-Si(OMe)$_3$	1 bar/22 °C	335	4050	130	2.6	31.2								[76]
APTCN-Si(OEt)$_3$	1 bar/22 °C	510	5000	153	3.3	32.7								[76]
APTCN-Si(OPr)$_3$	1 bar/22 °C	440	4100	84	5.2	48.8								[76]
APTCN-Si(OBu)$_3$	1 bar/22°C	440	3600	100	4.4	36								[76]
APTCN-(OPr)	1 bar/25 °C	6.64	179	6.4	1	28	500 psi/25°C	1.5	208	506	46.4	4.5	10.9	[75]
APTCN-(OPr)	1 bar/25°C						800 psi/25°C	1.5	293	739	57.6	5.1	12.8	[75]
APTCN-(SiMe$_3$)	1 bar/25°C	143.7	1800	84	1.7	21	500 psi/25°C	1.5	1828	4977	280	6.5	17.8	[75]
							800 psi/25°C	1.5	2341	6523	331	7.1	19.63	[75]
APN-(OPr)$_3$							500 psi/25°C	1.5	84.3	189	24	3.5	7.9	[75]
APN-(OPr)$_3$							800 psi/25°C	1.5	134	322	32.7	4.1	9.8	[75]
APN-Si(OEt)$_3$							800 psi/25°C	1.5	7766	18,254	985	7.9	18.5	[75]
APN-SiMe$_3$ [Pd]	1 bar/25 °C	950	8900			12.5								[77]

Polymers	Pure gas						Mixed gas							Ref #
	Pressure/ Temp	C_3H_8 (Barrer)	C_4H_{10} (Barrer)	CH_4 (Barrer)	α C_3H_8/CH_4	α C_4H_{10}/CH_4	Pressure/ Temp	C_4H_{10} mol %	C_3H_8 (Barrer)	C_4H_{10} (Barrer)	CH_4 (Barrer)	α C_3H_8/CH_4	α C_4H_{10}/CH_4	
APN-SiMe$_3$ [Ni]	1 bar/25 °C		1800	15,200		14.2								[77]
PVNB	1 bar/25 °C		149	37		4								[78]
Cp-PVNB	1 bar/25 °C		380	44		8.6								[79]
O-PVNB	1 bar/25 °C		27.5	7.1		3.9								[79]
S-PVNB	1 bar/25 °C		4.7	1.5		3.1								[79]
XL-APTCN	1 bar/25 °C	1450	10,800	1030	1.4	10.5								[80]
APTCN-Si-b-APT CNSiOEt (3 mol%)	1 bar/22 °C	1030	1790	14,640	1.7	14.2								[81]
XL-APTCN-Si-b-APTCNSiOEt (3 mol%)	1 bar/22 °C	960	1800	15,460	1.9	16.1								[81]
APTCN-Si-b-APTCN SiOEt (10 mol%)	1 bar/22 °C	830	1800	16,700	2.2	20.1								[81]
XL-APTCN-Si-b-APTCNSiOEt (10 mol%)	1 bar/22 °C	770	1360	—	1.8	—								[81]
APTCN-SiMe$_3$	1 bar/22 °C	1880	14,730	1130	1.7	13								[82]
APTCN-Si(OEt)$_3$	1 bar/22 °C	153	510	5000	3.3	32.7								[82]

Table 7.
C_{3+} hydrocarbon properties in high free volume glassy polymeric membranes.
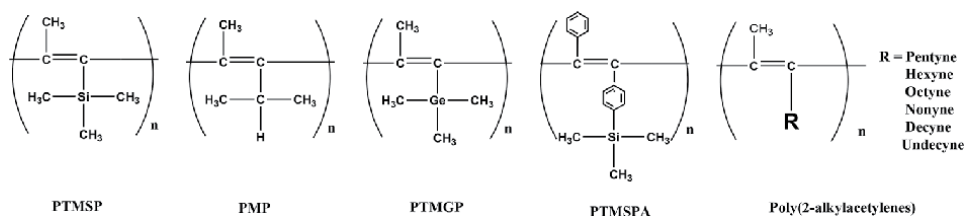
Figure 10.
Chemical structures of selected branched polyacetylene-based polymers (i.e. PTMSP, PMP, PTMGP, PTMSPA) and linear poly(2-alkylacetylenes) (i.e. i.e., poly(2-hexyne), poly(2-octyne), poly(2-nonyne), poly (2-decyne), and poly-(2-undecyne)).
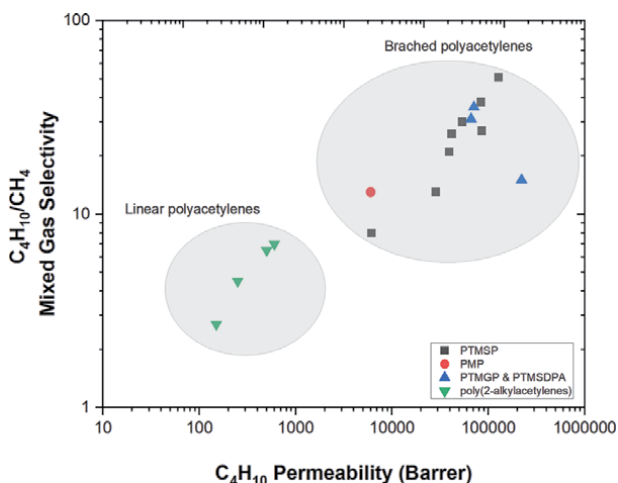

Figure 11.
Mixed gas C_4H_{10} permeability and C_4H_{10}/CH_4 selectivity for selected branched polyacetylene (i.e. PTMSP, PMP, PTMGP and PTMSDPA) and linear poly(2-alkylacetylenes) (i.e. poly(2-hexyne), poly(2-octyne), poly (2-nonyne), poly(2-decyne), and poly-(2-undecyne)) membranes.

5.1.2 PIM-1

PIMs are spirobisindane-based rigid, glassy polymers with high fractional free volume (FFV = 0.26), excellent chemical stability and good solvent resistance. PIM-1 is the most studied PIMs for gas separation, and it shows high CO_2 permeability with moderate CO_2/CH_4 selectivity, which is exceeding the upper bounds [97]. A new perspective on the role of PIMs and its functionalized ladder PIMs (e.g. PIM-polyimide copolymers) in key energy-intensive membrane-based gas separations, including O_2/N_2, H_2/N_2, H_2/CH_4, CO_2/CH_4, H_2S/CH_4, C_2H_4/C_2H_6, and C_3H_6/C_3H_8, was described in detail in a recent review paper by Wang et al. [98]. Similar as PTMSP, PIM-1 is also particularly permeable to hydrocarbon vapors (**Table 7**). Thomas et al. [16, 17] investigated the pure- and mixed-gas permeation properties of PIM-1, it exhibits C_4H_{10}/CH_4 and C_4H_{10}/H_2 mixed gas selectivities up to 25 and 27, respectively, under a mixture of 2 vol% C_4H_{10} in CH_4. Since PIM-1 has better solvent resistance than PTMSP, it could find applications as an advanced membrane material for the separation of organic vapor/permanent gas mixtures [17], and further membrane performance evaluation under industrially relevant feed streams and testing conditions will be the topic of future studies in the research groups.

1. Polynorbornene-based polymers

Another promising reverse-selective glassy polymer class for C$_{3+}$ hydrocarbon separation and removal are substituted polynorbornenes (PNBs). Many valuable correlations between gas-permeability and polynorbornene structure have been summarized in prior reviews [12, 19, 71]. More recently, the development in the field of next generation polynorbornene-based polymers, their limitations and challenges for targeted gas separations was discussed also in a recent review [99]. These studies show that solubility-controlled permeation of gaseous hydrocarbons (C$_1$ − C$_4$) is characteristic for both addition polymerization-type polynorbornenes (APNBs) with Si-containing side-groups and ring opening metathesis polymerization type polynorbornenes (ROMP PNBs) with flexible Si-O bonds in side-groups (**Figure 12**). Summary of C$_{3+}$ hydrocarbon permeation properties for APNBs and ROMP PNBs membranes under pure- and mixed-gas can be found in **Table 7**. In general, the membrane C$_4$H$_{10}$/CH$_4$ selectivity increased significantly as increasing the length of side groups (e.g. Me, Et, *n*-Pr, *n*-Bu). Among these polynorbornene-based polymers, both distributed APNBs-Si(OPr)$_3$ and ROMP-Si(OBu)$_3$ membranes exhibited higher C$_4$H$_{10}$/CH$_4$ pure gas selectivities of 48.8 and 32.4, respectively [76].

Although many studies investigated the permeation properties using pure gases, fewer reported separation performance under multicomponent gas feed streams [21]. Sundell et al. [75] reported a route toward the production of *exo* ROMP and addition-type polynorbornenes and polytricyclononenes (APTCN) through the stereochemical control afforded by the reductive Mizoroki−Heck reaction. All addition-type and tricyclononene-based polymer membranes (e.g. APTCN-SiMe$_3$ and APTCN-Si(OEt)$_3$) show improved mixed gas C$_4$H$_{10}$/CH$_4$ selectivities compared to APBNs-Si(OEt)$_3$ and ROMP-Si(OEt)$_3$ membranes (**Figure 13**) under the same testing conditions, due to the increased polymeric chain-spacing. These polynorbornene-based polymers demonstrate solubility-selective permeation with mixed gas selectivities that exceed commercially used PDMS.
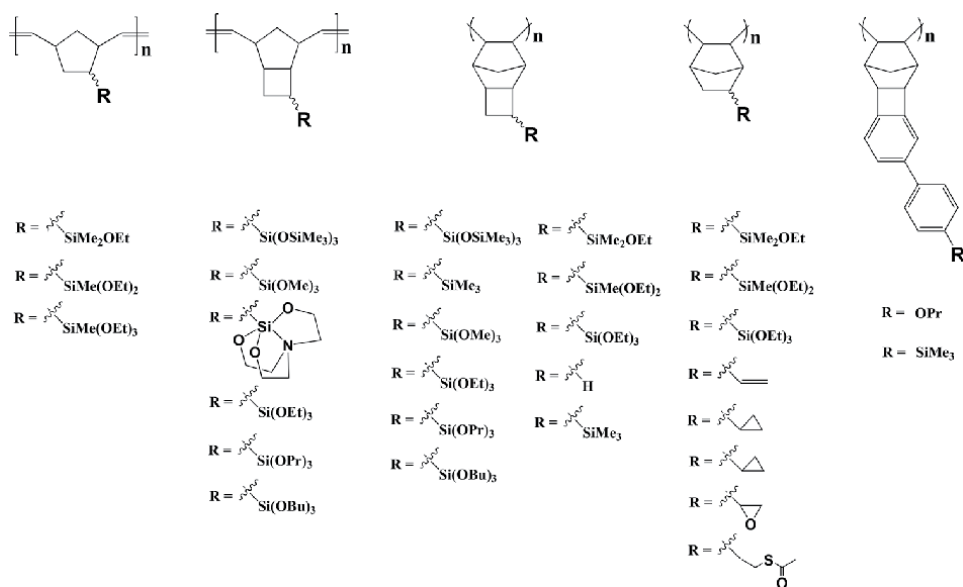

Figure 12.
Structures of metathesis and addition polynorbornenes bearing different substituents for gas separation applications.
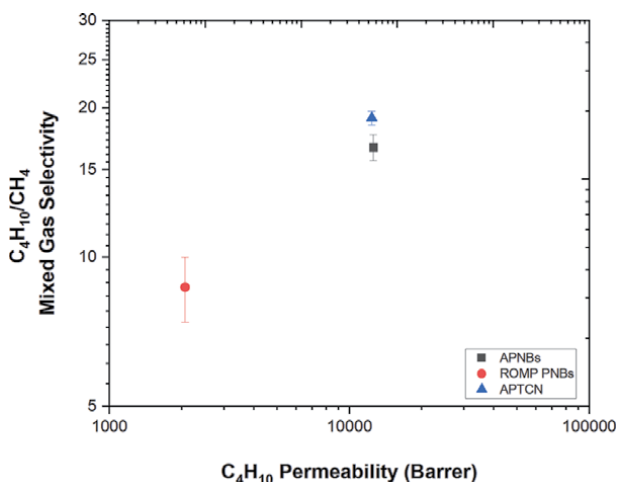
Figure 13.
Mixed gas C_4H_{10} permeability vs.C_4H_{10}/CH_4 selectivity for APBNs-Si(OEt)$_3$ (black squares), ROMP-Si(OEt)$_3$ (red circles) and substituted-APTCN (blue triangles) under C_{3+} rich multicomponent gas mixtures containing 1.5–4 vol% C_4H_{10} at 25°C and 800 psi.

5.2 Rubbery polymers

5.2.1 Rubbery siloxane-containing homo-and copolymers

Application of PDMS based rubbery siloxane membranes for selective removal of hydrocarbons and recovery of various organic components [3, 100–102] is considered. Summary of C_{3+} hydrocarbon permeation properties of PDMS, POMS and modified rubbery siloxane membranes in pure and mixed gases can be found in **Table 8**.

PDMS has low T_g ($\sim$−123°C), flexible chains, and large free volume. The permeability, solubility, and diffusivity of hydrocarbons in PDMS membranes have been studied in previous literature [52, 83], and results show that feed gas compositions and testing conditions significantly affect membrane separation performance. The effect of chemical compositions on the permeation properties of PDMS membrane by introducing substituted groups in both side and main chains was compressively studied by Stern et al. [90, 103–105] and summarized in previous reviews [12, 23]. Results show that the substitution of functional groups in the side-groups of siloxane polymers has the same general effect on polymer permeability and selectivity as the substitution of such groups in the polymer main chains [104] (**Figure 14**). When the size of the side-groups (e.g. –CH$_3$, –C$_2$H$_5$, –C$_3$H$_7$, –C$_8$H$_{17}$, − C$_{10}$H$_{11}$–, CH$_2$CH$_2$CF$_3$, –C$_6$H$_5$, etc.) and main chains (e.g. –(CH$_2$)$_2$, −(CH$_2$) $_2$, −(CH$_2$)$_8$, −m-C$_6$H$_4$, −p-C$_6$H$_{24}$) increased, the chains become less flexible resulting in the increases in T_g (from −123°C to −28°C) and the decreases in permeability, especially for those condensable gases with larger kinetic diameters (e.g. C$_3$H$_8$) [23].

Compared to PDMS with (Me$_2$SiO)$_x$ backbone chain, membranes based on POMS with (OctMeSiO)$_x$ backbone chain exhibited enhanced C_{3+} hydrocarbon separation performance (C_{3+}/CH$_4$ selectivities) [14, 56, 57, 88, 89]. Schultz et al. [14] reported that POMS was one of two promising polymers for separation of C_{3+} hydrocarbons among the total 45 different polymers that were tested under C$_4$H$_{10}$/CH$_4$ binary gas mixture (97/3 mol%). Since POMS is a soft material, it is susceptible to compression and thus the permeability goes down significantly with increase in the feed pressure as shown in **Figure 15**.

Polymers	Pure gas						Mixed gas							Ref. #
	Pressure/temp	C_3H_8 (Barrer)	C_4H_{10} (Barrer)	CH_4 (Barrer)	α C_3H_8/CH_4	α C_4H_{10}/CH_4	Pressure/temp	C_4H_{10} mol %	C_3H_8 (Barrer)	C_4H_{10} (Barrer)	CH_4 (Barrer)	α C_3H_8/CH_4	α C_4H_{10}/CH_4	
Polydimethylsiloxane (PDMS)														
PDMS	0.01 bar/25°C	4100		1200	3.4									[22]
							250 psi/23°C	2		7200	1200		6	[59]
	240 psi/35°C	4100		1200	3.4									[16]
	4.4 atm/35°C	7400		1298	5.7									[83]
							150 psi/25°C	2		12,900	1250		10.3	[83]
							11 atm/25°C	1		12,400	1240		10	[83]
							11 atm/25°C	2		12,900	1250		10.3	[83]
							11 atm/25°C	4		13,700	1280		10.7	[83]
							11 atm/25°C	6		16,100	1400		11.5	[83]
							11 atm/25°C	8		17,400	1450		12	[83]
	98.6 psi/35°C	10,000		1350	7.4									[23]
	4.4 atm/35°C	6400												[62]
	4.4 atm/25°C		17,800	1200		14.8	4.4 atm/25°C	6		17,600	1250		14.1	[52]
	4.4 atm/35°C		15,900	1350		11.8	4.4 atm/35°C	6		16,100	1400		11.5	[52]
	4.4 atm/5 °C		13,300	1500		8.90	4.4 atm/50°C	6		13,500	1550		8.7	[52]
	5 bar/35°C	17,000		1500	11.3									[53]
							5 atm/35°C		1000		90	11		[54]
	1 bar/35°C	5500		1600	3.4									[84]
	2 bar/35°C	10,000		1600	6.3									[85]
	15 bar/35°C	4100	7500	1200		6.25								[86]
PDA@PDMS	6 bar/20°C	160 GPU												[87]
PDMS							200 psi/25°C	3	3025	6279	497	6.1	12.6	[21]
							500 psi/25°C	3	4722	9709	672	7	14.4	[21]
							800 psi/25°C	3	6041	12,539	874	6.9	14.3	[21]
							200 psi/25°C	4	3567	6668	581	6.1	11.5	[21]

Polymers	Pure gas — Pressure/temp	C_3H_8 (Barrer)	C_4H_{10} (Barrer)	CH_4 (Barrer)	α C_3H_8/CH_4	α C_4H_{10}/CH_4	Mixed gas — Pressure/temp	C_4H_{10} mol %	C_3H_8 (Barrer)	C_4H_{10} (Barrer)	CH_4 (Barrer)	α C_3H_8/CH_4	α C_4H_{10}/CH_4	Ref. #
							500 psi/25°C	4	5198	9533	849	6.1	11.2	[21]
							800 psi/25°C	4	6184	11,084	1082	5.7	10.2	[21]
PDMS w/net	0.8 bar/25°C	5600	18,200	1300	14	14								[56]
PDMS	0.8 bar/25°C	5200	17,000	1200	14.2	14.2								[57]
							800 psi/25°C	4	7891	15,468	1097	7.1	16.0	[75]
	2 bar/20°C	6900	33,800	1170	28.9	28.9	800 psi/25°C	0.5	4260	7380	1033	4.1	7.1	[25]
							800 psi/25°C	1.5	5971	11,710	1173	5.1	10.0	[25]
							800 psi/25°C	4	11,016	21,496	1636	6.7	13.1	[25]
Side-chain substituted PDMS														
POMS	0.01 bar/25°C	2029		314			6 bar/35°C	3	5[1]	5[1]	0.5[1]		10	[14]
POMS	0.8 bar/25°C	1980	7500	300	6.6	25								[22]
POMS	0.4 bar/30°C	1560		270	5.8									[56]
POMS	0.5 bar/20°C		7.5[1]	0.2[1]		15.6								[88]
POMS							10 bar/20°C	5		7[1]	0.31[1]		22.5	[57]
POMS							30 bar/20°C	5		13.2[1]	0.49[1]		27	[57]
POMS							40 bar/30°C	5		9.8[1]	0.56[1]		17.5	[89]
POMS	98.6 psi/35°C	2300		310	7.4									[23]
PHexMS	0.8 bar/25°C	1392	8160	340	5.8	24								[56]
PDecMS	0.8 bar/25°C	1608	6480	240	6.7	27								[56]
PEtMS	98.6 psi/35°C	3800		470	8.1									[23]
PPrMS	98.6 psi/35°C	4200		570	7.4									[23]
PEtF$_3$MS	98.6 psi/35°C	450		200	2.3									[23]
PPhMS	98.6 psi/35°C	170		36	4.7									[23]
PPrMS	0.01 bar/25°C	8120		1450	5.6									[22]
PDMSM	0.4 atm/25°C	837	2807	130	6.44	21.6								[90]
PDMSTM	0.4 atm/25°C	37	240	8.4	4.4	28.6								[90]

Polymers	Pure gas						Mixed gas							Ref. #
	Pressure/temp	C$_3$H$_8$ (Barrer)	C$_4$H$_{10}$ (Barrer)	CH$_4$ (Barrer)	α C$_3$H$_8$/CH$_4$	α C$_4$H$_{10}$/CH$_4$	Pressure/temp	C$_4$H$_{10}$ mol %	C$_3$H$_8$ (Barrer)	C$_4$H$_{10}$ (Barrer)	CH$_4$ (Barrer)	α C$_3$H$_8$/CH$_4$	α C$_4$H$_{10}$/CH$_4$	
PDMSM/PDMSTM (75/25)	0.4 atm/25°C	547	2340	113	4.8	20.7								[90]
Main-chain substituted PDMS														
PDMS-PEtMS	98.6 psi/35 °C	4200		600	7.0									[23]
PDMS-PHxMS	98.6 psi/35 °C	3400		400	8.5									[23]
PDMS-POMS	98.6 psi/35 °C	2800		360	7.8									[23]
PDMS-P*m*PhMS	98.6 psi/35 °C	800		110	7.3									[23]
PDMS-P*p*PMS	98.6 psi/35 °C	40		1.2	33.3									[23]
Ter-PDMS	2 bar/20 °C	3950	21,200	430	9.19	49.3	800 psi/25°C	0.5	2781	5703	469	5.9	12.2	[25]
Ter-PDMS							800 psi/25°C	1.5	3615	8185	505	7.2	16.2	[25]
Ter-PDMS							800 psi/25°C	4	9199	19,524	1073	8.6	18.2	[25]
Polyurethane (PU)														
PTMG–HDI–BDO	2 bar/30°C	182		36.7	5									[91]
PCL–HDI–BDO	2 bar/30°C	61.4		12.8	4.8									[91]
PPG–HDI–BDO	2 bar/30°C	200		44.1	4.5									[91]
PTMG–TDI–BDA	2 bar/30°C	190		34.8	5.5									[91]
PDMS-PU (50/50)	1 bar/30°C		300			6–8								[92]
Poly(ether-b-amide) copolymers														
Pebax 1074							800 psi/25°C	1.5	46	105	9	5.2	12.0	[93]
Pebax 1657							800 psi/25°C	1.5	29	67	6	4.7	10.7	[93]
Pebax 2533							800 psi/25°C	1.5	340	894	51	6.7	17.6	[93]
Pebax 3000							800 psi/25°C	1.5	64.5	156.8	13.2	4.9	12.0	[93]
Pebax 5513							800 psi/25°C	1.5	17.2	41.3	4.3	4.1	9.8	[93]

$^t_m N^3/(m^2 . h. bar)$.

Table 8.
C$_{3+}$ hydrocarbon properties in rubbery polymeric membranes.

Side Groups   Main Chains

$R_1 =$ - CH_3
         - C_2H_5
         - C_3H_7
         - C_8H_{17}
         - $C_{10}H_{21}$
         - $(CH_2)_2CF_3$
         - C_6H_5

$R_2 =$ - (CH_2) -
         - $(CH_2)_2$ -
         - $(CH_2)_6$ -
         - $(CH_2)_8$ -
         - m-C_6H_4 -
         - p-C_6H_4 -
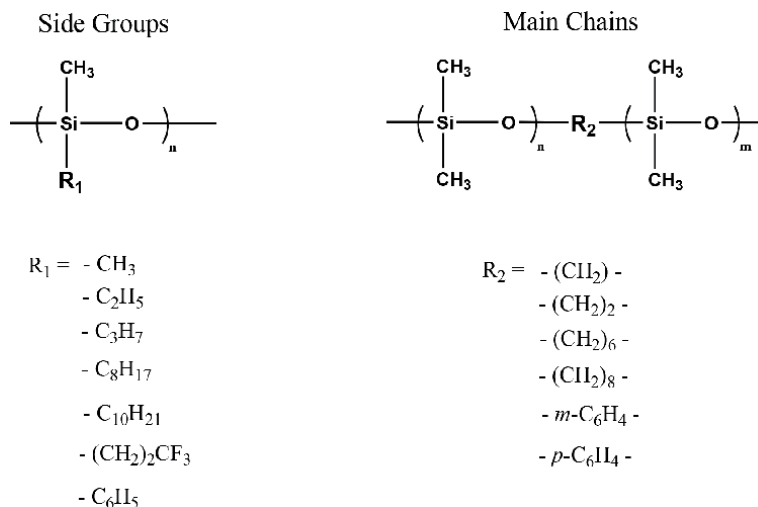
Figure 14.
Chemical structures of PDMS-based siloxane polymers with different side and main chains.

More recently, Grushevenko et al. [56] synthesized siloxane rubbery membranes by using an *in-situ* technique with the introduction of side alkyl groups followed by polymer chains crosslinking in the same reaction mixture. Results showed that POMS membrane demonstrated higher C_4H_{10}/CH_4 ideal selectivity (α = 25) than that of PDMS membrane (α = 14). The gas permeation properties of polyhexyl-methylsiloxane (PHexMS) and polydecylmethylsiloxane (PDecMS) were further studied. With the increase of substituent length from C_8 to C_{10}, C_4H_{10} permeability (6480 Barrer) of PDecMS membranes decreased but C_4H_{10}/CH_4 selectivity increased to 27 due to reducing diffusion coefficient. These results show that polyalkylmethylsiloxanes with longer side chains (e.g. PDecMS) are promising to be applied as materials for the purpose of C_{3+} extraction from natural gas (**Figure 16**).

In addition, a novel class of silicon-organic polymers, silmethylene rubbery polymers including more robust Si-C bonds, has been developed for separation of C_{3+} hydrocarbons from natural gas. Alentiev et al. [90] reported a thermally initi-ated polymerization technique to synthesize polydimethylsilmethylene (PDMSM) and polydimethylsiltrimethylene (PDMSTM) homo-polymers that include only more robust Si–C bonds (**Figure 17**). These silicon-containing rubbery polymers
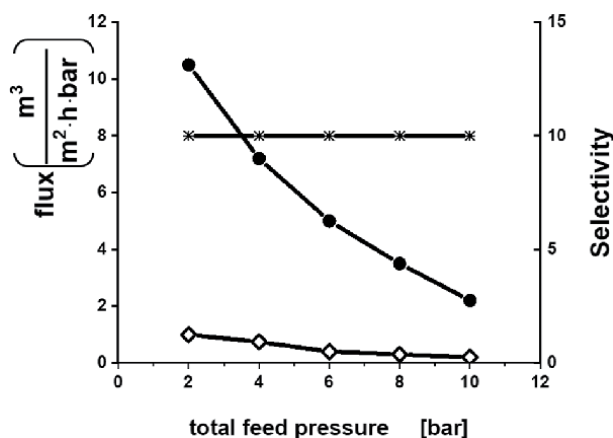
Figure 15.
Pressure behavior of the POMS under C_4H_{10}/CH_4 (97/3 Mol%) binary gas mixture, where compression decreases flux with feed pressure methane, • butane, x selectivity [14].
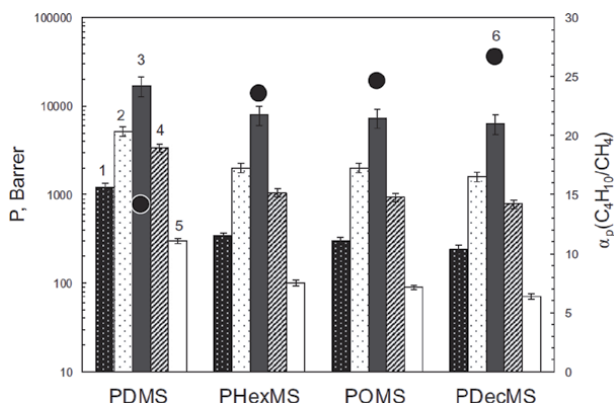
Figure 16.
Permeability (1-CH$_4$, 2-C$_3$H$_8$, 3-C$_4$H$_{10}$, 4-CO$_2$, 5-N$_2$) and C$_4$H$_{10}$/CH$_4$ selectivity of polyalkylmethylsiloxane membranes (feed pressure:0.8 bar, temperature: 25°C) [56].

and its copolymers have relatively high T_g (−92°C to −76°C) and excellent chemical stability (decomposition in air >240°C), compared to conventional PDMS. In addition, these novel rubbery polymers distinctly reveal solubility-controlled permeation behavior, but the permeabilities of C$_{3+}$ hydrocarbons in PDMSM and PDMSTM are lower than those in PDMS.

A comprehensive survey of the recent developments on the synthesis, properties, and applications of silicon-containing copolymers was provided in the literature [106], including silicone-urea and silicone-urethane copolymers, silicone-ester copolymers, silicone-amide copolymers, silicone-imide copolymers etc. These silicon-containing copolymers which combine unique properties of PDMS in the polymer backbone have been evaluated as gas separation membranes, such as CO$_2$/N$_2$ and CO$_2$/CH$_4$ separations [92, 107–110], but few reported C$_{3+}$ hydrocarbon separation and removal from natural gas. Gomesa et al. [92] reported the synthesis of poly (ether siloxane urethane urea) membrane materials for C$_4$H$_{10}$/CH$_4$ separation. Results show that the higher the content of soft siloxane segments, the higher are the permeabilities of C$_4$H$_{10}$ and CH$_4$ due to higher chain mobility, while the C$_4$H$_{10}$/CH$_4$ single gas selectivity (6–8) does not change so much as permeability (2–320 Barrer).

A series of silicon-containing terpolymers with Si-O-Si and Si-(CH$_2$)$_2$- in polymer backbone and side chains were synthesized for enhanced C$_{3+}$ hydrocarbon recovery from natural gas by Yang et al. [95]. The partially octyl substituted crosslinked rubbery siloxane membranes were prepared by crosslinking vinylmethylsiloxane terpolymer (Ter-PDMS) composed of (VinylMeSiO)$_p$(Me$_2$-SiO)$_m$(OctMeSiO)$_n$ backbone chains via an addition curing process [25]. Improved
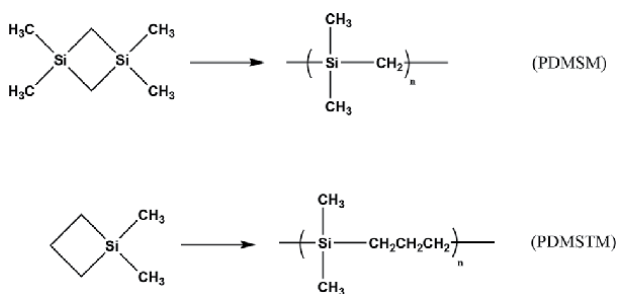
Figure 17.
The scheme of synthesis of silmethylene rubbery polymers: polydimethylsilmethylene (PDMSM) and polydimethylsiltrimethylene (PDMSTM).

gas permeation performances were observed for this modified siloxane Ter-PDMS membrane with C_4H_{10}/CH_4 ideal selectivity of 49.1 (2 bar and 20°C), with lower C_4H_{10} permeability (19,800 Barrer) compared to conventional PDMS membrane (33,800 Barrer C_4H_{10} permeability). Such decrease in permeability compared to conventional PDMS was induced by a reduction of chain flexibility with partial substitution of functional groups in the side chains after crosslinking in membrane matrix. Moreover, this modified siloxane Ter-PDMS membrane also showed enhanced C_{3+} separation performance (143% increase in C_4H_{10}/CH_4 mixed gas selectivity) under high pressure (up to 800 psi) 7-component gas mixtures compared to conventional PDMS membrane [25].

5.2.2 Polyurethane rubbery polymers

Polyurethanes have found commercial applications using in a diversity of products in industry, from coatings and adhesives for automotive, shoe soles, mattresses, and foam insulation. Polyurethanes are rubbery polymers which are introduced for different gas pair separations vastly, such as CO_2/N_2, CO_2/CH_4, O_2/N_2. The solubility and diffusivity of gases indicate solubility domination of gas transport in these membranes. Varies researchers have shown that the permeability of polyurethane membranes increases, while the selectivity decreases with the decrease the hard segment content (urethane or urea), or the increase the soft segment (polyether or polyester) molecular weight [111–115].

Poly(urethane–urea) (PUU) membranes display moderate C_{3+}/CH_4 selectivity for removal of C_{3+} hydrocarbons from natural gas. Sadeghi and coworkers [91] evaluated the separation performance of a series of PUU membranes synthesized with different type of diisocyanates and polyols. It was found that PUU membranes with polypropylene glycol (PPG) polyol had the maximum C_3H_8 permeability of 200 Barrer and C_3H_8/CH_4 selectivity of 5.5 because of its higher rubbery property and higher phase separation. In their recent paper [116], two series of PUU membranes containing aromatic and aliphatic side chains with different sizes were developed for separating of C_2H_6 and C_3H_8 from CH_4. The longer aliphatic side chain based PUU provides the best hydrocarbon separation performance with C_3H_8 permeability of 186 Barrer and C_3H_8/CH_4 idea selectivity of 6.5.

5.2.3 Poly(ether-b-amide) rubbery copolymers (Pebax®)

Pebax®—product of Arkema, is a group of thermoplastic elastomers, containing polyamide "hard" segment (e.g., nylon-6, nylon-12), and polyether "soft" segment (e.g., poly (ethylene oxide) [PEO], poly (tetramethylene oxide) [PTMEO]), which maintain the highly desirable combination of the toughness traditionally associated with polyamides and the flexibility/elasticity with polyether. Various Pebax® copolymers with different polyether/polyamide ratios were designed and synthesized to meet the requirements for different applications. Typical grades of commercial Pebax® 2533, 3533, 4011, 4033, 5533, 6633, 1074 and 1657 have been widely studied in literature for gas separation applications. For example, Pebax® 1657 containing 60 wt% polyether segment is a promising material showing good performance in CO_2 separation from CH_4 or N_2 [117]. MTR has also demonstrated favorable economics for a hybrid separation process that utilized Pebax® 4011 in conjunction with an amine absorption polishing step for sour gas separation [118]. However, fewer reported C_{3+} hydrocarbon separation and removal from natural gas. Harrigan et al. [93] recently investigated the sour gas separation performance of five different grades of commercial Pebax® 2533, 5513, 3000, 1074 and 1657 under high pressure 6-component gas mixtures containing C_{2+} hydrocarbons.

Results show that Pebax® 1074 and 1657 containing low of polyether segment (50–60 wt%) retained the highest CO_2/CH_4 selectivity (α = 16–19) but lower C_{3+}/CH_4 selectivities (C_3H_8/CH_4 = 4.7–5.2; C_4H_{10}/CH_4 = 11–12). Surprisingly Pebax® 2533 containing higher polyether segment (80 wt%) exhibited higher C_3H_8/CH_4 selectivity of 6.7 and C_4H_{10}/CH_4 selectivity of 17.6), which are greater than the C_3H_8/CH_4 selectivity of 5.3 and C_4H_{10}/CH_4 selectivity of 10.5 for commercially available PDMS membrane under the same testing conditions (800 psi, 25°C) [25]. However, Pebax® 2533 membrane shows 93% and 91% decrease in C_3H_8 and C_4H_{10} permeabilities, respectively, compared with that of PDMS.

5.3 Mixed matrix membranes (MMMs)

MMMs have been explored to develop materials for enhanced separation performance of conventional membrane. Different types of inorganic fillers, such as silica, TiO_2, fumed silica, graphene oxide (GO), activated carbon (AC), MOFs, zeolites, ZIFs, POSS etc., have been incorporated into PDMS, POMS, PTMST, and PU membrane matrix for air separation [119], CO_2 removal and capture [120, 121], pervaporation [122], hydrogen separation [83, 123], and hydrocarbon separation [10, 65, 94, 124–129]. The concept of using MMMs for light and heavy hydrocarbons separation and recovery in petrochemical and chemicals industries has attracted much interest and research in recent years. Several studies, such as olefin/paraffin separations (e.g. C_2H_4/C_2H_6, C_3H_6/C_3H_8, n-C_4H_8/i-C_4H_{10}), aromatic/aliphatic separations (e.g. toluene/n-hexane, p-xylene/o-xylene), vapor/gas separations (e.g. C_{3+}/N_2, C_{3+}/H_2 and C_{3+}/CH_4) were discussed in a recent review by Najari and coworkers [125]. Here, summary of C_{3+} hydrocarbon permeation properties of mixed matrix membranes (e.g. PTMSP, PTMGP, PDMS, POMS, PU and modified rubbery siloxane) in pure and mixed gases can be found in **Table 9**. Khanbabaei et al. [55] prepared PDMS-fumed silica MMMs for removing C_4H_{10} from CH_4. Results show the decreased C_4H_{10}/CH_4 mixed gas selectivity for both neat membrane and MMMs. The MMMs exhibited 38% increment in C_4H_{10} permeability and simultaneous 30% increase in C_4H_{10}/CH_4 selectivity under C_4H_{10}/CH_4 (3/97 mol%) binary gas mixture with adding >10 wt% of fumed silica, compared to neat PDMS membrane. Mushardt et al. [89] evaluated the separation of C_{3+} hydrocarbons of MMMs composed of POMS and 10–40 wt% AC from permanent gas streams under varying operating conditions (e.g. feed and permeate pressure, temperature, feed gas compositions). Best performance was achieved at highest average fugacity of C_4H_{10} caused by increasing feed pressure, high permeate pressure and high concentration of C_4H_{10} in feed mixture. At 40 bar, POMS/20 wt% AC MMMs exhibited higher C_4H_{10}/CH_4 mixed gas selectivity of 33 and C_4H_{10} permeance of 18 mN^3/(m^2.h.bar) under multicomponent gas mixtures including 2 vol% of C_4H_{10}. Gomes et al. [65] reported the preparation of PTMSP/silica MMMs with incorporation of 20–40 nm silica by sol–gel copolymerization of tetraethoxysilane (TEOS) with different organoalkoxysilanes. When methyltriethoxysilane (MTEOS) or n-octyltriethoxysilane (OTEOS) were used, the obtained MMMs exhibited higher separation performance (C_4H_{10}/CH_4 mixed gas selectivities of 12.7 and 13.9 at 1 bar and 30°C, respectively).

In a recent investigation, Yang et al. [95] described a method to design and produce novel, crosslinked siloxane/POSS MMMs for enhanced C_{3+} hydrocarbon recovery from natural gas. Dual-functional POSS nanofiller (OS-POSS-VTMO) containing silicon hydride moiety ($\equiv$–Si–H) and trimethoxylsilicon groups (–Si(OMe)$_3$) was synthesized and used as both a crosslinking agent and nanofiller (**Figure 18**) in modified rubbery siloxane (Ter-PDMS) membrane matrix. Under

Polymers	Fillers	Loading %	Pure Gas						Mixed Gas							Ref. #
			Pressure/temp	C_3H_8 (Barrer)	C_4H_{10} (Barrer)	CH_4 (Barrer)	α C_3H_8/CH_4	α C_4H_{10}/CH_4	Pressure/temp	C_4H_{10} mol %	C_3H_8 (Barrer)	C_4H_{10} (Barrer)	CH_4 (Barrer)	α C_3H_8/CH_4	α C_4H_{10}/CH_4	
PTMSP	EH-5 silica	30							150 psi/25°C	2		54,288	2326		23	[61]
	TS-610 silica	50							150 psi/25°C	2		114,655	4980		23	[61]
	Silica(TEOS/ OMDEOS1:0)	6.2	1.4 atm/30°C	1890	2390	470	4.0	5.1	1 atm/30°C	2		2420	350		6.8	[65]
	Silica(TEOS/ OMDEOS1:1)	5.2	1.4 atm/30°C	390	900	180	2.2	5.0	1 atm/30°C	2		790	110		7.4	[65]
	Silica(TEOS/ OMDEOS1:2)	2.8	1.4 atm/30°C	440	1190	350	1.3	3.4	1 atm/30°C	2		1440	190		7.6	[65]
	Silica(TEOS/ OMDEOS2:1)	2.2	1.4 atm/30°C	140	42	150	0.9	0.3	1 atm/30°C	2		470	90		5.4	[65]
	Silica(TEOS/ MTEOS1:1)	3.5	1 atm/30°C						1.4 atm/30°C	2		6280	495		12.7	[65]
	Silica(TEOS/ OTEOS1:1)	6.4	1 atm/30°C	480	240	960	1.8	4.0	1.4 atm/30°C	2		3850	280		13.7	[65]
	Silica(TEOS/ DTEOS1:1)	1	1 atm/30°C	520	300	1350	1.7	4.5	1.4 atm/30°C	2		1280	160		8	[65]
	Silica(TEOS/ HDTMOS1:1)	0.6	1 atm/30°C						1.4 atm/30°C	2		1110	140		7.9	[65]
PTMGP (85% trans content)	TiO$_2$	10	3.5 psi/30°C		14,300	7490		1.9	1 bar/30°C	1.6		56,280	1840		30.6	[67]
	TiO$_2$	5	3.5 psi/30°C		17,700	8240		2.1	1 bar/30°C	1.6		36,350	1210		30	[67]
	TiO$_2$	10	3.5 psi/30°C		18,300	8120		2.3	1 bar/30°C	1.6		66,890	2130		31.4	[67]
	TiO$_2$	20	3.5 psi/30°C		17,000	7990		2.1	1 bar/30°C	1.6		62,280	1990		31.3	[67]
PU	ZMS-5	5	2 atm/30°C	92.5		31.8	2.91									[94]
	ZMS-5	10	2 atm/30°C	101		32.4	3.12									[94]
	ZMS-5	15	2 atm/30°C	110		33.1	3.33									[94]

Polymers	Fillers	Loading %	Pure Gas						Mixed Gas							Ref. #
			Pressure/ temp	C_3H_8 (Barrer)	C_4H_{10} (Barrer)	CH_4 (Barrer)	α C_3H_8/CH_4	α C_4H_{10}/CH_4	Pressure/ temp	C_4H_{10} mol %	C_3H_8 (Barrer)	C_4H_{10} (Barrer)	CH_4 (Barrer)	α C_3H_8/CH_4	α C_4H_{10}/CH_4	
	ZMS-5	20	2 atm/30°C	117		32.3	3.63									[94]
PDMS	Silica	0.5	2 bar/35°C	9500		1350	7.0									[85]
	Silica	2	2 bar/35°C	30,000		1050	28.6									[85]
	Silica	0.5	7 bar/35°C	22,500		1350	16.7									[85]
	Silica	2	7 bar/35°C	24,500		950	25.8									[85]
	fumed Silica	5.5	1.5 atm/30°C		7500	360		21	10 atm/30°C	3		2962	455		6.5	[55]
	fumed Silica	11	1.5 atm/30°C		10,500	620		17	10 atm/30°C	3		4665	752		6.2	[55]
	fumed Silica	16.5	1.5 atm/30°C		9500	570	16.5		10 atm/30°C	3		4448	370		6.4	[55]
POMS	activated carbon	10							40 bar/20°C	5		4.9[1]	0.28[1]		17.5	[89]
	activated carbon	20							40 bar/20°C	5		3.2[1]	0.15[1]		21	[89]
	activated carbon	40							40 bar/20°C	5		1	0.06[1]		18	[89]
	activated carbon	20							40 bar/20°C	5		4[1]	0.2[1]		20	[89]
	activated carbon	20	0.5 bar/20°C		4.2[1]	0.12[1]		14.6	30 bar/20°C	1		3.8[1]	0.17[1]		22	[57]
	activated carbon	20							30 bar/20°C	2		4.5[1]	0.19[1]		24	[57]
	activated carbon	20							30 bar/20°C	5		9[1]	0.28[1]		32.5	[57]
	activated carbon								30 bar/20°C	2[2]		13[1]	0.41[1]		31.5	[57]
Ter-PDMS	OS-VTM-POSS	50	1 bar/25°C	1627	7480	217	7.5	34.6	800 psi/25°C	1.5[3]	2839	6730	401	7.1	16.8	[95]
	OS-VTM-POSS	50							800 psi/25°C	0.5[4]	2025	4881	262	7.7	18.7	[95]

$1 mN^3/(m^2 \cdot h \cdot bar)$.
[2]Multicomponent gas mixture: 1% C_5H_{12}/2% C_4H_{10}/6% C_3H_8/10% C_2H_6/79% CH_4/2% CO_2.
[3]Multicomponent gas mixture: 1.5% C_4H_{10}/3% C_3H_8/5% C_2H_6/66.5%% CH_4/12% CO_2/12% N_2.
[4]Multicomponent gas mixture: 0.5% C_4H_{10}/2% C_3H_8/5% C_2H_6/77.9%% CH_4/14% N_2/500ppm BTEX.

Table 9.
C_{3+} hydrocarbon properties in mixed matrix membranes.
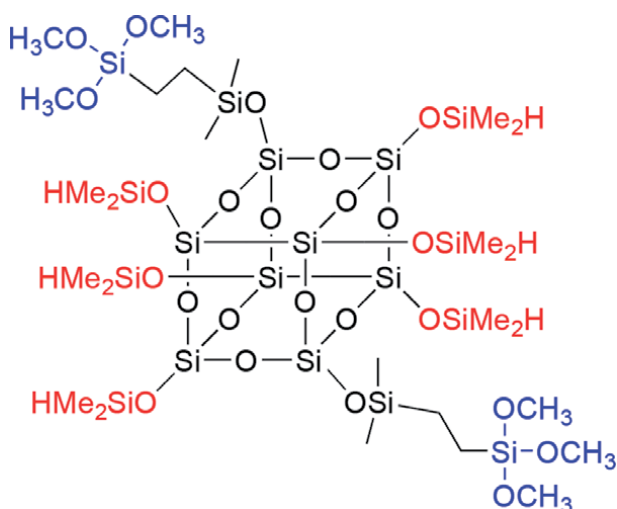
Figure 18.
Molecular structure of dual-functionalized POSS crosslinking agent (OS-POSS-VTMO) containing silicon hydride moiety ($\equiv$–Si–H) and trimethoxylsilicon groups –(Si(OMe)$_3$).

simulated typical field gas streams and testing conditions (e.g. feed pressure up to 800 psi for multicomponent gas mixture consisting C_1-C_5 hydrocarbons, CO_2, N_2 and BTEX). The produced novel, crosslinked Ter-PDMS/POSS MMMs exhibited better separation performance (e.g. 89% and 163% increase in C_3H_8/CH_4 and C_4H_{10}/CH_4 mixed gas selectivities) and enhanced swelling resistance, compared to conventional PDMS membrane. At 800 psi, Ter-PDMS/POSS MMM had a mixed gas C_4H_{10} permeability of 4880 Barrer and C_4H_{10}/CH_4 mixed gas selectivity of 18.7, respectively.

6. Conclusions and outlook

Membrane-based separations have emerged as an economically favorable alternative due to its small footprint, reduced capital, and energetic cost. Membranes for C_{3+} hydrocarbon recovery from natural gas have been practiced in the chemical and petrochemical industries, the improved C_{3+} hydrocarbon separation and removal process from natural gas will be beneficial of these industries.

This chapter summarizes C_{3+} hydrocarbon separation and removal from natural gas using polymeric membrane-based technologies. More specifically, it addresses the removal of C_3H_8 and C_4H_{10} from CH_4 by perspective polymer architectures based on reverse-selective glassy polymers with stiff chains and rubbery polymers with flexible chains. At present PDMS, POMS and poly(ether-*b*-amide) rubbery polymer membranes are used by industries in the field for C_{3+}/CH_4 separation. However, improved mixed gas selectivity of C_{3+}/C_1 with high flux will have a positive impact of the economics of the C_{3+} hydrocarbon recovery from natural gas. In case of reverse selective glassy polymers, membrane separation performance can be improved by introducing new groups or additives into membrane matrix, however, the loss of permeances due to physical aging restrains their applications in industry. This chapter also accounts the effect of the chemical structure of rubbery polymers on their permeation properties for C_{3+} hydrocarbons recovery from natural gas. Modified siloxane rubbery polymers-based membranes may be seen in future in the field for enhanced C_{3+} hydrocarbons recovery from natural gas since these membrane materials display improved mixed gas C_{3+}/CH_4 selectivity than

commercial membranes. In addition, only few studies regarding MMMs approach for enhanced C$_{3+}$ heavy hydrocarbons removal from natural gas are reported in the literature. More research efforts are needed in the future from the selection of right nanofillers and understanding the dynamic interactions between polymers and nanofillers regarding mixed gas permeation in the membrane matrix.

The permeation properties of the polymeric and mixed polymer matrix membrane materials have been reviewed and compared under varying operating parameters by many research groups. These results emphasize the observation that C$_{3+}$ hydrocarbon separation performance is strongly related to the testing condition, feed compositions and chemical structures. However, a thorough evaluation of C$_{3+}$ hydrocarbon separation properties is rarely reported in the literature under industrially relevant feed streams and testing conditions. Thus, there is a need for further research and testing of advanced membrane materials that are resistance to swelling and satisfy the practical requirements during the actual industrial gas processes.

Acknowledgements

Author details

John Yang[1*], Milind M. Vaidya[2], Sebastien A. Duval[2] and Feras Hamad[2]

1 Aramco Services Company: Aramco Research Center—Boston, Cambridge, MA, USA

2 Research and Development Center, Saudi Aramco, Dhahran, Saudi Arabia

*Address all correspondence to: john.yang@aramcoamericas.com

IntechOpen

References

[1] The BP Statistical Review of World Energy. 70th ed. 2021. Available from: https://www.bp.com/content/dam/bp/business-sites/en/global/corporate/pdfs/energy-economics/statistical-review/bp-stats-review-2021-full-report.pdf

[2] Statistics report "Key World Energy Statistics 2021", IEA September 2021. Available from: https://iea.blob.core.windows.net/assets/52f66a88-0b63-4ad2-94a5-29d36e864b82/KeyWorldEnergyStatistics2021.pdf

[3] Baker RW. Membrane Technology and Applications. 2nd ed. New York: John Wiley and Sons; 2004

[4] Bernardo P, Drioli E, Golemme G. Membrane gas separation: A review/state of the art. Industrial and Engineering Chemistry Research. 2009;**48**:4638-4663

[5] Baker RW. Membrane gas-separation: Applications. Membrane Operations: Innovation Separation and Transformations. Wiley-VCH Verlag GmbH Co; 2009;**8**:167-194

[6] Gas Separation Membranes—Global Market Trajectory and Analytics. Global Industry Analyst Inc; 2021. Available from: https://www.businesswire.com/news/home/20220120005591/en/Global-Gas-Separation-Membranes-Market-Trajectory-Analytics-Report-2021-Asia-Pacific-Poised-to-Drive-Market-Growth-Europe-and-US-Hold-Significant-Share—Forecast-to-2026—ResearchAndMarkets.com

[7] Baker RW. Future directions of membrane gas separation technology. Industrial and Engineering Chemistry Research. 2002;**41**:1393-1411

[8] Ismail AF, Ridzuan N, Rahman SA. Latest development on the membrane formation for gas separation.

Songklanakarin Journal of Science and Technology. 2002;**24**:1025-1042

[9] Sanders DF, Smith ZP, Guo R, Robeson LM, McGrath JE, Paul DR, et al. Energy-efficient polymeric gas separation membranes for a sustainable future: A review. Polymer. 2013;**54**:4729-4761

[10] Ravanchi RM, Kaghazchi T, Kargari A. Application of membrane separation processes in petrochemical industry: A review. Desalination. 2009;**235**:199-244

[11] Scholes CS, Stevens GW, Kentish SE. Membrane gas separation applications in natural gas processing. Fuel. 2012;**96**:15-28

[12] Yampolskii Y. Polymeric gas separation membranes. Macromolecules. 2012;**45**:3298-3311

[13] Baker RW, Lokhandwala K. Natural gas processing with membranes: An overview. Industrial and Engineering Chemistry Research. 2008;**47**:2109-2121

[14] Schultz J, Peinemann KV. Membranes for separation of higher hydrocarbons from methane. Journal of Membrane Science. 1996;**110**:37-45

[15] Toy LG. Pinnau I. Natural Gas Treatment Process Using PTMSP Membrane. U.S. Patent 55017221

[16] Merkel TC, Bondar V, Nagai K, Freeman BD. Gas sorption, diffusion, and permeation in poly(dimethylsiloxane). Journal of Polymer Science Part B: Polymer Physics. 2000;**38**:273-296

[17] Thomas S, Pinnau I, Dub N, Guiver MD. Pure- and mixed-gas permeation properties of a microporous spirobisindane-based ladder polymer (PIM-1). Journal of Membrane Science. 2009;**333**:125-131

[18] Thomas S, Pinnau I, Du N, Guiver MD. Hydrocarbon/hydrogen mixed-gas permeation properties of PIM-1, an amorphous microporous spirobisindane polymer. Journal of Membrane Science. 2009;**338**:1-4

[19] Yampolskii Y, Starannikova L, Belov N, Bermeshev M, Gringolts M, Finkelshtein E. Solubility controlled permeation of hydrocarbons: New membrane materials and results. Journal of Membrane Science. 2014;**453**: 532-545

[20] Jue ML, Lively RP. Targeted gas separations through polymer membrane functionalization. Reactive and Functional Polymers. 2015;**86**:88-110

[21] Vaughn JT, Harrigan DJ, Sundell BJ, Lawrence JA, Yang J. Reverse selective glassy polymers for C$_{3+}$ hydrocarbon recovery from natural gas. Journal of Membrane Science. 2017;**522**:68-76

[22] Stern SA, Shah VM, Hardy BJ. Structure-permeability relationships in silicone polymers. Journal of Polymer Science Part B: Polymer Physics. 1987; **25**:1263-1298

[23] Semenova SI. Polymer membranes for hydrocarbon separation and removal. Journal of Membrane Science. 2004;**231**(1–2):189-207

[24] Abang T, Vaidya MM, Prada IC, Duval SA, Ballaguet J-PR, Mohammad AF, et al. Membrane application for NGL production enhancement. In: GPA Europe / GPA GCC joint Annual Conference, Athens, 21-23 September, 2016. Available from: https://gpaeurope. com/library/secure/membrane-applica tion-ngl-production-enhancement

[25] Yang J, Vaidya MM, Harrigan DJ, Duval SA, Hamad F, Bahamdan AA. Modified rubbery siloxane membranes for enhanced C$_{3+}$ hydrocarbon recovery from natural gas: Pure and multicomponent gas permeation

evaluation. Separation and Purification Technology. 2020;**242**:116774

[26] Rao HX, Liu FN, Zhang ZY. Preparation and oxygen/nitrogen permeability of PDMS crosslinked membrane and PDMS/ tetraethoxysilicone hybrid membrane. Journal of Membrane Science. 2007;**303**: 132-139

[27] Haider B, Dilshad MR, Rehman MAU, Schmitz JV, Kaspereit M. Highly permeable novel PDMS coated asymmetric polyethersulfone membranes loaded with SAPO-34 zeolite for carbon dioxide separation. Separation and Purification Technology. 2020;**248**:116899

[28] Haider B, Dilshad MR, Rehman MAU, Akram MS, Kaspereit M. Highly permeable innovative PDMS coated polyethersulfone membranes embedded with activated carbon for gas separation. Journal of Natural Gas Science and Engineering. 2020;**81**:103406

[29] Bakonyi P, Bogdán F, Kocsi V, Nemestóthy N, Bélafi-Bakó K, Buitrón G. Investigating the effect of hydrogen sulfide impurities on the separation of fermentatively produced hydrogen by PDMS membrane. Separation and Purification Technology. 2016;**157**:222-228

[30] Liang C-Z, Yong W-F, Chung T-S. High-performance composite hollow fiber membrane for flue gas and air separations. Journal of Membrane Science. 2017;**541**:367-377

[31] Moradi MR, Chenar MP, Noie SH. Using PDMS coated TFC-RO membranes for CO$_2$/N$_2$ gas separation: Experimental study, modeling, and optimization. Polymer Testing. 2016;**56**: 287-298

[32] Scholes CA, Bacus J, Chen GQ, Tao WX, Li G, Qader A, et al. Pilot plant performance of rubbery polymeric

membranes for carbon dioxide separation from syngas. Journal of Membrane Science. 2012;**389**:470-477

[33] Uwitonze H, Hwang KS, Lee I. Improving NGL recovery process with dividing-wall column for offshore applications. Chemical Engineering and Processing: Process Intensification. 2020;**147**:107747

[34] White Paper: "Liquid Hydrocarbon Drop Out in Natural Gas Infrastructure". NGC+ Liquid Hydrocarbon Drop Out Task Group; 2005. Available from: https://www.beg.utexas.edu/files/cee/legacy/NGC_HDP_Paper.pdf

[35] Mehra R. Conversion of Lean Oil Absorption Process to Extraction Process for Conditioning Natural Gas. U.S. Patent 4696688

[36] Dragomirova R, Stöhr M, Hecker C, Lubenau U, Paschek D, Wohlra S. Desorption-controlled separation of natural gas alkanes by zeolite membranes. RSC Advances. 2014;**4**: 59831-59834

[37] Yu L, Grahn M, Hedlund J. Ultra-thin MFI membranes for removal of C_{3+} hydrocarbons from methane. Journal of Membrane Science. 2018;**551**:254-260

[38] Arruebo M, Coronas J, Menéndez M, Santamaría L. Separation of hydrocarbons from natural gas using silicalite membranes. Separation Science and Technology. 2001;**25**:275-286

[39] Ribeiro MA, Ferreira A, Santos JC, Seo YK, Lee UH, Chang JS, et al. Separation of C_3/C_4 hydrocarbon mixtures by adsorption using a mesoporous iron MOF: MIL-100(Fe). Microporous and Mesoporous Materials. 2012;**153**:178-190

[40] Wijmans JW, Baker RW. The solution-diffusion model: A review. Journal of Membrane Science. 1995;**107**: 1-21

[41] Bhide BD, Voskericyan A, Stern SA. Hybrid processes for the removal of acid gases from natural gas. Journal of Membrane Science. 1998;**140**:27-49

[42] Denbeigh K. The Principles of Chemical Equilibrium. Cambridge: Cambridge University Press; 1960

[43] Singh-Ghosal A, Koros AJ. Energetic and entropic contributions to mobility selectivity in glassy polymers for gas separation membranes. Industrial and Engineering Chemistry Research. 1999; **38**:3647-3654

[44] Raharjo RD, Freeman BD, Sanders ES. Pure and mixed gas CH_4 and n-C_4H_{10} sorption and dilation in poly (dimethylsiloxane). Journal of Membrane Science. 2007;**292**:45-61

[45] Lau CH, Li P, Chung TS, Paul DR. Reverse-selective polymeric membranes for gas separations. Progress in Polymer Science. 2013;**38**:740-766

[46] Jiang X, Kumar A. Performance of silicone-coated polymeric membrane in separation of hydrocarbons and nitrogen mixtures. Journal of Membrane Science. 2005;**25**:179-188

[47] Merkel TC, Bondar VI, Nagai K, Freeman BD, Pinnau. Gas sorption, diffusion, and permeation in poly (dimethylsiloxane). Journal of Polymer Science Part B: Polymer Physics. 2000; **38**:415-434

[48] Khanbabaei G, Vasheghani-Farahani E, Rahmatpour A. Permeability, solubility, and diffusivity of methane and butane in diphenylsiloxane-dimethylsiloxane copolymer membranes. Journal of Macromolecular Science Part B Physics. 2011;**50**:2376-2392

[49] Iyer GM, Liu L, Zhang C. Hydrocarbon separation by glassy polymer membranes. Journal of Polymer Science. 2020;**58**:2482-2517

[50] Jordan SM, Koros WJ. Permeability of pure and mixed gases in silicone rubber at elevated pressures. Journal of Polymer Science Part B: Polymer Physics. 1990;**28**:795-809

[51] Pinnau I, He Z. Pure-and mixed-gas permeation properties of poly-dimethyl siloxane for hydrocarbon/methane and hydrocarbon/hydrogen separation. Journal of Membrane Science. 2004;**244**:227-233

[52] Raharjo RD, Freeman BD, Paul DR, Sarti GC, Sanders ES. Pure and mixed gas CH_4 and $n\text{-}C_4H_{10}$ permeability and diffusivity in poly(dimethylsiloxane). Journal of Membrane Science. 2007;**306**(9):75-92

[53] Sadrzadeh M, Shahidi K, Mohammadi T. Effect of operating parameters on pure and mixed gas permeation properties of a synthesized composite PDMS/PA membrane. Journal of Membrane Science. 2009;**342**: 327-340

[54] Ghadimi A, Sadrzadeh M, Shahidi K, Mohammadi T. Ternary gas permeation through a synthesized PDMS membrane: Experimental and modeling. Journal of Membrane Science. 2009;**344**:225-236

[55] Khanbabaei G, Vasheghani-Farahani E, Rahmatpour A. Pure and mixed gas CH_4 and $n\text{-}C_4H_{10}$ permeation in PDMS-fumed silica nanocomposite membranes. Chemical Engineering Journal. 2012;**191**:369-377

[56] Grushevenko EA, Borisov IL, Bakhtin DS, Bondarenko GN, Levin IS, Volkov AV. Silicone rubbers with alkyl side groups for C$_{3+}$ hydrocarbon separation. Reactive and Functional Polymers. 2019;**134**:156-165

[57] Mushardt H, Muller M, Shishatskiy S, Wind J, Brinkmann T. Detailed investigation of separation performance of a MMM for removal of higher hydrocarbons under varying operating conditions. Membranes. 2016;**6**:16

[58] Low ZX, Budd PM, McKeown NB, Patterson DA. Gas permeation properties, physical aging, and its mitigation in high free volume glassy polymers. Chemical Reviews. 2018;**118**: 5871-5911

[59] Pinnau I, Toy LG. Transport of organic vapors through poly(1-trimethylsilyl-1-propyne). Journal of Membrane Science. 1996;**116**:199-209

[60] Pinnau I, Casillas CG, Morisato A, Freeman BD. Hydrocarbon/hydrogen mixed gas permeation in poly(1-trimethylsilyl-1-propyne) (PTMSP), poly(1-phenyl-1-propyne) (PPP), and PTMSP/PPP blends. Journal of Polymer Science Part B: Polymer Physics. 1996; **34**:2613-2621

[61] Pinnau I, He Z. Filled Super Glassy Membrane. U.S. Patent 6316684

[62] Prabhakar RS, Merkel TC, Freeman BD, Imizu T, Higuchi A. Sorption and transport properties of propane and perfluoropropane in poly(dimethylsiloxane) and poly(1-trimethylsilyl-1-propyne). Macromolecules. 2005;**38**:1899-1910

[63] Raharjo RD, Freeman BD, Paul DR, Sanders ES. Pure and mixed gas CH_4 and $n\text{-}C_4H_{10}$ permeability and diffusivity in poly(1-trimethylsilyl-1-propyne). Polymer. 2007;**48**:7329-7344

[64] Grinevich Y, Starannikova L, Yampolskii Y, Gringolts M, Finkelshtein E. Solubility controlled permeation of hydrocarbons in novel highly permeable polymers. Journal of Membrane Science. 2011;**378**:250-256

[65] Gomes D, Nunes SP, Peinemann K-V. Membranes for gas separation based on poly(1-trimethylsilyl-1-propyne)–silica nanocomposites. Journal of Membrane Science. 2005;**246**:13-25

[66] Morisato A, Pinnau I. Synthesis and permeation properties of poly (4-methyl 2-pentyne). Journal of Membrane Science. 1996;**121**:243-250

[67] Yave W, Peinemann KV, Shishatskiy S, Khotimskiy V, Chirkova M, Matson S, et al. Synthesis, characterization, and membrane properties of poly(1-trimethylgermyl-1-propyne) and its nanocomposite with TiO_2. Macromolecules. 2007;**40**:8991-8998

[68] Hu Y, Shiotsuki M, Sanda F, Freeman BD, Masuda T. Synthesis and properties of Indan-based polyacetylenes that feature the highest gas permeability among all the existing polymers. Macromolecules. 2008;**41**: 8525-8532

[69] Pinnau I, Morisato A, He Z. Influence of side-chain length on the gas permeation properties of poly(2-alkylacetylenes). Macromolecules. 2004;**37**:2823-2828

[70] Finkelshtein E, Makovetsii K, Gringolts M, Rogan Y, Golenko T, Starannikova L, et al. Addition-type polynorbornenes with $Si(CH_3)_3$ side groups: Synthesis, gas permeability, and free volume. Macromolecules. 2006;**39**: 7022-7029

[71] Yampolskii Y, Starannikova L, Belov N, Gringolts M, Finkelshtein E, Shantarovich V. Addition—type polynorbornene with $Si(CH_3)_3$ side groups: Detailed study of gas permeation, free volume and thermodynamic properties. Membrane Gas Separation. 1st ed. John Wiley and Sons Ltd; 2010;**3**:43-57

[72] Gringolts ML, Bermeshev MV, Starannikova LE, Rogan YV, Yampol'skii YP, Finkel'shtein ES. Synthesis and gas separation properties of metathesis polynorbornenes with different positions of one or two $SiMe_3$ groups in a monomer unit. Polymer Science, Series A. 2009;**51**:1233-1240

[73] Bermeshev MV, Syromolotov AV, Gringolts ML, Starannikova LE, Yampolskii YP, Finkelshtein ES. Synthesis of high molecular weight poly [3-{tris(trimethylsiloxy)silyl} tricyclononenes-7] and their gas permeation properties. Macromolecules. 2011;**44**:6637-6640

[74] Gringolts M, Bermeshev M, Yampolskii Y, Starannikova L, Shantarovich V, Finkelshtein E. New high permeable addition poly (tricyclononenes) with $Si(CH_3)_3$ side groups. Synthesis, gas permeation parameters, and free volume. Macromolecules. 2010;**43**:7165-7162

[75] Sundell BJ, Lawrence JA III, Harrigan DJ, Lin S, Headrick TP, O'Brien JT, et al. Exo-selective, reductive heck derived polynorbornenes with enhanced molecular weights, yields, and hydrocarbon gas transport properties. ACS Macro Letters. 2020;**9**: 1363-1368

[76] Alentiev DA, Egorova ES, Bermeshev MV, Starannikova LE, Topchiy MA, Asachenko AF, et al. Anus tricyclononene polymers bearing tri(n-alkoxy)silyl side groups for membrane gas separation. Journal of Materials Chemistry A. 2018;**6**:19393-19408

[77] Alentiev DA, Bermeshev MV, Starannikova LE, Bermesheva EV, Shantarovich VP, Bekeshev VG, et al. Stereoselective synthesis and polymerization of Exo-5-trimethylsilylnorbornene. Journal of Polymer Science, Part A: Polymer Chemistry. 2018;**56**:1234-1248

[78] Wozniak AI, Bermesheva EV, Andreyanov FA, Borisov IL, Zarezin DP, Bakhtin DS, et al. Modifications of addition poly(5-vinyl-2-norbornene) and gas-transport properties of the obtained polymers. Reactive and Functional Polymers. 2020;**149**: 104513

[79] Wozniak AI, Borisov IL, Bermesheva EV, Zarezin DP, Volkov AV, Finkelstein ES, et al. Influence of the nature of chemical modification of addition poly (5-vinyl-2-norbornene) on the gas permeability of hydrocarbons. Polymer Science, Series B. 2020;**62**:218-224

[80] Alentiev DA, Dzhaparidze DM, Bermeshev MV, Starannikova LE, Filatova MP, Yampolskii YP, et al. Addition copolymerization of silicon-containing tricyclononene with 2,5-norbornadiene dimer. Polymer Science, Series B. 2019;**61**:812-816

[81] Alentiev DA, Egorova ES, Bermeshev MV, Starannikova LE, Yampolskii YP, Finkelshtein ES. Crosslinking of addition copolymers from tricyclononenes bearing $(CH_3)_3Si$- and $(C_2H_5O)_3Si$-groups as a modification of membrane gas separation materials. Polymer Engineering and Science. 2019; **59**:2502-2507

[82] Alentiev DA, Egorova ES, Bermeshev MV, Starannikova LE, Topchiy MA, Asachenko AF, et al. Janus tricyclononene polymers bearing tri(n-alkoxy)silyl side groups for membrane gas separation. Journal of Materials Chemistry A. 2018;**6**:19393-19408

[83] Pinnau I, He Z. Pure- and mixed-gas permeation properties of polydimethylsiloxane for hydrocarbon/methane and hydrocarbon/hydrogen separation. Journal of Membrane Science. 2004;**244**:227-233

[84] Sadrzadeh M, Shahidi K, Mohammad T. Preparation and C_3H_8/gas separation properties of a synthesized single layer PDMS membrane. Separation Science and Technology. 2010;**45**:592-603

[85] Farno E, Ghadimi A, Kasiri N, Mohammadi T. Separation of heavy gases from light gases using synthesized PDMS nano-composite membranes: Experimental and neural network modeling. Separation and Purification Technology. 2011;**81**:400-410

[86] Chen B, Ruan X, Xiao W, Jiang X, He G. Synergy of CO_2 removal and light hydrocarbon recovery from oil-field associated gas by dual-membrane process. Journal of Natural Gas Science and Engineering. 2015;**26**:1254-1263

[87] Fang M, Zhang H, Chen J, Wang T, Liu J, Li X, et al. A facile approach to construct hierarchical dense membranes via polydopamine for enhanced propylene/nitrogen separation. Journal of Membrane Science. 2016;**499**:290-300

[88] Grushevenko EA, Borisov IL, Bakhtin DS, Legkov SA, Bondarenko GN, Volkov AV. Membrane material based on octyl-substituted polymethylsiloxane for separation of C_3/C_1 hydrocarbons. Petroleum Chemistry. 2017;**57**:334-340

[89] Mushardt H, Kramer V, Hülagü D, Brinkmann T, Kraume M. Development of solubility selective mixed matrix membranes for gas separation. Chemie Ingenieur Technik. 2014;**86**:83-91

[90] Alentiev A, Economou IG, Finkelshtein E, Petrou J, Raptis VE, Sanopoulou M, et al. Transport properties of silmethylene homo-polymers and random copolymers: experimental measurements and molecular simulation. Polymer. 2004; **45**:6933-6944

[91] Khosravi A, Sadeghi M. Separation performance of poly(urethane–urea) membranes in the separation of C_2 and C_3 hydrocarbons from methane. Journal of Membrane Science. 2013;**434**:171-183

[92] Gomesa D, Peinemann KV, Nunes SP, Kujawski W, Kozakiewicz J. Gas transport properties of segmented poly (ether siloxane urethane urea) membranes. Journal of Membrane Science. 2006;**281**:747-753

[93] Harrigan DJ, Yang J, Sundell BJ, Lawrence JA, O'Brien JT, Ostraat ML. Sour gas transport in poly(ether-*b*-amide) membranes for natural gas separations. Journal of Membrane Science. 2020;**595**:117497

[94] Tirouni I, Sadeghi M, Pakizeh M. Separation of C_3H_8 and C_2H_6 from CH_4 in polyurethane–zeolite 4Å and ZSM-5 mixed matrix membranes. Separation Science and Technology. 2015;**141**: 394-402

[95] Yang J, Vaidya MM, Tammana VVR, Harrigan D. Modified Siloxane Composite Membranes for Heavy Hydrocarbon Recovery. U.S. Patent 10293301

[96] Masuda T, Isobe E, Higashimura T, Takada K. Poly[1-(trimethylsilyl)-1-propyne]: A new high polymer synthesized with transition-metal catalysts and characterized by extremely high gas permeability. Journal of the American Chemical Society. 1983; **105**:7473-7474

[97] Budd PM, Msayib KJ, Tattershall CE, Ghanem BS, Reynolds KJ, McKeown NB, et al. Gas separation membranes from polymers of intrinsic microporosity. Journal of Membrane Science. 2005;**251**:263-269

[98] Wang Y, Ma X, Ghanem BS, Alghunaimi F, Pinnau I, Han Y. Polymers of intrinsic microporosity for energy-intensive membrane-based gas separations. Materials Today Nano. 2018;**3**:69-95

[99] Wang X, Wilson TJ, Alentiev DA, Gringolts M, Finkelshtein E, Bermeshev M, et al. Substituted polynorbornene membranes: A modular template for targeted gas separations. Polymer Chemistry. 2021;**12**:2947-2977

[100] Zhan X, Wang M, Gao T, Lu J, He Y, Li L. A highly selective sorption process in POSS-g-PDMS mixed matrix membranes for ethanol recovery via pervaporation. Separation and Purification Technology. 2020;**236**:116238

[101] Hu M, Wu Z, Sun L, Guo S, Li L, Lia J, et al. Improving pervaporation performance of PDMS membranes by interpenetrating polymer network for recovery of bio-butanol. Separation and Purification Technology. 2019;**228**: 115690

[102] Si Z, Liu C, Li G, Wang Z, Li J, Xue T, et al. Epoxide-based PDMS membranes with an ultrashort and controllable membrane-forming process for 1-butanol/water pervaporation. Journal of Membrane Science. 2020;**612**: 118472

[103] Shan VM, Hardy BJ, Stern SA. Solubility of carbon dioxide, methane and propane in silicon polymers. Effect of polymer side chains. Journal of Polymer Science Part B: Polymer Physics. 1986;**24**:2033-2047

[104] Stern SA, Shah VM, Hardy BJ. Structure-permeability relationships in silicone polymer. Journal of Polymer Science Part B: Polymer Physics. 1987; **25**:1263-1298

[105] Shan VM, Hardy BJ, Stern SA. Solubility of carbon dioxide, methane and propane in silicon polymers. Effect of polymer backbone chains. Journal of Polymer Science Part B: Polymer Physics. 1993;**31**:313-317

[106] Yilgor E, Yilgor I. Silicone containing copolymers: Synthesis, properties and applications. Progress in Polymer Science. 2014;**39**:1165-1195

[107] Ghosh A, Sen SK, Dasgupta B, Banerjee S, Voit B. Synthesis, characterization and gas transport properties of new poly (imide siloxane) copolymers from 4,4-(4,4-isopropylidenediphenoxy) bis (phthalicanhydride). Journal of Membrane Science. 2010;**364**:211-218

[108] Powell CE, Qiao G, Kebtish SE. Gas Separation Membranes and Processes for the Manufacture Therefor U.S. Patent Publication 2010/0313752

[109] Hong T, Chatterjee S, Mahurin SM, Fan F, Tian Z, Jiang D, et al. Impact of tuning CO_2-philicity in polydimethylsiloxane-based membranes for carbon dioxide separation. Journal of Membrane Science. 2017;**530**:213-219

[110] Madhavan K, Reddy BSR. Poly (dimethylsiloxane-urethane) membranes: Effect of hard segment in urethane on gas transport properties. Journal of Membrane Science. 2006;**283**: 357-365

[111] Sadeghi M, Talakesh MM, Ghalei B, Shafiei M. Preparation, characterization and gas permeation properties of a polycaprolactone based polyurethane–Silica nanocomposite membrane. Journal of Membrane Science. 2013;**427**: 21-29

[112] Talakesh MM, Sadeghi M, Pourafshari Chenar M, Khosravi A. Gas separation properties of poly(ethylene glycol)/poly(tetramethylene glycol) based polyurethane membranes. Journal of Membrane Science. 2012;**415–416**: 469-477

[113] Sadeghia M, Semsarzadehb MA, Barikanic M, Ghaleib B. The effect of urethane and urea content on the gas permeation properties of poly (urethane–urea) membranes. Journal of Membrane Science. 2010;**354**:40-47

[114] Sadeghi M, Semsarzadeh MA, Barikani M, Ghalei B. Study on the morphology and gas permeation property of polyurethane membranes. Journal of Membrane Science. 2011;**385–386**:76-85

[115] Isfahani AP, Ghalei B, Bagheri R, Kinoshita Y, Kitagawa H, Sivaniah E, et al. Polyurethane gas separation membranes with ethereal bonds in the

hard segments. Journal of Membrane Science. 2016;**513**:58-66

[116] Fakhar A, Sadeghi M, Dinaru M, Lammertink R. Comparative assessment of hydrocarbon separation performance of bulky poly(urethane-urea)s toward rubbery membranes. Journal of Natural Gas Science and Engineering. 2021;**27**: 104356

[117] Liu SL, Shao L, Chua ML, Lau CH, Wang H, Quan S. Recent progress in the design of advanced PEO-containing membranes for CO_2 removal. Progress in Polymer Science. 2013;**38**:1089-1120

[118] Amo K et al. Final Report to DOE *"Low-Quality Natural Gas Sulfur Removal/Recovery"*. Morgantown, WV: MTR; 1998

[119] Ogbole EO, Lou J, Ilias S, Desmane V. Influence of surface treated SiO_2 on the transport behavior of O_2 and N_2 through polydimethylsiloxane nanocomposite membrane. Separation and Purification Technology. 2017;**175**: 358-364

[120] Ha H, Park J, Ando S, Kim CB, Nagai K, Freeman BD, et al. Gas permeation and selectivity of poly (dimethylsiloxane)/graphene oxide composite elastomer membranes. Journal of Membrane Science. 2016;**518**: 131-140

[121] Molki B, Aframehr WM, Bagheri R, Salimi J. Mixed matrix membranes of polyurethane with nickel oxide nanoparticles for CO_2 gas separation. Journal of Membrane Science. 2018;**549**: 588-601

[122] Zhan X, Lu J, Xu H, Liu J, Liu X, Cao X, et al. Enhanced pervaporation performance of PDMS membranes based on nanosized octa [(trimethoxysilyl)ethyl]-POSS as macro-crosslinker. Applied Surface Science. 2019;**473**:785-798

[123] Rezakazemi M, Shahidi K, Mohammadi T. Hydrogen separation and purification using crosslinkable PDMS/zeolite A nanoparticles mixed matrix membranes. International Journal of Hydrogen Energy. 2012;**37**: 14576-14589

[124] Najari S, Saeidi S, Gallucci F. Mixed matrix membranes for hydrocarbons separation and recovery: A critical review. Reviews in Chemical Engineering. 2019;**37**(3):363-406

[125] Sadrzadeh M, Amirilargani M, Shahidi K, Mohammadi T. Pure and mixed gas permeation through a composite polydimethylsiloxane membrane. Polymers for Advanced Technologies. 2011;**22**:586-597

[126] Kim H, Kim H-G, Kim S, Kim SS. PDMS-silica composite membranes with silane coupling for propylene separation. Journal of Membrane Science. 2009;**344**:211-218

[127] Shen G, Zhao J, Guan K, Shen J, Jin W. Highly efficient recovery of propane by mixed-matrix membrane via embedding functionalized graphene oxide nanosheets into polydimethylsiloxane. AICHE Journal. 2017;**63**:3501-3510

[128] Woo M, Choi J, Tsapatsis M. Poly (1-trimethylsilyl-1-propyne)/MFI composite membranes for butane separations. Microporous and Mesoporous Materials. 2008;**110**:330-338

[129] Sundell BJ, Lawrence JA III, Harrigan DJ, Vaughn JT, Pilyugina TS, Smith DR. Alkoxysilyl functionalized polynorbornenes with enhanced selectivity for heavy hydrocarbon separations. RSC Advances. 2016;**6**: 51619-51628

Chapter 6

Pandemic Problems Related to Forecasting Natural Gas Consumption

Tomasz Chrulski

Abstract

There are many macroeconomic and atmospheric factors affecting the development of natural gas consumption forecasts. Recently, another factor has emerged that causes some problems in developing an accurate forecast. COVID-19 introduced many perturbations. It makes previous long-term natural gas consumption forecasts obsolete. This chapter presents the process of natural gas consumption in the U.S. and the implications that a pandemic will have on the forecasting process. Forecasts were developed using RStudio. The results clearly show the impact of the pandemic on the consumption of gaseous fuel by each area of life.

Keywords: forecasting, natural gas, COVID-19, consumption, energy

1. Introduction

Pandemics are not a new phenomenon in human history, from time to time crises occur in world history. An example of such a pandemic is the coronavirus that shocked humanity. It is the kind of shock that causes a global economic crisis. The coronavirus also introduced some shock in forecasting energy consumption, including natural gas. Natural gas consumption forecasts during a pandemic, even those for the shortest periods, are subject to large error. The problem with forecasting gas consumption is the inability to predict government decisions on restrictions and the lack of reliable estimates of the long-term forecast of the number of illnesses and the lack of predictions of people's behavior in following proper instructions.

This paper presents a coronavirus pandemic and its effects on natural gas consumption forecasting in the United States.

2. Natural gas consumption in the world

The International Energy Agency, in its 2021 Q1 Quarterly Report, estimates that global gas demand fell by 2.5% or 100 billion cubic meters (bcm) in 2020, the largest decline on record. This was due to slowing economies, resulting in lower energy intake. The other interesting development in 2020 was that natural gas prices reached historic lows and had high volatility [1]. However, the report presents the positive part, that is, it forecasts that global natural gas demand will grow by 2.8% in 2021 (about 110 bcm), slightly above the 2020 decline, allowing a return to 2019 levels.

3. Natural gas consumption in U.S.

U.S. Energy Information Administration, Agency says it will be some time before energy consumption returns to normal [2]. The speed of economic recovery, advances in technology, changes in trade flows, and energy incentives will determine what sources the United States uses to produce and consume energy in the future [3]. **Figure 1** shows a forecast of natural gas consumption with an increasing outlook. The US EIA (**Figure 2**) forecasts that natural gas will continue to play an important role in the industry.
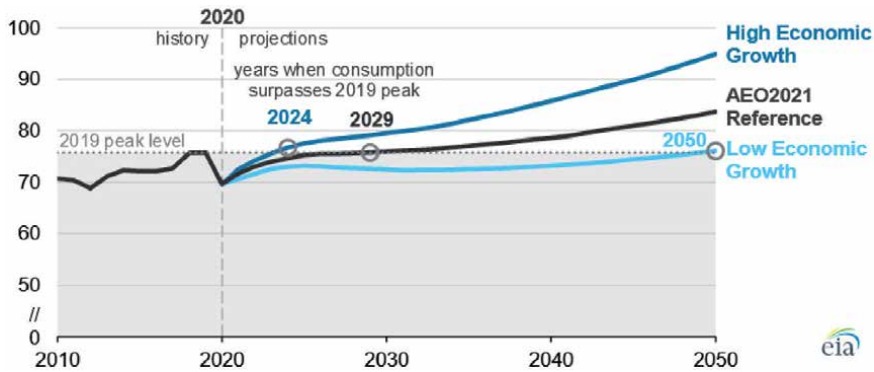
Figure 1.
EIA's AEO2021 explores the impact of COVID-19 on the U.S. energy mix through 2050 (quadrillion British thermal units).
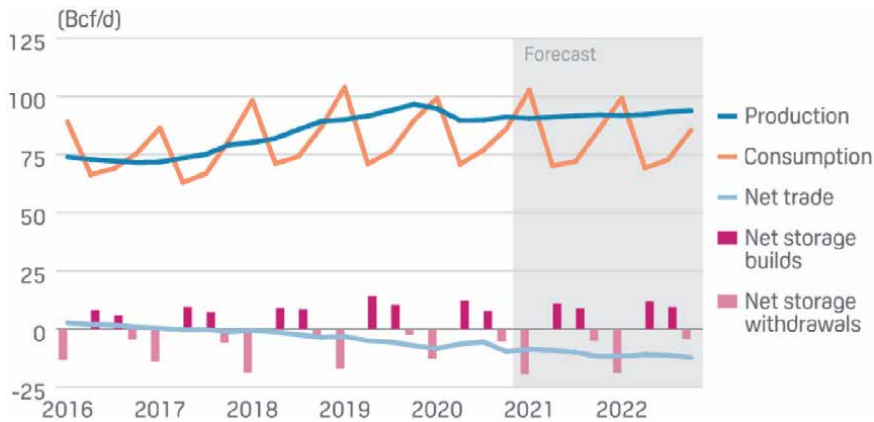
Figure 2.
US EIA lifts forecasts for 2021–2022 natural gas and power consumption.

Prices (dollars per thousand cubic feet)	2019	2020	2021 (forecast)
Henry Hub Spot	2.67	2.11	3.15
Residential Sector	10.46	10.83	11.04
Commercial Sector	7.59	7.48	7.98
Industrial Sector	3.90	3.29	4.23

Table 1.
Prices (dollars per thousand cubic feet).

Natural gas prices at the Henry Hub [4], which are a reference for U.S. natural gas prices, show that natural gas prices for the pandemic period are the lowest. **Table 1** shows forecasts using neural networks indicate that natural gas prices will increase. **Table 2** also indicates that natural gas supplies will be on an increasing trend. At the same time, **Table 3** shows that residential natural gas prices increased in 2020 due to higher residential natural gas consumption caused by remote work and being at home. In 2021, the price of natural gas is forecast to rise because the industrial economy is poised to recover.

The pandemic also reduced the supply of gaseous fuel, regardless of the type of supply chain. Coronavirus completely impacted overall natural gas consumption. The forecast for 2021 gas fuel supplies do not represent a sharp rebound. The forecast is for an increasing, fairly moderate trend.

The natural gas consumption forecast for 2021 is interesting. For the residential sector, commercial sector the trend is upward, while natural gas consumption by the electric power sector is forecast to decline, which may be due to the growth of the renewables industry and the increased interest in this energy source by this industry.

Data shows, natural gas in the residential sector, consuming natural gas for space heating, water heating, air conditioning, lighting, refrigeration, cooking and the use of many other appliances will continue to be important in the energy industry. In addition data shows that natural gas will play an important role in the industry's recovery. It will continue to be used to heat and cool processes and power machinery (**Table 4**) [5].

Supply (billion cubic feet per day)	2019	2020	2021 (forecast)
Marketed Production	100.04	98.84	98.90
Dry Gas Production	93.06	91.36	91.41
Pipeline Imports	7.37	6.84	7.08
LNG Imports	0.14	0.13	0.20

Table 2.
Supply (billion cubic feet per day).

Consumption (billion cubic feet per day)	2019	2020	2021 (forecast)
Residential Sector	13.74	12.70	13.23
Commercial Sector	9.62	8.60	9.18
Industrial Sector	23.07	22.56	23.91
Electric Power Sector	30.93	31.74	28.83
Total Consumption	85.15	83.26	82.93

Table 3.
Consumption (billion cubic feet per day).

Primary Assumptions (percent change from previous year)	2019	2020	2021 (forecast)
Heating Degree Days	0.6	−9.4	5.5
Cooling Degree Days	−5.2	1.6	−5.6
Commercial Employment	1.4	−6.6	3.2
Natural-gas-weighted Industrial Production	−0.4	−5.8	6.6

Table 4.
Primary assumptions (percent change from previous year).

Baseline assumptions (percentage change from previous year) show that Natural-gas-weighted Industrial Production will be increasing compared to 2020.

4. The impact of coronavirus on the U.S. gas industry

The emergence of the coronavirus has had a dramatic impact on natural gas intake, but also on the values of companies operating in the natural gas market area. The authors project that the net loss to U.S. GDP from COVID-19 will range from $3.2 trillion (14.8%) to $4.8 trillion (23.0%) over a 2-year period for the scenarios conducted [6].

The example of giant drilling services provider Schlumberger shows how the pandemic has affected the company's stock value and workforce reductions [7]. The above was presented in **Figure 3**.

5. Coronavirus as an additional external factor

The compiled data set by U.S. for Natural Gas Consumption by End Use clearly shows the impact of the pandemic on natural gas withdrawals [8]. The **Figure 4** definitively shows the growth in natural gas consumption in the U.S.

Figure 3.
Schlumberger limited (SLB). NYSE - Nasdaq real time Price. Currency in USD.
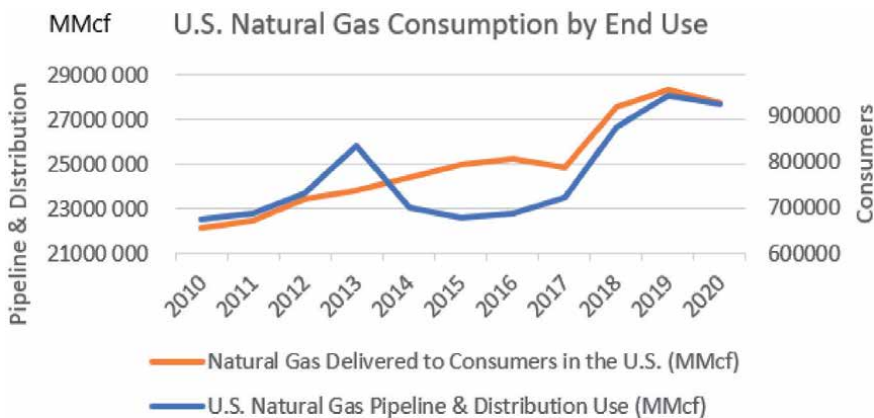
Figure 4.
U.S. natural gas consumption by end use.
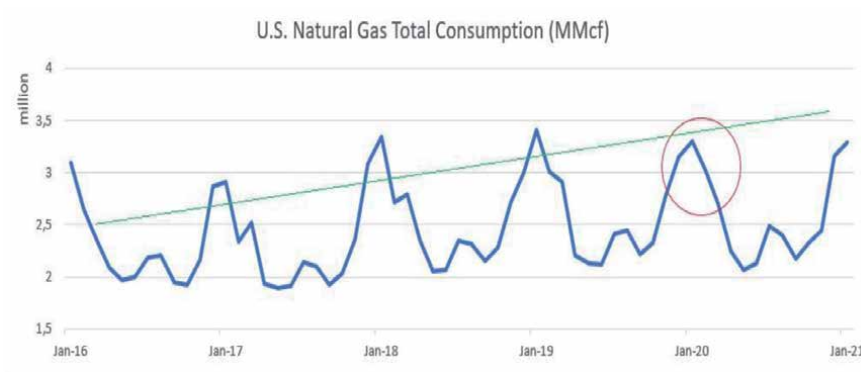
Figure 5.
U.S. natural gas consumption.

Figure 5 shows the impact of coronavirus on natural gas consumption. The trend of aggregate natural gas consumption in the U.S. has been slowed by a pandemic [9].

External factors, such as weather conditions [10], fuel availability, and price [11], influence the development of a forecast of natural gas consumption by consumers. In addition, a new factor affecting gas consumption dynamics is the economy, which depends on the number of cases of COVID-19. The first cases in North America were reported in the United States in January 2020 [12]. Forecasting assumes general economic stability and no significant changes in the industry or market.

The forecast should be developed on historical data that provides a guarantee of stability [13]. However, there is no guarantee that past conditions will hold in the future. Unexpected external events, e.g., the emergence of a pandemic, undermine assumptions and render the forecast invalid. It is impossible to take into account completely the number of future illnesses and the restrictions introduced by the government. Throughout the United States, officials are enacting a number of restrictions on distancing from the public. Ordinances vary by state, county, and even city. Restrictions are escalating in many areas as cases are increasing across the country [14].

6. Forecasting natural gas consumption

This research study investigates natural gas consumption forecasting using NNAR model (neural network autoregression). Artificial Neural Networks (ANN) were hypothesized as a method to imitate the human brain and its functions while it performs cognitive tasks, or when it learns [15]. The forecasting was done using RStudio software. Two forecasts were made for the year 2021–2022. The first one was made using historical data up to January 2020 and the next one collected historical data of the year 2020 where the pandemic was ongoing. **Figure 6** shows the consumption forecast with a horizon of one year. It does not take pandemics into account (**Figure 7**).

Figure 8 considers the pandemic.

For example, gas consumption by industry in the state of Alabama and Colorado are shown in **Figures 9** and **10**. The figure shows gas consumption for the years: 2018, 2019, 2020. It is clear that the first two years are essentially collinear with each other, making it possible to make a forecast of consumption for 2020. However, the
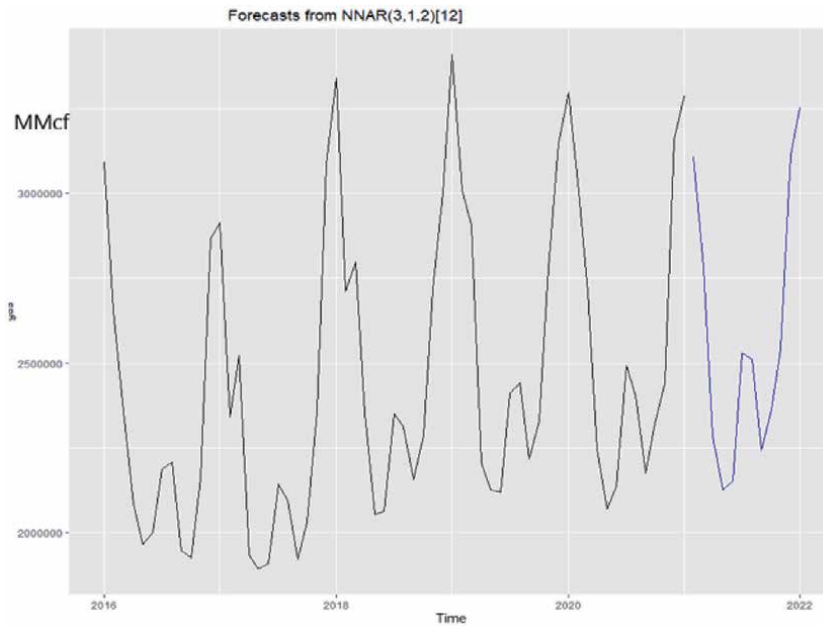
Figure 6.
U.S. natural gas consumption – Forecast including COVID-19.
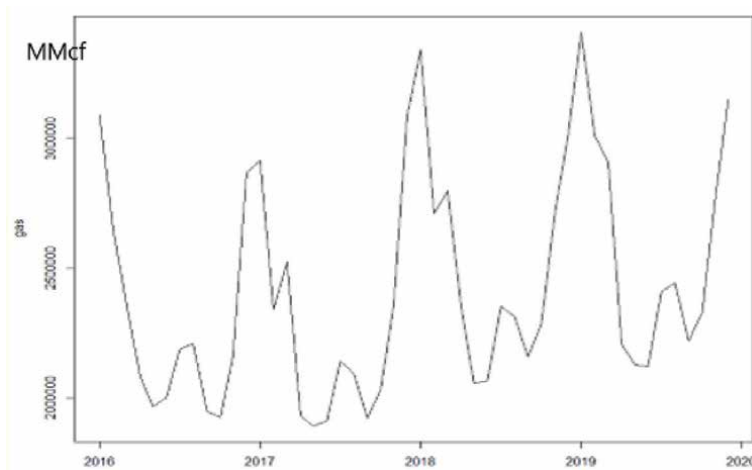
Figure 7.
U.S. natural gas consumption (2016–2020).

onset of the pandemic introduced a structural change in the time series and resulted in lower industrial gas consumption. Such a structural change causes distortion and becomes a problem in accurate forecasting. In order to carry out a natural gas forecast for 2021, it is therefore necessary to take into account, the structural change that occurred in 2020. In addition, an analysis of the impact of COVID-19 morbidity and economic dynamics should also be carried out.

The chapter presents the use of neural networks for forecasting. The use of machine learning can perfectly be used to predict natural gas consumption [16]. They can also be used to discuss the link between the number of COVID-19 cases and natural gas consumption [17].
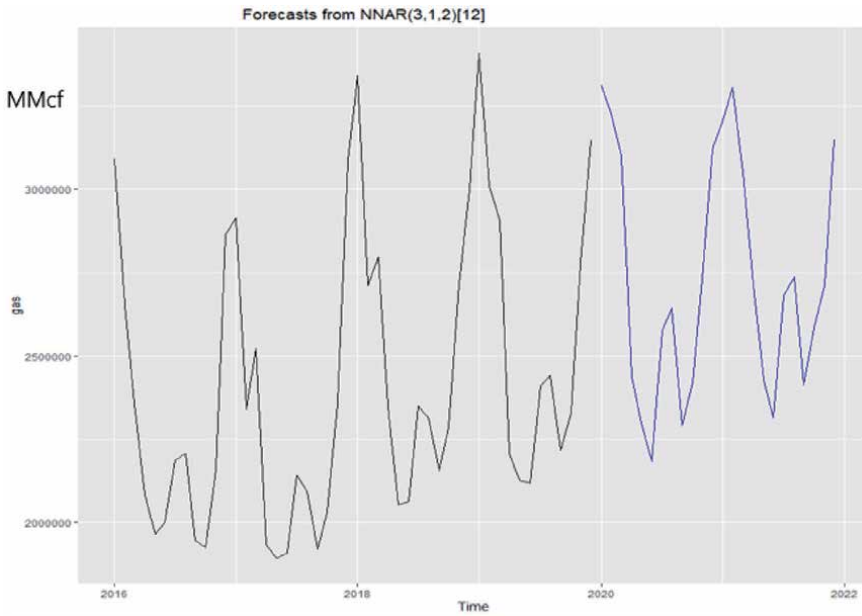
Figure 8.
U.S. natural gas consumption – Forecast without COVID-19.
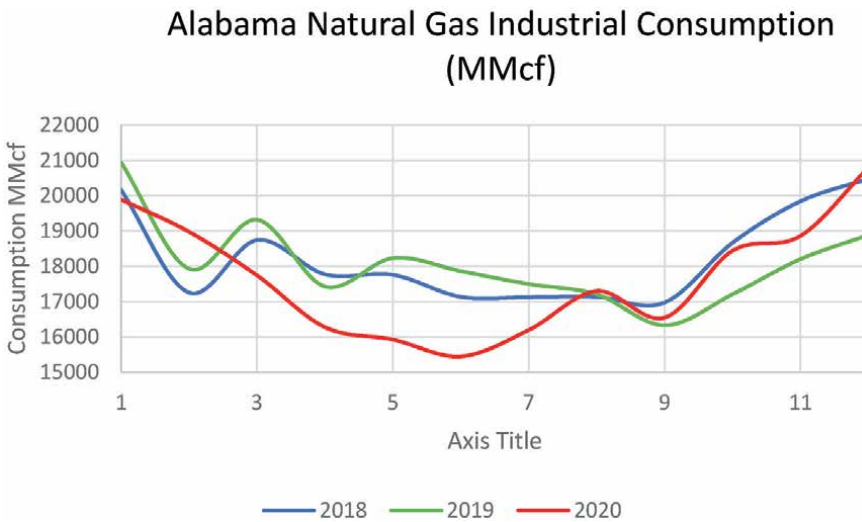
Figure 9.
Alabama natural gas industrial consumption (MMcf) in 2018–2020.

7. Conclusions

In conclusion, there is a definite impact of coronavirus on the dynamics of developing economies. The data presented in the article on the consumption of gaseous fuel by the industrial sector, households, natural gas transmission, shows a structural change in 2020. There is no sector that benefits from natural gas supply that has not been impacted by COVID-19. Pandemic has become a new external factor to consider when forecasting natural gas consumption.
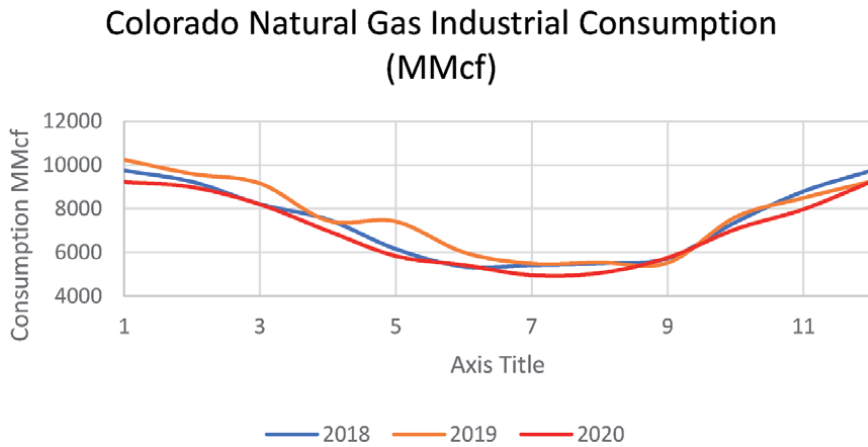
Figure 10.
Colorado natural gas industrial consumption (MMcf) in 2018–2020.

Developed forecasts by various research centers indicated that between 2020 and 2021, natural gas consumption will be on an upward trend. Unfortunately, the emergence of a pandemic in early 2020 introduced a shock. The pandemic has become a new factor to be taken into account when making a forecast. Unfortunately, it is not easy to estimate how further the pandemic will spread, the timing of government restrictions.

Thus, it can be definitely stated that the existing forecasts must be constantly updated, supplemented with new data. Even the latest available models are not able to estimate natural gas consumption in the long term very accurately. They may also be used to discuss the four key themes that shape the politics of a sustainable energy transition.

Author details

Tomasz Chrulski
Environmental Engineering, Mining and Energy, Doctoral School AGH,
Cracow, Poland

*Address all correspondence to: chrulski@agh.edu.pl

IntechOpen

References

[1] Gas Market Report, Q1-2021 [Internet]. 2021. Available from: https://www.iea.org/reports/gas-market-report-q1-2021 [Accessed: 2021-04-16]

[2] Annual Energy Outlook 2021 (AEO 2021) [Internet]. 2021. Available from: https://www.eia.gov/outlooks/aeo/ [Accessed: 2021-04-17]

[3] Short-Term Energy Outlook [Internet]. 2021. Available from: https://www.eia.gov/outlooks/steo/report/natgas.php [Accessed: 2021-04-15]

[4] Disavino, Scott; Krishnan, Barani (25 September 2014). "Henry Hub, king of U.S. natural gas trade, losing crown to Marcellus". Reuters. Retrieved 21 October 2014.

[5] Natural gas can revive the economy [Internet]. 2021. Available from: https://www.politico.com/story/2011/04/natural-gas-can-revive-the-economy 053574 [Accessed: 2021-04-15]

[6] The Impacts of the Coronavirus on the Economy of the United States [Internet]. 2021. Available form: https://link.springer.com/article/10.1007/s41885-020-00080-1 [Accessed: 2021-04-15]

[7] Schlumberger cuts 21,000 jobs after 'the most challenging quarter in past decades' [Internet]. Available from: https://www.offshoreenergy.biz/schlumberger-cuts-21000-jobs-after-the-most-challenging-quarter-in-past-decades/ [Accessed: 2021-04-15]

[8] Natural Gas [Internet]. 2021. Available from: https://www.eia.gov/dnav/ng/ng_cons_sum_dcu_nus_a.htm [Accessed: 2021-04-15]

[9] Global trends in the energy sector and their implication on energy security in NATO's southern neighbourhood [Internet]. 2021. Available from: http://www.realinstitutoelcano.org/wps/portal/rielcano_en/contenido?WCM_GLOBAL_CONTEXT=/elcano/elcano_in/zonas_in/defense+security/ari103-2020-berahab-global-trends-energy-sector-and-implication-on-energy-security-in-natos-southern-neighbourhood [Accessed: 2021-04-14]

[10] Timmer P., Lamb P., Relations between Temperature and Residential Natural Gas Consumption in the Central and Eastern United States. Journal of Applied Meteorology and Climatology. 2007. 46:1993-2013.DOI:10.1175/2007JAMC1552.1

[11] Natural gas explained Factors affecting natural gas prices [Internet]. 2021. Available from: https://www.eia.gov/energyexplained/natural-gas/factors-affecting-natural-gas-prices.php [Accessed: 2021-04-14]

[12] COVID-19 pandemic [Internet]. 2021. Available from: https://en.wikipedia.org/wiki/COVID-19_pandemic [Accessed: 2021-04-14]

[13] 5fundamentals of business forecasting [Internet]. 2021. Available from:

[14] COVID-19 restrictions [Internet]. 2021. Available from: https://eu.usatoday.com/storytelling/coronavirus-reopening-america-map/ [Accessed: 2021-04-14]

[15] Anagnostis A., Papageorgiou E., Bochtis D. Application of Artificial Neural Networks for Natural Gas Consumption Forecasting. Sustainability. 2020; 12: 6409; DOI:10.3390/su12166409

[16] Shigi O., J. Weiqi., C. Wei. Machine learning model to project the impact of COVID-19 on US motor gasoline

demand. Nature Energy, 5, 6660673 (2020).

[17] Helm D. The Environmental Impacts of the Coronavirus. Environmental and Resource Economics volume 76, pages 21-38 (2020).

Chapter 7

Role of Natural Gas in India: Recent Developments and Future Perspectives

Akhoury Sudhir Kumar Sinha,

Sanjay Kumar Kar, Umaprasana Ojha and

Marriyappan Sivagnanam Balathanigaimani

Abstract

India strives for increasing the share of natural gas to 15% by 2030 from 6.5% at present. This chapter highlights recent developments to achieve the targets set by the government. Further, we discuss regulatory and policy interventions to facilitate the growth of the natural gas market in the country. We analyze the opportunities and challenges to the smooth transition of the green economy with the greater role of natural gas. We present the infrastructure developments, including liquefied natural gas (LNG) importing terminals, cross-country natural gas pipelines network, LNG tankers, refueling stations, and city gas distribution (CGD) network. Finally, we present a futuristic perspective of natural gas in the energy transition. We conclude that India being a natural gas deficient country, import dependency would continue to grow. However, this would not deter the growth of natural gas in the economy. Proactive measures by the government and its agencies will boost investment to create the desired infrastructure for achieving higher natural gas penetration in India.

Keywords: natural gas, price, city gas distribution, import, India

1. Introduction

India commits to addressing climate change without compromising economic growth. It continues to expand its energy basket and reduce over-dependence on coal and oil. India is on the right path to managing its energy transition. It aims to increase the share of natural gas to 15% by 2030 [1] from 6.5% at present. Experts believe that India must go through multiple phases of the energy transition. In this context, many believe that natural gas could play the role of a transition fuel. However, we believe that natural gas has a more prominent role than just a bridge fuel. The government firmly pushes the adoption of natural gas as a clean fuel. In line with the United Nation's sustainable development goal # 7 [2], natural gas offers a solution to ensure modern and clean energy is accessible to millions of customers at an affordable price in India. Further, natural gas is a viable and affordable solution to reduce pollution in cities and industries. The transport sector, one of the biggest CO_2 emitters, stands to benefit from the higher penetration of natural gas in the country.

2. Natural gas market in India

India's natural gas market is at a growth stage. Its demand for natural gas has been growing steadily. India's unsaturated market has the potential to expand gas demand at a faster rate. This section highlights natural gas reserves, domestic production, consumption, deficit, and import.

2.1 Proved natural gas reserves

At the end of 2020, India's proven natural gas reserves stood at 1.32 trillion cubic meters (TCM) compared to just 0.731 TCM in 2000, 80.5% growth in 20 years. Despite India's rising natural gas reserves, its share is just 0.7% of the global reserves. Asia-Pacific, the world's most populous region holds 8.8% of the global reserves. In this region, China leads the table with a 4.5% share followed by Australia, India, Indonesia, and others. Global natural gas resources are quite unevenly distributed. Russia, Iran, and Qatar hold 19.9%, 17.1%, and 13.1% of the global reserves, respectively. These three countries collectively controlled 50% of the global natural gas reserves of 188 TCM in 2020 (**Figure 1**).

2.2 Domestic production

India's natural gas production has been a cause of concern for the government and the operating companies. The consuming industries, especially the power and fertilizer producers are at the receiving end. The falling natural gas production has severely impacted the power and fertilizer producers. If India continues to produce at the current rate the reserve to production ratio (R/P) suggests that natural gas can last for 56 years. However, the production rate is bound to increase in the future (**Figure 2**), thereby the R/P ratio will fall.

2.3 Demand projections

Petroleum and Natural Gas Regulatory Board (PNGRB), India had commissioned an industry study in 2011 to assess the realistic demand of natural gas by 2029–2030. The purpose was to advise the government about the development of related infrastructure for making the natural gas available, transport, creating re-gasification plants, and supply to various sectors. The industry group submitted
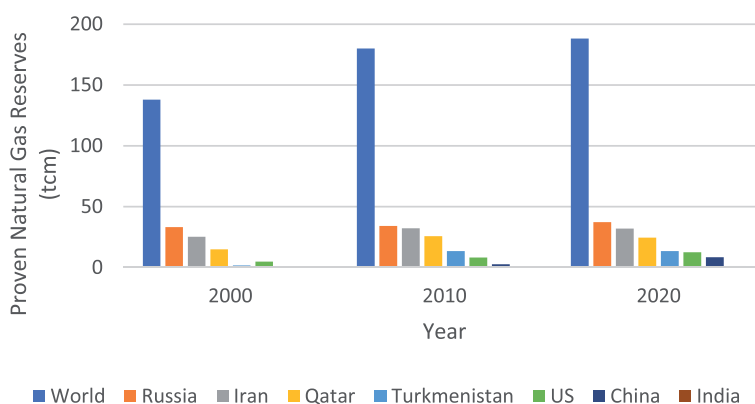

Figure 1.
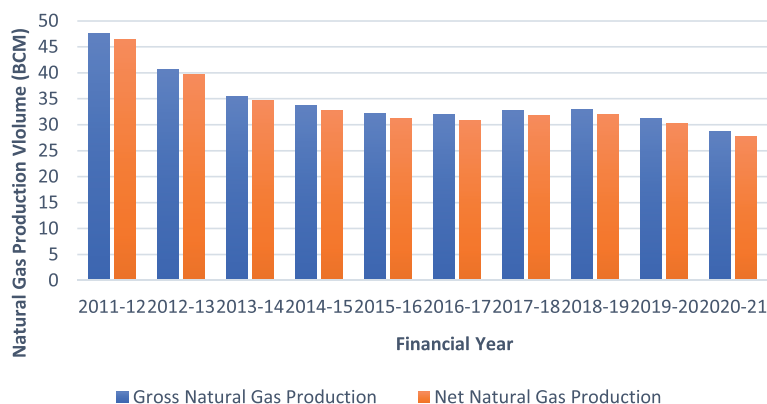*Proven natural gas reserves in India. Source: prepared by the authors using Statistical Review of World Energy 2021.*

Figure 2.
India's domestic natural gas production.

Consuming industry/sector	2021–2022	2026–2027	2029–2030
Power	238.88	308.88	353.88
Fertilizer	107.85	110.05	110.05
City gas distribution	46.25	67.96	85.61
Industrial	37.00	52.06	63.91
Petchem/refineries/Int. Cons	81.99	103.41	118.85
Sponge iron/steel	10.00	12.19	13.73
Total realistic demand	516.97	654.55	746.03

Source: PNGRB [3].

Table 1.
Projected natural gas demand in India [in MMSCMD].

its report in 2013. PNGRB projected that the demand for natural gas to expand up to 746 million standard cubic meters per day (MMSCMD) (**Table 1**) in 2029–2030 from the actual consumption of 176 MMSCMD in 2010–2011.

2.4 Consumption and deficit

Petroleum Planning and Analysis Cell (PPAC) records suggest that the average consumption of natural gas in the first 4 months of the financial year (FY) 2021–2022 was around 171 MMSCMD, which was 316 MMSCMD lower than the PNGRB projections. In fact, from the year 2012–2013 till 2020–2021, the trend of consumption of natural gas had been significantly lower than PNGRB's projections. India achieved about 34% of the natural gas demand projections for the FY 2020–2021 compared to 65% achievement in 2012–2013 (**Table 2**). During the said period, consumption of natural gas increased marginally but the actual consumption was markedly lower than the projections. The widening gap between projected demand and actual consumption could be due to sluggish natural gas demand in the industries and transport sector. The reasons for sluggish demand and slow penetration of natural gas could be ascribed to a combination of factors including lower domestic natural gas production, high import price, and infrastructure bottlenecks.

Arguably, the natural gas market development was slower than expectations. The natural gas market development was largely dependent on the ample supply of domestic natural gas at affordable prices [4]. The user of natural gas in power

Year	Projection	Actual consumption			Achievement against projections
		Domestic	**Import**	**Total**	
2012–2013	242.66	108.91	48.26	157.17	64.8%
2013–2014	265.33	94.72	48.77	143.49	54.1%
2014–2015	289.52	89.57	50.98	140.55	48.5%
2015–2016	326.16	85.29	58.60	143.89	44.1%
2016–2017	378.06	84.51	68.08	152.59	40.4%
2017–2018	409.05	86.93	75.18	162.11	39.6%
2018–2019	438.02	87.83	78.74	166.57	38.0%
2019–2020	465.19	82.90	92.84	175.74	37.8%
2020–2021	490.76	76.12	90.03	166.15	33.9%

Source: prepared by the authors based on projections of PNGRB [3] and actual consumption data of PPAC.

Table 2.
Natural gas consumption in India (MMSCMD).

plants, fertilizer plants, cement plants, ceramic industries, refineries, and petro-chemical plants were expected to strongly drive natural gas market development, which did not happen.

The gas-based power plants expected domestic gas to address their long-standing supply concerns. Unfortunately, falling domestic natural gas production aggravated their pain points. The natural gas consumption by power plants declined from 22,628 MMSCM in 2011–2012 to 11,020 MMSCM in 2019–202020. The share of natural gas consumption by power plants fell from 35% in 2011–2012 to 17% in 2019–20. During the period, natural gas consumption in refineries, fertilizer plants, and the city gas distribution (CGD) network improved (**Figure 3**). The government prioritized natural gas allocation to the CGD network, especially for the domestic and transport segments, which resulted in higher consumption.

It is evident from **Table 2** that domestic supply shrank from approximately 109 MMSCMD in 2012–2013 to 76 MMSCMD. Consequently, during the same period, liquefied natural gas (LNG) import increased from 48 MMSCMD to 90 MMSCMD. LNG import registered 88.5% growth to maintain the share of natural gas and meet rising natural gas demand.
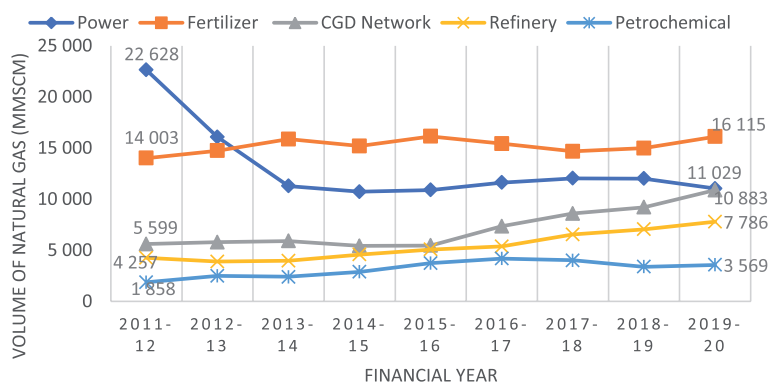

Figure 3.
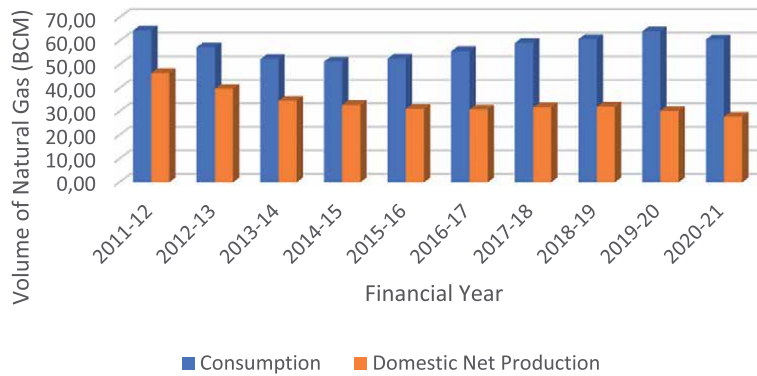*Natural gas consumption by selected sectors in India [5].*

Figure 4.
India's widening natural gas deficit. Source: prepared by the authors using PPAC data [7].

The higher contribution of natural gas in India's primary energy basket will be severely constrained without boosting demand in the industries, especially power and fertilizer plants. The refineries, petrochemical plants, and CGD network will continue to augment natural gas consumption. CARE Ratings—a leading credit rating agency [6] indicated that higher urea production will foster demand for natural gas. However, the fertilizer plants will need natural gas supply at a competitive price, supply of domestic natural gas will be desirable.

India's natural gas domestic production has been lower than consumption. It is evident from **Figure 4** that natural gas consumption has been fluctuating. The slack domestic natural gas production failed to meet the demand, therefore, the deficit kept widening. So, India's dependence on natural gas imports continued to rise. Due to a lack of import options through a pipeline, India primarily relied on the import of liquefied natural gas (LNG).

2.5 LNG import

Globally LNG trade registered a strong improvement over the previous decade. By December 2020, global LNG trade reached 350 million tons. By February 2021, the global LNG regasification capacity in 39 markets hit 850 million tons per annum (MMTPA). According to the International Gas Union Report (2021), the leading natural gas deficit countries like Japan, China, South Korea, India, and Spain depended on LNG imports. The rising demand of LNG in the Asia-pacific region resulted in the liquefaction capacity addition in the middle east, Russia, and Australia.

Due to India's rising natural gas deficit the import of LNG escalated from 18 billion cubic meters (BCM) in 2012 to 33.8 BCM in 2020 (**Figure 5**). Owing to severe Covid-19 linked disruptions including national and state lockdowns, natural gas consumption slowed down in 2020–2021. As a result, the import of LNG was marginally lower than the previous year. India largely depended on Qatar for its LNG import. However, newer import destinations like Russia and USA offered an opportunity to reduce over-dependence on any single-sourcing country.

India's LNG import would continue to increase in the near and long term. Recently Petronet LNG CEO stated that "India needed to increase its LNG import capacity to 155 MMTPA considering 80% utilization to enhance the use of the cleaner fuel" [8]. The capacity expansion will depend on pipeline connectivity for evacuating re-gasified LNG (R-LNG), the price of imported LNG, and acceptance of R-LNG at the price point by the consuming industries. High LNG price often hampers buyer acceptance; therefore, it slows down LNG infrastructure
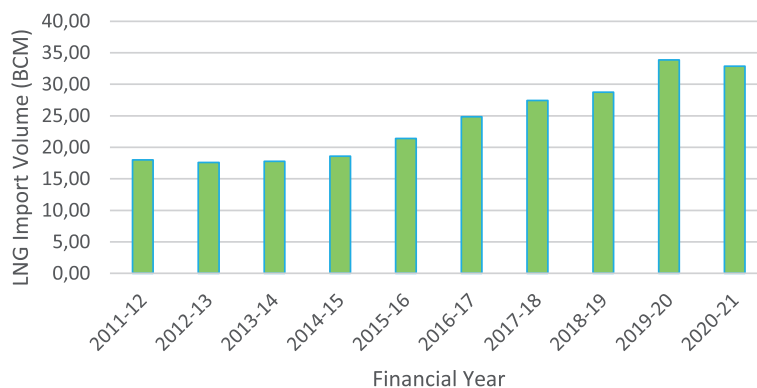
Figure 5.
LNG import in India. Source: prepared by the authors using data available on the PPAC website [7].

development. However, investment in LNG infrastructure is long-term in nature, so temporary LNG price fluctuations should not deter LNG infrastructure build-up.

3. National gas grid

India aspires to raise natural gas's share to 15% by 2030 from 6.5% in 2020, which necessitates the development of associated infrastructure. Often the natural consumption centers are away from production centers, so pipeline connectivity or virtual pipelines are critical to meet the demand. India's natural gas grid would expand to 32,559 km from the existing operational network of 17,016 km (**Table 3**).

India's plan for creating an interconnected "National Gas Grid" shall support the wider supply and distribution of R-LNG throughout the nation. Indian natural gas pipeline network is less penetrated compared to the developed countries. At present, for every million population only about 12.3 km of natural gas pipeline exists in India. India's 17,016 km of natural pipeline network is insufficient to connect all demand centers. Therefore, the government wants to develop a pan-India natural gas grid of 32,559 km, which can address the existing regional disparities of the natural gas pipeline network. A fully functional national gas grid will improve natural gas accessibility throughout India.

As per the data available on the Petroleum Planning and Analysis Cell website the average capacity utilization of natural gas pipelines stood at 54% during

	Pipeline	Authorized length (km)	Authorized capacity (MMSCMD)
1	Operational natural gas pipelines	12,654	337.3
2	Natural gas pipelines partly commissioned[#]	13,680	406.5
3	Natural gas pipelines under construction	6225	180.9
	Total	32,559	924.7

[#]*Commissioned length 4362 km.*
Source: compiled from published sources [9].

Table 3.
India's natural gas grid (as on June 30, 2020).

2018–2019. Only nine pipelines had capacity utilization above 50% and Dahej-Vijaipur (DVPL)-Vijaipur-Dadri (GREP) pipeline had a capacity utilization of 67% and Dabhol-Bengaluru Pipeline (Including spur) had 8% capacity utilization. Most of the existing pipelines are underutilized and the operators are trying to enhance the productivity of the pipelines. Pipeline Infrastructure Limited, now the owner of East-West Pipeline has decided to inject green hydrogen into its pipeline, which will help improving the capacity utilization of the pipeline.

4. LNG Infrastructure in India

Natural gas consumption should expand from 165–170 MMSCMD to 640–700 MMSCMD by 2030 to reach 15% of primary energy consumption. Given the fact that domestic production may not go beyond 100 MMCMD from the current levels of 75 MMSCMD, the gap shall have to be filled with the import of LNG for which adequate regasification terminals should be created. At end of 2020, India had six operational LNG terminals with a cumulative capacity of 42.5 MMTPA (**Table 4**). Petronet LNG Limited operated the largest LNG terminal at Dahej, Gujarat with a capacity of 17.5 MMTPA. The Petronet LNG Limited was the largest operator with

Sl. no.	Place	State	Developer(s)	Year of commissioning	Annual capacity (MMTPA)
Commissioned					
1	Dahej	Gujarat	Petronet LNG Limited (PLL)	2004	17.5
2	Hazira	Gujarat	Shell Energy India	2005	5
3	Dabhol	Maharashtra	GAIL (India) Limited	2013	5
4	Kochi	Kerala	PLL	2013	5
5	Ennore	Tamil Nadu	Indian Oil Corporation	2019	5
6	Mundra	Gujarat	GSPC LNG	2020	5
Total commissioned					42.5
Under construction					
7	Jaigarh	Maharashtra	Western Concessions Private Limited	2021*	5
8	Dhamra	Odisha	Adani-Total	2022*	5
9	Jafrabad	Gujarat	Swan LNG	2022*	5
10	Chhara	Gujarat	HPCL & Shapoorji Pallonji Group	2022*	5
Total under construction					20
Grand total					62.5

Expected.
Source: compiled from published sources [10–14].

Table 4.
Operational, under construction, and planned LNG terminals in India.

54% of the total commissioned LNG terminal capacity. The Dahej and Kochi terminals handled 254 and 14 LNG cargoes respectively in the financial year 2020–2021. Utilization of Kochi terminal improved due to commissioning of Mangalore section of GAIL's Kochi Mangalore pipeline in 2020–2021.

Upcoming LNG terminals in Jaigarh (Floating Storage and Regasification Unit), Dhamra, Jafrabad (Floating Storage Regasification Unit), and Chhara will strengthen India's LNG infrastructure. Especially, the LNG terminal in Dhamra, Odisha will augment natural gas supply in eastern India and enhance natural gas penetration in the underpenetrated demand centers. Dhamra LNG terminal can expand its capacity up to 10 MMTPA. Dhamra will bolster the CGD network development in Odisha, West Bengal, and Bihar. LNG infrastructure development now spreads across the coastal states in the country, which was not the case earlier. Even then the share of LNG infrastructure is still concentrated in the west coast of India. Well-developed ports, natural gas pipeline connectivity, and early adoption of natural gas in Gujarat, and Maharashtra supported LNG infrastructure in the west coast. On the contrary, despite the strong coastal presence, the eastern and southern states like Odisha, West Bengal, Andhra Pradesh, and Tamil Nadu remained less attractive for developing LNG terminals.

In the coming years, LNG will have greater use, especially LNG as a transport fuel, which will create a market for LNG. Considering the emerging market scenario, LNG has significant growth potential. The new and upcoming consumption centers will create additional demand for LNG.

The existing capacity of LNG regasification terminals will not meet the rising demand. Therefore, the existing LNG infrastructure requires much-needed augmentation to address the supply concerns. So, there is an urgent requirement of creating additional LNG regasification capacity to the tune of 75–80 MMTPA.

5. City gas distribution

Apart from the anchor customers like the power/fertilizer/petrochemical plants, and the refineries, the City Gas Distribution would remain the other most important sector. The government wanted to boost clean fuel adoption in the transport, domestic, and transport sectors, so PNGRB granted 136 authorizations to CGD entities under the 9th and 10th rounds of bidding. This has the potential to cover 53% of the geographical area (GA) of the country and 70% of the population. The number of compressed natural gas (CNG) stations will increase from existing 1838 to over 10,000. In the same way, the number of domestic PNG connections is proposed to be increased from 5.5 million to 40 million. The CGD sector will need investment in the range of Rs. 900–1200 billion by 2030.

The CGD networks growth has taken off only in the last 5–6 years. The historical progress of the award of CGD networks is given in **Table 5**.

In addition to the above, PNGRB has already announced the 11th round of bidding under which an additional 65 geographical areas could get a CGD network. The government and the PNGRB are constantly striving to expand the CGD network in the country. The government offers the necessary push to build up CGD infrastructure across the country. However, the shift from competing fuels to natural gas will take place only when it becomes cost-competitive. Customers are primarily concerned about the economics of natural gas vs. the competing fuels [16, 17], therefore availability of domestic natural gas or imported LNG at a competitive price will improve the adoption of natural gas.

	Category	Year	Category-wise % area of India	Cumulative	Category-wise population coverage (%)	Cumulative population coverage (%)	Category-wise GA	Cumulative GA
1	Pre-PNGRB		3.02	3.02	9.67	9.67	31	31
2	Round 1	2008	0.03	3.05	0.33	10.00	6	37
3	Round 2	2009	0.03	3.08	0.23	10.23	3	40
4	Round 3	2010	1.21	4.29	0.77	11.00	6	46
5	Round 4	2013	1.29	5.58	2.27	13.27	9	55
6	Round 5	2015	1.82	7.40	2.04	15.31	8	63
7	Round 6	2015	2.02	9.42	2.07	17.38	18	81
8	Round 7	2016	0.46	9.88	0.36	17.74	1	82
9	Round 8	2016	0.57	10.45	0.94	18.68	6	88
10	Section 42		0.61	11.06	1.57	20.25	6	94
11	Round 9	2018	23.82	34.88	26.38	46.63	86	180
12	Round 10	2018	19.92	52.8	24.32	70.86	50	230

Source: compiled by authors from published sources [15].

Table 5.
CGD network expansion in India.

6. Gas market developments

In addition to the domestic, transport, and industrial segments, there are multiple areas where natural gas could find users. Room heating and cooling offer opportunities for use of natural gas. Higher penetration of the CGD network will facilitate the adoption of CNG for intra-city transport, especially public transport. Despite the economic advantage of CNG over competing fuel, CNG refueling stations remained a major hurdle for inter-city travel. Within the city, mobile refueling units (MRUs) could address refueling concerns as the customers can refuel at their doorstep. MRUs have been working successfully in countries like Mexico, Colombia, Peru, Indonesia, Vietnam, Russia, Korea, etc. India introduced its first MRU (CNG) in June 2021. Due to its flexibility, cost efficiency, and convenience, it has the potential to expand across the country.

The telecom service tower could shift to natural gas/LNG-based generators from diesel generators. There are over 5,20,000 such towers on a pan-India basis and growing. These generators use diesel in case of power outages. The use of natural gas/LNG will be economical as well as environment friendly. LNG use for long-distance transport, inland waterways, LNG bunkering in fishing/marine vessels offers considerable opportunities for adoption as a cleaner fuel.

In addition to the above, the CGD sector will throw open ample opportunities for equipment and spare suppliers in the areas like mechanical meters, smart meters, PNG regulators, PE pipes, online compressor, booster compressor, dispenser, and cascade, etc.

Expansion of the natural gas market will bring along several benefits like socio-economic empowerment, import-substitution, emission reduction, and green energy solutions at affordable prices. Further, natural gas shall address India's energy security concerns to a greater extent.
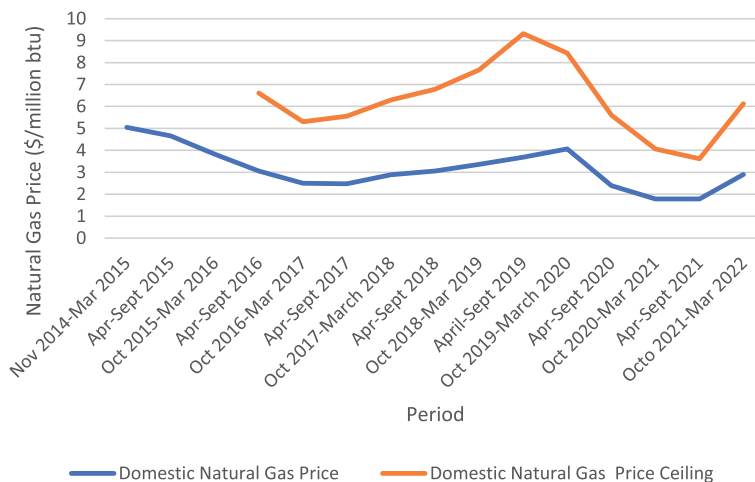
Figure 6.
Domestic natural gas price trend in India. Source: prepared by the authors using PPAC data [18].

7. Enablers for natural gas market growth

The government and regulators have created a conducive environment for investment in gas market development. Consequently, large private players are involved in the entire natural gas value chain. Domestic natural gas allocation policy prioritized gas allocation to the CGD sector, which catalyzes market expansion.

The domestic gas price trends (**Figure 6**) suggest that the market-based pricing mechanism augurs well for the market development. The domestic natural gas price was fixed at $2.90 per million British thermal units (mbtu) for October 2021–March 2022. The ceiling price for natural gas was fixed at $6.13 per mBtu for October 2021–March 2022.

The government's decision to develop a pan-India natural gas grid will be one of the biggest enablers for gas market growth. Less penetrated regional markets in north-east, east, and south India will get access to natural gas. The availability of natural gas will boost industrial, economic, and social progress in those regions.

8. Impediments for natural gas market growth

For a long period impediments like insufficient infrastructure for the import of natural gas, low cross-country pipeline penetration, and lack of cost-competitiveness of natural gas hampered market growth in India. Despite rising environmental concerns and lower emphasis on polluting fuel, natural gas faces continued challenges from coal. Further, falling renewable electricity price challenges natural gas's cost competitiveness. The high cost of imported LNG becomes a dampener for power plants to use natural gas. Insufficient availability of domestic natural gas does not offer any hope for the stranded power plants. The Standing Committee on Energy (2020–2021) in its eleventh report pointed out that change in domestic gas allocation policy adversely impacted the stranded power plants. This committee observed that the gas-based power plants which developed based on assured domestic gas supply are unviable on imported R-LNG [19]. High R-LNG price, which is at times twice the price of domestic gas is not sustainable for power plants. Therefore, most of the natural gas-stranded power plants are stressed assets.

The ministry of power stated that the unit cost of power produced from imported R-LNG was around Rs.7/kWh [19], which was expensive compared to coal and renewable power. Solar-based power cost has declined to a record low of Rs 2/kWh, which is comparable to coal-based electricity cost.

Natural gas has been kept outside the purview of goods & services tax (GST), which is an impediment for growth of the sector. Various industry bodies including the Federation of Indian Petroleum Industry recommend bringing natural gas under the ambit of GST [20]. The current tax regime allows states to levy varying amounts of value-added tax, which goes against "one nation one tax" philosophy. Further, buyers of natural gas do not get input credit, consequently, it adds up to the production cost of the industrial customer.

Lack of sufficient cross-country pipeline network remains a major impediment for natural gas market development. The pipeline network has better connectivity in the west coast compared to eastern and north-eastern India. However, the government has taken several steps to build pan-India natural gas pipeline network.

9. Strategic initiatives for natural gas market growth

The government has been pushing for expansion of the natural gas market with a heightened focus on increasing city gas distribution network penetration including CNG at retail outlets across the country. Further, the government emphasizes building cross country pipeline networks to remove the supply bottleneck. The government offers viability gap funding for the infrastructure build-up. For instance, the government committed 60% viability gap funding for Northeast Gas Grid with an estimated project cost of Rs 92.65 billion [21]. The Indradhanush Gas Grid Limited shall connect eight north-eastern states with a 1656 km natural gas pipeline. The government encourages investors to develop LNG terminals for import of LNG and regasification of LNG. In addition, it aspires for developing 1000 LNG refueling stations across all the major "highways, industrial corridors, and mining areas". LNG refueling stations development would attract investment of Rs. 100 billion soon. The first 50 LNG refueling outlets shall be along the golden quadrilateral and major national highways [22]. Ministry of Petroleum and Natural Gas must strongly push for including natural gas in the GST regime. Such a move will bring tax rationality and benefit customers across the country.

The presence of an active and independent regulator in the form Petroleum and Natural Gas Regulatory Board serves as an enabler for faster progress of the natural gas market in India [4]. The regulator brings transparency and establishes fair competition.

10. Conclusions

India's under-penetrated natural gas market will expand till it saturates. There are plenty of scopes for expansion in the north-east, eastern, and southern India. City gas distribution will be a prime driver for natural gas market growth. The existing infrastructure including LNG importing terminals, pipelines, and refueling stations needs a boost. Despite the emergence of multiple green energy options, the share of natural gas will increase. The government's progressive policies including viability gap funding for cross-country pipeline and promotion of LNG/hydrogen-CNG as transport fuels will spur natural gas market developments. Additionally, the government is committed to removing the bottlenecks to enhance penetration of natural in the country. Natural gas will play a critical role in developing India's green economy.

Acknowledgements

Authors are thankful to the editors and anonymous reviewers for their comments and observations.

Conflict of interest

The authors declare no conflict of interest.

Acronyms

Btu	British thermal unit
BCM	billion cubic meter
CGD	city gas distribution
CNG	compressed natural gas
LNG	liquefied petroleum gas
MMTPA	million tons per annum
MMSCMD	million standard cubic meter per day
PNGRB	Petroleum and Natural Gas Regulatory Board
Rs.	Indian rupee
TCM	trillion cubic meter
CARE	Credit Analysis & Research Ltd

Author details

Akhoury Sudhir Kumar Sinha*, Sanjay Kumar Kar, Umaprasana Ojha
and Marriyappan Sivagnanam Balathanigaimani
Rajiv Gandhi Institute of Petroleum Technology, Jais, India

*Address all correspondence to: asksinha@rgipt.ac.in

IntechOpen

References

[1] Ministry of Petroleum & Natural Gas. Indian Petroleum and Natural Gas Statistics 2019-20. 2021

[2] United Nation. The SDGs in Action. 2015. Available from: https://www.undp.org/sustainable-development-goals?utm_source=EN&utm_medium=GSR&utm_content=US_UNDP_PaidSearch_Brand_English&utm_campaign=CENTRAL&c_src=CENTRAL&c_src2=GSR&gclid=EAIaIQobChMI0buikJrW8wIV3_fjBx0OjAUVEAAYASAAEgL3uvD_BwE

[3] PNGRB. Vision 2030: Natural Gas Infrastructure in India. 2013. Availble from: https://www.pngrb.gov.in/Hindi-Website/pdf/vision-NGPV-2030-06092013.pdf

[4] Kar SK, Gupta A, editors. Natural Gas Markets in India. Singapore: Springer Singapore; 2017. DOI: 10.1007/978-981-10-3118-2

[5] Govt. of India. Energy Statistics—India 2021. 2021. Availble from: http://www.mospi.nic.in/sites/default/files/reports_and_publication/ES/Energy%20Statistics%20India%202021.pdf

[6] CARE Ratings. Natural Gas—April-February 2021 Update & FY22 Outlook. 2021

[7] PPAC. Import of LNG in India 2021. Availble from: https://www.ppac.gov.in/content/153_1_ImportNAturalgas.aspx

[8] Verma N. LNG's share of Indian gas demand to rise to 70% by 2030—Petronet CEO. Availble from: https://www.reuters.com/world/india/lngs-share-indian-gas-demand-rise-70-by-2030-petronet-ceo-2021-06-17/ [Accessed: September 9, 2021]

[9] PNGRB. Natural Gas Pipeline Network in India. 2020. Availble from: https://www.pngrb.gov.in/data-bank/NGPLReports27082020.pdf

[10] Petronet LNG Ltd. Dahej LNG Terminal. 2021. Availble from: https://petronetlng.in/Dahej_LNG_Terminal.php

[11] Petronet LNG Ltd. Kochi LNG Terminal 2021. Availble from: https://petronetlng.in/kochi-terminal.php

[12] Shell Energy India. LNG Terminal. 2021. Availble from: https://www.shell.in/shellenergy/shell-energy-india/lng-terminal.html#knowmore

[13] Indian Oil LNG. Terminal. 2021. Availble from: https://www.indianoillng.com/

[14] Australina Govt. Insight—LNG infrastructure in India. 2021. Available from: https://www.austrade.gov.au/news/insights/insight-lng-infrastructure-in-india

[15] PNGRB. CGD Network. 2021. Available from: https://www.pngrb.gov.in/eng-web/CGD-network-BID.html

[16] Kumar Kar S, Kumar Sinha P, Mishra S. Sabarkantha Gas Limited: Challenges of marketing natural gas. Asian Case Research Journal. 2016;**20**:177-217. DOI: 10.1142/S0218927516500073

[17] Kumar Kar S, Sahu S. Managing natural gas business: A case of Bharat Natural Gas Company Limited. Emerging Markets Case Studies. 2012;**2**:1-22. DOI: 10.1108/20450621211214450

[18] PPAC. Natural Gas Price. 2021. Available from: https://www.ppac.gov.in/content/151_1_ProductionNaturalGas.aspx

[19] Lok Sabha. Standing Committee on Energy. 2021. Available from: https://doi.org/http://164.100.47.193/lsscommittee/Energy/17_Energy_11.pdf

[20] Business Standard. Bring natural gas under GST to push for gas-based economy: Industry. 2021

[21] PIB. Cabinet approves Capital Grant as Viability Gap Funding to Indradhanush Gas Grid Limited for setting up the North East Natural Gas Pipeline Grid. 2020. Available from: https://pib.gov.in/Pressreleaseshare. aspx?PRID=1598709 [Accessed: September 25, 2021]

[22] BusinessLine. Clean fuel: Centre plans to invest ₹10,000 cr to set up LNG stations. 2020

Demand Response Applications for the Operation of Smart Natural Gas Systems

Lina Montuori and Manuel Alcázar-Ortega

Abstract

This chapter discusses different aspects related to the operation of natural gas systems in the framework of the new configuration of energy systems based on the smart grid concept. First of all, different experiences performed worldwide regarding the application of demand response principles to increase the efficiency and operability of natural gas networks are presented. Next, the characteristics of the natural gas system to be configured according to the smart grid architecture are discussed, including the necessary agents for the proper functioning of such infrastructure. After that, the current state of installation of gas smart meters in some European countries is presented, according to the massive rollout process promoted by the European Union. Barriers that prevent the full exploitation of demand response resources related to natural gas systems are presented in the next section. After that, technical constraints which may be solved by using demand response are presented. Finally, last tendencies related to the development of natural gas systems, such as the injection of hydrogen, are considered.

Keywords: demand response, smart grid, smart city, energy management, natural gas infrastructure, consumer's flexibility, optimization, energy consumption, renewable energy

1. Introduction

The concepts of Smart Grid and Smart City have rapidly expanded worldwide with the objective to raise sustainability standards, quality of life, and economic dynamism of future cities. At present, cities are responsible for more than 75% of waste, 70% of greenhouse gas emissions, and 75% of energy consumption [1]. This trend is going to be more and more significant due to the increase in population of urban areas. By 2045, according to the World Bank[1], the number of people living in cities will increase by 1.5 times to 6 billion. This fact emphasizes the importance of increasing sustainability, reducing waste energy, and 'smart' management of the available resources. In this context, natural gas systems, similarly to the rest of energy systems, are evolving towards a highly technified structure, where the consumer is called to play a starring role. The implementation of a natural gas smart infrastructure requires the proper development of smart metering and communication protocols to be able to give real-time and remote consumption readings and provide advanced services to the users.

---

[1] http://www.worldbank.org/en/topic/urbandevelopment.

The implementation of this smart architecture is ongoing in some European countries and abroad as will be discussed in the following sections.

Demand response programs are the best candidates to promote the consumers' flexibility, empowering the smart natural gas infrastructure to be a resilient and feasible energy network. Future trends in the development of natural gas systems will be focused on, exploring the huge potential that remains unexplored on the natural gas demand side, which could be used by gas network operators for the solution of technical constraints, balance services, or optimization of programming of underground storage. This potential is especially interesting at this moment, when the massive rollout of gas smart meters is taking place [2, 3]. In this context, smart gas systems would facilitate the use of demand response resources for the better operation of gas networks, similarly to how it happens in power systems.

The chapter will be organized as follows: at first, the state of the art of the massive rollout of smart meters currently ongoing worldwide will be presented. Then, demand response programs currently used in natural gas systems around the world will be explored and analyzed, including a review of some international experiences on this matter. Before, the novel application of smart grid concepts, exclusively used up to now for power systems, will be proposed for the architecture of the smart natural gas system, including the analysis of existing barriers that prevent the implementation of demand response programs in this kind of networks. Finally, the future developments required to optimize the use of this energy resource and to improve the operation of natural gas systems will be presented, identifying new agents and new energy resources (such as hydrogen) that are expected to contribute to developing the natural gas systems in the coming years.

2. State of art of the smart metering infrastructure

The implementation of a smart city requires the proper development of a smart metering infrastructure, a system for the intelligent measurement of the energy consumption of each user, through smart meters able to give real-time and remote consumption readings of different services (electricity, water, gas, and district heating), providing advanced services to the users[2].

In order to reach the proper integration of different energy supplies, such as electricity, gas, water, district heating and energy produced by waste[3], and service systems such as the internet, video terminal, and e-cars, it is necessary to promote the use of different electronic meters (e.g. electric, water, heating, and gas meters) and different sensors integrated into a distributed architecture, able to gather and analyses heterogeneous data. So as to achieve this objective, the following subsystems should be implemented:

- Smart Grids: Intelligent interconnected networks, which have a bidirectional data flow between the service center and the end user.

- Smart Buildings: Commercial and residential buildings that respect the environment and have integrated energy production systems.

- Smart Sensors: Sensors with the function of collecting data from the necessary variables at the smart city. They are fundamental to managing energy and avoiding waste.

---

[2] https://www.endesaeduca.com/Endesa_educa/recursos-interactivos/smart-city.

[3] http://www.autorita.energia.it/it/com_stampa/14/140908cs.htm.

- Information and Communication Technology Infrastructure (ICT): ICT infrastructure must be able to control the different subsystems of the smart city, through which citizens and administrative operators can actively participate in the management of the different facilities and uses [4].

- Smart Citizens: They have to actively participate in smart solutions and smart programs. From the energy perspective, it is the energy consumer.

2.1 Pilots and cases of application

Smart city pilot projects have largely spread out in Europe (Spain, Germany, France, Finland, or Italy). In 2010, the Association "Genova Smart City" drew up a project to turn the capital city of Liguria into a smart city, meeting the requirements of the European Commission [5]. In 2015, into the framework of "Flexemeter project[4]—Flexible smart metering for multiple energy vectors with active prosumers", two pilot applications have been performed in Turin (Italy) and Malmo (Sweden). Both projects involved the local DSOs and volunteer "prosumers[5]" on real systems and were predominantly focused on the integration of the electricity and heating district supply. By 2030, supported by the European Commission, Geneva (Switzerland) will become a smart city for the electric, heating, and cooling networks, with the integration of renewable energies (wind turbines).

The diffusion of flexible multi-utilities and multiservice system is the crucial step to improve energy and market efficiency, to optimize the energy management during the peak periods, and to promote the integration of DR programs profiled on more efficient energy demand prediction [6]. In that framework, a fundamental role is played by the smart meters. At present, a smart metering infrastructure able to collect, aggregate, and analyze real-time data is essential to properly manage the different energy resources and to reduce greenhouse emissions as required by the COP21 [1].

The European Smart Metering Landscape report [7] has presented the best practices in the smart metering field. Different smart metering pilot projects have been successfully carried out in Europe: in Finland, the smart metering project was based on the monitoring of the cottage's electricity consumption in real time and its impact on the carbon footprint. Another example was carried out in Spain, where consumers equipped with smart meters received specific information to allow an evaluation on how to reduce their average electrical consumption. In Germany, a German start-up company created a Social Metering App that allows users to view and share smart metering data in terms of carbon emissions, kWh, or monetary costs for all energy carriers (electricity, gas, and oil), and water meters.

Under the Third Energy Package[6], Member States are required to ensure the implementation of smart metering for electricity, gas, water, and heating. In this framework, long-term cost benefits analysis (CBA) has been carried out so as to decide the implementation of a smart metering infrastructure [8].

In contrast with the Electricity Directive, which required that 80% of consumers should have smart electricity meters by 2020, the Gas Directive does not specify how many consumers should have smart meters or provide a deadline for deployments following a positive CBA. The following section will show the current situation of the rollout of smart meter gas in Europe.

---

[4] http://flexmeter.polito.it/index.php/project.

[5] Prosumer is a neologism applied to consumers which also are able to produce electricity that can be delivered to the grid.

[6] http://eur-lex.europa.eu/legal-content/EN/TXT/PDF/?uri=CELEX:32009L0072&from=en.

3. Architecture of the smart natural gas system

The main purpose of the gas system is to supply gas to consumers with the required safety and quality characteristics at a reasonable cost. In order to fulfill this target in a cost-effective manner, different agents are necessary; each of them will be assigned some specific role.

The gas transmission network is the physical medium through which consumers can obtain the amount of gas they need. Depending on the type of network (characterized, among other parameters, by the pressure level and its capacity), there are transmission and distribution networks. Distribution networks are structures connected to the transmission network and carry the gas to the final consumers. The owners of the network, which are in charge of maintenance and development of those infrastructures, will therefore be transmitters and distributors.

Distribution (low and medium pressure network) is the final link of the chain in delivering natural gas to customers. While some large industrial or commercial customers, as well as power generators fueled by gas, receive natural gas directly from high-capacity interstate and intrastate pipelines, most users receive natural gas from their local gas utility, also called local distribution company (LDC).

Unlike other energy sources, the gas can be stored in large amounts at different points of the grid. The network operator, whose mission is to ensure that the gas system remains balanced and stable so that energy transactions can be performed safely and reliably, can use these gas stores.

Depending on the type of network they manage, these operators may be transmission or distribution operators. The operation of the network is an activity that could be developed by agents different from the owners of the infrastructures, so that these operators would be different from the transmitters and distributors previously defined.

Other agents that should be established according to size and characteristics of the gas system, as well as the configurations that the network can adopt, are the aggregators, whose mission is grouping small distributed demand resources into larger packages that can provide significant value to the system as a whole.

Finally, the figure of the gas retailer appears as an intermediary of the retail market between the final consumers (small amounts of energy) and the mechanisms of the wholesale market and gas production (large amounts of energy). The different agents and the activities they would carry out within the new framework that smart grids offer to the natural gas market are further discussed subsequently.

3.1 Agents in a smart natural gas system

When the natural gas system is structured according to a smart grid architecture, the need for specific agents arises to make the whole network work properly. The different agents that would be involved in the proper performance of a smart natural gas system, including the provision or utilization of DR resources were identified in the research of Montuori et al. [2] and they could be summarized as follows:

- End users, who consume natural gas and pay the supplier the price requested. Moreover, end users in smart natural gas systems may provide the grid operator with demand response services.

- Producers, who explore, investigate, and exploit the gas deposits.

- Gas storage managers, who handle storage facilities to adapt the gas supply according to the end users' needs and the availability of resources in real time.

- Aggregators, who group small end users so as to create significant blocks of flexible demand that can be used by grid operators, as well as any other stakeholder needing demand response resources.

- Transmitters, who manage the gas network infrastructure at high pressure.

- Distributors, who, similarly to transmitters, manage the gas network to supply end users.

- Retailers, who behave as buyers in the wholesale market and sellers in retail markets to supply the natural gas to end users.

- Wholesale energy traders, who buy natural gas in international markets and incorporate it into the system, reselling it to retailers or to large end users, as well as to transmitters or distributors for operation purposes.

- Transmission System Operator (GSO), who operates the transmission gas network and guarantees the supply according to security standards and regulations in force.

- Distribution network operator, who operates a regional distribution network.

Market operator, who manages the necessary mechanism to exchange natural gas between the parties in the wholesale market (**Figure 1**).

The aforementioned activities refer to roles but not entities. Therefore, it is possible that some agent (for example, a distribution company) plays more than one role (distributor and distribution network operator).

3.2 New agents: aggregators

The role of the aggregator in smart natural gas system has been discussed in detail in previous research of Montuori et al. [2, 9]. This agent aggregates small and middle gas consumers, behaving as DR providers, and the stakeholders interested in using those services (such as transmission system operators, distribution network operators, retailers, etc.), who behave as DR requesters.

Aggregation in smart natural gas systems could be understood in two different ways:

- Traditional aggregation, which would be based on the joint management of gas consumptions of end users that actually use natural gas directly (similarly to what this agent does in power systems). This is the case of consumers using gas in a boiler or a burning system for heating purposes.

- District heating operators. This is a real novel approach, further detailed in [9], that considers the aggregation not of direct gas consumption, but of thermal energy that is produced in a centralized way by consuming natural gas. Therefore, the district heating operator, that is the actual gas consumer, may offer some kind of flexibility by managing the aggregated thermal consumption of the steam or hot water consumers within its portfolio.

One essential requirement for aggregators is to have appropriate monitoring and control equipment so as to offer reliable operation services to some particular stakeholders. Therefore, the massive rollout that is taking place in some countries, as mentioned earlier, will have a positive impact on this point since it will

help to further develop the role of the aggregator in smart natural gas systems (**Figure 2**).

One of the main advantages of aggregation would be related to the balancing of natural gas, which would avoid the need for the transmission system operator to purchase natural gas in the wholesale market during high prices periods. In this case, aggregators may offer the same service by increasing or reducing the amount of gas of their consumers. Moreover, this aggregated service would make the system behave more efficiently since the activation of a demand response service when more gas is required is translated into a reduction of the gas level in the network, which also reduces the risk of congestion. Additionally, demand response reduces the greenhouse emissions when the amount of gas is reduced but not shifted to other periods.
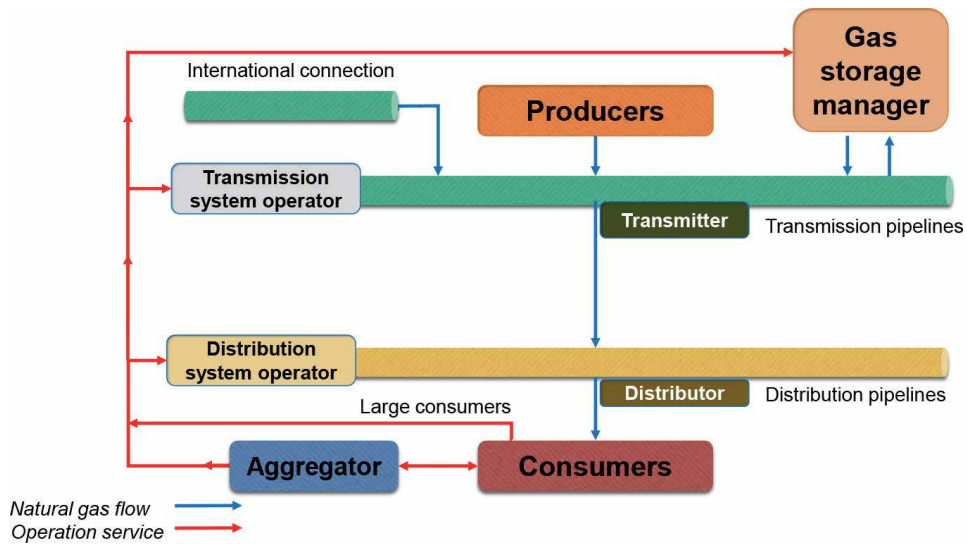
Figure 1.
Roles to be played in a smart natural gas system [2].
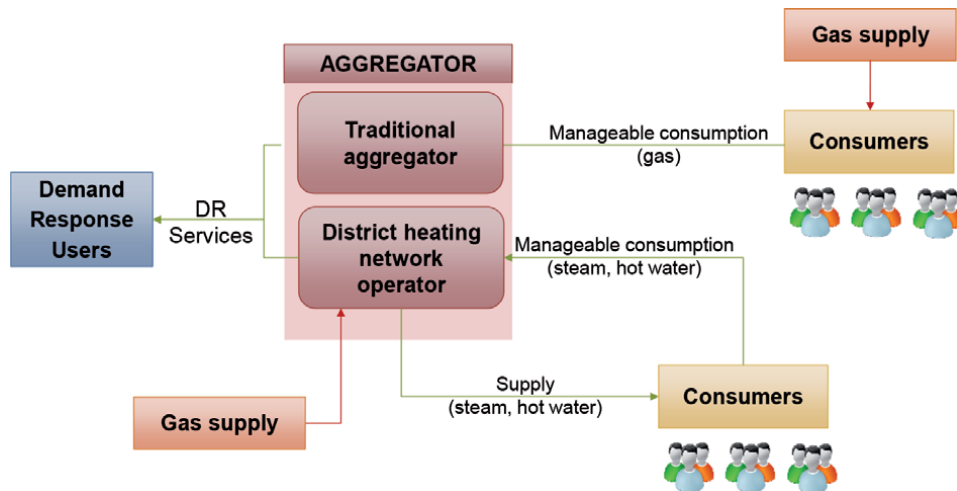
Figure 2.
Activities of the aggregator.

4. Massive rollout of smart gas meters in Europe

In recent years, the European Union has played a leading role in promoting the reduction of greenhouse gas emissions in line with the ambitious new targets that fix the GHG reduction emissions levels below at least 55% by 2030. In accordance with this de-carbonization process, deep changes are required to meet these standards and a new settlement of the gas retail market needs to be held.

In order to enforce the transition to a more efficient organization for the gas system, the introduction of gas smart meters and smart metering network concepts have to be promoted as it has been already done in the electrical sector. To support these innovative changes, a new concept of consumer like a more aware and active participant in the marketplace needs to be promoted [10]. Similarly, the role of aggregators also needs to be empowered as an intermediary between small customers and network operators willing to use customers' services (DR resources) so as to manage their infrastructures more efficiently. With regard to the metering instruments and in prospective to the development of multiservice smart cities, the European Directive MID 2014/32/UE defines the functionality of measuring instruments for the promotion of efficient consumer behavior and for their active participation in the energy market. In spite of that, the Directives on the Internal Market for Electricity and Gas (Directives 2009/72/EC and 2009/73/EC) included in the Third Energy Package does not oblige European countries to participate in the rollout of the smart meter gas and does not state a deadline to complete it either. This lack of a mandatory regulation on this matter derives into different behaviors in each European country.

Similarly, to that previously done in the electrical sector, European countries have carried out a CBA for participation in the smart meter gas rollout [11].

As shown in **Figure 3**, the results were dissimilar and a slower approach to the smart meters gas introduction was registered:

- In 2017, just five member states (Ireland, Italy, Netherlands, Luxembourg, and the United Kingdom) decided to introduce smart meters by 2020.

- In 2019, also France, Austria, Hungary, and Denmark set up a strategy for the massive smart gas meters rollout implementation.

In 2013, 19 European countries conducted a CBA with 12 countries showing negative CBA results (Germany, Spain, Portugal, Romania, Finland, Sweden, Poland, Czech Rep, Belgium, Greece, and Latvia). In 2018, eight Member States carried out a new CBA, obtaining coherent results with the previous one except for Austria and Ireland, where the first CBA was positive and this new one had a slightly negative result. Seven Member States did not conduct any CBA (Bulgaria, Croatia, Estonia, Greece, Hungary, Poland, and Portugal). Finally, states without natural gas networks have not been considered (Cyprus and Malta).

The latest conducted analysis among the State Members EU-28 has recognized different factors that push a country to install a gas smart meter. On one side, the two main driving factors are the digitalization of the distribution network and the optimization of the grid operation, together with the digitalization of the retail market that enables new services for private players [12]. Moreover, smart metering helps to reduce operating costs through savings in manual meter readings, theft protection, process improvement, better scheduling, and balancing processes, as well as consumer engagement opportunities. However, the participation in the massive rollout and the results of the CBA are also influenced by other factors, such as density of gas customers, gas customer expenditure, and competitiveness
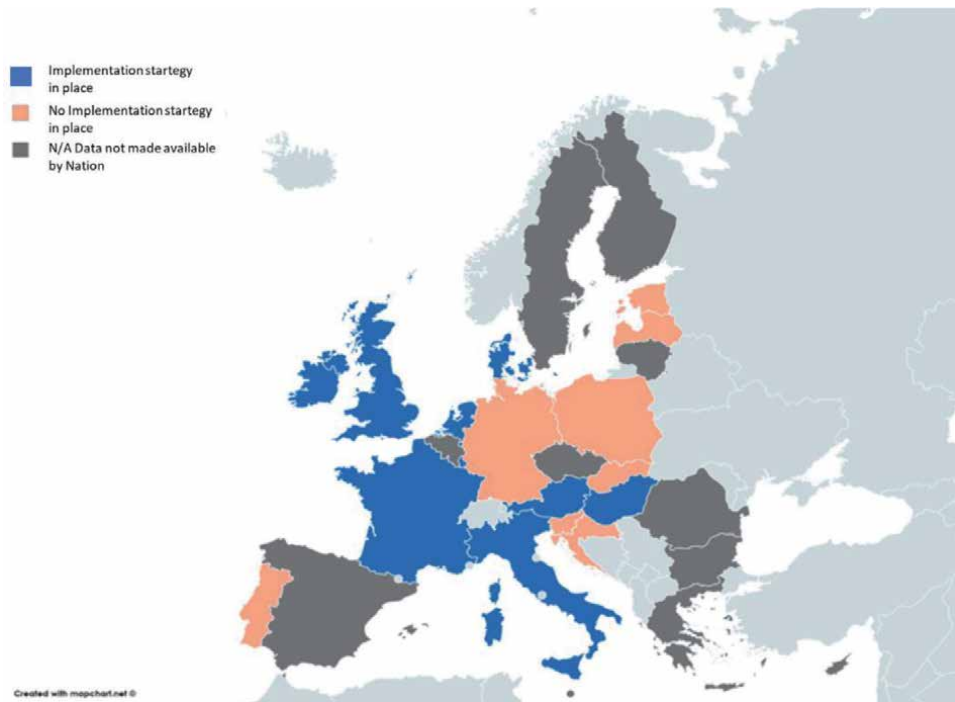
Figure 3.
Gas smart metering rollout in Europe (source: [12]).

of supply market and need for consumer engagement, meter location, and meter ownership [11]. Currently, countries with a high density of gas customers and a significant share of gas bills such as the UK and Italy were more favorable to the smart metering rollout. Additional benefits of taking part in the rollout of gas smart meters could be derived from the higher transparency and awareness about the gas consumption and from the reduction of GHG emissions improving energy efficiency. These social benefits, together with the introduction of DR programs, should be driving factors to enlarge the number of EU countries enrolled in this program.

Germany is the largest gas consumer country in the EU. However, it does not accept the mandatory rollout due to unclear costs-benefit ratio of the smart metering gas implementation, according to the report of Wissne and Stronzik [13]. In addition, the saving costs derived from theft protection were not as high in Germany as in the other countries, as this is not a frequent problem in that country. Similarly, Sweden rejected the participation in the rollout because the low number of gas consumers (around 40.000) made it not attractive, as highlighted by Brodin et al. [14]. On the other side, Spain has a much higher amount of gas customers (over 7 million) but, despite that, the CBA had negative results. The most significant results obtained in the countries which have adopted the rollout are described in the following sections.

4.1 Italy

The Italian CBA showed a positive net benefit, coming from the reduction of the operation costs mainly due to two reasons: the lower cost of metering compared to the manual reading and the reduction of energy theft. The CBA does not consider the installation of In-Home Display (IHD) as underlined Poletti et al. [15].

According to the Plan of the Authority for the Electric, Gas and Water, the mass market rollout started in Italy in 2013. The gas smart meter deployment target adopted was more ambitious than those set by other European countries pretending to end the mass-market stage of the rollout by the end of 2018. Conversely, the installation of electronic meters is still ongoing due to several disruptions (lack of funding and infrastructure) even if it shows a considerable growth, according to Bianchini et al. [16]. The new target period to complete the wide-scale rollout has been extended up to 2023 with the installation of 85% smart gas meters.

During 2020, almost three-quarters of domestic customers, 85% of condominiums, 75% of public service activities, and two-thirds of customers with other uses (**Figure 4**) were installed. By the end of 2020, the total number of gas smart meters installed was 23,854 thousand while the number of remaining traditional smart meters was 7432 thousand (comprising class from G4 up to G40) [17].

4.2 Luxembourg

Luxembourg is one of the EU countries, which had two positive CBAs, the first in 2013 and the second in 2018. At the first instance, the government chose to start a mandatory rollout with the introduction of gas smart meters and electrical smart meters by 2020 for at least 95% coverage. Now, the end of the massive rollout is expected by the end of 2021, reaching 90% of the total. The smart metering rollout started in 2015, and it included the development of an energy grid for the integration not just of electricity and natural gas consumptions but also distributed energy resources such as solar, wind, biogas, and heat pumps [7].

4.3 Ireland

In 2013, the CBA had in Ireland the strongest positive result, especially for the fast rollout scenario with the combination of energy statement with In-Home display (IHD) and variable tariff. Regarding the additional benefits from reduced emissions of greenhouse gases, all the considered scenarios were positive. However, in 2018 the trend changed and the CBA was reviewed with a slightly negative result that was considered neutral by the European Commission. The new deadline for the large-scale rollout has been set up in 2024 [12].
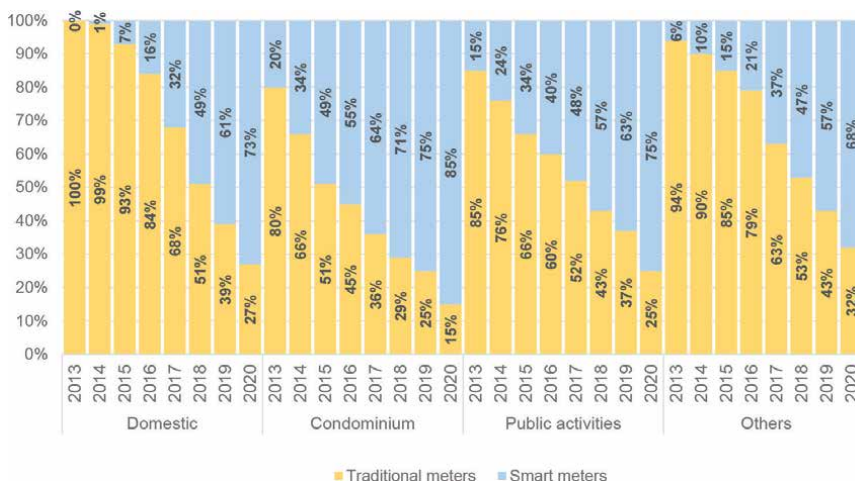

Figure 4.
Percentage of smart meter gas installed in Italy 2013-2020 (Source: [17]).

The company Gas Networks Ireland[7] (GNI) currently supports the National Smart Metering program, which is focused on both gas and electricity metering devices. The program includes the use of smart metering technology, variable time of use, and in-home displays according to the CBA results. A share communication infrastructure has been implemented for gas meters and electricity meters in order to leverage the costs. In future, the same infrastructure could be used also for water smart meters.

4.4 Netherlands

In 2009, due to privacy concerns, the mandatory rollout was not accepted by the Dutch Senate, so a voluntary rollout of 7 million consumers started. During 2012, the installation of smart meters was performed on a small scale and the company Oxxio (former Eneco Energie) provided over 200,000 smart meters using GPRS as the communication technology [18]. Considering that almost 100% of the households accepted the smart meter (with almost 100% standard readings), it would be expected a benefit of approximately 770 million euros, which is equivalent to 50 € per metering point according to the positive results of the CBA discussed by Bouw et al. [19]. In 2014, the Netherlands decided to implement a strategy for the smart meter gas rollout. In 2015, the rollout of smart meters in the Netherlands reached approximately 1.5 million domestic small meters installed. The target of the Dutch grid operator is to have at least 80% of all Dutch households connected to the network by a smart meter by the end of 2021.

4.5 United Kingdom

The CBA carried on by the UK Department of Energy and Climate Change in 2014 on the smart meters rollout was positive, with an estimation of net benefits equal to £6.2 billion (equivalent to 7.2 billion of euro) [20]. The UK's rollout is the largest project in the gas market, and it involves 30 million customers with a gas consumption equal to 50% of the household energy costs, as investigated by Segalotto [21]. Households can freely choose, if applying or not, for a smart meter of new generation, for the gas and electricity with an in-home display screen that shows in real time the exact amount of the energy consumption[8].

At the end of 2013, there were 295,700 smart meters already installed in domestic properties in the country. However, the British government started officially a smart meter rollout in 2016.

The home area network (HAN) implemented in the UK for the smart meters' remote reading uses a ZigBee Energy network. ZigBee Smart Energy is the network solution for electric meters, gas meters, and in-home displays, due to its maturity and popularity in Smart Energy application profile and its capability of ensuring robust communications architecture of a smart natural gas system [22]. At the end of 2020, there were 98,600 smart meters installed in non-domestic sites and, in spite of the delay due to the COVID-19 pandemic breakdown, smart meters installation showed the highest peak of the rollout (**Figure 5**).

On the other side, the installation in the domestic sites continued increasing in 2020 and reached a total of 3.1 million smart meters installed, as shown in **Figure 6** [23].

---

[7] http://www.gasnetworks.ie/en-IE/About-Us/Our-commitment/Marketplace/Smart-meters.
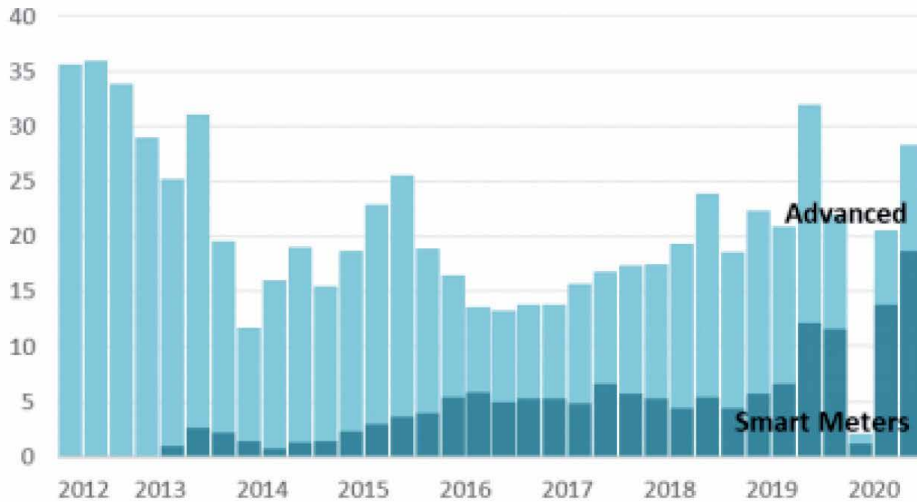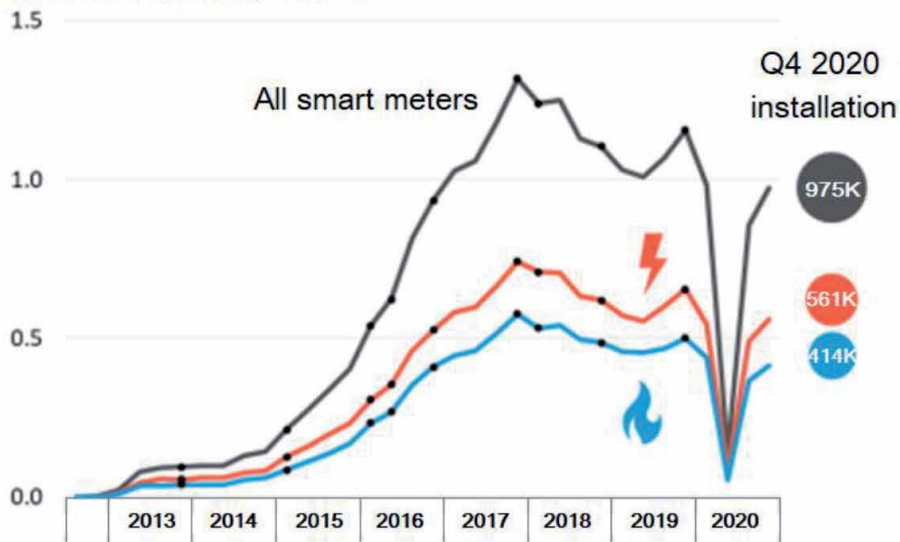
[8] https://www.smartenergygb.org/en/about-smart-meters/what-is-a-smart-meter.

Figure 5.
Non-domestic smart meter gas installed in Great Britain from 3rd quarter 2012 to 4th quarter 2020 (source: [23]).

Figure 6.
Domestic smart meter gas installed in Britain from 3rd quarter 2012 to 4th quarter 2020 (source: [23]).

4.6 France

In France, Electricité Réseau Distribution France (ERDF) carried out an initial gas smart meter pilot project in 2011. From the start of 2010, the pilot project was carried out for 18 months in four regions (Auch, Saint-Omer, Laval and Pierre Bénite, and Etampes) with the installation of 18,500 meters. The obtained results support the idea that the smart meter is essential to achieve efficiency and reliable

operation of the natural gas system. The utilization of smart meters made consumers aware of their consumption which, together with the use of demand response, resulted in savings of 0.9% in the gas consumption as gathered by Drozdowski and Vandamme [24].

In 2017, the French gas company GRDF started a huge smart gas meter rollout that should drive the replacement of 11 million traditional gas meters with an investment of 1 billion euros. To achieve this goal, the French gas infrastructure started an upgrade of the existing technological infrastructure to be able to meet the highest communication system standards. The full rollout of 11 million meters is expected to be complete by the end of 2022 [25]. Nowadays, the French rollout is ongoing according to the agreed planning. Six million meters had been already installed at the end of 2020, with an average value of 150,000 meters per month.

5. Demand response experiences in natural gas systems

DR concepts have been used for years (with different levels of development depending on countries) in the management of power systems [26]. Thus, DR programs, either offered by system operators or utilities, contribute to solving different matters that appear in the habitual operation of the power grid. Nevertheless, and in spite of the similarities existing between the power and natural gas systems, there are few successful experiences of DR applications in the natural gas system. However, as agreed by some researchers and professionals, DR concepts could be essential for the better and more efficient operation of natural gas systems, as can be deduced, among others, from the following factors highlighted by Srinivaspura [27]:

- Electricity and natural gas markets are closely related as this resource is more and more used for power generation. The main reasons are:

- Environmental issues related to the reduction of power production with such fuels as coal.

- The higher performance of natural gas power plants (especially in combined cycle facilities)

- The massive utilization of renewable energies, which makes necessary generation technologies able to quickly respond to the high variability of this kind of generation, providing power reliability and supply guarantee.

- The volatility of natural gas markets is increasing, especially due to the utilization of natural gas for power generation.

- Until the recent past, natural gas demand used to be quite stable and seasonal; however, this tendency is changing nowadays [29].

- Natural gas is replacing other fuels in hydrocarbon markets [28].

Until now, DR concepts have been applied worldwide as predominantly pilot projects, but results achieved have been promising [29]. In Canada, residential end-users have been asked to participate in DR programs based on the gas management through the regulation of the thermostat for heating applications. The energy savings estimated were influenced by the thermal oscillation (external Temperature) and the warmness of the season and could reach up to 21% [30].

Enernoc, the most active company in DR applications for small and medium customers in the electricity sector, is also trying to develop some experiences in the natural gas sector. In particular, this company has developed a platform, which is being tested in customers from National Grid in the State of New York, in order to shift consumptions to optimize the use of fuel sources based on weather availability. Therefore, Enernoc will try to demonstrate that DR concepts may help in winter to solve the same kind of problems that the power system (closely linked to the gas consumption) has during peak periods in summer [31].

Regarding Europe, Spain was a pioneer in the approval of an interruptible program in 2006[9], based on the need of establishing tools and mechanisms so as to make more flexible the natural gas system. By means of this program, the gas system operator has the possibility to interrupt the supply to large customers willing to do that in case of emergencies. This advanced mechanism has two types or modes of interruptibility:

- Mode A: This mode can be used between the gas trader and the final consumer so that the consumer may help the trader in case of imbalance due to incidents which may produce the lack of gas in the portfolio of such traders.

- Mode B: Interruptible fee. The agreement is established between the final consumer, the gas trader, and the gas system operator, so that the consumer is committed to reduce the consumption under requirement from the system operator due to the lack of gas in the system. In this case, a reduced access fee is applied to the consumer for using the infrastructures of the gas system.

Interruptible customers must be able to completely interrupt their consumption with a notification in advance of 24 h. The duration of the interruption may vary from 6 h up to 10 days. However, as mentioned earlier, only large customers with an annual consumption higher than 10 GWh and a daily consumption higher than 26 MWh and connected to a pipeline with a pressure higher than 4 bar can participate.

Another experience can be found in the United Kingdom, where there is a kind of interruptible program, but just at the distribution level and less developed than in Spain. Just a small group of large industrial consumers can participate, depending upon the commercial arrangements they have agreed to[10]. Interruptible customers receive discounted transportation charges when reducing their consumption in periods of high demand (especially in winter peaks). In 2010, just 27 customers participated in interruptible gas contracts in the UK [32].

In the Netherlands, a consortium of 11 entities called Energy Delta Gas Research (EDGaR)[11] coordinates the development of different scientific, applied, and technological research projects on natural gas. However, even if there are some research lines in the field of smart natural gas systems, none of them is dealing at the moment with DR applications in the natural gas sector. Said that, it is true that for this consortium, customer's flexibility is a key value in smart grids, and some ideas have arisen about the utilization of flexibility of electricity consumers for the management of power plants fueled by natural gas, as indicated in the research of Huitema et al. [33].

---

[9] The interruptibility program is regulated in the Resolution 25 July 2006 from the General Direction of Energy Policy and Mines. Available from: https://www.boe.es/diario_boe/txt. php?id=BOE-A-2006-14314.

[10] The characteristics of interruptible supplies are described in: http://www2.nationalgrid.com/uk/ Industry-information/Gas-transmission-system-operations/Interruptions-to-supply/.

[11] More information about this consortium is available at: http://www.edgar-program.com [Accessed: April 18, 2017].

All these experiences demonstrate the promising application of DR resources for a more efficient management of the natural gas systems, similarly to the power grid. However, most of them are just in the pilot phase at present or, in the best case, only large industrial customers are enabled to participate.

6. Constraints in the natural gas system

The present section has the aim to describe the technical constraints that may affect the natural gas system, highlighting the potential of demand response so as to overcome these limits and promote the development of a reliable natural gas system, able to quickly face sudden network failures.

Generally speaking, the physical/technical constraints of a gas network system are set by one or more of the following parameters:

- The capacity of the pipelines, which limits the quantity of gas that can be transmitted between two points.

- The pressure of the gas supply. Actually, a different reliability issue can derive from the natural gas operation. The gas network is characterized by variable flow for each arc, which determines a variable pressure at every node [34].

- The extension and meshing complexity of the network—areas not served by the pipelines cannot be supplied by gas.

Regarding the commercial constraints, they may be set by the following:

- Energy regulations. The energy regulations should be addressed to implement the efficiency of the gas network by providing incentives.

- Political stability. Sometimes, the presence of a large gas storage site or gas availability in countries defined as politically unstable could affect the trend of the natural gas market.

- Geographical position of a country. The geographical position of a country may facilitate more or less the connections with large gas reserves or with strategic gas transit hubs.

- Availability of other energy resources for thermal production. The presence of other energy resources guarantees energy independence from the natural gas network failure

Interruptions of gas supply that could occur in the gas system determine a non-continuity of the service. Traditionally, interruptions have been divided into short and long. Short interruptions are those whose duration is shorter than a standard value defined in regulation. For example, the Italian regulation defines an interruption as short when the duration is less than or equal to 120 min. However, interruptions are considered as long when exceeding such standard duration.

According to its nature, interruptions could be also classified as follows:

- Scheduled interruptions (also called interruptions with notice), which take place due to scheduled operations of maintenance of the system (transmission and distribution). Usually, operators notify the customers at least 24 h before

a planned interruption occurs, specifying the date, time, and duration for the scheduled activities. Generally, among the activities considered as scheduled interruptions, the more relevant are the following:

- Ordinary/planned system maintenance, scheduled by the network operator (replacements of working parts of valves, of piping, etc.)

- Extraordinary maintenance, scheduled by the network operator (the rollout of the meters replacing)

- Extraordinary maintenance, requested by the customers (request for a metrological test, leakage test, etc.)

- Unscheduled interruptions (or without notice), which are unexpected events that occur on the gas system network and cannot be forecasted by the network operators. Among the reasons, those which can motivate an interruption without notice can be considered:

- Congestion of the pipelines in specific nodes of the network, defined as the impossibility of the system to meet the energy needs of end users. It could be of two types:

- Commercial congestion, due to the not commercial availability of the gas on the wholesale market

- Technical congestion, due to the non-physical presence of sufficient quantity of gas to meet the energy needs

- Extraordinary maintenance operations because one of the following events occurs:

- Detection of gas leakage from any part of the supply system (meters, pipelines, compression cabin, valves, etc.)

- Presence of water in the gas pipelines or in the meters

- Tampering of the network system (vandalism act, close of the meter valve, damage)

- Blocking of the pressure regulator in the compression cabin

- Pressure level out of the range of the proper operation of the system

- Political issue that determines unpredictable events such as acts of public authorities or such as the gas crisis of 2014 because of the political instability in the relationship with Russia.

- Natural catastrophe, unusual natural events for which has been declared a state of emergency by the competent authority, such as the heart quake in the center of Italy, which happened in the summer of 2016, which determined the damage of several pipelines and compression cabins.

- Strikes or rejection of the authorization documents by the competent authority (not taken into account in this book chapter)

- A gas accident, defined as an event involving any apparatus of the gas network that determines serious injuries or deaths of people, or damage to people's goods not lower than an economic value established by the law. For example, in Italy, this economic value is 1000 euros (Article 28, paragraph 28.1). The causes of a gas accident could be multiple, such as gas leakage (voluntary or not); an uncontrolled combustion caused by insufficient ventilation, etc.

- An emergency, defined as an event that can put into risk the safety and the continuity of supply in large proportions of the distribution/transmission network. An emergency can be caused by:

- Unplanned unavailability of service at delivery points or interconnection points.

- Unplanned out of service at the high, medium, or low-pressure networks that result in the interruption of the gas distribution without notice to one or more end users.

- Gas leakage on the pipelines.

- Damage caused by excess or defect of pressure in the network compared to the values provided by the current technical standards.

Depending on country-specific regulation, an emergency could be defined in different ways. For example, in Italy, and according to Article 27, paragraph 27.1, an emergency is considered an event that causes the interruption of the gas distribution without notice to at least a number of 250 end users and for the duration of 24 hours.

6.1 Gas network constraints in the United States of America

In the United States, the wide network of interstate and intrastate pipelines that runs throughout the country has several open issues to solve in order to strengthen the stability and reliability of the American gas network:

Implementation of existing pipelines and infrastructure. In spite of the growth in consumption, the US transmission infrastructure does not properly cover all the country and large areas suffer the lack of sufficient pipelines with the adequate capacity for gas delivery, such as the Northwest and New England [35]. In order to face this constraint, new upcoming projects are expected to increase the number and capacity of the existing pipelines in order to transmit natural gas from production centers to consuming markets or exports terminals. Recent projects intended to increase the reach of natural gas produced in the Marcellus and Utica regions of the Northeastern United States (see **Figure** 7). New infrastructures are expected to be built from the Appalachia production between 2015 and 2025.

Implementation of new pipelines and processing infrastructure. Forecast of energy needs beyond 2025 expects a significant impact of the growth in demand for gas-fired power generation on the existing pipeline system. In particular, to face the growth in electric demand, additional pipelines are needed in order to ensure the system's reliability. The gas demand for power generation will increase by 73% between 2014 and 2025, in comparison to the 39% increase between 2005 and 2014. New pipelines and processing infrastructure are required to face this growing demand and to connect the end user to new supply source [37].
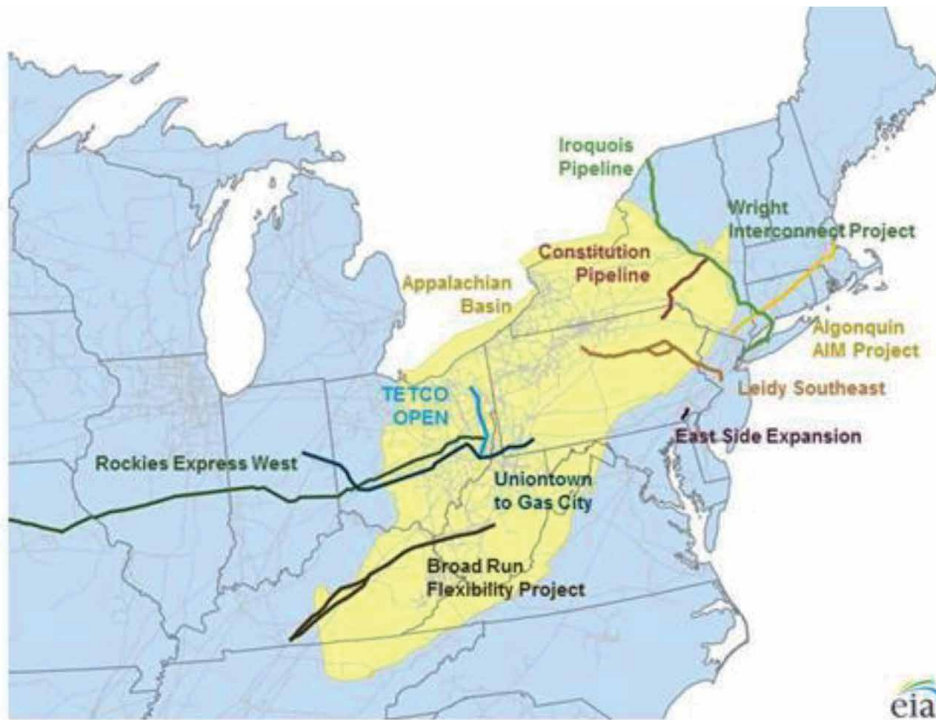
Figure 7.
Implementation of new pipelines in USA (source: [36]).

- Reduction of natural gas losses. Local distribution companies (LDCs) have been pursuing the replacement of leak-prone pipes in order to reduce natural gas losses from infrastructure systems, contributing to the increase in safety of the transmission system. Now, the mileage of cast iron distribution pipes has been reduced just for 25% between 2005 and 2014 [38].

- Increment in state incentives. New capital expenditures have to be provided by State legislators for building new pipelines and expanding or repurposing existing ones. Such investments should be applied also to other infrastructures, such as compressor and pumping stations [39]. In spite of the growing awareness of the stakeholders about the potential environmental benefits of reducing natural gas losses, many reforms are required on the natural gas infrastructure.

- Introduction of DR programs. The introduction of new DR programs for the management of the consumption could help to face the temporary lack of sufficient pipelines with the adequate capacity for the NG delivery (such as Northwest and New England). Indeed, putting in evidence the advantage of this kind of strategies is one of the main objectives of this book chapter.

6.2 Gas network constraints in Europe

Past gas supply disruptions as a result of the political turbulence between Russia and Ukraine increased EU dependency on gas imports and the risks of the security supply. Therefore, a reliable and interconnected system able to face the EU domestic
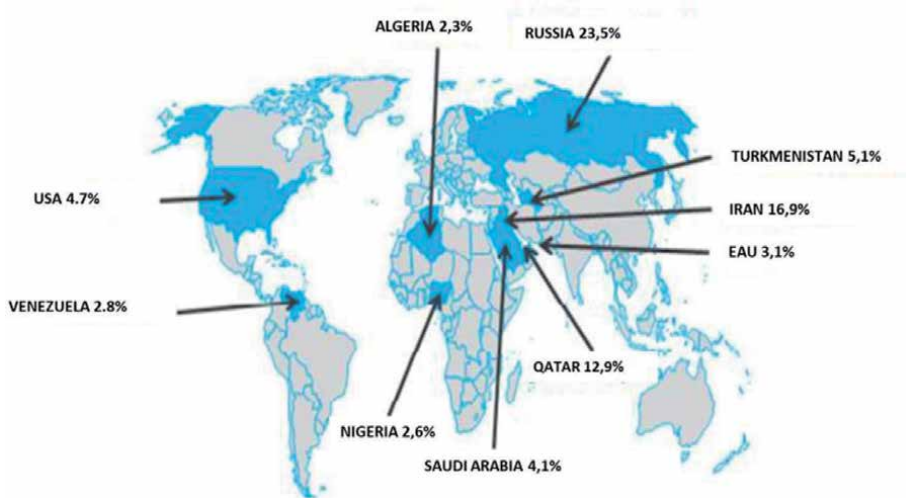
Figure 8.
Proven reserves of natural gas worldwide. Top 10 countries (source: [40]).

energy needs should be implemented. Depending on the duration and on the level of the demand, ENTSOG[12] shows that potential disruptions may directly affect the majority of EU Member States, except France, Spain, and Portugal, which may be supplied from the south interconnections. Indirect effects would include increases in the prices of LNG for the entire EU. The resilience of the gas infrastructure needs to get improved, carrying on the following implementations:

- Improvement of the existing pipelines. The increasing dependence on imports needs the improvement of the existing pipelines. The major issue is the limited connections between the Western pipeline and the Eastern infrastructures. In order to facilitate the creation of a reliable and robust gas system throughout Europe, the European Network of Transmission System Operators for Gas (ENTSOG), in cooperation with Gas Infrastructure Europe (GIE) implemented the Gas Infrastructure Map, which provides an overview of the existing gas infrastructures and establishes a reference for information of their trends over time.

- Diversification of supply routes. In order to reduce the dependency of imports from Russia (the owner of the 23% of the total proved reserves of natural worldwide, as shown in **Figure 8**) and unstable transit countries, new pipelines need to be built re-routing the Russian imports (i.e. Nord Stream, Yamal, and Blue Stream).

- Implementation of reverse flow pipelines. Even if establishing a reverse flow is relatively easy since a technical point of view, there are still many restrictions in the main pipelines, which both hinder competition and decrease the security of supply. The potential to operate pipelines in two directions increases the resilience in case of a supply disruption [41].

- Improvement of energy efficiency. It should be considered a potential in the energy-efficient design of the transmission system. These days, 5% of the energy is lost in the transmission grid.

---

[12] ENTSOG is the European Network of Transmission System Operators for gas. More information ca be found at: http://www.entsog.eu.

- Harmonization of the standards. The diversification and non-integration of the standards adopted by the different countries for technical building and daily operations do not favor the system management across the system borders. A higher degree of standardization is required. Efforts are required so as to regulate the third-party access to the grid (TPA) in free conditions, as well as to improve information requirements to ensure transparency.

- Improvement of the security of supply. After the physical breakdowns of energy transmission networks following the crises with transit countries (Ukraine in 2006 and 2008 and Belarus in 2007), EU has been forced to adopt the strategy of diversifying supply routes which would gradually reduce its dependence on such transit countries. An improvement in the energy network and strict cooperation between states is essential so as to ensure a timely response in case of crises.

- Introduction of DR programs. The implementation of the DR programs could reduce the vulnerability to gas supply shocks, facilitating the development of an integrated gas market, reducing the import dependency and the variation of natural consumption due to the climate change issue. Some of the most significant benefits of DR programs in the short term in European countries may be:

- Management of sudden supply disruption due to catastrophic events (heart quake) and/or to political issues such as in the case of disruption of all supplies from Russia.

- Management of the seasonal storage. The EU's gas storage, together with increased scope for reverse flows, can play a mitigating role in the event of supply disruption.

- Management of the growing variable trend of natural gas consumption and network congestion. The demand for natural gas has traditionally been characterized by a highly cyclic trend depending on the season and on the climatic changes. Generally speaking, gas demand is expected to be higher in January and February, and lower during the months of July and August. Correspondently, and in order to meet the cyclical demand, the base-load storage capacity is typically withdrawn in winter (to meet increased demand, while storage injection typically takes place in summer (to store excess gas in preparation for the next upcycle). The recent increase in the use of gas for power generation has resulted in an anomalous and variable behavior of the gas demand. Hence, the increasing use of natural gas so as to generate electricity results in a peak of demand during the warmest months, whose magnitude is as pronounced as the peak in electricity consumption for air conditioning and lighting systems.

7. Barriers to the implementation of demand response strategies in the natural gas system

Barriers and handicaps related to the implementation of DR in power systems have been discussed in many studies. One of the most recent examples can be found in Alcázar-Ortega et al. [42], which results from the European project DRIP. Among other results, this project produced a methodology for the systematic evaluation of handicaps, which prevents the implementation of DR strategies in the operation of power systems. Considering this work and based on the similarities previously identified between

power and natural gas systems, a preliminary evaluation of barriers can be assessed or referred to the gas side.

One of the main barriers is the difficulty for customer's acceptance: customers are not willing to reduce their consumption. The first reason is that consumers are not aware of the potential they may have, and they do not know that someone could be willing to pay in exchange for such flexibility. Another reason is that, when being aware of this potential, customers perceive that the economic incentives they may receive are not attractive enough. This barrier can be faced by providing customers with evidence about the economic profitability that DR actions may provide to their energy bills. While this is a difficult task, there are some tools for this purpose (some examples are provided by the aforementioned DRIP project), developed in the last years for the electricity markets that may be used for this purpose but applied to the natural gas sector.

Tools are also necessary so as to jump barriers on the side of retailers or system operators, as the potential offered by customers is difficult to forecast, and the benefits that DR may mean for their business are not easy to assess. However, the benefits of DR have been also proved in power systems for these activities, so similar results can be expected in the natural gas sector. Retailers can find in DR resources a help for the optimization of their portfolio and the reduction of imbalances, with significant cost savings. Regarding the gas system operators, the most significant barrier for them is probably the utilization of small and medium flexible consumptions. In fact, the few examples that can be found about the utilization of DR in natural gas systems are just related to very large consumers (as discussed in Section 2.3). Therefore, the empowering of the figure of the aggregator in natural gas systems is essential for the proper integration of DR resources coming from the residential and commercial sectors, as well as medium and small industries. A significant role can be played here by the managers of district heating networks, as they can provide the system operator with flexible customers willing to play not only with their gas supply but also their hot water or steam utilization. The system operator can utilize the potential offered by flexible customers so as to solve technical constraints related to the maximum capacity of pipelines in periods of peak demand. Additionally, the usage of natural gas storage can be optimized, allowing the system operator to combine both storage and DR resources to guarantee the optimum management of the whole system.

The development of the concept of Smart Energy Systems in recent times, which provides a strong metering and communication structure of the natural gas network, is definitely enabling energy grids for the easier utilization of customer's flexibility. However, as indicated in [5], the impact of DR programs, most of which would be similar to those existing for power systems, has to be evaluated and validated. At present, except for the few examples mentioned in this section, there are no real experiences demonstrating this potential. Therefore, the implementation of pilots arises as one essential step to provide credibility for considering DR.

There are some opinions against the utilization of DR strategies in the natural gas sector since some experts think that DR programs for gas consumers may be alluring but impractical [43]. Nevertheless, this book chapter proves the suitability of DR strategies applied to the natural gas sector, where similar problems to those arising in power systems can be afforded by this media.

8. Novel resources: hydrogen

One of the most promising tendencies in clean energy sources is the utilization of hydrogen, which has been identified as the fuel for the energy transition of the

21st century by many institutions and scientists as remarked by Cheli et al. [44]. Indeed, mixing hydrogen with natural gas improves the utilization rate of this hydrocarbon while it also reduces greenhouse gas emissions and pollutants [45].

Natural gas and hydrogen may be mixed in the range from 10–20% in order to be compatible with existing natural gas infrastructures [46]. Indeed, in Italy, the gas system operator, Snam, has demonstrated the feasibility of introducing hydrogen into the natural gas pipelines at rates between 5% and 10% [47]. Some experiences have also taken place regarding the metering devices in the natural gas infrastructure, concluding that fractions of hydrogen up to 15% in the natural gas system do neither affect the reliability nor durability of diaphragm gas meters [48].

Hydrogen can be obtained by electrolysis, applying an electrical current. Therefore, this method can be used when renewable energy production is higher than demand during valley periods, which would increase the efficiency of the whole energy system [44]. Such efficiency increment could be maximized by allowing the participation of consumers by means of demand response services, as discussed in the previous sections.

9. Conclusions

Demand Response has been used for years in the operation and management of power systems. However, few experiences exist in the natural gas sector, where the application of DR strategies is almost non-existing.

The most significant experiences on DR utilization in the gas sector, as well as the main issues to take into account for the implementation of DR actions in gas networks, have been highlighted in this chapter. This kind of mechanisms offers many benefits either for customers and other stakeholders within the gas sector and may increase significantly the efficiency of the gas system when used in balance services by the gas system operator. Moreover, due to the similarities existing between the power and natural gas systems, the application of similar strategies used in electric systems for the gas sector should be considered as the natural evolution for a more efficient and operative management. Together with that, new strategies such as the injection of hydrogen in the gas network may also contribute to the higher efficiency of the whole system, reducing emissions and helping to integrate renewable resources.

The barriers that may prevent the utilization of DR resources in the natural gas system are also discussed here. However, many of them can be solved, thanks to the new structure that today is being given to the energy systems based on the concept of smart grid, which is discussed in this chapter. It is indeed in energy systems structured according to the smart grid configuration, where the application of DR is more useful and profitable.

Conflict of interest

The authors declare no conflict of interest.

Author details

Lina Montuori* and Manuel Alcázar-Ortega
Universitat Politècnica de València, Institute for Energy Engineering,
Valencia, Spain

*Address all correspondence to: lmontuori@upvnet.upv.es

IntechOpen

References

[1] United Nations. Cities and Climate Change: Global Report on Human Settlement 2011. Nairobi, UN; 2012

[2] Montuori L, Alcázar-Ortega M, Álvarez-Bel C. Methodology for the evaluation of demand response strategies for the management of natural gas systems. Energy. 2021;**234**:121283

[3] Dababneh F, Li L. Integrated electricity and natural gas demand response for manufacturers in the smart grid. IEEE Transaction on Smart Grid. 2018;**4**(10):4164-4174

[4] Focus Group on Smart Sustainable Cities. Smart Sustainable Cities: An Analysis of Definitions. International Telecommunication Union; 2014

[5] Benevolo C, Dameri P. La smart city come strumento di green development. Il caso de Genova Smart City. Electronic Journal of Management. 2013;**1-30**(3): 1-36

[6] Patti E, Pons E, Martellacci D, Castagnetti FB, Acquaviva A, Maci E. Architecture for energy vectors with active prosumers. In: International Conference on Smart Cities and Green ITC Systems. Lisbon: Springer; 2015

[7] USmartConsumer Project. European Smart Metring Landscape Report. Utilities and Consumers. Madrid: European Commission; 2016

[8] Institute of Communication & Computer Systems of the National Technical University of Athens. Study on cost benefit analysis of Smart Metering Systems. European Commission; 2015

[9] Montuori L, Alcázar-Ortega M. District heating as DR aggregator: Estimation of the potential in the Italian peninsula. Energies. 2021;**14(21)**(7052):1-19

[10] Autorità per l'energia elettrica, il gas e il sistma idrico. Schema di linee strategiche per il quadriennio 2015-2018. Roma: AEEGSI; 2014

[11] Muallem D, Smart gas metering Europe—an untapped opportunity? Metering & Smart Energy International. June 07, 2013

[12] European Commission. Benchmarking Smart Metering Deployment in the EU-28 Final Report. Bruxelles: Tractebel Impact; 2019

[13] Wissne M, Stronzik M. Smart Metering Gas. WIK Consult; 2014

[14] Brodin E, Elwén A, Grahn E, Larsson E, Abrahamsson K, Morén G, et al. The Swedish Electricity and Natural Gas Markets 2015—Ei R2016:10. Eskilstuna: The Swedish Energy Markets Inspectorate; 2016

[15] Poletti C, Cervigni G, Di Castelnuovo M, Sileo A. Costs and Benefits of the Italian Smart Gas Metering Programme. Milan: The Center for Research on Energy and Environmental Economics and Policy at Bocconi University; 2011

[16] Bianchini A, Saccani C, Guzzini A, Pellegrini M. Gas smart metering in Italy: State of the art and analysis of potentials and technical issues. In: Conference: Summer School Francesco Turco. Palermo, Italy: Associazione Italiana Docenti Impianti Industriali (AIDI); 2018

[17] ARERA. Relazione Annuale sullo stato dei servisi e sull'attivitá svolta. Autoritá di Regolazione per Energia Reti e Ambiente; 2021

[18] IBM. Oxxio Uses Smart Utility Metering Technology to Give More Control and Options to Customers. IBM Corporation; 2006

[19] Bouw A, Oost J, Gibiino S. Smart Meters in the Netherlands—DSOs Are Leading the Way. IBM Corporation; 2013

[20] Department of Energy. Smart Meter Roll-Out for the Domestic and Small and Medium Non-Domestic Sectors (GB): Impact Assessment. British Government; 2015

[21] Segalotto J-F, Bigliani R. Gas Smart Metering in Italy: Rollout Update and Emerging Communications Technologies for Utility-Grade IoT. IDC Energy Insights; 2016

[22] Silicon Labs. ZigBee Propagation for Smart Metering Networks. Silicon Laboratories Inc.; 2013

[23] Department for Business, Energy & Industry Strategy. Smart Meter Statistics in Great Britain: Quarterly Report to end December 2020. Official Statistics; 2021

[24] Drozdowski R, Vandamme M. Smart gas meters: Assessment of customer response to improved information about their energy consumption. In: ECEEE 2013 SUMMER STUDY Proceedings. Belambra Les Criques, Toulon/Hyères, France: European Council for an Energy Efficient Economy; 2013

[25] GRDF France. Smart gas meter France [Online]. Available from: https://www.grdf.fr/grdf-en/smart-gas-meter-france. [Accessed: August 30, 2021]

[26] Montuori L, Alcázar-Ortega M. Demand response strategies for the balancing of natural gas systems: Application to a local network located in The Marches (Italy). Energy. 2021;**225**(120293):1-13

[27] Srinivaspura C. Demand Response for Natural Gas. 2017 [Online]. Available from: http://www.energycentral.com/c/pip/demand-response-natural-gas. [Accessed: February 27, 2017]

[28] U.S. Energy Information Administration. Annual Energy Outlook 2016. Washington DC: EAI; 2016

[29] Faruqui A, Weiss J. Gas Demand Response. Spark Forthnightly; 2010

[30] Manning M, Swinton M, Szadkowski F, Gusdorf J, Ruest K. The effects of thermostat set-back and set-up on seasonal energy consumption, surface temperatures and recovery times at the CCHT twin house facility. ASHRAE Transactions. 2007;**113**(1):1-12

[31] Tweed K. EnerNOC moves into demand response for natural gas. Greentech Media. April 18, 2012

[32] Backer A. Britain's Interruptible gas contracts. Reuters. January 08, 2010

[33] Huitema G, Szirbik N, Wortmann H, Ittoo A, Dzousa A. Embedding flexibility in combined gas and electricity infrastructures. In: 4th Research Day EDGaR. Hilversum, Netherlands: Netherlands Environmental Assessment Agency; 2012

[34] Dilaveroglu S. Optimization for Design and Operation of Natural Gas Transmission Networks. College Station, TX: ASM University; 2012

[35] Petrihos N, VanWhye K. U.S. Natural Gas Pipelines. All Infrastructure Crisis. American Action Forum; 2016

[36] U.S. Energy Information Administration. New pipeline projects increase Northeast natural gas takeaway capacity. Washington DC: EIA; 2016

[37] O'Neil B, Hopkins P, Gressley J. The Economic Benefits of Natural Gas Pipeline Development on the Manufacturing Sector. IHS Economics; 2016

[38] U.S. Department of Energy, Office of Energy Policy and Systems Analysis

(DOE). Natural Gas Infrastructure Modernization Programs at Local Distribution Companies: Key Issues and Considerations. Washington DC; 2017

[39] Hagan H, Ruege E. Unlocking Demand for Natural Gas Pipelines. White & Case LLP; 2014

[40] ENI Group. World Gas and Renewables Review. San Donato Milanese, Italy: ENI; 2012

[41] Bjornmose J, Roca F, Turgot T, Hansen D. An Assessment of Gas and Oil Pipelines in Europe. Brussels: European Parliament; 2009

[42] Alcázar-Ortega M, Calpe C, Theisen T, Carbonell-Carretero J-F. Methodology for the identification, evaluation and prioritization of market handicaps which prevent the implementation of demand response: Application to European electricity markets. Energy Policy. 2015;**86**: 529-543

[43] Coffee GA. Gas Demand Response Programs Are Appealing but Impractical. Winston & Strawn LLP; 2016

[44] Cheli L, Guzzo G, Adolfo D, Carcasci C. Steady-state analysis of a natural gas distribution network with hydrogen injection to absorb excess renewable electricity. International Journal of Hydrogen Energy. 2021;**46**:25562-25577

[45] Kong M, Feng S, Xia Q, Chen C, Pan Z, Gao Z. Investigation of mixing behavior of hydrogen blended to natural gas in gas network. Sustainability. 2021;**13**(4255):1-17

[46] National Grid, Atlantic Hydrogen Inc. Hydrogen-Enriched Natural Gas: Bridge to an Ultra-Low Carbon World. Fredericton, NB: Atlantic Hydrogen; 2009

[47] Alverà M. Rivoluzione idrogeno: La piccola modelocal che può salvare il mondo. Trento: Mondadori; 2020

[48] Jaworski J, Kułaga P, Blacharski T. Study of the effect of addition of hydrogen to natural gas on diaphragm gas meters. Energies. 2020;**13**(3006): 1-20

Analysis of Efficiency of Natural Gas Absorption Process from Water Impurities

Fatimata Tall

Abstract

The composition of natural gas varies depending on the field, formation, or reservoir from which it is produced. Since the composition of natural gas is never constant, there are standard test methods that can be used to determine the composition of natural gas and thus prepare it for use. The impurities contained in the gas are led to the formation of hydrates causing the blockage of the pipelines. Determining the optimal technological parameters of the drying plant and recommending a good choice of drying and glycol regeneration process will improve the field gas preparation system. Absorption using triethylene glycol (TEG) is one of the most popular methods for the dehydration of natural gas. However, the thermodynamic parameters of the gas as well as the parameters of the TEG always remain conditions to be studied to ensure an optimization of the process of regeneration of the glycol. The available experimental data were selected and correlated using a thermodynamic model based on the Peng-Robinson equation of state. The results obtained show that the model provided is a valuable tool for the design of the natural gas dehydration process.

Keywords: natural gas, absorption, dehydration, water, triethylene glycol, hydrate

1. Introduction

Absorption is known to be the most common drying method among the various gas drying processes.

During the absorption process, water vapor in the gas stream is absorbed in the liquid solvent stream. The liquid solvents used are glycols and the most commonly used are triethylene glycol and diethylene glycol.

The main technological parameters of the absorption process are temperature, pressure, the nature of the absorbent, the concentration of the regenerated absorbent, and the frequency of circulation of the absorbent.

However, according to several studies, TEG is the most used because of its ease of regeneration at concentrations from 98 to 99.9% as they approach properties that meet the criteria for commercial use [1, 2].

In general, the choice of the process mode and absorbent depends on the required depression of the gas dew point.

The depth of gas drying from moisture significantly depends on the concentration of glycol at the inlet to the absorber.

To deepen gas drying, vacuum desorption of moisture from glycol is used (at a pressure of 0.060–0.080 MPa and a temperature of about 205°C). The concentration of regenerated glycol, in this case, increases to 99.5%, and the dew point depression increases to 50–70°C [3].

The aim of this study is to dehydrate natural gas and evaluate the influence of the parameters involved in the absorption process in order to be able to optimize the absorption process using the most optimal parameters in accordance with the desired level of dehydration.

At present, di- and tri-ethylene glycol are used as absorbents for gas preparation [4].

The choice of solvent depends on the application. Typically, the solvent must meet the following criteria—high solubility of the solute to reduce the amount of solvent used; low volatility to reduce losses; does not cause corrosion; low viscosity for a high rate of mass transfer; safe; does not foam.

Glycols meet these criteria in the case of gas dehydration. The most popular glycol used for offshore gas processing is triethylene glycol (TEG).

The efficiency of natural gas dehydration by the absorption method depends on the nature of the absorbent, the concentration of the absorbent at the inlet to the absorber, the circulation rate of the absorbent, and the thermodynamic parameters of absorption [5].

2. Absorption process simulation

This process is a "traditional" dehydration process based on triethylene glycol (TEG). The goal is to reduce the amount of water in natural gas using TEG, which is used as an extraction solvent. This process is necessary to avoid the formation of hydrates at low temperatures or corrosion problems due to the presence of carbon dioxide or hydrogen sulfide which are regularly found in natural gas.

The effectiveness of the gas dehydration method is measured by the water content in the dry product gas. Most gas sale contracts specify the maximum amount of water vapor allowed in the gas. The maximum amount of water vapor is estimated at 7 lbs./MMscf. Standard gas specifications also limit the water dew point to −10°C to ensure flow in export pipelines on the seabed [6]. Distribution specifications depend on the geographic region in which they are applied. For example, in Russia, the dew point temperature of the water during winter is −20°C, and during summer it is −14°C for natural gas at a pressure between 4 and 7 MPa [7].

The composition, temperature, and pressure of the Yamburg X-field gas were selected to simulate wet gas dehydration in Unisim Design R460.

Table 1 represents the composition of the gas of the X field and **Table 2** represents the parameters of the gas and the triethylene glycol.

The moisture content of the gas is 600 mg/m^3, this value exceeds the specification (100 mg/m^3), so the gas must be recycled.

We accept the multiplicity of the TEG, equal to 1.500 m^3/h, the mass percentage is 99.7%.

The mass flow rate of moisture in the gas is calculated by the formula:

$$Qm. = Wi \times V \tag{1}$$

where V is the volumetric amount of hydrocarbon raw materials, m^3/h.

Wi—initial moisture content.

In most installations, the rate of the TEG absorbent is 1–10 m^3/h and depends on the degree of gas purification [8].

Composition	Mass percentage
N_2	0.0018
CO_2	0.065
CH_4	0.81
C_2H_6	0.054
C_3H_8	0.036
$n-C_4H_{10}$	0.0095
$i-C_4H10$	0.019
Sum	1

Table 1.
Gas composition.

Parameters	Values	
	Wet gas	**TEG 99.7%**
Temperature	25°C	25°C
Pressure	4 MPa	3.800 MPa
Flow rate	330,000 m^3/hr	(1700 kg/hr)
Initial water content	0.600 g/m^3	

Table 2.
Parameters of the initial wet gas and TEG.
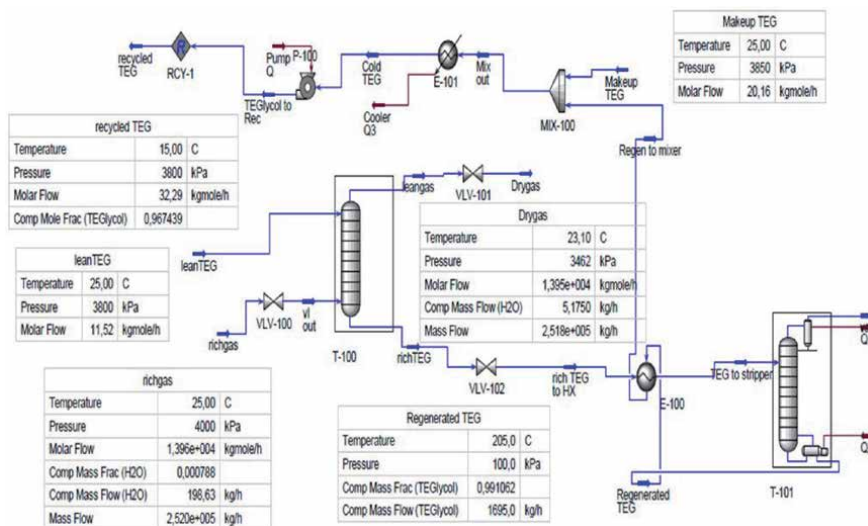
Figure 1.
Gas dehydration process in Unisim.

Unisim's simulation of a typical absorption gas dehydration process is shown in **Figure 1** and combines gas absorption and glycol recovery.

The drying process illustrated in **Figure 1** is explained below.

The wet gas is first directed to a valve that operates to reduce the gas pressure.

The wet gas enters the absorber column from below and the lean TEG enters from the top, falling into the absorber when it comes into contact with the wet gas

flowing upward. Wet gas enters the T100 contactor at a pressure of 3862 kPa. This column absorbs part of the water contained in the gas thanks to the presence of triethylene glycol.

The dried gas is directed to the valve and then leaves it at a pressure of 3462 kPa.

The rich TEG leaves the bottom through the level control, passes through a valve where it is depressurized, and exits at a pressure of 3080 kPa.

The TEG containing water and hydrocarbons is sent to a stripping column (T101). The regenerator distillation column includes a reboiler operating at 205°C to prevent degradation of the TEG. The outgoing gases are condensed by the condenser, so the water vapor is directed to the outlet. The regenerated TEG sent to the bottom of the column (Regen Bottom), passing through the heat exchanger, will be sent to the mixer and mixed with a quantity of glycol to compensate for the losses of glycol.

2.1 Simulation results

The simulation results allow us to know a large number of process parameters, as well as the dew point temperature of the gas after absorption, which will allow us to know if the gas meets the conditions of the transport specification.

At a dry gas pressure of 3462 kPa, the gas dew point temperature is −26°C (**Table 3**).

2.1.1 Absorption column profile

We see that the temperature gradually increases, starting from the 2nd stage to the 9th stage, and then decreases to the 10th stage. This can be explained by the fact that as the gas goes up to meet the glycol, and heat transfer becomes more and more important; and this allows the glycol to absorb more water from the gas before saturation. At stage 10, when the glycol loses its ability to absorb water the temperature drops.

As shown, the pressure increases when moving up the stage, this is because the absorption phenomenon occurs at high pressure, in contrast to the regeneration phenomenon.

- Temperature dew point

Stages	Temperature (°C)	Pressure (kPa)	Pure liquid (kgmol/hr)	Pure vapor (kgmol/hr)
1	23.53	3600	13.24	
2	23.54	3611.11	14.19	2.4128
3	23.55	3622.22	15.06	2.4129
4	23.56	3633.33	19.91	2.413
5	23.59	3644.44	16.78	2.4131
6	23.61	3655.55	17.72	2.4132
7	23.62	3666.66	18.8	2.4133
8	23.628	3677.77	20.14	2.4134
9	23.621	3688.88	21.94	2.4135
10	23.6	3700		2.4137

Table 3.
Profile of the absorption column.

Composition	Molar fraction
N_2	0.001181
CO_2	0.027063
CH_4	0.915635
C_2H_6	0.032489
C_3H_8	0.014767
n-C_4H_{10}	0.002954
i-C_4H10	0.005907
H_2O	0.000025
TEG	0.000000

Table 4.
Composition of dry gas.

Water dew point temperature	−26°C
Moisture contents	0,015 г/м^3
Critical temperature	−63°C
Critical pressure	6170 кПа
Critical compressibility	0.300

Table 5.
Composition of dry gas.

Distillation type		Glycol concentration (%)	Glycol loss (kg/hr)
Atmospheric pressure (kPa)	100	93.420	0.665
Vacuum pressure (kPa)	80	94.423	1.242
	60	96.512	2.313
	35	98.061	5.701

Table 6.
Concentration of glycol after regeneration.

After drying, the gas comes out with a composition and pressure different from the original composition and initial pressure. The dew point temperature of this new gas composition can be determined by using the Unisim software (**Tables 4** and **5**).

2.1.2 Regeneration column profile

Triethylene glycol is recovered in a distillation column containing a reboiler and a condenser. The reboiler temperature is 205°C to avoid decomposition of the glycol, and the condenser is at 102°C because the boiling point of water is 100°C. The reboiler is pressurized to below atmospheric pressure to increase the glycol purity. Under these conditions, glycol is recovered by 98.06% in molar percentage or 99.10% in mass percentage (**Table 6**).

2.2 Analysis and optimization of absorption process

An analysis of the various parameters involved in the absorption process will allow us to better understand the effect of these variables on the process. The result of this analysis will allow us to select variable parameters to obtain the most optimal process. The most important process parameters are the solvent flow rate in the absorber, the gas contact temperature, the number of equilibrium stages in the absorber, and the stripping gas used (if a very concentrated TEG is required).

2.2.1 Influence of TEG flow rate on dry gas content

To determine the influence of the number of equilibrium stages in the absorber, as well as the TEG flow, the feed gas is taken into account and the TEG flow rate and the number of stages are varied. The water content of the gas will be calculated for each option. The TEG flow rate was varied between 1500 and 3000 kg/h (**Figure 2**).

The result of the analysis shows that the water content in the dry gas decreases with an increase in the circulation rate of the triethylene glycol.

It can be seen that starting from 1500 kg/h, the water content in the gas is 0.019 g/m^3, and with an increase in the TEG consumption, the water content decreases.

With regard to the optimization of the TEG circulation, it can be seen that 1700 kg/h allows a water content of 0.015 g/m^3 to be achieved, which corresponds to the specification for the water content in the gas. Therefore, it is preferable to reduce the amount from 2500 to 1700 kg/h and it will be more cost-effective from an economic point of view.
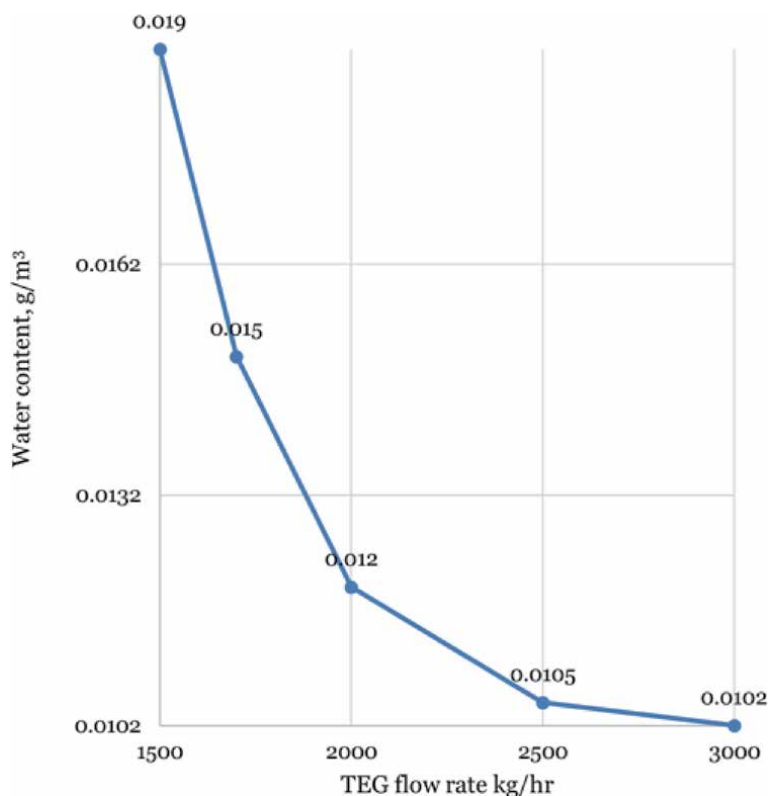

Figure 2.
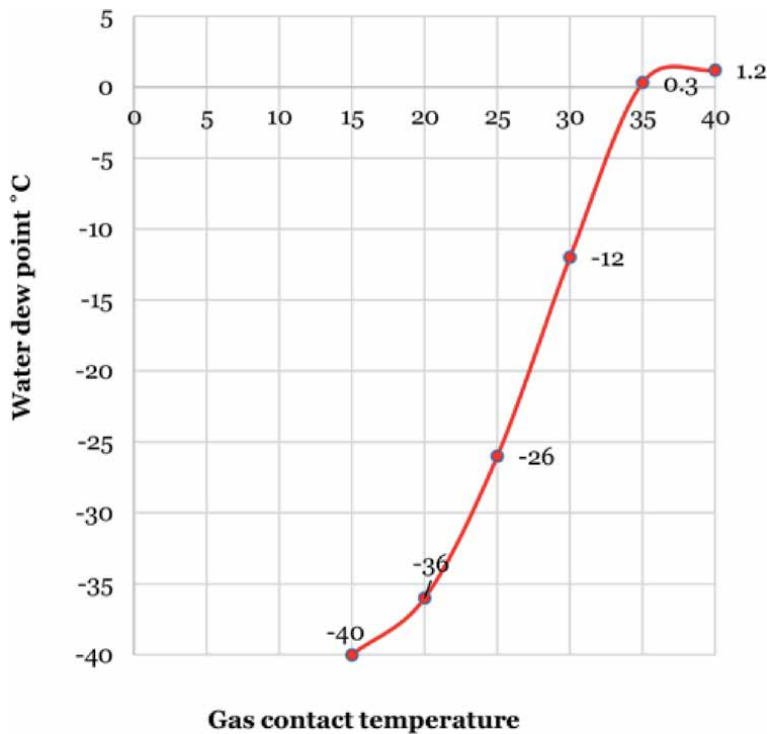*Influence of TEG flow rate on dry gas content.*

Figure 3.
Influence of gas contact temperature on water dew point.

In addition, high circulation rates can overload the reboiler and prevent proper glycol regeneration. The heat required for the reboiler is directly proportional to the circulation rate. Thus, increasing the circulation rate can lower the reboiler temperature, reduce the lean glycol concentration, and actually reduce the amount of water that the glycol removes from the gas.

2.2.2 Influences of gas contact temperature on water dew point

To determine the effect of the gas contact temperature, the given feed gas is taken into account and the temperature is varied. The water dew point of the gas will be calculated for each option (**Figure 3**).

The graph shows that as the gas contact temperature decreases, the amount of water contained in the gas after drying also decreases. This is due to the fact that low temperatures increase the capacity of absorbents, allowing them to absorb more water contained in the gas; therefore, the lower the gas temperature, the lower its equilibrium moisture capacity and then low water dew point. In addition, high temperatures increase TEG losses. The lower the process temperature, the lower the calculated concentration of glycol is used to obtain the target gas dew point. A decrease in temperature also leads to the destruction of the heat consumption for the operation of the regeneration unit, since the amount of water extracted from the gas decreases.

2.2.3 Effects of the stripping gas on TEG regeneration

After drying the gas, it is necessary to check the flows to determine at what temperature the gas will be hydrated.

Formation temperature	−22,18
Freezing temperature	−26,54
Type of hydrate	types I and II

Table 7.
Hydrate formation conditions.

Pressure (kPa)	Temperature (°C)
429	−38
908	−32
1838	−26
3431	−21
4362	−19
5469	−17
6058	−16,68
6419	−16,23
6616	−16,01
6703	−15,9
6722	−15,89
6694	−15,92

Table 8.
Thermodynamic range of hydrate formation.

The analysis of the conditions of hydrate formation of dry gas at a pressure of 3462 kPa and a temperature of 23°C conditions is given in **Table 7**.

At a pressure of 3462 kPa and a temperature of 23°C, dry gas can be transported without the formation of hydrates.

The formation of hydrates in process plants and pipelines can occur within a few minutes; therefore, it is necessary to know the range of hydrates formation.

Table 7 shows the range of temperatures and pressures at which hydrates are formed (**Table 8**).

The following figure allows better visualization of hydrate formation as a function of temperature and pressure (**Figure 4**).

The diagram shows the critical properties of the dry gas flow; critical temperature Tcr = −63.12°C, critical pressure Pcr = 6170 kPa.

The figure shows the temperatures and pressures indicated in **Table 2** at which the hydrate is formed.

Thus, in order to ensure the transportation of gas without the formation of hydrates, it is necessary that the transportation be carried out outside these values of temperature and pressure.

2.2.4 Effects of the stripping gas on TEG regeneration

Stripping gas is an optional element that is used to achieve very high glycol concentrations that cannot be obtained with normal regeneration. This will ensure maximum dew point reduction and greater dehydration. It is also used to ensure
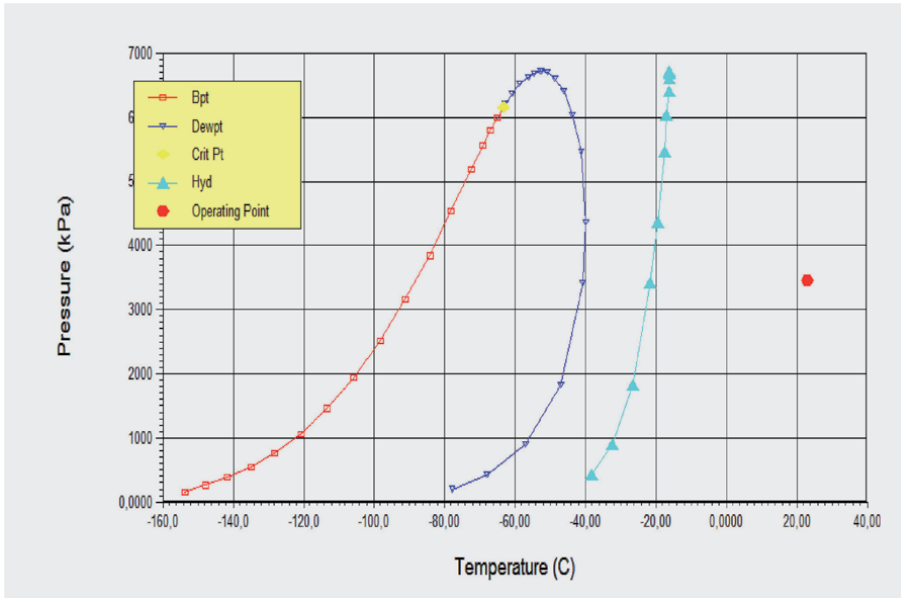
Figure 4.
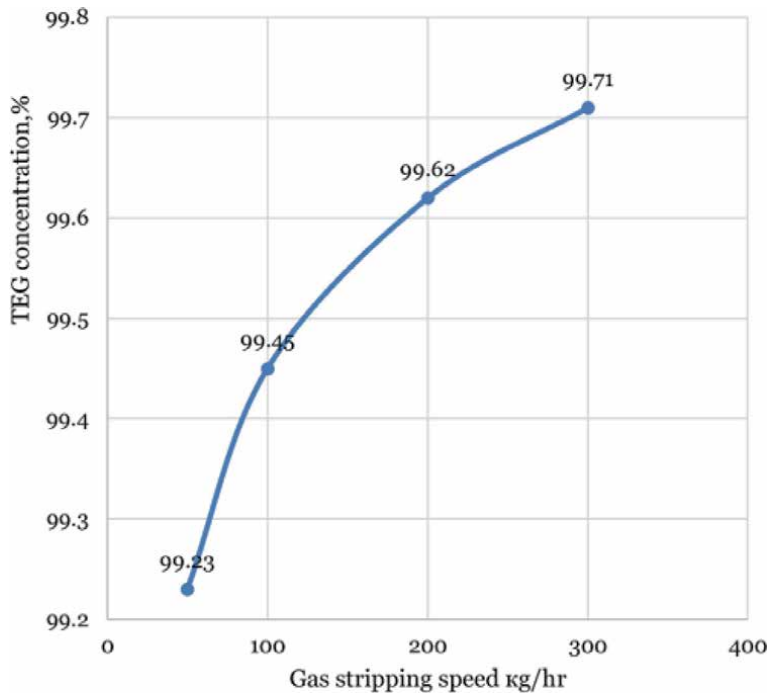*Diagram of the formation of hydrates.*

Figure 5.
TEG concentration versus stripping gas velocity.

intimate contact between hot gas and lean glycol after most of the water has been removed by distillation.

The concentration of the regeneration glycol depends on the rate of circulation of the stripping gas. We will analyze the effect of the boil-off gas flow rate adopted for dry gas on the glycol purity. The speed varies from 50 to 300 kg/hr (**Figures 5** and **6**).
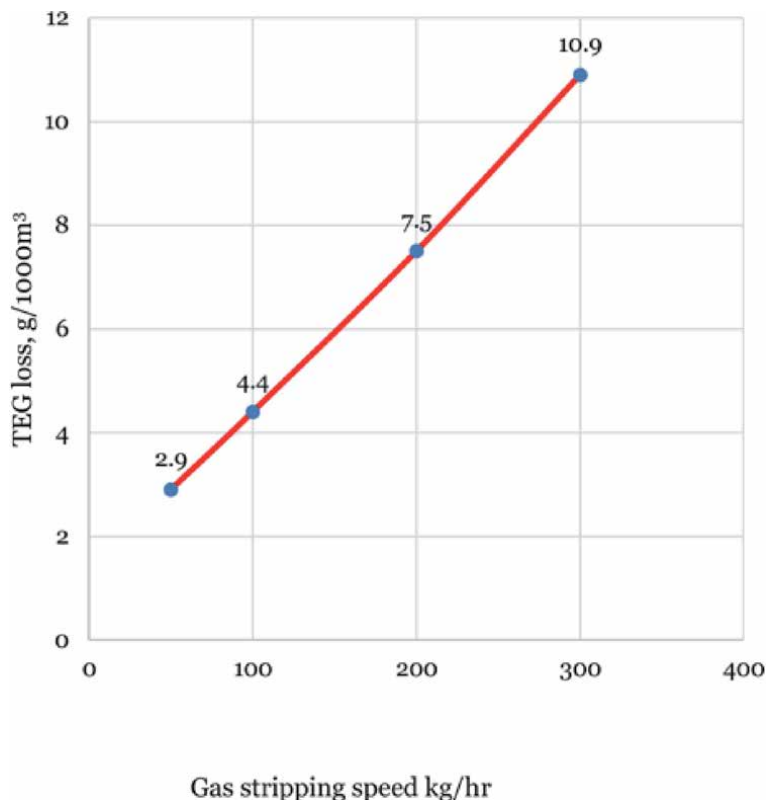
Figure 6.
TEG losses versus stripping gas velocity.

By analyzing the effect of the stripping gas flow rate, it can be seen that at a reboiler pressure of 100 kPa, the more the stripping gas flow rate increases, the more the glycol concentration increases, but on the other hand, there is little glycol loss. The amount of stripping gas produces a cleaner glycol but causes an increase in glycol loss.

To optimize the operation and from an economic point of view, it is recommended to work on a plant where the reboiler pressure is set at 100 kPa with a boil-off gas flow rate of 200 kg/h, which will allow us to recover glycol up to 99.62% with a loss of 7.5 g/1000 m^3.

2.2.5 Regeneration of glycol with an azeotropic agent

The agent is used to form a ternary azeotrope with the mixture.

The DRIZO process provides glycol enrichment by using its own internal stripping medium, a mixture of paraffinic and aromatic hydrocarbons with a boiling range of C_5 +.

The patent works with an isooctane solvent, but the typical composition of the stripping medium is aromatic hydrocarbons, naphthene, and paraffin.

In our study case, hexane is used to separate binary water and triethylene glycol.

Based on the DRIZO process principle, a 100% hexane hetero-azeotrope is used as our gas does not contain C_5+ hydrocarbons (**Figure 7**).

Azeotropic distillation was carried out at various reboiler pressure and the results allowed us to see the concentration of regenerated glycol and the loss of glycol according to the parameters (**Table 9**).
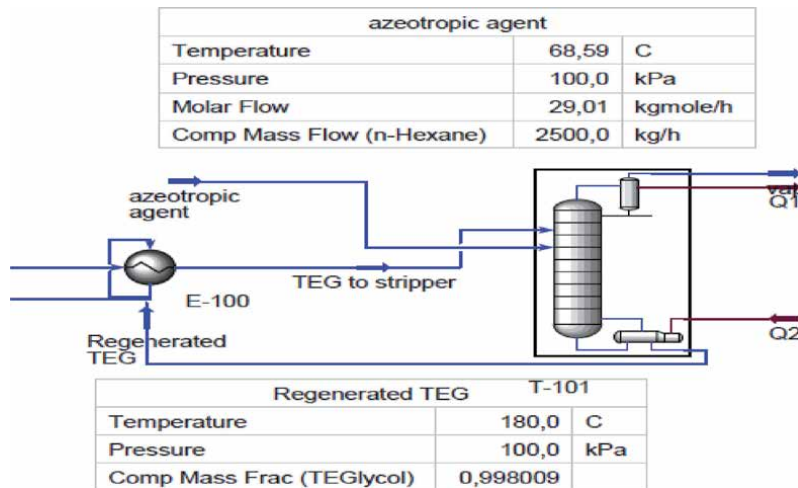
azeotropic agent		
Temperature	68,59	C
Pressure	100,0	kPa
Molar Flow	29,01	kgmole/h
Comp Mass Flow (n-Hexane)	2500,0	kg/h

Regenerated TEG	T-101	
Temperature	180,0	C
Pressure	100,0	kPa
Comp Mass Frac (TEGlycol)	0,998009	

Figure 7.
The process of regeneration using an azeotropic agent.

Reboiler temperature (°C)	Glycol concentration (%)	TEG glycol (kg/hr)
200	99.981	2.432
180	99.914	2.315
140	99.792	2.193

Table 9.
Results of the regeneration process.

Analyzing the results, we see that at atmospheric pressure and a reboiler temperature of 200°C, we can achieve a glycol concentration of 99.981% with a loss of 2.432 kg/h.

Lowering the temperature of the reboiler does not significantly reduce the TEG concentration; therefore, to reduce the heat consumption, the temperature of the reboiler can be set to 140°C.

3. Conclusion

The modeling of the absorption process was carried out using the Unisim program. The study of the various parameters allowed to identify their influence on the whole process in particular on the gas dew point and also on the glycol concentration after regeneration.

The simulation results showed that the parameters that have the greatest influence on the efficiency of the process are the gas contact temperature, the rate of circulation of triethylene glycol, as well as the stripping gas if regeneration of glycol with a high concentration is required.

A decrease of the gas contact temperature to 25°C led to a decrease in the amount of water in the dried gas.

A high TEG circulation rate results in dry gas with less water but can overload the reboiler and reduce good glycol recovery.

To increase the degree of TEG regeneration, a stripping gas and an azeotropic agent were used at atmospheric pressure.

With the stripping gas, the TEG was regenerated up to 99.71% by mass at a reboiler temperature of 205°C, while with the azeotropic agent the regeneration is 99.914% by mass for a temperature of 180°C and for a temperature of 200°C it is 99.981% by mass.

The particular conclusion of this study is that increasing the temperature of the reboiler does not allow a great increase in the purity of the regenerated triethylene glycol; therefore, to reduce the heat consumption, the temperature of the reboiler can be reduced.

Author details

Fatimata Tall
Department of Petroleum Engineering, Tomsk Polytechnic University, Russia

*Address all correspondence to: fatimatatall29@gmail.com

IntechOpen

References

[1] Makogon YF. Hydrates of natural gases. Moscow: Nedra (Mineral Ressources) press; 1974. p. 208 (In Russian)

[2] Gironi F, Maschietti M, Piemonte V. Natural Gas Dehydration: A Triethylene Glycol-Water System Analysis. Energy Sources, Part A: Recovery, Utilization, and Environmental Effects. 2010; **32**(20):1861-1868

[3] Eirini GP, Cristina C, Georgia DP, Giuseppe C, Epaminondas CV. Sensitivity analysis and process optimization of a natural gas dehydration unit using triethylene glycol. Journal of Natural Gas Science and Engineering. 2019;**71**:1875-5100

[4] Nikolaev VV, Busygina NV, Busygin IG. The main processes of physical and physicochemical gas processing. Moscow: Nedra Publishing House; 1998. p. 184

[5] https://www.researchgate.net/ publication/340417842_Natural_gas_ Processing_course

[6] Demirbas A. Methane Gas Hydrate. London: Green Energy and Technology; 2010. p. 192

[7] STO Gazprom 089-2010. Combustible natural gas supplied and transported through main gas pipelines. Technical conditions. Moscow: JSC "Gazprom"; 2010. p. 19 (In Russian)

[8] Erich VN, Rasina MG, Rudin MG. Chemistry and technology of oil and gas. Chemistry: Leningrad; 1972. p. 464 (In Russian)

Chapter 10

Catalysts for the Simultaneous Production of Syngas and Carbon Nanofilaments via Catalytic Decomposition of Biogas

Buthainah Ali Al-Timimi and Zahira Yaakob

Abstract

The possibility of alleviation of methane and carbon dioxide levels in the atmosphere are of major global interest. One of the alternatives that attracts much scientific attention is their chemical utilization, especially because both of these gases are components of the biogas. Thus, the rapid and extensive shale gas development makes them abundant raw materials. The development of an effective catalytic process that could be scaled-up for industrial purposes remains a great challenge for catalysis. As well, understanding of the mechanisms of molecular activation and the reaction pathways over active centers on heterogeneous catalysts needs to be advanced. It has been shown that biogas is a very interesting source of renewable energy. Because of its elevated methane content, biogas has excellent potential, as reflected in its year-over-year rise in production. This is because its manufacturing promotes the use of organic waste, prevents uncontrolled dumping and minimizes atmospheric methane and carbon dioxide emissions. Moreover, its use as an energy source is in some cases an alternative to fossil fuels and can help to minimize energy dependence. Another aspect of interest is that it can be used in situ, allowing agro-livestock farms or small industrial plants to achieve energy self-sufficiency.

Keywords: biogas, catalyst, renewable energy, decomposition, syngas, carbon nanofilaments

1. Introduction

Due to the elevated level of population growth, energy consumption has risen over the recent decade [1]. This increase in energy demand over the years has changed the energy scenario through manufacturing [2]. Furthermore, even with the current low oil price, the world's energy demand is anticipated to continue to rise in the future according to the international energy agency's new policy situation [3], from 13.2% in 2011 up to 17.6% in 2035 as shown **Figure 1**.

Currently, dependence on fossil fuels such as petroleum, gas and coal to satisfy energy demand has caused environmental issues owing to anthropogenic greenhouse gas generation. Methane (CH_4) and carbon dioxide (CO_2) are the most
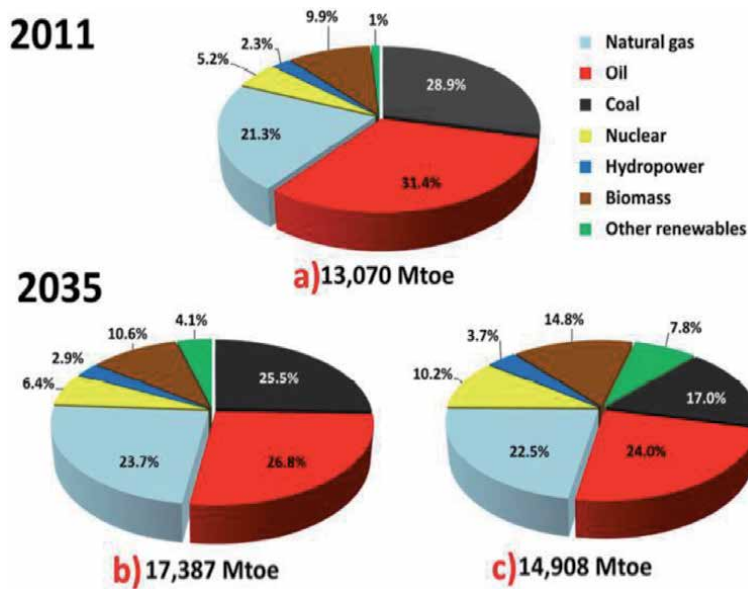
Figure 1.
Primary energy demand in Mtoe (million tonnes of oil equivalent) (a) 2011, (b) 2035 "new policies scenario" and (c) 2035 "450 scenario" (adapted from Ref. [3]).

abundant greenhouse gasses and have lately contributed significantly to climate change issues [4]. While the level of methane in the environment is smaller than that of carbon dioxide [5], it is surprising that around 20% of worldwide warming occurs is caused by it [6]. Conventionally, there are two main sources of methane emissions including nature occurring activities and anthropogenic activities. Examples of the first source are termites, grasslands, coal beds, lakes, wetlands and forest fires, while examples from the second source are landfills, oil and gas treatment, wastewater treatment plants, coal mining, rice production, livestock and agricultural activities [7]. According to the US Environmental Protection Agency [8], methane manufacturing from landfill sites accounts for almost one-third of all methane produced in the United States alone, where landfill gas consists of 40–45% methane and 55–60% carbon dioxide by quantity by volume [9]. Notwithstanding, the reality that methane is a significant element of natural gas, a big quantity of natural gas is burned globally owing to technological constraints and the high price of carrying this valuable gas from its reservoirs, which are often far from industrial fields and the prospective market [10]. These actions have wasted an important source of hydrocarbons and contributed to global warming by releasing greenhouse gases into the atmosphere [11]. Carbon dioxide capture and storage (CCS) has been implemented globally to decrease carbon dioxide emissions due to pressure to combat global climate change and guarantee viable power sources [12]. In addition, renewable energy is required instantly to replace oil resources to decrease the heavy dependence on crude oil and its unwanted impacts on the atmosphere [13].

In the last few years, the resources of renewable energy, particularly, biogas, have gained massive attention around the world as a substitute for traditional fossil fuels [14]. In Southeast Asia, palm oil biomass is considered one of the most plentiful renewable resources and has enormous potential for the sustainable production of chemical substances and fuels. Liquid waste, known as palm oil mill effluent (POME) generated along with crude palm oil production, is one of Southeast Asia's environmental problem due to its high pollution characteristics. Therefore, digestion, an aerobic treatment, is widely adopted in the oil palm industries as a reliable and

effective treatment for POME. The biogas generated during POME's anaerobic decomposition is not restored for use, but can be dissipated into the atmosphere [15]. The biogas produced contains two greenhouse gases: methane (60–70%) and carbon dioxide (30–40%) with traces of hydrogen sulfide which can be utilized after purification for heat generation, electricity production, bio-methane production and of synthesis gas (referred to as syngas, mixture of H_2 and CO) [16]. In fact, POME could become a significant source for biogas production due to its high organic content [17]. According to the World Meteorological Organization [18], methane and carbon dioxide levels were reported at 1845 ppm (parts per million) and 400.1 ppm (parts per million) respectively in 2015. Methane levels in the environment have been revealed to be below carbon dioxide levels, but have caused about 20% of worldwide warming [19]. Methane production was estimated at 6875 million metric tons which equals the total amount of carbon dioxide from all anthropogenic sources in 2010 [20]. Methane is frequently considered an important natural gas component with small amounts of other hydrocarbons such as ethane, propane and butane containing inert substances such as molecular oxygen (O_2) and carbon dioxide [21]. When monitoring the negative impact of methane and carbon dioxide, it is paramount to reduce their concentrations so that to avoid the high concentration of the greenhouse gases that lead to negative environmental conditions and increased temperature.

A great deal of extensive studies has been conducted to discover efficient methods of converting methane and carbon dioxide into precious products and thus reducing their elevated atmospheric quantity. Because of its comparatively low price and stability relative to other methods, converting carbon dioxide and methane into syngas is one of the most prevalent technologies [22]. It is one of the most important processes to convert hydrocarbons in the chemical industries to produce syngas [23]. In many distinct applications, such as Fischer-Tropsch (F-T) petroleum synthesis and the manufacturing of methanol and other precious fluid fuels and chemicals, syngas can be regarded as a construction block [24].

Recently, there have been many attempts that have prompted interest in producing alternative fuels by using renewable and environmentally friendly sources of energy, one of the few alternative sources is biogas. Even so, it is not entirely greenhouse gas-free; it does not, however, lead to global warming. Biogas is an appealing alternative for converting fuel to transport and generate electricity [25]. The vital route that will be of benefit to the power generation industry is the direct conversion of biogas, composed of methane and carbon dioxide to hydrocarbons under catalytic decomposition processes.

The use of catalysts in the catalytic reaction is essential in growing syngas manufacturing, as they assist to alter and enhance the reaction rate without consumption in the process [26]. Catalysts operate by offering an alternative mechanism that decreases energy activation, which implies the system needs less energy to achieve the state of transition. While catalytic reaction needs elevated temperatures to operate due to its heat-absorbing nature, the existence of catalysts can significantly decrease the reaction temperature [27].

Recently, there have been many attempts to use monometallic catalysts such as Ni, Co, Fe and Cu in the catalytic process because they are cheap and have a strong magnetization ability [28, 29]. Furthermore, bimetallic such as Ni-Co, Ni-Fe, and Ni-Cu have become very attractive to researchers due to their properties and the diversity of applications when compared with their individual mono-metal counterparts. The incorporation of nickel into Co, Fe, and Cu metals decreases the use of expensive noble metals [30]. Bimetallic catalysts success is thought to be due to the synergy of their parent metals they consist of two separate metals that display elevated dispersion and active sites. Moreover, the physical and chemical properties of the bimetallic catalysts are enhanced due to the formation of the solid solution

[31]. For example, Pudukudy et al. [32] and Pinilla et al. [33] revealed a greater carbon output from a bimetallic catalyst compared to a monometallic catalyst.

2. Energy and environment: current and difficult situations

At the moment, the adverse effect on the environment from the burning of fossil fuels, coal and compressed natural gas has become one of the main global issues [34]. Climate change occurs when the greenhouse effect rises, as demonstrated by flash floods, wind storms, heat waves and sudden droughts in a number of nations [35]. In addition, worldwide demand for energy is growing while fossil-fuel energy sources are quickly declining. Fossil fuels are one of the non-renewable energy resources that will be depleted in several decades if large-scale sources of energy are continually used [36]. As shown in **Figure 2**, the world production of fossil oil is at the peak of the production, and it is expected to diminish by the year 2050 [37]. Because of these situations, it is essential to replace petroleum consumption, minimize future expenses and eliminate the adverse effect on health and the environment. Thus, the replacement of non-renewable energy source with renewable resources is imperative to fulfill the needs of the energy demand without causing harm to the environment and mankind [38]. Due to this crisis, various kinds of energy are used to meet the large demand for petroleum-based fuel such as wind turbines, river dams, solar panels, geothermal power and biofuels [39].

The conversion of methane into liquid fuels or greater hydrocarbons has been performed extensively. Bradford and Vannice [40] studied the growth of methanol, formaldehyde, propanol, benzene and other aromatics through direct oxidative conversion of methane. Unfortunately, all the aforementioned processes produce low yields or they are not recommended for an industrial scale. Today, various technologies are available for the production of syngas from natural gas. This gas is a component of precious fluid fuels and chemicals like Fischer-Tropsch oil, methanol and dimethyl ether [41].
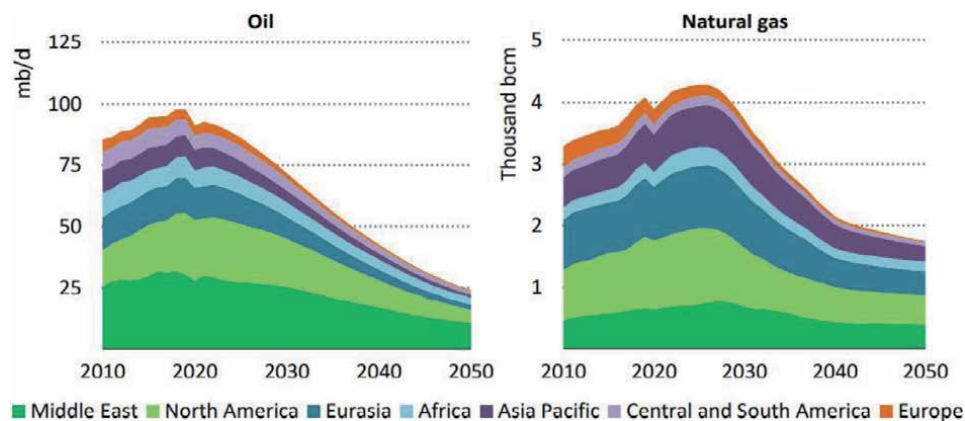

Figure 2.
Oil and natural gas production in the NZE (adapted from Ref. [37]).

2.1 Biogas

The most significant renewable energy sources in the globe are biomass and hydropower. However, the use of other renewable resources is necessary to

minimize the negative climate impacts caused by the excessive use of fossil fuels. In that sense, biogas will play an important role in the future. The biogas primary energy has increased 70% between 2008 and 2013 [42] and its production is expected to double in 2022 up to 45×10^9 m^3. Biogas is a gas consisting primarily of methane and carbon dioxide generated from anaerobic digestion of organic matter from agricultural waste, landfills, urban wastewater and industrial wastewater. It is considered, therefore, a renewable energy source [43].

Based on the residue, biogas can contain traces of other compounds that hinder its use in the production of energy, making it necessary to install costly purification systems. Among them, the most significant are H_2S, NH_3, halogenated hydrocarbons and siloxanes. Biogas has traditionally been regarded a non-value by-product usually burned in flares to avoid hazards to humans and the environment and then released into the atmosphere. Recently, various options for biogas use such as heat, electricity, mixed heat and energy or the manufacturing of bio-methane have been suggested. Nevertheless, from an economical point of view, all the previous biogas applications depend on government feed in tariff policies. Besides, different countries like Malaysia, Germany, Spain or Italy, have reduced or even removed the cost-based compensation creating an unstable scenario for the renewable energy producers [44]. Therefore, the manufacturing of fresh biogas products is not only interesting but essential in order to reduce the obstacles to profitability.

One of the alternatives considered is the manufacturing of syngas that consists of a blend of H_2 and CO and is the basis of C1 chemistry [45]. Depending on the syngas H_2:CO ratio, it can be used to produce methanol, dimethyl ether (DME), liquid hydrocarbons (Fischer-Tropsch process) or H_2. Syngas can be acquired from several procedures such as methane steam reforming, partial methane oxidation or dry methane reforming.

2.2 Catalytic decomposition of biogas

Due to overdependence on fossil-based fuels and increasing environmental concerns, the resources of renewable energy, in particular biogas, have gained massive attention around the world as a substitute for traditional fossil fuels. Biogas is obtained from the process of the anaerobic digestion of organic compounds. Methane (40–70%) and carbon dioxide (30–60%) are the primary compounds of biogas [46]. One of its most common applications is the direct combustion for energy recovery through co-generation plants that produce electricity and heat. Nevertheless, the use of renewable sources of methane like the one contained in biogas (biomethane) for different applications like the production of hydrogen is a more interesting option than the use of fossil methane [47].

In this context, the catalytic decomposition of methane (CDM) (Eq. (1)) is being studied as an alternative to steam reforming of methane (SRM) to produce CO_2-free hydrogen. The CDM in a single step produces a mixture of hydrogen and unconverted methane, which can be directly used as fuel in internal combustion engines or, even directly used to power a fuel cell [47].

$$CH_4 \rightarrow C + 2H_2 \quad , \quad \Delta H^{\circ}_{298K} = 75.0 \text{ kJ mol}^{-1} \quad (1)$$
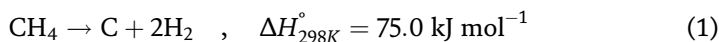
The catalysts traditionally used in the CDM consist of transition metals belonging to group VIII (Ni, Fe, Co) supported over different metal oxides such as Al_2O_3, MgO, La_2O_3, and CeO_2 [48, 49]. These catalysts are characterized by promoting the formation of carbon nanostructures (carbon nanofibers or carbon nanotubes) varying their textural and structural properties as a function of the catalyst composition and the operational conditions [50]. These carbon nanostructures have very

interesting properties for their use in applications where thermal and electrical conductivity of materials is a key factor. However, one of the problems of the CDM is the deactivation over time of the catalysts due to carbon deposition that encapsulates the metal particles disabling their active sites [51].

Co-feeding with CH_4 different oxidizing agents such as H_2, H_2O or CO_2, can increase the life of the catalyst. Co-feeding with H_2, inhibits the deactivation of the catalyst at the expense of a desired product, which reduces the efficiency of the process while the use of CO_2 as Co-feeding induces Boudouard reaction (Eq. (2)) thereby resulting in gasification of graphitic carbon produced during the CDM reaction.

$$2CO \rightarrow C + CO_2 \quad , \quad \Delta H^{\circ}_{298K} = 172.0 \text{ kJ mol}^{-1} \quad (2)$$
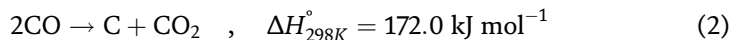
The use of CO_2 in the CDM process has been studied by two approaches: some authors have suggested a cyclical process consisting of a methane decomposition step followed by another stage of gasification of the deposited carbon with CO_2. Other authors have studied the decomposition of mixtures CH_4:CO_2 in conditions that favor the formation of nanostructured carbon. Nagayasu et al. [52] observed a slow deactivation of a Ni based catalyst to be used in the CDM in the presence of CO_2. They also noted an increase in carbon accumulation capacity in the form of nanotubes by increasing the partial pressure of CO_2 co-fed along with that of CH_4.

Asai et al. [53] confirmed the inhibition of the deactivation of the catalyst studied in the decomposition of methane in the presence of CO_2, suggesting a mechanism based on the gasification of graphitic carbon layers that encapsulate the catalyst particles, allowing the formation of carbon in the form of nanotubes. Indeed, co-feeding of CH_4 and CO_2, which are the main components of biogas as previously mentioned, modifies the reaction mechanism of methane decomposition into carbon and H_2, to a process called dry reforming, which produces a mixture of H_2 and CO. This is a highly endothermic reaction that takes place by way of a catalyst in the temperature range between 600 and 800°C, producing syngas with a molar ratio 1:1 [54].

This syngas can be used in multiple applications such as fuel for solid oxide fuel cells or Fischer-Tropsch synthesis to produce environmental friendly liquid fuels, when using a renewable source such as biogas [55]. If the aim is to produce H_2, then a water gas shift reaction followed by CO_2-H_2 separation should be accomplished. The practical implementation of the dry reforming of methane (DRM) faces many key challenges, which also apply to the biogas decomposition, and one of the most important is the deactivation of the catalysts due to the formation of carbon during the reactions of CH_4 decomposition and CO_2 disproportionation [56]. Also, Edwards and Maitra [57] reported that it is convenient to work at high temperatures and low ratios of CH_4:CO_2 (<1), to minimize carbon formation from a thermodynamic point of view. However, from the industrial point of view it would be much more desirable to work at moderate temperatures and CH_4:CO_2 ratios close to one, despite these are conditions under which carbon formation is thermodynamically favored.

Another issue that should be addressed is the high sulfur content of the biogas. This can provoke severe metal catalysts deactivation, therefore an exhaustive desulphurization of the biogas fed to the catalytic decomposition of biogas (CDB) reactor would be required when using a real biogas. The most commonly used methods for hydrogen sulphide removal can be found in [58]. The more active catalysts that promote the lower carbon deposition are precious metals, but its high price provokes that the most widely used catalysts for dry reforming are based on Ni, Co and Fe [59], which are the same catalysts traditionally used in the CDM.

Since the typical CH_4:CO_2 ratio in biogas composition is higher than 1 (CH_4 concentration in biogas can be as high as 70% depending on its origin), avoiding carbon deposition in the biogas decomposition reaction is not a task easy to accomplish. Thus, as previously mentioned, the presence of CO_2 along with the selection of optimum operating conditions for the deposition of carbon could prevent the rapid deactivation of the catalyst, resulting in a new biogas recovery process in which a gas with a suitable composition for its use in an internal combustion engine and carbon nanofibers (CNF) with multiple applications in sectors such as energy and transport are obtained. Direct decomposition of a gas simulating a typical biogas composition by means of metal catalysts under conditions that are favorable for carbon deposition has been studied by Muradov and Smith [60]. The problem associated to carbon deposition through decomposition of CH_4:CO_2 mixtures with ratio >1 was solved by adding small amounts of steam, prolonging the catalyst life. Some previous works by De Llobet et al. [61] focused on a study of CDB, conducted at moderate temperatures and using typical catalysts previously used in the CDM, promoting the formation of nanostructured carbon and syngas. As per their report, the Ni/Al$_2$O$_3$ catalyst exhibited high activity as well as stability, allowing them to obtain high CH_4 conversion together with the high-yield production of fishbone-like nanocarbon.

2.3 Chemistry of carbon dioxide

Figure 3 illustrates a key aspect of the thermodynamics of any possible CO_2 conversion. The figure also demonstrates the free emission of CO_2 from Gibbs and its associated substances. It is evident that CO_2 is an extremely stable molecule; it therefore requires significant energy input, optimized reaction conditions and (almost invariably) active catalysts for any chemical conversion of CO_2 into a carbonaceous fuel.
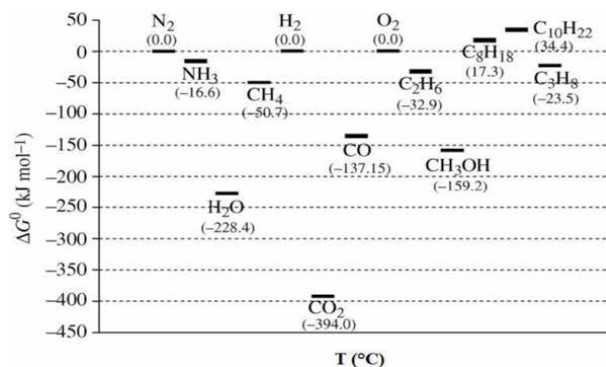

Figure 3.
Gibbs free energies of formation of selected chemicals (adapted from Ref. [62]).

However, it is important to note that chemical reactions (conversions) arise due to the difference in the Gibbs free energy between the reactants and products of a chemical reaction (under certain conditions). This is illustrated by the Gibbs-Helmholtz relationship (Eq. (3)):

$$\Delta G^{\circ} = \Delta H^{\circ} - T\Delta S^{\circ} \qquad (3)$$

Therefore, the comparative stability of the ultimate response products must be taken into consideration in the effort to use CO_2 as a chemical feedstock compared to the use of reactants. Both terms (ΔH° and $T\Delta S^{\circ}$) of the Gibbs free energy are not

favorable for the conversion of CO_2 to other molecules [63]. Since the carbon-oxygen bonds are relatively strong, substantial energy input is necessary for their cleavage, in terms of carbon reduction. Similarly, the entropy term ($T\Delta S^o$) makes little to no contribution to the thermodynamic driving force for any reaction involving CO_2. Most importantly, the enthalpy term, ΔH^o, can be taken as a good initial guide for the assessment of thermodynamic stability and feasibility of any CO_2 conversions.

Freund and Roberts [63] highlighted the significant contribution of CO_2 surface chemistry. They claimed that any progress in the use of CO_2 as a useful reactant can be achieved in relation to fuel synthesis by using novel catalytic chemistry wisely. They attempted to illustrate that the greatest potential impact lies in this area of material chemistry, physics and engineering. These researchers also pointed out that a positive change in free energy should not be considered as a reason enough not to pursue potentially useful CO_2 reactions. This is because, ΔG^o only provides information as to the yield of products at equilibrium through the relationship (Eq. (4)), and the kinetics of such a process is indeed favorable.

$$\Delta G^{\circ} = -RT \ln K \qquad (4)$$

Since the kinetics are favorable, CO_2 decrease to CO (a key step in all conversion reactions), the primary step in all transformation responses, may also be feasible on metal surfaces or other catalytic materials, for instance on nano- and mesoporous metal particles [62]. Presently, a large number of industrial-scale chemical manufacturing processes worldwide operate on the basis of strong endothermic chemicals. The SRM to yield syngas and hydrogen is a classic example (Eq. (5)):

$$CH_4 + H_2O \rightarrow CO + 3H_2 \quad , \quad \Delta H^{\circ}_{298K} = +206 \text{ kJ mol}^{-1} \qquad (5)$$
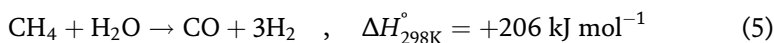
It is important to emphasize that the above-mentioned, highly endothermic reaction is used to produce large quantities of 'merchant hydrogen' in the gas, food and fertilizer industries worldwide. The corresponding DRM reflects the important reaction of CO_2 with hydrocarbons, which will be central to our idea of converting CO_2 into flue gases to produce chemical fuels (Eq. (6)):

$$CH_4 + CO_2 \rightarrow 2CO + 2H_2 \quad , \quad \Delta H^{\circ}_{298K} = +247.3 \text{ kJ mol}^{-1} \qquad (6)$$
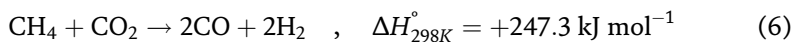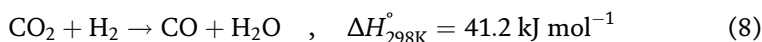
The energy input for DRM requires about 20% more energy input than the SRM, but there is definitely no restricted additional energy cost for this chemical reaction. It is important that these two reactions lead to syngas with different H_2:CO molar ratios. For the final production of liquid fuels, both are useful for the formation of horns.
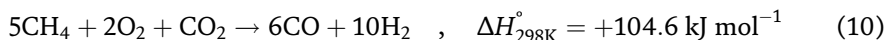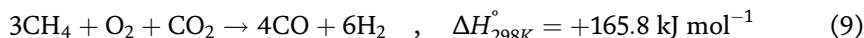
Figure 4 shows the enthalpy of the chemical reactions of the CO_2 conversion. This means that CO_2 is thermodynamically much easier to use as a co-reactant, usually with a higher (i.e. less negative) Gibbs free energy, such as H_2 or CH_4. These hydrogen-containing energy carriers give their internal chemical energy to promote the conversion of CO_2. Therefore, the heat of reaction (enthalpy of reaction) from CO_2 to CO production is important and obvious as the individual reactive and CO_2 energy as a key factor. Compare the thermal decomposition energies of CO_2 (Eqs. (7) and (8)).

$$CO_2 \rightarrow CO + \tfrac{1}{2}O_2 \quad , \quad \Delta H^{\circ}_{298K} = +293 \text{ kJ mol}^{-1} \qquad (7)$$
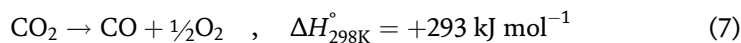
With that of the reaction of CO_2 with H_2 (Eq. (8))

$$CO_2 + H_2 \rightarrow CO + H_2O \quad , \quad \Delta H^{\circ}_{298K} = 41.2 \text{ kJ mol}^{-1} \tag{8}$$

This aspect may be further illustrated by the process of 'oxyforming', whereby the amount of oxygen in the dry reforming reaction is increased deliberately. In doing so, the reaction enthalpy of reaction is significantly reduced (Eqs. (9) and (10)):

$$3CH_4 + O_2 + CO_2 \rightarrow 4CO + 6H_2 \quad , \quad \Delta H^{\circ}_{298K} = +165.8 \text{ kJ mol}^{-1} \tag{9}$$

$$5CH_4 + 2O_2 + CO_2 \rightarrow 6CO + 10H_2 \quad , \quad \Delta H^{\circ}_{298K} = +104.6 \text{ kJ mol}^{-1} \tag{10}$$

The fundamental material challenge in this area lies in the fact that, generally, the reaction between CO_2 and H_2 occurs at high temperatures on multi-component heterogeneous catalysts [64].
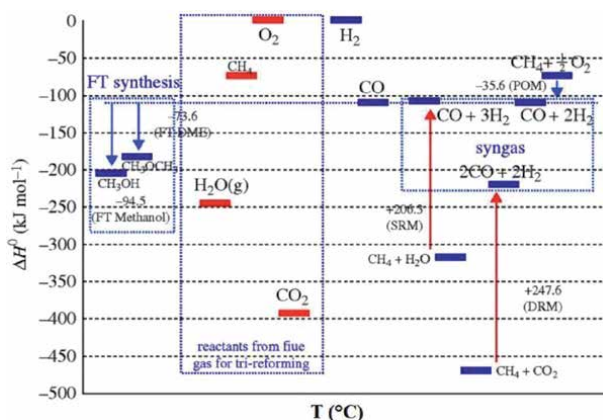

Figure 4.
The enthalpy of reaction for syngas production and Fischer-Tropsch (FT) synthesis of methanol and dimethyl ether (adapted from Ref. [62]).

2.4 Syngas

Syngas is a blend of carbon monoxide and coal with a tiny quantity of methane and carbon dioxide. In the ever changing energy landscape, it is not only versatile, but also an increasingly important commodity. There are various carbon sources that happen through gasification or catalytic reformation for the manufacturing of syngas. Coal, natural gas (mainly methane), petroleum, and biomass could be the sources of carbon. The primary technical problem with fossil fuel syngas manufacturing is the complicated purification and conditioning procedures of syngas. The main reasons why the world has become more interested in the producing of biomass-derived syngas are therefore to decrease over-dependence on fossil fuels, to impose stricter CO_2 emission standards and to verify the accessibility of resources. Roddy [65] claimed that biomass could originate from industrial, domestic, agricultural and urban waste sources as a feedstock for syngas production. The use of biomass or waste as the raw material for syngas manufacturing is theoretically two-pronged: the generation of clean energy and an effective way to reduce waste as reported by Markets and Markets [66], a compound annual growth rate (CAGR) of 8.7% is anticipated to achieve 117,400 MW (Megawatts) heat in 2018. Boerrigter and Rauch [67] estimated the future market for syngas to increase to 50,000 petajoules (PJ) per annum, equivalent to 13.9×10^9 MWh per annum in, 2040. This amounts to replacing an average 30% fossil fuel usage is 10% of the complete world power consumption. They also projected that syngas will be used

primarily in gas-to-liquid (GTL) procedures, with 49% for gas-to-product (GTP) procedures and 39% for renewable gas and hydrocarbon manufacturing. In, 1993, Shell Malaysia built the world's first commercial GTL plant in Bintulu, Sarawak. Since, 2003, as many as for 14,700 barrels of high-quality GTL products have been produced per day. This is clearly an upgrade in the production from its original capacity of 12,500 barrels per day. As reported by the Borneo Post, Shell's GTL plant plans to invest RM (Malaysian ringgit) 48.36 million to rejuvenate its plant in Bintulu in, 2015. The world's largest GTL plant is located in Qatar, with a production capacity of 140,000 barrels of product per day.

In short, the development of the market for syngas is accelerating, the important increase in syngas consumption is due to its use as an energy precursor. The presence of CO, H_2 and CH_4 gases, which possess certain heating value, makes it highly in demand. Syngas also includes approximately 50% of natural gas's power density. Subramani et al. [68] reported that 1 kg of H_2 contains the same amount of energy as 2.6 kg of CH_4, which is equivalent to 3.1 kg of gasoline. H_2 is used at low temperatures because of its elevated energy content; fuel cells are used to produce electricity, power cars or even in the synthesis of Fischer – Tropsch. In addition to serving as an energy carrier, it has traditionally been used as a feedstock for the mass production of significant chemicals, such as methanol, ammonia or fertilizers.

2.5 Carbon nanofilaments

Carbon nanofilaments are nanometric filaments with diameters between 1 and 200 nm and lengths of up to several microns. These materials are composed mainly of graphite type carbon whose basic structural component is graphene [69]. Graphene can be defined as the combination of carbon atoms with sp^2 hybridization, where each carbon atom joins three others forming a flat hexagonal tessellation (basal plane or graphene layer) [70]. The parallel stacking of several of these layers' outcomes in graphite characterized by an elevated structural order and a distance of 0.3354 nm between the distinct graphene layers (crystalline domain or interplanar distance, d_{002}) (**Figure 5**).

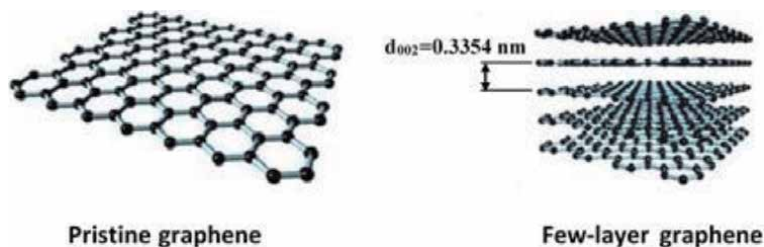**Pristine graphene**   **Few-layer graphene**

Figure 5.
Representative scheme of crystal structures of graphene (adapted from Ref. [71]).

On the other hand, carbon nanofilaments have a structural order inferior to that of graphite and according to the Franklin classification [72] correspond to turbostratic type materials, that is, they have crystalline domains greater than graphite and smaller than non-graphitic carbons ($0.3354 < d_{002} < 0.344$ nm).

Within carbon nanofilaments we can distinguish two types: carbon nanotubes (CNT) and carbon nanofibers (CNF). The CNT can be considered as layers of graphene rolled into hollow tubes [73]. Depending on the number of layers that make up the CNT, they are classified as single wall CNT (SWCNT), formed by a single layer, or multiple wall CNT (MWCNT), formed by 2 or more concentrically coiled layers (**Figure 6a**) [73]. On the other side, the CNF can be hollow or strong
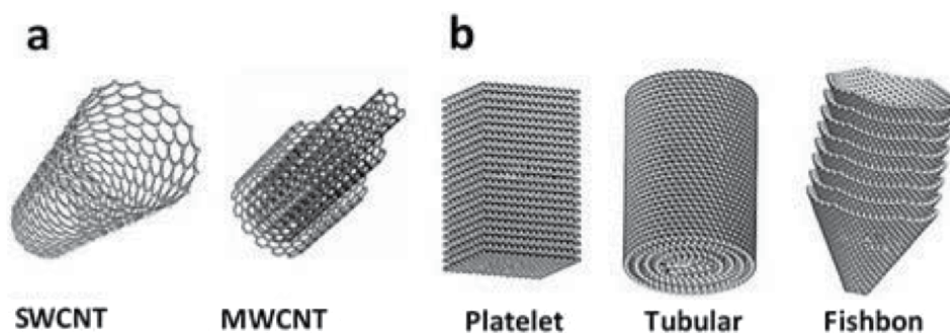
Figure 6.
Simplified representation of the different kinds of (a) carbon nanotubes (SWCNT and MWCNT), and (b) carbon nanofibers (platelet, tubular, fishbone) (adapted from Ref. [73]).

and are categorized with regard to their longitudinal axis according to the angle they form graphene layers (α). The most common types of CNF are platelet, parallel (also named ribbon or tubular) and fishbone (**Figure 6b**) [73]. Platelet CNF are characterized by the fact that the graphene sheets are arranged perpendicular to the growth axis of the CNF (α ≈ 180°), while in the fishbone type the angle α is between approximately 20–160° [74].

They are also called Herringbone. Finally, the parallel types would be those in which the sheets are parallel to the longitudinal axis of the CNF (α ≈ 0°). Unlike **Figure 6b**, this sort of structure can also be tubular and therefore it is not feasible to distinguish them from MWCNT by using electronic microscopy methods. However, there is some controversy, parallel type CNF tend to present areas along their structure in which the graphene layers are not oriented in parallel (α > 0°) as well as numerous imperfections such as the union of the layers' graphene inside the nanofiber (loops). Along with these three morphologies, in the CNF world there are other types of less common structures such as bamboo CNF, which are characterized by having internal holes that occur periodically due to the movement of the catalytic particle during the growth of the CNF, or the octopus-type NFCs that are generally produced when a Ni catalyst doped with Cu [75] is employed. Although there is a bibliography related to the formation of carbon filaments since the late nineteenth century, it was the discovery of the transmission electron microscope (TEM) in 1939 that really represented a breakthrough in this field since it allowed the observation in detail the morphology of this type of structures [76]. Initially, the interest in carbon formation derived from the problems that its accumulation caused in the processes of conversion of hydrocarbons (deactivation and destruction of catalysts or plugging of reactors) and therefore, the objective was to understand how and why it was generated in order to avoid their formation [77]. However, since the discovery of CNT by Iijima [78] in the 90s and due to the properties that carbon nanofilaments present (high specific surfaces and high electrical conductivities and thermal, the approach changed and numerous studies were initiated to optimize their production [79].

3. Current reforming technologies

Numerous reform techniques have been created to fulfill the long list of demands required in downstream chemicals procedures. Dry Reforming of methane is the most prevalent technique used in the syngas sector through one of three reforming procedures: (1) steam reforming of methane (SRM), (2) partial oxidation

of methane (POM) and (3) dry reforming of methane (DRM). The difference between the three techniques is based on the oxidant used, the kinetics and reaction energy, and the percentage of syngas produced (H_2:CO).

3.1 Steam reforming

The SRM approach produces a higher H_2:CO ratio of 3:1 compared to the ratio required for Fischer-Tropsch (F-T) synthesis of 2:1 [80]. Due to its endothermic nature, SRM requires an extensive energy input so it is very expensive. In addition, a higher H_2O:CH_4 ratio is required to achieve a higher H_2 output, making the SRM process less favorable and speeding up the activation of catalysis. Moreover, SRM faces corrosion problems and requires a desulfurization unit [81].

3.2 Partial oxidation of methane

In the case of POM approach, this process is suitable for producing larger amounts of hydrocarbons and naphtha. Typically, POM has a very short residence time, high selectivity, and high conversion rates [82]. However, the exothermic nature of the reaction causes the induction of hot spots in the catalyst and makes it difficult to control the process. In addition, POM requires a cryogenic unit to separate oxygen from air. In the case of POM, this process is suitable for producing larger amounts of hydrocarbons and naphtha. POM typically has a very short period of residence, high selectivity and high conversion rates. The exothermic nature of the response, however, allows warm spots in the catalyst to be induced and makes the method hard to regulate and POM requires a cryogenic unit to separate oxygen from air [83].

4. Dry reforming of methane

DRM approach is the most promising of all techniques, as it utilizes two greenhouse gases (CO_2 and CH_4) to generate industry-significant syngas while at the same moment lowering excessive greenhouse gas emissions. The DRM method is also cheaper than other techniques, as it eliminates the complicated gas separation of finished products. It generates the ratio H_2:CO that can be used to synthesize oxidized chemicals and F-T synthesis long-chain hydrocarbons. DRM can also be extended to biogas (CO_2, CO, and CH_4) as a raw material for cleaner and eco-friendly fuels. DRM syngas is also a solar or nuclear energy storage facility [84]. Since reaction is endothermic, the process is generally carried out at temperatures between 450 and 900°C. In addition, the utilization of a catalyst is required in order to obtain acceptable CH_4 conversions. The practical application of the DRM faces many significant obstacles and one of the most significant is the deactivation of the catalysts due to carbon formation during CH_4 decomposition and CO_2 disproportionate responses. Working at elevated temperatures and low CH_4:CO_2 ratios (<1) is useful from a thermodynamic point of perspective to prevent carbon formation. From an industrial point of perspective, however, work at mild temperatures and CH_4 would be much more desirable: CO_2 ratios close to one. Nevertheless, circumstances under which thermodynamic carbon formation is favored [85].

In this context, the DRM's attempts focus on developing a catalyst that demonstrates elevated activity and stability and low carbon formation and price at the same moment. In one of the first works related to the DRM, Fischer and Tropsch studied different metals belonging to groups 8, 9 and 10 (Ni, Co, Fe, Mo, W, Y, Cu). Among them, only Ni and Co showed a good activity ($X_{CH_4} \approx 90\%$). Years later,

Gadalla et al. [86] tested different commercial Ni-based catalysts, obtaining CH_4 conversions near 100% during 70 h of operation. Nonetheless, in order to avoid carbon deposition and catalyst deactivation they used $CH_4:CO_2$ ratios below 0.5 and temperatures above 900°C. Due to their high activity and lower carbon formation as compared to Ni, noble metals have been extensively studied as catalysts for the DRM [87]. However, their high cost and low availability make other metals more attractive from an industrial point of view. Due to their reduced cost compared to noble metals, Ni, Co and Fe were also widely researched and in the last years, bimetallic catalysts have stood out.

In order to synthesize an enhanced catalyst, these catalysts aim to potentiate the features of both metals. Ni-Co bimetallic catalysts showed a very healthy conduct among them. In any event, carbon deposition issues are even more important when using biogas. Biogas usually has higher $CH_4:CO_2$ ratios than one that ultimately leads to bigger quantities of carbon depositions that quickly deactivate the catalysts. However, distinct types of carbon are created during the decomposition of hydrocarbons and luckily not all of them are directly liable for the deactivation of catalysts. The sort and location of carbon atoms is more important than the amount generated when considering catalytic activity, according to Pinilla et al. [88]. Generally, only carbon encapsulation is directly liable for deactivation of the catalyst owing to active center coverage, while other carbon structures, such as carbon nanofilaments, can only cause operational issues when manufactured in big amounts as reactor blockage.

4.1 Kinetics and mechanistics of dry reforming approach

Studies of DRM's kinetics and mechanisms were conducted to determine an appropriate reaction rate model, either empirically or on the basis of a theoretical response mechanism to best suit the relevant experimental information and possibly describe the response rate and the chemical process. This understanding can further optimize the design and layout of the chemical system catalysts (the reactor), which can further improve DRM's overall development with more cost-effective technology [89]. Although, from a mechanistic point of perspective, steam reforming has received much attention, there has been a resurgence of interest in dry reforming over the previous centuries. A series of catalysts for DRM were researched as a consequence. This has resulted in a number of mechanistic measures for DRM being published in the literature. The DRM reaction mechanism was explored by Aldana et al. [90] over a Ni-based catalyst.

Aldana et al. reported that H_2 dissociates on Ni^0 locations while carbon dioxide is activated on ceria-zirconia assistance to generate carbonates that can be hydrogenated into formats and then into methoxy species. This mechanism includes weak fundamental support sites for carbon dioxide adsorption and includes a stable interface between metal and support. Compared to Ni-silica, which activates both carbon dioxide and hydrogen on Ni^0 particles, these characteristics lead in much better operations of these catalysts [90]. This mechanism is also supported by Pan et al. [91]. Meanwhile, Ayodele et al. [92] conducted a DFT analysis of the DRM over Ru nanoparticles supported on TiO_2 (101).

4.2 Influence of process variables on reaction rates

Extensive research was carried out to study the impacts of altering process variables on catalyst performance for the DRM reaction. This inquiry is essential as various process factors may result in variable catalyst performance [93]. The notion of activation energy should be considered as it will determine the response rate.

Table 1 tabulates the activation energy (E_a) values of CH_4 and CO_2 obtained from different types of Ni-based catalysts in DRM. For most catalysts, the activation energy of CH_4 is higher than that of CO_2 since the molecules of CH_4 are more stable than those of CO_2. Therefore, more energy is required to activate the more stable molecules. Moreover, the basicity of the assistance for the catalyst has resulted to variations in the activation barrier. Kathiraser et al. [93] think the activation energy in DRM is fully dependent on the catalyst's type of catalyst support, promoter and bimetallic interactions.

Catalyst	Preparation method	Total flowrate (mg)	Catalyst Amount (kJ/mol)	$E_{a(CH_4)}$ (kJ/mol)	$E_{a(CO_2)}$ (kJ/mol)	Ref.
Ni/Al_2O_3 (400–650°C)	Wet impregnation	28	500	—	64.4	[94]
$4.82Ni/Al_2O_3$ (750–850°C)	Incipient wetness	100–980	—	242.67	115.86	[95]
$7Ni/MgO$ (550–750°C)	Incipient wetness-impregnation	—	10	105	99	[96]
$5Ni/MgAl_2O_4$ (600–800°C)	Co-precipitation	30	20	26.39	40.43	[97]
$13.5Ni-2K/5MnO-Al_2O_3$ (550–800°C)	Impregnation	400	50	113.8	—	[98]
$0.3Pt-10Ni/Al_2O_3$ (580–620°C)	Sequential impregnation	100	5	112.55	98.74	[99]
$8\%Ni/\alpha-Al_2O_3$ (550–750°C)	Wet impregnation	360	40	89.1	88.6	[100]

Table 1.
E_a values over several Ni-based catalysts for DRM reaction.

In the meantime, Cui et al. [100] conducted a thorough study of the DRM mechanism over $Ni/\alpha-Al_2O_3$ using steady-state and transient kinetic methods at 550–750°C temperatures. Their results show that the CH_4 dissociation and CO_2 conversion E_a values could be classified as follows: low (550–575°C), middle (575–650°C) and high (650–750°C). In low and high temperature areas, the response was constant but fluctuated in the region of medium temperature. It is suggested that the dissociation of CH_4 into CH_x and hydrogen species in the Ni active sites at temperatures above 650°C has attained a level of balance. In addition to the activation energy, it is essential to correctly formulate the suitable catalyst's inherent kinetic models based on basic measures in order to reach a compromise between economic feasibility and process effectiveness. However, this kinetics of reaction is affected by the reactants 'mass transport. When eliminating the impact of mass transport, the conversions observed can be directly ascribed to the catalyst's inherent kinetics.

According to Kathiraser et al. [93], distinct gas hourly space velocities (GHSVs) need to be tested to eliminate internal mass transport resistance. The aim of this experiment is to verify that the conversions have reached a stable value and that a further shift in GHSV does not influence the conversion of reactants. The contact time, which plays a significant part in CO_2 and CH_4 conversions, is another consideration. When the contact time value is high, CO_2 or CH_4 conversions stay unaffected. The particle size of the catalyst should be held as small as possible to eliminate inner mass transport resistance, so that a further reduction in size does not impact conversions.

Kim et al. [101], explored the use of a CO_2-photoacoustic signal (PAS) to analyze kinetically the DRM reaction on a Ni catalyst supported on Al_2O_3 and TiO_2. They

discovered that the reason why mass flow rates low are used is because this method generates heat periodically because when a material absorbs a modulated laser beam, the photoacoustic signal is produced. It is essential to remember the characteristics of kinetic curves that act as the reaction mechanism's blueprints. These include the point of inflection, a brief period of induction or breakpoints. No particular GHSV can be found from all the results to eliminate the impacts of constraints on mass transfer. This indicates that the development of inherent kinetic models is critical in preliminary research.

4.3 Catalysts for dry reforming approach

Numerous studies on the development of active and coking-resistant DRM reaction catalysts have been published [102, 103]. Common DRM catalysts are backed by noble metal catalysts like Ru, Rh and Pt and backed by transition metal catalysts like Ni and Co [104–106]. The calculations for the result showed that noble Ru and Rh metals exhibit greater activity than Ni as long as the particle sizes and dispersion are the same [106]. While noble metals such as Ru, Rh and Pt in the DRM response are very effective and more resistant to coking than other transition metals, they are not readily accessible and are also costly [104].

4.3.1 Nickel based catalyst material

Ni-based catalysts are the most frequently used for commercial purposes on an industrial scale. In order to commercialize the industrial sector DRM response, the primary focus is on developing inexpensive and cost-effective catalysts with high activity and high carbon deposition resistance. Researchers performed research on the sort of assistance used and the impacts of adding promoters to Ni-based catalysts in order to define the most efficient way to enhance their coking resistance. In addition, latest efforts to enhance catalytic activity and inhibit carbon formation are aimed at combining two or three metals as active locations [105, 107]. Pretreatment process preparation method and catalyst also play a crucial role in altering structural characteristics, implementing behavior decrease and enhancing catalytic efficiency [108]. Besides establishing the Ni-based catalyst with certain modifying agents in the catalyst preparation, the incorporation of Ni particles in the mesoporous aid could also enhance the conversion of reactants and the yield of products by preventing the sintering of metal particles and improving the metal-supporting connection. This metal produces desirable results due to the high specific region of mesoporous materials which can increase the dispersion of Ni particles on the supported catalyst [109].

In addition, the strong interaction between metal and support stabilizes the Ni particles incorporated in the mesoporous matrix. Multiple contact regions between the Ni particles and the support could improve thermal stability and support metal cooperation and support. The incorporation of Ni-based catalysts into mesoporous supports such as MCM-41, SBA-16, TUD-1, meso-Al_2O_3 and meso-ZrO_2 has, as reported in the literature, demonstrated high catalytic activity and high carbon resistance in DRM. Catalyst supports can also be synthesized from plants, which is crucial for the effectiveness of DRM catalysts. The use of polymers from trees has been an interesting region among scientists in latest years with the aim of increasing the velocity of chemical reactions. In addition to generating high-quality chemicals, catalysts installed on commonly accessible cellulose incur low manufacturing expenses [110].

Abimanyu et al. [111] reported that the main steps to synthesize catalyst supports are pretreatment and hydrolysis. Ni-based catalysts have been used

industrially as metal precursors in DRM, but the need to refine the metal to improve catalyst performance has recently attracted the interest of many scientists, as these particles demonstrated promising physical and chemical properties with elevated technological applications potential.

The preparation technique significantly affected a catalyst's physico-chemical characteristics and efficiency, according to Jang et al. [112]. It has therefore been noted that impregnation and co-precipitation are the most commonly used standard techniques of catalyst preparing. Another less prevalent technique for preparing catalysts is sol-gel, which generates a distribution of fine size. This method reduces the deactivation rate, offers high thermal resistance to agglomeration and creates a product of high quality compared to conventional methods.

A new non-thermal glow discharge plasma method has recently been developed to improve metal support interaction, boost the distribution of Ni particles and improve the activity and stability of the catalyst [113]. However, in comparison with simpler preparation techniques, plasma therapy is comparatively costly. This would improve the activity and stability of the catalyst in the DRM response by combining novel catalytic material and techniques.

Supported bimetallic catalysts demonstrate increased DRM activity and stability based on Zhang et al. [114] study. The preparation technique is one of the main variables responsible for the bimetallic catalyst's outstanding catalytic results. During catalyst preparing, the use of high calcining temperature outcomes in strong interactions between metal and support, which converts the catalyst into stable frame-like constructions. In particular, carbon formation is efficiently blocked during the catalyst decrease by using Ni-Co alloy compared to using single Ni sites. The synthesis method of different catalysts also affects the reaction effectiveness. For example, the method of co-precipitation may produce smaller sizes of metal particles compared to the use of wet impregnation.

4.3.2 Catalysts developed for CO_2 reforming

There are focuses on the development of DRM catalysts for catalysts with the following features: greater activity and greater stability towards coke formation, sintering, the formation of inactive chemical species and metal oxidation [115]. The catalytic efficiency could be improved by changing the catalyst's active sites by adding supports and promoters during catalyst preparing to increase conversion and selectivity [116]. **Table 2** shows several catalysts that have been developed recently, including Ni-based catalysts applied to the DRM reaction.

4.4 Catalyst deactivation

Deactivation of catalyst relates to loss of activity of catalyst during the response. It is the significant drawback of metal-based catalysts, as it not only creates product reductions that affect the response rate, but also costs industry millions of cash to replace the catalyst. Catalyst deactivation basically relates to three elements, according to Bartholomew and Farrauto [122] chemical, mechanical and thermal. Catalysts for metal reforming are frequently deactivated by coking, poisoning, fouling and sintering. **Table 3** describes the mechanisms of catalyst deactivation.

4.4.1 Poisoning

Poisoning relates to the powerful adsorption in the feed of chemical substances such as impurities. Poisoning of catalysts may be reversible (temporary) or irreversible (permanent) [122]. The catalyst may be retrieved by air oxidation or

Catalyst	Preparation method	GHSV (mL/gh)	Temperature (°C)	CH$_4$ conversion (%)	CO$_2$ conversion (%)	H$_2$/CO ratio	Ref.
Co-, Cu- and Fe-doped Ni/Al$_2$O$_3$	Fusion	12,000	650	34–40	NA	NA	[30]
25–55%Ni/MeO$_x$(Me = Al, Mg, Ti, and Si)	Evaporation-induced self-assembly	48,000	600	76	NA	NA	[50]
Ni/Ce-Al$_2$O$_3$ and Ni/Ce-Zr-Al$_2$O$_3$	Wet impregnation	21,000	800	66.7–79.5	45.2–86.9	NA	[58]
5% Ni/MgAl$_2$O$_4$	Microwave-assisted combustion	NA	850	83	—	≈1	[102]
5,10,15%Ni/MgAl$_2$O$_4$	Homogenous precipitation	12,000	700	78	89	NA	[103]
K,Mg,Ce-2,8% Ni/Al$_2$O$_3$	Wet impregnation	NA	160	31.6	22.8	2.2	[107]
5–100%NiH-Ce	Co-precipitation	20,000	550	35–55	35–45	0.55–1.60	[115]
5,10,15% NiMgAlCe	Co-precipitation	29,000	750	33–48	57–69	0.78–0.96	[116]
Pd, Pt-55%Ni-Cu/MgO·Al$_2$O$_3$	Wet impregnation	48,000	675	84	NA	0.55–1.50	[103]
15%Ni/ZrTiAlO$_x$	Sol-gel & impregnation	45,000	600	85	95	0.95	[117]
10Ni + 3%Ce/8% PO$_4$ + ZrO$_2$	Wet impregnation	28,115.4	800	95	96	NA	[118]
Ni-Mo$_2$C/MgO	Sol-gel	30,000	850	90	85	NA	[119]
NiO–10Al$_2$O$_3$–ZrO$_2$	One-step synthesis method	48,000	700	92	90	0.73	[120]
Ni-W/Al$_2$O$_3$-MgO	Co-precipitation	36,000	777.29	87.6	93.3	1	[121]

Table 2.
Catalysts developed for the DRM reaction.

steaming to wash its surface for reversible toxicity. For irreversible poisoning, however, the toxins cannot be removed, so replacing current catalysts with a fresh batch is essential. Sulfur species such as hydrogen sulfide are common poisons in all catalytic processes with reduced metals as the active site. S-poisoning, as in procedures of F-T synthesis and steam reform, is always a disaster.

In 2011, Bartholomew and Farrauto illustrated the mechanism of sulfur poisoning [122]. Firstly, the S atom adsorbs or blocks the reaction or active sites of the catalyst physically (geometric effect). Then, the S atom alters the metal atoms electronically. The metal ions subsequently alter their adsorbability or their capacity to dissociate with reactant molecules like H$_2$ and CO. The S atom also alters the surface area and creates major catalytic characteristics alterations. This hinders the accessibility of adsorbed reactants to each other and thus slows down the adsorbed reactants' surface propagation. **Table 4** describes the typical poisons of industrial catalysts for different types of reaction. The avoidance of sulfur toxicity and sulfur strength can be improved by modifying the structure of the catalysts by

Mechanism	Type	Definition
Poisoning	Chemical	Strong chemisorption of species on catalytic sites, thereby blocking sites for catalytic reaction
Fouling	Mechanical	Physical deposition of species from fluid phase onto the catalytic surface and in catalyst pores
Thermal degradation (Sintering)	Thermal	Thermally induced loss of the catalytic surface area due to crystalline growth, support area and active phase support reactions
Vapor formation	Chemical	Reaction of gas with catalyst phase to produce volatile compound
Vapor-solid and solid-solid reactions	Chemical	Reaction of fluid, support, or promoter with catalytic phase to produce inactive phase
Attrition/crushing	Mechanical	Loss of catalytic material due to abrasion Loss of internal surface area due to mechanical induced crushing of the catalyst particle

Table 3.
Mechanisms of catalyst deactivation.

Reactions	Catalyst	Poisons
Steam reforming	Ni/Al_2O_3, Ni	H_2S, As, HCl
CO hydrogenation	Ni, CO, Fe	H_2S, As, COS, NH_3, HCN, metal carbonyls
Automotive catalytic converters	Pt, Pd	Pb, P, Zn, S
Ammonia synthesis	Fe	CO, CO_2, H_2O, O_2, S, C_2H_2, Bi, Se, Te, P, VSO_4
Catalytic cracking	SiO_2-Al_2O_3, Zeolites	Organic bases, NH_3, hydrocarbon, Na, heavy metals

Table 4.
Poisons of the industrial catalysts.

incorporating certain additives, such as molybdenum and boron, which adsorb sulfur selectively or change the response circumstances. According to Bartholomew and Farrauto [122], reduction in the temperature of steam reforming over Ni/Al_2O_3 catalysts from 800 to 500°C will decrease the strength of S adsorption, hence reducing sulfur poisoning from 5 ppm to only 0.01 ppm.

4.4.2 Sintering effect (thermal degradation)

Bartholomew and Farrauto [122], Christensen et al. [123], and Argyle and Bartholomew [124] describe the sintering of a heterogeneous catalyst as the loss of the catalytic layer, which is generally irreversible owing to the development of crystallite either on the supporting material or after thermal degradation in the active stage. Bartholomew and Farrauto [122] revealed two significant sintering parameters. The first is the sintering of temperature, including above the catalyst atmospheric temperature. The next is the sintering rate, which is impacted by the support structure and morphology, the metal particle size distribution, and the support's phase transition. These two catalyst sintering processes are crystallite migration (coalescence) and nuclear or vapor transport (ripening of Ostwald). Christensen et al. [123] outlined that crystallite migration involves entire crystallite migration followed by collision and coalescence. In the meantime, Argyle and Bartholomew [124] addressed that Ostwald ripening relates to the migration of

metal transport species emitted from one crystallite over the assistance or through the gas phase and caught by another crystallite. The author also stated that the sintering method is due to elevated temperatures and that owing to the presence of water vapor there is an increase in the sintering speed. Due to sintering impacts, **Figure 7** demonstrates the conceptual models of crystallite development.

Lif and Skoglundh [125] found that the co-impregnation of nickel catalysts with the oxides of alkali metals, alkaline earths or lanthanides suppresses the sintering effect. In addition, it was also shown that the catalyst preparation sequential impregnation technique improves the catalyst's stability towards sintering. To conclude, it is extremely desirable that it possesses the following characteristics for the growth of a fresh catalyst: heat resistance, coking resistance and stability in syngas manufacturing.
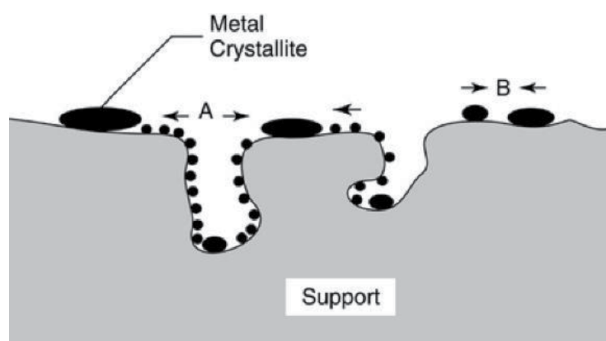

Figure 7.
Conceptual models for crystallite growth due to sintering by (A) Ostwald ripening and (B) crystallite migration (adapted from Ref. [124]).

4.4.3 Carbon deposition

Fouling is a physical (mechanical) deactivation that causes the loss of catalyst activity owing to coke deposition that blocks the reactive sites. Steam reforming utilizes catalysts primarily based on Ni. Coke deposition is a prevalent cause of deactivation of Ni-based catalysts. Temperature-programmed hydrogenation (TPH) and Temperature-programmed oxidation (TPO) methods are used to analyze carbon deposition on the used catalyst. The methods of TPH and TPO are used to define the features of the kinds of carbon species created during reaction on the catalysts [126]. According to Bartholomew and Farrauto [122], the types of carbon that may be formed during reforming are C_α, C_β, C_V, C_γ and C_C (see **Table 5**).

CH_4 cracking (Eq. (1)) and CO disproportionation are the two primary reasons for coke deposition during DRM (Eq. (6)). There are three possible carbon fouling mechanisms for the metal catalyst. The first mechanism is carbon, which deposits reactive sites on the catalyst and impedes binding of the reactants to the active locations. The carbon would otherwise encapsulate the catalyst's reactive site and deactivate the catalysts. Another deactivation option resides in the coke being deposited in the catalyst pores, thereby stopping the reactants from crystallizing on it. The third mechanism involves carbon-forming needle-like filaments in the active site of the nickel catalyst, to some extent breaking the catalysts. **Figure 8** shows the conceptual model of the mechanisms of carbon fouling of a catalyst.

Quincoces et al. [135] used DRM catalyst Ni/γ-Al$_2$O$_3$. They found that there were no rises in carbon deposition while the molar ratio of the reactants, CH_4/CO_2, was maintained in unity. This finding shows that by changing the response circumstances, such as the molar ratio of reactant feed, carbon deposition can be

No.	Structural type	Designation	Temperature of formation (K)	Peak temperature (K) for reaction with H_2	Ref.
1	Adsorbed, atomic (dispersed, surface carbide)	C_α	473–673	473	[127, 128]
2	Polymeric, amorphous films or filament	C_β	523–773	673	[127, 129, 130]
3	Vermicular (polymeric amorphous) a. filaments b. fibers c. whiskers	C_ν	573–1273	673–873	[127, 131–133]
4	Nickel carbide (bulk)	C_γ	423–523	548	[127]
5	Graphitic (crystalline) a. platelets b. films	C_C	773–823	823–1123	[127, 128, 131, 132, 134]

Table 5.
Forms and reactivity of carbon formed by decomposition of CO on Ni.
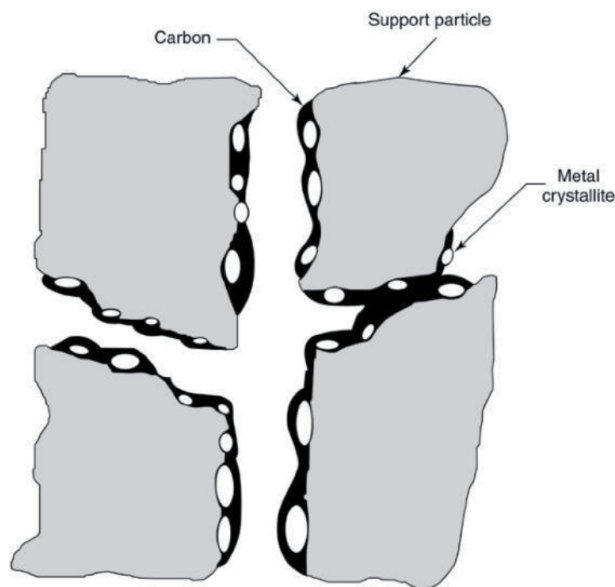
Figure 8.
Conceptual models of fouling, crystalline encapsulation and pore plugging of a supported metal catalyst (adapted from Ref [124]).

minimized. In their research, they discovered that a filamentous or whisker-like morphology was shown by the carbon deposit on Ni/γ-Al$_2$O$_3$. This finding is comparable to Kępiński et al. [136] reporting. Meanwhile, on a backed metal catalyst, Toebes et al. [137] recorded carbon formation with metal crystallites in addition to carbon filaments. The growth of carbon filaments has pushed the metal crystallites from the surface of the catalyst support.

Ito et al. [138] also proposed that CO_2 could reduce the impacts of the fouling system. While the increasing carbon filaments remove the Ni metal, the introduced CO_2 responds to CO through a reverse-Boudouard response with the carbon

whiskers. One of the findings of their study was that after the removal of the carbon whisker, there is a decrease in bulk Ni. This renders the catalyst to be inactive for carbon deposition. However, there is an increase in the reforming activity of CH_4, which is due to the newly exposed Ni active sites from the bulk Ni.

Cheng et al. [139] report a reduction in the Brunauer-Emmett-Teller (BET) surface area and the amount of pore used carbon catalyst. As a result of this phenomenon, catalyst activity is lost. Wagner et al. [140] noted that a vapor reforming catalyst's acidity is proportional to its coke formation tendency. They also asserted that using basic support or basic mixed oxide support named K, the coking strength of the reforming catalysts could be improved. Li et al. [141] and Zanganeh et al. [142] also endorsed this argument, whereby nickel catalyst deactivation can be weakened if the nickel is backed by a strong Lewis base oxide like MgO, CaO, SrO or BaO.

Subsequently, the present research project introduces DRM to investigate the level of resistance of the catalyst towards carbon formation. Zanganeh et al. [142] suggested that an increase in the CO_2/CH_4 ratio during DRM and increasing the temperature to a high level may minimize carbon formation thermodynamically.

Ito et al. [138] also agreed that the increased CO_2-to-CH_4 feed ratio would eliminate the CH_4 decomposition reaction. Koo et al. [143] found that introducing less than 1wt percent of Mg into the Ni catalyst would enhance their coking strength. Adding promoter like Mo could therefore allay the coke formation phenomenon on the Ni catalyst. Another proposal to reduce the carbon deposition of a catalyst with a small surface area is to reduce the Ni load of the assistance. A CO_2/CH_4 molar ratio of more than 3.0 should be used to prevent the boudouard reaction.

5. Conclusion

Throughout this work, it has been shown that biogas is a very interesting source of renewable energy. Because of its elevated CH_4 content, biogas has excellent potential, as reflected in its year-over-year rise in production. This is because its manufacturing promotes the use of organic waste, prevents uncontrolled dumping and minimizes atmospheric CH_4 and CO_2 emissions. In addition, its use as an energy source is in some cases an alternative to fossil fuels and can help to minimize energy dependence. Another aspect of interest is that it can be used insitu, allowing agro-livestock farms or small industrial plants to achieve energy self-sufficiency. A lot of studies on DRM over Ni-based catalysts has been carried out in latest decades to better comprehend the mechanism and techniques of response to improve carbon deposition resistance. Several methods were suggested to minimize the trend of Ni-based catalyst coke formation. One is the use of the appropriate catalyst preparation technique. Another is the use of metal oxides with strong Lewis basicity as supports or promoters (since Lewis acidity is identified to encourage coke buildup). Future study in this area is likely to focus on the use of catalysts based on bimetallic nickel, such as the incorporation of Co with Ni catalyst.

The bimetallic catalysts showed stable activity and elevated inactivation resistance, although carbon deposition occurs. Catalyst activity should be considered, as the primary reason for catalytic inactivation is the encapsulating carbon, which is deposited directly in the catalyst's active places instead of the carrier's surface. Also, when it is generated in large quantities, it can cause clogging of the reactor. The problem of carbon formation is exacerbated when biogas is used for this process, because the CH_4:CO_2 ratio of biogas is greater than that which can lead to the formation of large carbon deposits in a short time. However, carbon atoms are more essential in type and place than the quantity of carbon generated. Averting the

deposition of carbon is therefore a challenging task. Also, this problem can be addressed from a completely different perspective. Rather than trying to avert carbon formation, it can be promoted as carbon filamentous. Previously, many researchers have effectively accomplished the synthesis of carbon filamentous thru electric arc-discharge and laser ablation and chemical vapor deposition techniques. Nevertheless, the cost-efficient and the controlled synthesis of carbon filamentous with varies morphologies by those techniques has not been reported.

Given the broad range of applications and the growing demand for biogas in different areas, the superb characteristics of biogas indicate its growing potential as a source of syngas for a broad range of renewable energies, where high purity and low manufacturing costs are significant factors. Thus, producing high-purity syngas and the controlled production of value-added carbon filamentous over cheap, efficient, tunable and simply synthesized catalysts is very important and is the main interest in this subject.

Acknowledgements

Conflict of interest

The authors declare no conflict of interest.

Author details

Buthainah Ali Al-Timimi[1,2]* and Zahira Yaakob[1,2]

1 Faculty of Engineering and Built Environment, Chemical and Process Engineering Department, Universiti Kebangsaan Malaysia, UKM Bangi, Selangor, Malaysia

2 Faculty of Engineering and Built Environment, Research Center for Sustainable Process Technology (CESPRO), Universiti Kebangsaan Malaysia, UKM Bangi, Selangor, Malaysia

*Address all correspondence to: buthainahali@gmail.com

IntechOpen

References

[1] Tanksale A, Beltramini JN, Lu GM. A review of catalytic hydrogen production processes from biomass. Renewable and Sustainable Energy Reviews. 2010;**14**: 166-182

[2] Aguilera RF, Ripple RD. Using size distribution analysis to forecast natural gas resources in Asia Pacific. Applied Energy. 2011;**88**(12):4607-4620

[3] IEA. World Energy Outlook 2013. International Energy Agency; 2013. ISBN: 978-92-64-20130-9. Available from: https://www.iea.org/re ports/world-energy-outlook-2013

[4] Noor Z, Yusuf R, Abba A, Hassan M, Din M. An overview of energy recovery from municipal solid wastes (MSW) in Malaysia scenario. Renewable and Sustainable Energy Reviews. 2013;**20**: 378-384

[5] Talyan V, Dahiya RP, Anand S, Sreekrishnan TR. Quantification of methane emission from municipal solid waste disposal in Delhi. Resources, Conservation and Recycling. 2007; **50**(236):240-259

[6] Wuebbles DJ, Hayhoe K. Atmospheric methane and global change. Earth-Science Reviews. 2002;**57**: 177-210

[7] Yusuf R, Noor Z, Abba A, Hassan M, Din M. Methane emission by sectors: A comprehensive review of emission sources and mitigation methods. Renewable and Sustainable Energy Reviews. 2012;**16**:5059-5070

[8] EPA. Inventory of U.S. Greenhouse Gas Emissions and Sinks: 1990-2016. United States Environmental Protection Agency (EPA) EPA 430-R-18-003; 2016. Available from: https://www.epa. gov/ghgemissions/inventory-us-greenhouse-gas-emissions-and-sinks-1990-2016

[9] Raco B, Battaglini R, Lelli M. Gas emission into the atmosphere from controlled landfills: an example from Legoli landfill (Tuscany, Italy). Environmental Science and Pollution Research. 2010;**17**:1197-1206

[10] Lunsford JH. Catalytic conversion of methane to more useful chemicals and fuels: A challenge for the 21st century. Catalysis Today. 2000;**63**: 165-174

[11] Elvidge CD, Ziskin D, Baugh KE, Tuttle BT, Ghosh T, Pack DW, et al. A fifteen year record of global natural gas flaring derived from satellite data. Energies. 2009;**2**:595-622

[12] Yang N, Wang R. Sustainable technologies for the reclamation of greenhouse gas CO_2. Journal of Cleaner Production. 2015;**103**:784-792

[13] Fayaz F, Danh HT, Nguyen-huy C, Vu KB, Abdullah B. Promotional effect of Ce-dopant on Al_2O_3-supported Co catalysts for syngas production via CO_2 reforming of ethanol. Procedia Engineering. 2016;**148**:646-653

[14] Bian Z, Das S, Wai MH, Hongmanorom P, Kawi S. A review on bimetallic nickel-based catalysts for CO_2 reforming of methane. ChemPhysChem. 2017;**18**(22):3117-3134

[15] MayJi C, Eong PP, Ti TB, Seng CE, Ling CK. Biogas from palm oil mill effluent (POME): Opportunities and challenges from Malaysia's perspective. Renewable and Sustainable Energy Reviews Journal. 2013;**26**:717-726

[16] Abdelsalam E, Samer M, Attia YA, Abdel-Hadi MA, Hassan HE, Badr Y. Effects of Co and Ni nanoparticles on biogas and methane production from anaerobic digestion of slurry. Energy Conversion and Management. 2017;**141**: 108-119

[17] Chan YJ, Chong MF, Law CL. An integrated anaerobic-aerobic bioreactor (IAAB) for the treatment of palm oil mill effluent (POME): Start-up and steady state performance. Process Biochemistry. 2012;**47**(3):485-495

[18] WMO. Greenhouse Gas Bulletin 2015: The State of Greenhouse Gases in the Atmosphere Based on Global Observations through 2015. Vol. 12. World Meteorological Organization (WMO); 2016. pp. 1-8. Available from: https://public.wmo.int/en/resources/library/wmo-greenhouse-gas-bulletin

[19] Popa M, Vollmer M, Jordan A, Brand W, Pathirana S. Vehicle emissions of greenhouse gases and related tracers from a tunnel study: CO: CO_2, N_2O:CO_2, CH_4:CO_2, O_2:CO_2 ratios, and the stable isotopes ^{13}C and ^{18}O in CO_2 and CO. Atmospheric Chemistry and Physics. 2014;**14**:2105-2123

[20] Johari A, Ahmed S, Hashim H, Alkali H, Ramli M. Economic and environmental benefits of landfill gas from municipal solid waste in Malaysia. Renewable and Sustainable Energy Reviews. 2012;**16**:2907-2912

[21] Karavalakis G, Durbin TD, Villela M, Miller JW. Air pollutant emissions of light-duty vehicles operating on various natural gas compositions. Journal of Natural Gas Science and Engineering. 2012;**4**: 8-16

[22] Bahari MB, Phuc NHH, Abdullah B, Alenazey F, VO, D. V. N. Ethanol dry reforming for syngas production over Ce-promoted Ni/Al_2O_3 catalyst. Journal of Environmental Chemical Engineering. 2016;**4**(4):4830-4838

[23] Alirezaei I, Hafizi A, Rahimpour MR, Raeissi S. Application of zirconium modified Cu-based oxygen carrier in chemical looping reforming. Journal of CO_2 Utilization. 2016;**14**: 112-121

[24] Peña MA, Gdmez J, p., Fierro, J. L. G. New catalytic routes for syngas and hydrogen production. Applied Catalysis A: General. 1996;**144**:7-57

[25] Ullah Khan I, Hafiz Dzarfan Othman M, Hashim H, Matsuura T, Ismail AF, Rezaei-DashtArzhandi M, et al. Biogas as a renewable energy fuel—A review of biogas upgrading, utilisation and storage. Energy Conversion and Management. 2017;**150**:277-294

[26] Cai X, Hang Y. Advances in catalytic conversion of methane and carbon dioxide to highly valuable products. Energy Science & Engineering. 2019;**7**: 4-29

[27] Ali B, Payam A, Zahira Y, Ali NT, Wadhah N. Non-supported nickel-based coral sponge-like porous magnetic alloys for catalytic production of syngas and carbon bio-nanofilaments via a biogas decomposition approach. Nanomaterials. 2018;**8**(12):1053

[28] Tanios C, Bsaibes S, Labaki M, Cazier F, Billet S, Lucette H, et al. Syngas production by the CO_2 reforming of CH_4 over Ni-Co-Mg-Al catalysts obtained from hydrotalcite precursors. International Journal of Hydrogen Energy. 2017;**42**(17): 12818-12828

[29] Ray K, Sengupta S, Deo G. Reforming and cracking of CH_4 over Al_2O_3 supported Ni, Ni-Fe and Ni-Co catalysts. Fuel Processing Technology. 2017;**156**:195-203

[30] Daniel Torres JLP, I. S. Co-, Cu- and Fe-doped Ni/Al_2O_3 catalysts for the catalytic decomposition of methane into hydrogen and carbon nanofiber. Catalysis. 2018;**8**(300):1-15

[31] Chen L, Zhu Q, Wu R. Effect of Co-Ni ratio on the activity and stability of Co-Ni bimetallic aerogel catalyst for methane Oxy-CO_2 reforming.

International Journal of Hydrogen Energy. 2011;**36**(3):2128-2136

[32] Pudukudy M, Kadier A, Yaakob Z, Takriff MS. Non-oxidative thermocatalytic decomposition of methane into CO_x free hydrogen and nanocarbon over unsupported porous NiO and Fe_2O_3 catalysts. International Journal of Hydrogen Energy. 2016; **41**(41):18509-18521

[33] Pinilla JL, de Llobet S, Moliner R, Suelves I. H_2-rich gases production from catalytic decomposition of biogas: Viability of the process associated to the co-production of carbon nanofibers. International Journal of Hydrogen Energy. 2017;**42**(37):23484-23493

[34] Demirbas A. Biofuels sources, biofuel policy, biofuel economy and global biofuel projections. Energy Conversion and Management. 2008; **49**(8):2106-2116

[35] Gangadharan P, Kanchi KC, Lou HH. Evaluation of the economic and environmental impact of combining dry reforming with steam reforming of methane. Chemical Engineering Research and Design. 2012;**90**(11): 1956-1968

[36] Hasnan NSN, Timmiati SN, Lim KL, et al. Recent developments in methane decomposition over heterogeneous catalysts: An overview. Materials for Renewable and Sustainable Energy. 2020;**9**(8):1-8

[37] IEA. Net Zero by 2050 A Roadmap for the Global Energy Sector. International Energy Agency; 2021. ISBN: 978-92-64-20130-9. Available from: https://www.iea.org/reports/net-zero-by-2050

[38] Pang J, Zheng M, Sun R, Wang A, Wang X, Zhang T. Synthesis of ethylene glycol and terephthalic acid from biomass for producing PET. Green Chemistry. 2016;**18**:342-359

[39] Faizal M, Wardah YH, Husna M, Husna A, Amirah YHT A. Energy, economic and environmental impact of palm oil biodiesel in Malaysia. Journal of Mechanical Engineering Research and Developments. 2018;**41**(3):24-26

[40] Bradford M, Vannice M. CO_2 reforming of CH_4. Catalysis Reviews. 1999;**41**:1-42

[41] Li D, Nakagawa Y, Tomishige K. Methane reforming to synthesis gas over Ni catalysts modified with noble metals. Applied Catalysis A: General. 2011;**408**: 1-24

[42] Comparetti A, Febo P, Greco C, Orlando S. Current state and future of biogas and digestate production. Bulgarian Journal of Agricultural Science. 2013;**19**(1):1-14

[43] Goswami R, Chattopadhyay P, Shome A, Banerjee SN, Chakraborty AK, Mathew AK, et al. An overview of physico-chemical mechanisms of biogas production by microbial communities: A step towards sustainable waste management. 3Biotech. 2016;**6**(1):1-12

[44] Maulud AL, Saidi H. The Malaysian fifth fuel policy: Re-strategising the Malaysian renewable energy initiatives. Energy Policy. 2012;**48**:88-92

[45] Keim W. C1 chemistry: Potential and developments. Pure and Applied Chemistry. 1986;**58**(6):825-832

[46] Musamali R, Isa YM. Decomposition of methane to carbon and hydrogen: A catalytic perspective. Energy Technology. 2019;**7**(6):1-40

[47] Chen L, Qi Z, Zhang S, Ji S, Somorjai GA. Catalytic hydrogen production from methane: A review on recent progress and prospect. Catalysts. 2020;**10**(8):858

[48] Pudukudy M, Yaakob Z, Takriff MS. Methane decomposition

over unsupported mesoporous nickel ferrites: Effect of reaction temperature on the catalytic activity and properties of the produced nanocarbon. RSC Advances. 2016;**6**(72):68081-68091

[49] Pudukudy M, Yaakob Z, Takriff MS. Methane decomposition into CO_x free hydrogen and multiwalled carbon nanotubes over ceria, zirconia and lanthana supported nickel catalysts prepared via a facile solid state citrate fusion method. Energy Conversion and Management. 2016;**126**(October):302-315

[50] Rastegarpanah A, Rezaei M, Meshkani F, Zhang K, Zhao X, Pei W, et al. Mesoporous Ni/MeO_x (Me = Al, Mg, Ti, and Si): Highly efficient catalysts in the decomposition of methane for hydrogen production. Applied Surface Science. 2019;**478**(11): 581-593

[51] De Llobet S, Pinilla JL, Moliner R, Suelves I. Relationship between carbon morphology and catalyst deactivation in the catalytic decomposition of biogas using Ni, Co and Fe based catalysts. Fuel. 2015;**139**:71-78

[52] Nagayasu Y, Asai K, Nakayama A, Iwamoto S, Yagasaki E, Inoue M. Effect of carbon co-feed on decomposition of methane over Ni catalysts. Journal of Japan Petroleum Institute. 2006;**49**: 186-193

[53] Asai K, Takane K, Nagayasu Y, Iwamoto S, Yagasaki E, Inoue M. Decomposition of methane in the presence of carbon dioxide over Ni catalysts. Chemical Engineering Science. 2008;**63**:5083-5088

[54] Nikoo MK, Amin NAS. Thermodynamic analysis of carbon dioxide reforming of methane in view of solid carbon formation. Fuel Processing Technology. 2011;**92**(3):678-691

[55] Mohamedali M, Henni A, Ibrahim H. Recent advances in supported metal catalysts for syngas production from methane. ChemEngineering. 2018;**2**(9):1-25

[56] De Llobet S, Pinilla JL, Lazaro MJ, Moliner R, Suelves I. CH_4 and CO_2 partial pressures influence and deactivation study on the catalytic decomposition of biogas over a Ni catalyst. Fuel. 2013;**111**:778-783

[57] Edwards JH, Maitra AM. The chemistry of methane reforming with carbon dioxide and its current and potential applications. Fuel Processing Technology. 1995;**42**(2–3):269-289

[58] Izquierdo U, García-García I, Gutierrez Á, Arraibi J, Barrio V, Cambra J, et al. Catalyst deactivation and regeneration processes in biogas tri-reforming process. The effect of hydrogen sulfide addition. Catalysts. 2018;**8**(12):1-19

[59] Dębek R, Motak M, Galvez ME, Da Costa P, Grzybek T. Catalytic activity of hydrotalcite-derived catalysts in the dry reforming of methane: On the effect of Ce promotion and feed gas composition. Reaction Kinetics, Mechanisms and Catalysis. 2017;**121**(1): 185-208

[60] Muradov N, Smith F. Thermocatalytic conversion of landfill gas and biogas to alternative transportation fuels. Energy & Fuels. 2008;**22**:2053-2060

[61] De Llobet S, Pinilla JL, Lázaro MJ, Moliner R, Suelves I. Catalytic decomposition of biogas to produce H_2-rich fuel gas and carbon nanofibers. Parametric study and characterization. International Journal of Hydrogen Energy. 2012;**37**(8):7067-7076

[62] Piumetti M, Fino D, Russo N. Photocatalytic reduction of CO_2 into fuels: A short review. Journal of Advanced Catalysis Science and Technology. 2014;**1**(2):16-25

[63] Freund H-J, Roberts MW. Surface chemistry of carbon dioxide. Surface Science Reports. 1996;**25**(8):225-273

[64] York A, Xiao T, Green M, Claridge J. Methane oxyforming for synthesis gas production. Catalysis Reviews. 2007;**49**:511-560

[65] Roddy D. A syngas network for reducing industrial carbon footprint and energy use. Applied Thermal Engineering. 2013;**53**:299-304

[66] Markets and Markets. Syngas Market and Derivatives (Methanol, Ammonia, Hydrogen, Oxo Chemicals, N-Butanol, DME) Market, by End Use Application, Feedstock, Technology, and Gasifier Type-Global Trends & Forecast to 2018 (online). Top Market Reports. CH 2043; 2013

[67] Boerrigter H, Rauch R. Review of applications of gases from biomass gasification. Energy Research Centre of the Netherlands 2006;**ECN-RX-06**:1-31

[68] Subramani V, Sharma P, Zhang L, Liu K. Catalytic Steam Reforming Technology for the Production of Hydrogen and Syngas. Hydrogen and Syngas Production and Purification Technologies. New Jersey: John Wiley & Sons, Inc.; 2010

[69] Walker PL. Carbon: An old but new material revisited. Carbon. 1990;**28**(2–3):261-279

[70] Nolan PE, Lynch DC, Cutler AH. Graphite encapsulation of catalytic metal nanoparticles. Carbon. 1996;**34**(6):817-819

[71] Xie J, Chen Q, Shen H, Li G. Review—Wearable graphene devices for sensing. Journal of the Electrochemical Society. 2020;**167**(3):037541

[72] Franklin RE. The structure of graphitic carbons. Acta Crystallographica. 1951;**4**(3):253-261

[73] Goldmann E, Górski M, Klemczak B. Recent advancements in carbon nano-infused cementitious composites. Materials. 2021;**14**(18):5176

[74] Ros TG, Van Dillen AJ, Geus JW, Koningsberger DC. Surface structure of untreated parallel and fishbone carbon nanofibres: An infrared study. ChemPhysChem. 2002;**3**(2):209-214

[75] Alstrup I, Tavares MT, Bernardo CA, Sørensen O, Rostrup-Nielsen JR. Carbon formation on nickel and nickel-copper alloy catalysts. Materials and Corrosion - Werkstoffe und Korrosion. 1998;**49**(5):367-372

[76] Nolan PE, Schabel MJ, Lynch DC, Cutler AH. Hydrogen control of carbon deposit morphology. Carbon. 1995;**33**(1):79-85

[77] Allaedini G, Aminayi P, Tasirin SM. The effect of alumina and magnesia supported germanium nanoparticles on the growth of carbon nanotubes in the chemical vapor deposition method. Journal of Nanomaterials. 2015;**2015**:1-6

[78] Ali B, Biak DRA, Sapuan SM, Zaidan AW, Aluuami W, Yusoff HM, et al. Preparation of carbon nanotubes via chemical technique (modified Staudenmaier method). Nanoscience &Nanotechnology-Asia. 2017;**7**(1):113-122

[79] Allaedini G, Tasirin SM, Aminayi P. Yield optimization of nanocarbons prepared via chemical vapor decomposition of carbon dioxide using response surface methodology. Diamond and Related Materials. 2016;**66**:196-205

[80] Oyama ST, Hacarlioglu P, Gu Y, Lee D. Dry reforming of methane has no future for hydrogen production: Comparison with steam reforming at high pressure in standard and membrane reactors. International Journal of Hydrogen Energy. 2012;**37**(13):10444-10450

[81] Carvalho L, Martins A, Reyes P, Oportus M, Albonoz A, Vicentini V, et al. Preparation and characterization of Ru/MgO-Al$_2$O$_3$ catalysts for methane steam reforming. Catalysis Today. 2009;**142**:52-60

[82] Larimi AS, Alavi SM. Ceria-zirconia supported Ni catalysts for partial oxidation of methane to synthesis gas. Fuel. 2012;**102**:366-371

[83] Ruckenstein E, Hang Hu Y. Methane partial oxidation over NiO/MgO solid solution catalysts. Applied Catalysis A: General. 1999;**183**:85-92

[84] Selvarajah K, Phuc NHH, Abdullah B, Alenazey F, VODVN. Syngas production from methane dry reforming over Ni/Al$_2$O$_3$ catalyst. Research on Chemical Intermediates. 2016;**42**(1):269-288

[85] Abdullah B, Abd Ghani NA, Vo D-VN. Recent advances in dry reforming of methane over Ni-based catalysts. Journal of Cleaner Production. 2017;**162**:170-185

[86] Gaddalla A, Sommer M. Carbon dioxide reforming of methane on nickel catalysts. Chemical Engineering Science. 1989;**44**:2825-2829

[87] Al-Doghachi FAJ, Rashid U, Taufiq-Yap YH. Investigation of Ce(III) promoter effects on the tri-metallic Pt, Pd, Ni/MgO catalyst in dry-reforming of methane. RSC Advances. 2016;**6**(13):10372-10384

[88] Pinilla JL, de Llobet S, Suelves I, Utrilla R, Lázaro MJ, Moliner R. Catalytic decomposition of methane and methane/CO$_2$ mixtures to produce synthesis gas and nanostructured carbonaceous material. Fuel. 2011;**90**(6):2245-2253

[89] Wang HY, Lua AC. Deactivation and kinetic studies of unsupported Ni and Ni-Co-Cu alloy catalysts used for hydrogen production by methane decomposition. Chemical Engineering Journal. 2014;**243**:79-91

[90] Aldana PAU, Ocampo F, Kobl K, Louis B, Thibault-Starzyk F, Daturi M, et al. Catalytic CO$_2$ valorization into CH$_4$ on Ni-based ceria-zirconia. Reaction mechanism by operando IR spectroscopy. Catalysis Today. 2013;**215**:201-207

[91] Pan Q, Peng J, Sun T, Wang S, Wang S. Insight into the reaction route of CO$_2$ methanation: promotion effect of medium basic sites. Catalysis Communication. 2014;**45**:74-78

[92] Ayodele BV, Khan MR, Nooruddin SS, Cheng CK. Modelling and optimization of syngas production by methane dry reforming over samarium oxide supported cobalt catalyst: Response surface methodology and artificial neural networks approach. Clean Technologies and Environmental Policy. 2017;**19**(4):1181-1193

[93] Kathiraser Y, Oemar U, Saw ET, Li Z, Kawi S. Kinetic and mechanistic aspects for CO$_2$ reforming of methane over Ni based catalysts. Chemical Engineering Journal. 2015;**278**:62-78

[94] Nagaoka K, Seshan K, Aika K, Lercher J. Carbon deposition during carbon dioxide reforming of methane—Comparison between Pt/Al$_2$O$_3$ and Pt/ZrO$_2$. Journal of Catalysis. 2000;**197**:34-42

[95] Abreu CAM, Santos DA, Pacífico JA, Lima Filho NM. Kinetic evaluation of methane_carbon dioxide reforming process based on the reaction steps. Industrial and Engineering Chemistry Research. 2008;**47**(14):4617-4622

[96] Wei J, Iglesia E. Isotopic and kinetic assessment of the mechanism of reactions of CH$_4$ with CO$_2$ or H$_2$O to form synthesis gas and carbon on nickel catalysts. Journal of Catalysis. 2004;**224**(2):370-383

[97] Guo J, Lou H, Zhao H, Chai D, Zheng X. Dry reforming of methane over nickel catalysts supported on magnesium aluminate spinels. Applied Catalysis A: General. 2004;**273**:75-82

[98] Pechimuthu NA, Pant KK, Dhingra SC, Bhalla R. Characterization and activity of K, CeO_2, and Mn promoted Ni/Al_2O_3 catalysts for carbon dioxide reforming of methane. Industrial and Engineering Chemistry Research. 2006;**45**(22):7435-7443

[99] Ozkara-Aydınoğlu S, Erhan Aksoylu A. A comparative study on the kinetics of carbon dioxide reforming of methane over $Pt-Ni/Al_2O_3$ catalyst: Effect of Pt/ Ni ratio. Chemical Engineering Journal. 2013;**215-216**: 542-549

[100] Cui Y, Zhang H, Xu H, Li W. Kinetic study of the catalytic reforming of CH_4 with CO_2 to syngas over Ni/α-Al_2O_3 catalyst: The effect of temperature on the reforming mechanism. Applied Catalysis A: General. 2007;**318**:79-88

[101] Kim J-W, Ha J-A, Jung H, Ahn B II, Lee S-H, Choi J-G. Kinetic analysis of supported Ni-catalyzed CO_2/CH_4 reactions using photoacoustic spectroscopy. Physical Chemistry Chemical Physics. 2007;**9**(43):5828-5833

[102] Braga RM, Rodrigues G. Nickel catalyst supported on magnesium and zinc aluminates ($MgAl_2O_4$ and $ZnAl_2O_4$) spinels for dry reforming of methane. Ceramica. 2017;**63**:77-81

[103] Meshkani F, Golesorkh SF, Rezaei M, Andache M. Nickel catalyst supported on mesoporous $MgAl_2O_4$ nanopowders synthesized via a homogenous precipitation method for dry reforming reaction. Research on Chemical Intermediates. 2017;**43**(1):545-559

[104] Kehres J, Jakobsen J, Andreasen J, Wagner J, Liu H. Dynamical properties of a $Ru/MgAl_2O_4$ catalyst during reduction and dry methane reforming. The Journal of Physical Chemistry C. 2012;**116**:21407-21415

[105] Rategarpanah A, Meshkani F, Wang Y, Arandiyan H, Rezaei M. Thermocatalytic conversion of methane to highly pure hydrogen over Ni–Cu/ $MgO·Al_2O_3$ catalysts: Influence of noble metals (Pt and Pd) on the catalytic activity and stability. Energy Conversion and Management. 2018; **166**(11):268-280

[106] Ocsachoque M, Pompeo F, Gonzalez G. Rh–Ni/CeO_2-Al_2O_3 catalysts for methane dry reforming. Catalysis Today. 2011;**172**:226-231

[107] Zeng YX, Wang L, Wu CF, Wang JQ, Shen BX, Tu X. Low temperature reforming of biogas over K-,Mg- and Ce-promoted Ni/Al_2O_3 catalysts for the production of hydrogen rich syngas: Understanding the plasma-catalytic synergy. Applied Catalysis B: Environmental. 2018;**224**(June): 469-478

[108] Chen J, Wu Q, Zhang J, Zhang J. Effect of preparation methods on structure and performance of Ni/ $Ce_{0.75}Zr_{0.25}O_2$ catalysts for CH_4-CO_2 reforming. Fuel. 2008;**87**:2901-2907

[109] Zhang Q, Wu T, Zhang P, Huang R, Song X, Gao L. Facile synthesis of hollow hierarchical Ni/γ-Al_2O_3 nanocomposites for methane dry reforming catalysis. RSC Advances. 2015;**4**:51184-51193

[110] Abatzoglou N, Fauteux-Lefebvre C. Review of catalytic syngas production through steam or dry reforming and partial oxidation of study liquid compounds. Wiley Interdisciplinary: Energy and Environment. 2015;**12**: 225-273

[111] Abimanyu H, Kim C, Ahn B, Yoo K. Synthesis of dimethyl carbonate by

trans esterification with various MgO-CeO$_2$ mixed oxide catalysts. Catalysis Letters. 2007;**118**:30-35

[112] Jang W, Jeong D, Shim J, Roh H, Son I, Lee S. H$_2$ and CO production over a stable Ni-MgO-Ce$_{0.8}$Zr$_{0.2}$O$_2$ catalyst from CO$_2$ reforming of CH$_4$. International Journal of Hydrogen Energy. 2013;**38**:4508-4512

[113] Hua W, Jin L, He X, Liu J, Hu H. Preparation of Ni/MgO catalyst for CO$_2$ reforming of methane by dielectric-barrier discharge plasma. Catalysis Communications. 2010;**11**:968-972

[114] Zhang J, Wang H, Dalai AK. Development of stable bimetallic catalysts for carbon dioxide reforming of methane. Journal of Catalysis. 2007;**249**(2):300-310

[115] Dębek R, Motak M, Galvez-parruca ME, Grzybek T, Costa D, Pieńkowski L. Ceria promotion over Ni-containing hydrotalcite-derived catalysts for CO$_2$ methane reforming Radosław. Energy and Fuels. 2017;**2039**(14):1-10

[116] Vallezi A, Lino P, Moreira E, José A, Assaf M. NiMgAlCe catalysts applied to reforming of a model biogas for syngas production. Catalysis Letters. 2018;**1**(1):1-13

[117] Shin SA, Alizadeh Eslami A, Noh YS, Song H-T, Kim HD, Ghaffari Saeidabad N, et al. Preparation and characterization of Ni/ZrTiAlO$_x$ catalyst via sol-gel and impregnation methods for low temperature dry reforming of methane. Catalysts. 2020;**10**:13-35

[118] Ibrahim AA, Al-Fatesh AS, Kumar NS, Abasaeed AE, Kasim SO, Fakeeha AH. Dry reforming of methane using Ce-modified Ni supported on 8% PO$_4$ + ZrO$_2$ catalysts. Catalysts. 2020;**10**(2):242

[119] Han B, Zhong J, Li W, Zhang Z, Bi G, Xie J. The promotional role of β-cyclodextrin on Ni-Mo$_2$C/MgO catalyst for biogas reforming. Molecular Catalysis. 2021;**515**:111897

[120] Wang Y, Wang Y, Li L, Cui C, Liu X, Da P, et al. Syngas production via CO$_2$ reforming of methane over aluminum-promoted NiO–10Al$_2$O$_3$–ZrO$_2$ catalyst. ACS Omega. 2021;**6**(34):22383-22394

[121] Yusuf M, Farooqi AS, Alam MA, Keong LK, Hellgardt K, Abdullah B. Response surface optimization of syngas production from greenhouse gases via DRM over high performance Ni–W catalyst. International Journal of Hydrogen Energy. 2021;**6**:1-14

[122] Bartholomew C, Farrauto R. Fundamentals of Industrial Catalytic Processes. New Jersey: John Wiley & Sons, Inc; 2011

[123] Christensen K, Chen D, Lodeng R, Holmen A. Effect of supports and Ni crystal size on carbon formation and sintering during steam methane reforming. Applied Catalysis A: General. 2006;**314**:9-22

[124] Argyle MD, Bartholomew CH. Heterogeneous catalyst deactivation and regeneration: A review. Catalysts. 2015;**5**(1):145-269

[125] Lif J, Skoglundh M. Stabilising alumina supported nickel particles against sintering in ammonia/hydrogen atmosphere. Applied Catalysis A: General. 2004;**274**:61-69

[126] Chen X, Yik E, Butler J, Schwank J. Gasification characteristics of carbon species derived from model reforming compound over Ni/Ce-Zr-O catalysts. Catalysis Today. 2014;**233**:14-20

[127] McCarty JG, Wise H. Hydrogenation of surface carbon on alumina-supported nickel. Journal of Catalysis. 1979;**57**(3):406-416

[128] Goodman DW, Kelley RD, Madey TE, Yates JT. Kinetics of the hydrogenation of CO over a single crystal nickel catalyst. Journal of Catalysis. 1980;**63**(1):226-234

[129] Pedersen K, Allan Skov JR, Rostrup-Nielsen. Catalytic aspects of high-temperature methanation. Preprints of Papers—American Chemical Society, Division of Fuel Chemistry. 1979;**25**(2):89

[130] Erekson EJ, Sughrue EL, Bartholomew CH. Catalyst degradation in high temperature methanation. Fuel Processing Technology. 1981;**5**(1–2): 91-101

[131] Rostrup-Nielsen J, Trimm DL. Mechanisms of carbon formation on nickel-containing catalysts. Journal of Catalysis. 1977;**48**(1–3):155-165

[132] Trimm DL. The formation and removal of coke from nickel catalyst. Catalysis Reviews. 1977;**16**(1):155-189

[133] Baker RTK. Catalytic growth of carbon filaments. Carbon. 1989;**27**(3): 315-323

[134] Baker RTK, Barber MA, Harris PS, Feates FS, Waite RJ. Nucleation and growth of carbon deposits from the nickel catalyzed decomposition of acetylene. Journal of Catalysis. 1972; **26**(1):51-62

[135] Quincoces C, Basaldella E, De Vargas S, Gonzalez M. Ni/γ-Al$_2$O$_3$ catalyst from kaolinite for the dry reforming of methane. Materials Letters. 2004;**58**:272-275

[136] Kępiński L, Stasińska B, Boro T. Carbon deposition on Ni/Al$_2$O$_3$ catalysts doped with small amounts of molybdenum. Carbon. 2000;**38**: 1845-1856

[137] Toebes M, Bitter J, de Jong K. Impact of the structure and reactivity of

nickel particles on the catalytic growth of carbon nanofibers. Catalysis Today. 2002;**76**:33-42

[138] Ito M, Tagawa T, Goto S. Suppression of carbonaceous depositions on nickel catalyst for the carbon dioxide reforming of methane. Applied Catalysis A: General. 1999;**177**: 15-23

[139] Cheng C, Foo S, Adesina A. Carbon deposition on bimetallic Co-Ni/Al$_2$O$_3$ catalyst during steam reforming of glycerol. Catalysis Today. 2011;**164**: 268-274

[140] Wagner A, Osborne R, Wagner J. Prediction of deactivation rates and mechanisms of reforming catalysts. Preprints of Papers-American Chemical Society, Division of Fuel Chemistry. 2003;**48**:748-749

[141] Li X, Hu Q, Yang Y, Wang Y, He F. Studies on stability and coking resistance of Ni/BaTiO$_3$-Al$_2$O$_3$ catalysts for lower temperature dry reforming of methane (LTDRM). Applied Catalysis A: General. 2012;**413-414**:163-169

[142] Zanganeh R, Rezaei M, Zamaniyan A. Dry reforming of methane to synthesis gas on NiO-MgO nanocrystalline solid solution catalysts. International Journal of Hydrogen Energy. 2013;**38**:3012-3018

[143] Koo K, Roh H, Seo Y, Yoon W, Park S. Coke study on MgO-promoted Ni/Al$_2$O$_3$ catalyst in combined H$_2$O and CO$_2$ reforming of methane for gas to liquid (GTL) process. Applied Catalysis A: General. 2008;**340**:183-190

Chapter 11

Storage of Natural Gas by CNTs

Mohsen Askaryan

Abstract

Carbon nanotubes (CNTs) have gained considerable attention over the past decade as up-to-date materials for storing renewable energy. The properties of CNTs, e.g., exceptionally high surface area, thermal conductivity, and electron mobility can be advantageous for applications toward energy storage. Conventional methods in natural gas storage include liquefaction (LNG) and compression (CNG) in the compression range of $2 \times 10^4 - 3 \times 10^4$ kPa in steel cylinders. But nanotubes carbon (CNT), which includes two models, is used for higher pressures (about 4×10^4 kPa). Single-walled carbon nanotubes (SWCNTs) and multiwalled carbon nanotubes (MWCNTs) are the two models in which the gas storage mechanism is superficial. Studies have also shown that the capacity of MWCNT to store natural gas can be enhanced by treating the nanotubes with acid. In the case of CO_2, however, positive CNT charging always enhances the adsorption while negative CNT charging always suppresses it. By doubling the nanotube diameter, the amount of the gas adsorption capacity increased by 45%.

Keywords: multiwalled carbon nanotube, single-walled carbon nanotubes, natural gas, adsorption, nanotechnology

1. Introduction

Natural gas is one of the cleanest and most useful forms of energy, with almost 90% of it being methane. In addition, natural gas contains a small amount of gases, such as ethane, propane, hydrogen, helium, carbon dioxide, nitrogen, hydrogen sulfide, and water vapor. The composition of natural gas varies depending on exploration wells and seasons. Due to the dissimilar distribution pattern of natural gas fields in the world and the increase in its use as a fuel, its transmission and storage are highly important [1]. The vast potential application of nanotechnology has propelled numerous research studies in various fields including the oil and gas sector. There are several challenges in the oil and gas industry that nanotechnology could address if articulately harnessed through research, and one of such challenges is natural gas storage and transportation. Several types of porous media for gas storage have been proposed, developed, and studied, and these include molecular sieve, activated carbon, zeolite, and carbon nanotubes (CNTs) [2]. Since the discovery of CNTs in the 1990s, they have been studied and used as adsorbents for various natural gases, alkanes, and noble gases. Due to the tubular shape, uneven structure with well-defined adsorption strategies and their exceptional specific surface area (up to 1550 m^2/g), carbon nanotubes are a better candidate for natural gas storage and separation especially compared with other porous adsorbents in the industry materials such as carbon and zeolite [3]. In general, the nanostructures

with high surface-to-volume ratio envisage a diversity of applications against the bulk materials. Particularly, one-dimensional carbon nanotubes (CNTs) exhibit the interesting features in nanotechnolo [4]. Research has shown that carbon nanotube (CNT), products of nanotechnology have the capacity to store natural gas through a comparatively cheap and efficient method, though investigations are still ongoing in solving the challenges facing this method. This chapter is thus aimed at reviewing the prospects of storing and transporting natural gas in CNT, and it highlights some factors that can enhance the gas storing capacity of methane in nanotubes [2].

2. Methods of gas storage

Natural gas storage and transport methods include underground gas storage (UGS) and adsorbed natural gas (ANG) [1]. Compression (compressed natural gas – CNG) and liquefaction (liquefied natural gas – LNG), but these methods are complex and expensive. In compression, the gas is stored as a supercritical fluid at room temperature but at high pressures of about $2 \times 10^4 – 3 \times 10^4$ kPa, reaching a density that is about 230 times higher (230 v/v) than the density of natural gas at standard temperature and pressure (STP) conditions [2]. In this case, the energy density is approximately 25% of that of gasoline. The disadvantages associated with this storage method include the risk of carrying highly pressurized tank in transit, high energy requirement for raising the pressure to $2 \times 10^4 – 3 \times 10^4$ kPa, the costs associated with acquiring the heavy thick-walled steel cylinders that can withstand such pressure, safety valves requirements, and the cost of transporting these heavy cylinders containing highly pressurized gas [2]. In the liquefied natural gas storage method, the gas is stored at a temperature of 112 K in a tank with a pressure of 1×10^3 kPa, in which case the gas has 72% of the total energy density of gasoline. Natural gas can be stored in CNTs, which are lightweight containers stuffed in a pressure vessel of about $2 \times 10^4 – 4 \times 10^4$ kPa. This method reduces cost; it reduces the risks associated with other storage methods and is a possible alternative for large-scale transportation of natural gas. A comparison between the natural gas storing capacity of CNT and CNG has shown that although CNT stores less amount of natural gas, it however does this at 83% storage pressure lower than CNG, which is a huge advantage that can be exploited to efficiently and economically store and transport natural gas [2]. Due to the problems of CNG, adsorbed natural gas (ANG) storage was introduced as a good alternative to CNG. In the ANG process, gas storage is done at a lower pressure than CNG. To be used on cheaper ships, work safety must be increased. Natural gas is absorbed through the embedded pores of the adsorbents. This adsorption process is performed at room temperature. The adsorption that an adsorbent performs depends primarily on the properties of the adsorbent. Materials that can be used to adsorb natural gas include highly porous materials such as activated carbon, zeolite, silica gel, activated alumina, carbon nanotubes, and a variety of material artificial adsorbents [1]. Activated carbon is usually used in ANG vessels. The maximum capacity of gas storage of activated carbon at 1500 psi and 298 K is reported to be 160 v/v, which compared with CNG has a lower storage volume. The amount of the pure methane adsorbed is more than when natural gas is used [1]. Studies show that under the same conditions, adsorption on carbon nanotubes is often greater than adsorption on activated carbon. It is also agreed that the nanoparticles used in nanotubes are the best option for absorbing and storing natural gas [1]. As already mentioned, the efficiency of ANG is lower than that of CNG. To solve this problem, natural gas storage can be considered in nanostructures. Another disadvantage of the adsorption process on

activated carbon, which has made these materials less popular, is their isothermal heat. Adsorption is a thermal phenomenon, and the high conductivity of activated carbon makes it act as an insulating material. Researchers try to use nanoscale adsorbents to adsorb more gas [1].

3. Natural gas as a clean energy source

Natural gas is a homogeneous mixture, having variable proportions of hydrocarbons. The general composition of natural gas includes methane (CH_4) constituting the major part, and it generally ranges from 55 to 98% in volume, ethane (C_2H_6), propane (C_3H_8), and other heavy constituents. There is a growing interest in the use of natural gases as an alternative source of energy especially because it is clean. Its thermal efficiency is higher than that of other fuels, and it produces mainly CO_2 and water vapor. The emissions of CO_2 are 25–30% lower than that generated from fuel-oil and 40–50% lower than coal per unit of produced energy [2]. As regards its use as a fuel, natural gas has many advantages. These include reduction in post combustion contaminants, reduction in maintenance costs compared with other fuels, reduction in suspended solid particles, which are associated with combustion of gasoline, absence of sulfur and sulfur dioxide (SO_2) emissions, which are typical contaminants from transportation vehicles. Compared with liquid fuels, the emissions from natural gas vehicle combustion are 76% less in carbon monoxide, 75% less in nitrogen compounds, 88% less in hydrocarbons, and 30% less in carbon dioxide [2]. Furthermore, the physiochemical properties of natural gas enable the use of catalysts for the combustion of gases, obtaining excellent results and minimizing emissions. In spite of the numerous advantages associated with the use of natural gas as a fuel over other forms of hydrocarbon fuels, its efficiency and economics in storage and transportation have constituted a major barrier to its usage. This could be attributed to its low energy density (heat of combustion/ volume) at standard temperature and pressure conditions [2].

4. Types and characteristics of carbon nanotubes (CNTs)

Elemental carbon in sp^2 hybridization can form a variety of amazing structures, such as graphite, graphene, CNTs, and fullerene [5]. Carbon nanotubes are allotropes of carbon with a concentric cylindrical shape of diameter in the order of nanometer and length of micrometer [2]. In particular, CNTs with very high length-to-diameter ratios (~132,000,000:1) have been constructed [6]. The carbon network of the shells is closely related to the honeycomb arrangement of the carbon atoms in the graphite sheets [5]. The structural shape of SWNTs is a tube several nanometers in diameter and several microns in length. They are also made of perforated graphene sheets. They are placed in one direction and next to each other to form the pipes. A MWNT is an arrangement of several to tens of hundreds of concentric tubes of graphite plates with adjacent ~0.34 nm shells separated (**Figure 1**) [5].

They are tubular cylinders of carbon atoms with extraordinary mechanical, electrical, thermal, optical, and chemical properties. CNTs were first discovered by Iijima in 1991; however, the first microscopic production of CNT was made by two researchers at Nippon Electric company limited fundamental research laboratory, and since then, there have been several developments of CNT [2]. Carbon nanotubes can be classified into chair-shaped and zigzag (**Figure 2**). Among them,
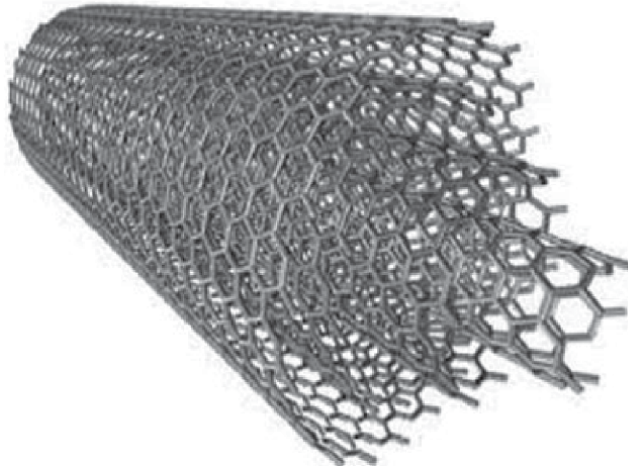
Figure 1.
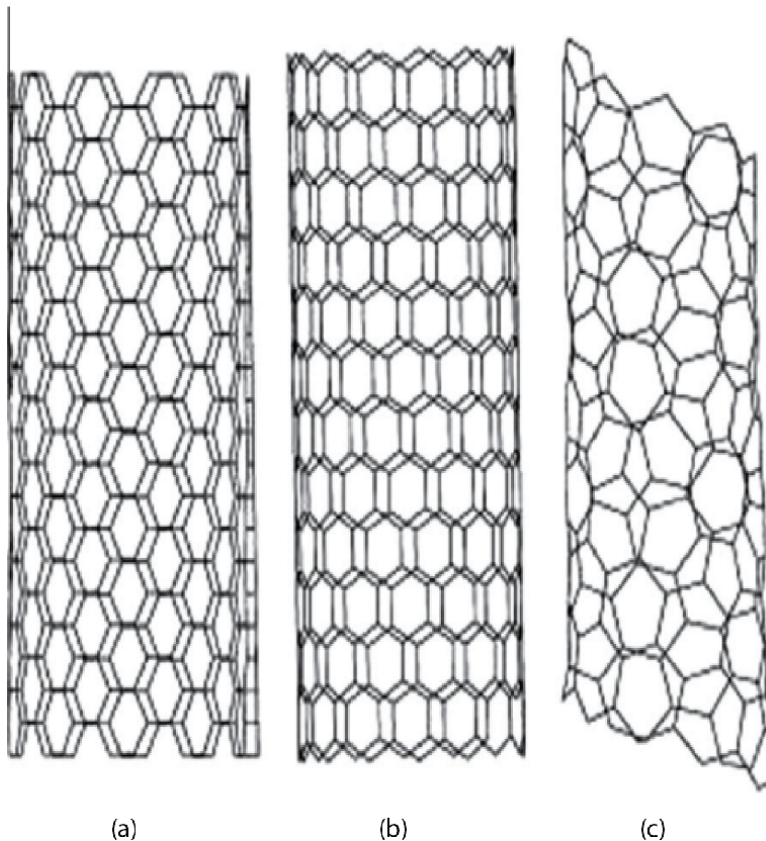*Scheme of MWNT [5].*

(a)   (b)   (c)

Figure 2.
Scheme of different SWNTs: armchair (a); zigzag (b); and chiral (c) [5].

only nanotubes have metal sex seats, chiral semiconductor tubes and zigzag tubes have 1–3 narrow slits and 2–3 large slits, respectively [5].

Methods of producing CNTs include arc evacuation, chemical vapor deposition (CVD), laser ablation, electrolysis, pyrolysis, flame synthesis, electron or ion beam

irradiation, and solar approaches. Laser abrasion and arc discharge are common methods for producing CNTs from carbon vapor. Carbon nanotubes made by these two methods can maintain good quality with less structural defects due to the presence of impurities in their constituents. In both methods, the growth process is performed at high temperatures, and re-firing properly ensures that the defects in the shape of the tubular graphene are reduced. In these techniques, it is difficult to control growth on patterned substrates at a reasonable rate. It should be noted that these production methods are expensive due to the need for high temperatures. To solve such problems, CVD production methods have been considered and used to allow the growth of various CNT structures. CVD seems to be a practical process due to its low required temperature range ($\sim$500–1200 °C). In addition, because CVD provides better control over the diameter, length, and number of CNT walls, their application can be extended to nanoelectronics, field diffusion, and more. However, researchers continue to emphasize the development of more efficient, cost-effective, and environmentally friendly alternatives to large-scale CNTs. Recycling waste or disposable materials into higher-value products (such as ceramics and steel) has encouraged researchers to synthesize CNTs from waste sources for a variety of applications. The use of waste as a source for the synthesis of carbon nanotubes can simultaneously reduce solid waste and construction costs [6]. But the most popular and most widely used method of synthesis is the chemical vapor deposition method [2]. Today, many advances have been made to obtain carbon materials with very fine porous pores that have very high adsorption properties for most gases. Pores at the molecular scale can absorb large amounts of gas, the adsorption potential of porous walls increases the density of the adsorbed material inside the pores. The major advantage of CNTs is related to the fact that the carbon structure is practically known. This aspect has permitted the correlation of experimental data with theoretical predictions [5]. Since the discovery of CNTs to date, scientists have made great efforts to design, synthesize, and characterize CNT layouts, including single-walled, double-walled, and multiwalled CNTs (SWCNTs, DWCNTs, and MWCNTs). Due to the strong van der Waals (VDW) forces between the carbon atoms of adjacent pipes, CNTs tend to form in stable molds on their own. This geometric shape creates different adsorption sites that differ in the amount of energy required to absorb the gas. Most scientists agree that the so-called groove area (g) between the two CNTs is the best absorption region (see **Figure 3**). The best CNT geometry for maximum adsorption depends strongly on the applied pressure. Thus it can happen that the adsorption strength does not change monotonically as a function of the nanotube diameter D and the inter-tube distanced [7].

Undoubtedly, yeast fermentation plays a critical role in the formation of CNTs. Therefore, an in-depth understanding of the CNT formation mechanism is required [8]. Molecular surface engineering is based on the construction of CNTs through the chemical route. This is related to the adjustable structure of CNTs, for example, crystallinity, number of walls, cavities, and length with the help of variables such as proper growth control, use of suitable catalysts and carbon sources. The cost of manufacturing CNTs can be easily calculated with the help of the selected chemical route and process control [6]. There are two types of carbon nanotube based on the number of layers or walls: the single-wall carbon nanotubes (SWCNTs) and the multi-wall carbon nanotubes (MWCNTs). The SWCNT can be described as a graphene sheet rolled into single cylindrical shape so that the structure is one-dimensional with axial symmetry. Most SWCNTs typically have diameters in the range of 1–1.3 nm and a few micrometers long. SWNT can be formed in three different designs: armchair, chiral, and Zig-Zag. The design of nanotubes depends on the complexity of the graphene in a tube, which can be represented by an index pair (n, m). The integers n and m represent the number of unit vectors in two
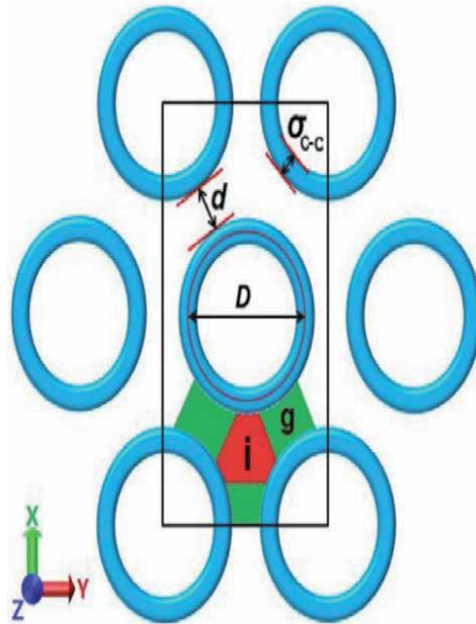
Figure 3.
Schematic arrangement of a parallel aligned three dimensionally SWCNT array in a simulation box (i.e. the black framework) of volume $L_x \times L_y \times L_z$ nm³. D is the nanotube diameter. The parameter d is the surface to surface intertube distance beyond VDW diameter σ_{C-C} = 0.34 nm of carbon atoms. It is defined as d = d_{CNT} - σ_{C-C} with d_{CNT} denoting the shortest separation between carbon atoms of adjacent tubes. Interstitial and groove regions are represented by i and g, respectively. Note that there is some ambiguity on how to discriminate between i and g [7].

directions in the graphene crystal lattice. If m = 0, this type of nanotube is called zigzag; if n = m, those nanotubes produced are called chair nanotubes, and in the third case, if m $\neq$ n, it is called chiral nanotube. The values of the integers n and m greatly affect the property of SWNT. The MWCNT is a multilayer of graphene sheets rolled and superimposed on each other. The outer diameters are typically in the range of 2–100 nm while the inner diameters are in the range of 1–3 nm, and the length is one to several micrometers. SWCNTs are more flexible than MWCNTs. They can be twisted, flattened, and bent into small circles or around a sharp bend without breaking, thereby increasing its applicability. SWCNTs have the unique electronic and mechanical properties, which can be used in applications such as field emission displays, nanocomposite material, nanosensors, and logical elements. MWCNTs exhibit some advantages over SWCNTs such as higher surface-to-volume ratio, they are easier to produce in high volume quantities, the product cost per unit is low, and its thermal stability and chemical stability are enhanced. However, MWCNTs have regions of structural imperfection, which may reduce its desirability for application. CNTs are light in weight and have the strongest tensile strength as compared with any synthetic fiber. This strength results from the covalent Sp^2 bonds formed between the individual carbon atoms. A standard SWCNT can withstand a pressure of 25 GPa without deformation. In terms of thermal conductivity, nanotubes are good conductors along the tube axis but good insulators lateral to the tube axis. Measurements carried out show that SWCNTs have better thermal conductivity compared with copper under the same conditions. MWCNTs exhibit a striking telescoping property whereby an inner nanotube core can slide almost without friction within its outer nanotube shell, thus creating an atomically perfect linear or rotational bearing. The symmetry and unique electronic structure of

graphene strongly affect its electrical properties. All CNTs have a large surface area and a high level of adsorption [2]. The type of adsorption in CNTs can be easily divided into three modes: (1) internal adsorption in which only the CNT interior space can be used, (2) external adsorption where adsorption can only be done in the space between CNTs (e.g., areas intermediate and groove; see **Figure 1** and (3) unlimited absorption in which both sides of the CNT, i.e., inside and outside, can be used. Among them, unlimited recruitment is the only thing that matters in the industry [7].

5. Storage mechanism of gas in carbon nanotubes

CNTs store gas through the process of adsorption. Adsorption of a gas is a process that gains one or more constituents of the gas in the region of the gas-solid interface where the molecules of the gas are bounded to the surface of the adsorbent as illustrated in **Figure 4**. Gas absorption in CNT is superficial, and this phenomenon involves increasing the density of the gas near the contact surface, and because the process is spontaneous, Gibbs free energy changes are negative. And because the entropy change is also negative (decreasing the degree of release of gas molecules during the process), the enthalpy changes are less than zero, so the process is hot. There are two types of absorption: physical adsorption and chemical adsorption. In physisorption, the bounding of the gas molecules is superficial because the gaseous molecules are not chemically bounded to the walls of the adsorbent. Weak van der Waals forces are responsible for holding the molecules of the gas to the adsorbent. The adsorption of methane on CNT is most likely through the process of physisorption where the adsorbents require an elevated exposed surface per gram of material called specific surface area, and it is expressed in cubical centimeters of adsorbate per gram of adsorbent. When the elemental constituents of the solid get smaller, the specific surface area gets larger. CNTs that have diameters in the order of nanometers and with hollow cylindrical surfaces present good specific surface areas and are an excellent adsorbent for adsorption of gases. As the pores of a CNT surface decrease, the gas storage capacity increases [2]. The doping of CNTs with metal atoms (such as Li or K) or functional groups (such as COO or NH^{3+}) is a possible way to enhance their adsorption capability [7].
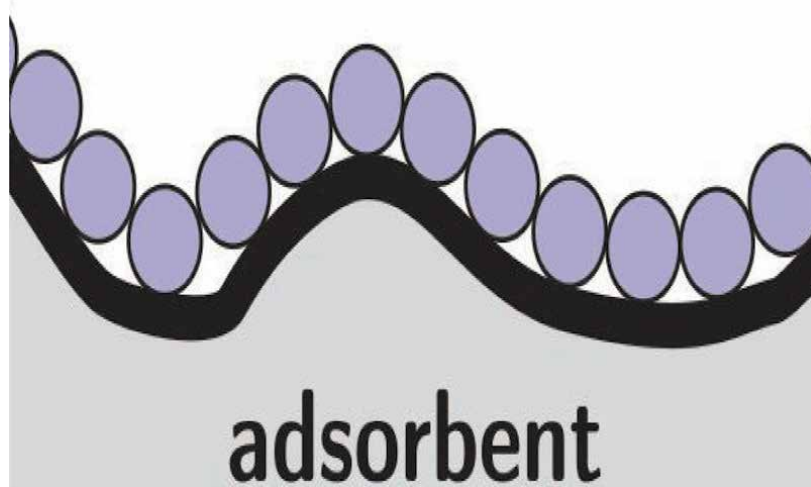

Figure 4.
Representation of the adsorption process of a gas on a solid surface [2].

6. Factors that affect the storage capacity of natural gas in CNT

In general, carbon nanotubes (SWCNT with a diameter of 2040 nm and MWCNT with a diameter of 3060 nm) are stable in the temperature range of 25–600°C. Also, an increase in the thermal capacity of carbon nanotubes has been reported by shortening the length of CNT diameter nanotubes in the range of 60–100 nm. While thermal stability increases with increasing nanotube length [6]. In a conducted simulation work to study the storage capacity of SWCNT at different temperatures and pressures, it was observed that methane is weakly adsorbed in SWCNT. Results showed that as pressure increases, the amount of methane adsorbed on SWCNT increased but as temperature increased, the amount of methane adsorbed on SWCNT decreased. It was reported that the binding energies for methane on the defected SWCNT increased by about 56% over the defect-free SWCNT showing that the presence of defects on the structure of nanotubes increases its methane adsorption capacity. Furthermore, for the encapsulated methane molecules inside the defected nanotubes, results showed about 68% increase in binding energy compared with the confined molecules in the defect-free nanotubes. It was pointed out that introducing surface curvatures in the nanotubes could reduce the binding energy between the methane molecules and the substrate. Thus, some factors that affect methane adsorption in SWCNT are pressure, temperature, structural defects, and curvatures. The methane storage capacity of MWCNT has been studied by several researchers. One set of results showed that a type of MWCNT strongly adsorbed methane at a maximum value of 5.44 mmol/g at a temperature of 283.15 K and a pressure of 40 bars. It was also reported that increasing pressure increased the amount of methane adsorbed, while increasing temperature decreased the amount of adsorbed methane. Another report has it that treating MWCNT with acids such as HCl and HNO_3 improves its methane adsorption capacity. The results of experiments conducted using acid-treated MWCNT and untreated MWCNT at the same pressures revealed that acid treatment of nanotubes enhances methane adsorption capacity especially at low pressures. In another work, the methane adsorptions on MWCNT treated with sulfuric and nitric acids, nitric acid, and alkaline were compared with the methane adsorption capacity of untreated MWCNT. Reported results showed that sulfuric and nitric acid–treated MWCNT adsorbed more methane than all other treated and untreated nanotubes. This was followed by nitric acid–treated case before the alkaline-treated nanotubes. The methane adsorption capacity on all the treated nanotubes was higher than the untreated cases showing that treating MWCNT with acids enhances its methane adsorption capacity. This work also showed that increase in pressure increases methane adsorption while increase in temperature decreases methane adsorption on MWCNT [2]. A group of scientists found in their research that the initial slopes of isotherms increased sharply, which indicates that active sites are created on the adsorbent during the functionalization step. Existence of functional groups on MWCNTs causes the adsorption capacity to increase gas at low pressures. At low pressures, adsorption on MWCNTs is affected by the fluid adsorbent interaction; therefore, functional groups led to increased fluid adsorbent interactions. But at higher pressures, fluid interactions become more important than fluid adsorbent interactions, and the role of functional groups is reduced [9].

7. Neutral and charged CNTs

Scientists considered the absorption of gas by loaded nanotubes to absorb CO_2-N_2 gas in a hexagonal CNT pipeline. They found that positive charges on CNTs

increased both CO_2 uptake and N_2-CO_2 uptake. Negative charges in a neutral CNT lead to weaker CO_2-N_2 uptake. Undoubtedly, charge distribution, both on CNTs and on adsorbent molecules, plays an important role in the uptake of gases into pregnant CNTs. In this work, they performed a large Monte Carlo simulation to evaluate the absorption and separation of dual gas mixtures of CO_2, SO_2, and H_2S in neutralized and charged. Carbon nanotubes at low pressure and 303 K at SWCNT with a diameter of 2.17, 2.71, and 3.26 nm and inter-tube distance of 1.0 nm were modeled. Certain loads from -0.04 q to +0.04 q were placed on each nanotube to investigate the effect of the load. It has been shown that the behavior of mixed gases in pregnant SWCNTs follows the same rules as pure gases. Due to the additional strong coulomb force between the adsorbent and the charged SWCNTs, the amount of polar molecule adsorption increases significantly when mixed with CO_2, while CO_2 adsorption is usually suppressed as a result of adsorption competition [3]. In addition to the general change in local charge distribution by doping or cavitation, electric oscillation absorption (ESA) provides another way to increase gas absorption by carbon-based adsorbents. Therefore, non-fading electric charges on the absorber can be generated and removed by charging and discharging and enable the rapid absorption and disposal of gases. For example, using GCMC simulations, some scientists have studied H2 uptake on charged SWCNTs. At temperatures 77 K and 298 K, they observed that charging of SWCNTs leads to a significantly better hydrogen storage than accessible in uncharged SWCNT systems. For positively charged CNTs, they observed a larger CO_2 adsorption than in neutral samples, while the opposite has been detected for CNT systems with a negative charge. Negative charges lead to a weaker adsorption and to a reduced CO_2/N_2 selectivity than a neutral CNT bundle [7]. With the criterion of unloaded CNT samples, it is easy to understand that the absorption in a positively charged pregnant CNT is always greater than that in a negatively charged pregnant CNT. Compared with the neutral CNT mode, negative overloads increase adsorption in areas with low pressure and suppress adsorption in areas with high pressure, while positive overloads always increase adsorption [7].

8. Prospects of CNT as a natural gas storage device

Carbon nanotubes have many industrial applications, but more attention is currently given to it as a material for natural gas storage. Several research studies have been conducted to investigate the adsorption behavior of methane, which is a major component of natural gas on SWCNT and MWCNT. The key to successful commercialization of CNT for gas storage is the adsorption capacity of the nanotubes at standard conditions, that is, the ratio of the volume of adsorbed natural gas to the volume of storage container (Vg/Vs). There are indications that substantial volume of methane can be stored in activated carbon pellets at atmospheric conditions, in fact an adsorption capacity of 126 Vg/Vs has been reported. Commercial development of CNT for adsorption of natural gas requires high storage gas capacity greater than 150 Vg/Vs. There are other advances in gas storage on CNT that can be leveraged on to improve the natural gas storage capacity on nanotubes. It should however be noted that a volumetric capacity of about 160 Vg/Vs for methane adsorption on SWCNT has been reported. One of the challenges facing the wide use of CNT as a major adsorbent for natural gas storage is achieving consistency in storage densities and replicable manufacturing capacity. The methods used to manufacture the carbon nanotubes that give the required capacity are quite rigorous, and research in its reproducibility is still ongoing. There is need to control the pressure, temperature, and the flow rate at which gas is efficiently filled and

released from the CNT tanks for automotive application. These conditions affect the performance of the storage system since the adsorption process is exothermic. The cost of producing, purifying, and tuning the CNT to obtain the required diameter in large quantity makes the existing methods economically viable [2].

9. Mathematical modeling

9.1 Geometry creation

As mentioned, natural gas adsorption on nanotubes depends on its varied features, including the diameter of nanotubes, construction method, gas arrangement in the nanotube structure, pressure, and temperature. The free spaces of nanotubes have the highest potential for natural gas adsorption. With an increase in the loading pressure, adsorption increases, but as the temperature of the adsorption medium enhances, adsorption decreases. A model was developed for natural gas storage in a vessel containing nanotubes. In fact, the adsorption phenomenon and gas storage of natural gas were modeled here. It was seemed that multi-wall nanotube could be a best choice for adsorbent, and so, multiwall carbon nanotube was used as adsorbent in this chapter. A container with a volume of about 100 ml and has inlet and outlet diameters of 6.35 mm, which we see in **Figure 5**. This container has an inner diameter of 35.85 mm and a height of 25.3 mm. It also has a porosity of 98.4%. Multiwalled nanotubes are uniformly placed inside the container, which can be considered as a porous medium [1].

The hypotheses that must be considered before solving the problem are:

- The porous environment is the same in all areas.

- The properties of the nanotubes do not change during the process.

- Convective heat transfer is established in the wall of the vessel and the surrounding fluid is in the experimental reference of the bath water.

- Radial heat transfer occurs inside the vessel.

- No chemical reaction occurs between the nanotubes and natural gas.

In addition, the properties and composition are listed. According to the assumptions mentioned above, the governing equations are obtained [1]. To simulate natural gas storage in carbon adsorbents, the equations must be solved
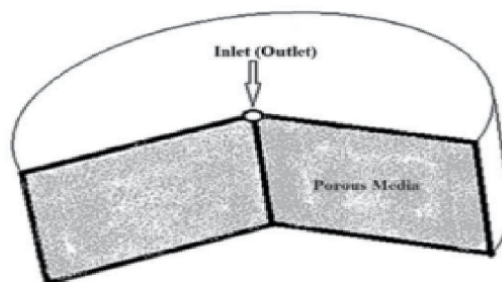

Figure 5.
Schematic of the geometry used here [1].

simultaneously. Several equations are calculated and obtained, and other equations are collected from other sources. To answer the equations of adsorption and storage of natural gas in nanoparticles, the equations of adsorption isotherm, adsorption heat, kinetics, energy, and mass must be used. To obtain the mass and energy equations, it is first necessary to write the equilibrium equations and then, using the conditions and assumptions governing the problem, the final equation is obtained. Due to the small physical dimensions, especially the thickness, it is not necessary to solve the problem in all dimensions. After examining this issue with Comsol software, it was proved that considering multidimensional or one-dimensional problem does not cause a difference in the results obtained, which is another reason for not solving the problem in all dimensions. To solve the existing equations, a radial system was considered to study temperature changes along the radius and other volumetric and mass values were calculated. Because the pressure gradient in ANG storage tanks is less than 700 kPa, there is no need to solve the Navier-Stokes equation [1].

9.2 Adsorption isotherm

Since the process of adsorption of natural gas on carbon nanotubes is similar to the adsorption of gas by ANG method, it was considered as a possible type of interaction between nanotubes and natural gas. The adsorption equilibrium depends on the pressure, temperature, and geometry of the adsorbent, which makes adsorption isotherms to be used to obtain the adsorption equilibrium. The Sips equation has the highest consistency with the experimental data to explain the adsorption of natural gas in nanotubes; thus, it can be used to describe the behavior of the adsorption process. The equation of the Sips adsorption isotherm is shown below:

$$q_e = \frac{q_m (b\rho)^{\frac{1}{n}}}{1 + (b\rho)^{\frac{1}{n}}} \tag{1}$$

$$\frac{1}{n} = \frac{1}{n_o} + \alpha \left(1 - \frac{T}{T_o} \right) \tag{2}$$

where b is adsorption/desorption constant (Pa^{-1}), n is adsorbate/adsorbent interaction parameter, p is pressure (Pa), q_e is adsorption equilibrium (mmol/gr), q_m is maximum adsorption (mmol/gr), T is temperature (K), T_o is reference temperature (K), and b_o, n_o, and α are constant parameters of adsorption isotherm. Eq. (2) proves that the amount of equilibrium adsorption in the original equation is pressure-dependent, and the dependence of the Sips model on parameters b and n on temperature is proved. In addition, the reference temperature is 283.15 K. The other parameters are different depending on the type and structure of the adsorbent, which are shown in **Table 1**.

$$b = b_o \exp \left[\frac{Q}{RT_O} \left(\frac{T}{T_o} - 1 \right) \right] \tag{3}$$

where Q is isosteric heat adsorption during the half-life of adsorption (kJ/mol), R is universal gas constant (j/mol K), T is temperature (K), and T_o is reference temperature (K). Absorption is heat, and when the temperature of the adsorption medium increases, isothermal heat has a negative effect on the process and reduces the adsorption capacity. The Clausius-Clapeyron equation is used to calculate isothermal heat. Each of the adsorption equations can be used to calculate the adsorption heat:

Parameter	Unit	Nanotube type	Value
q_m	mmol/gr	C	80.92
		Si	65.83
b_o	Pa^{-1}	C	0.0143e−5
		Si	0.262e−5
n_o	–	C	0.884
		Si	1.164
Q	Kj/mol	C	7.595
		Si	12.5
α	–	C	0.726
		Si	0.5909

Table 1.
Constant parameters of equations [1].

$$Q_{st} = RT^2 \left(\frac{\delta ln\rho}{\delta T} \right)_q \tag{4}$$

$$Q_{st} = Q - anRT_o \ln \left(b_p \right) \tag{5}$$

where Q_{st} is isosteric heat adsorption. Simultaneously with environmental conditions, equilibrium time has a great impact on the process. The kinetic equation (6) is used to obtain the absorption capacity at a given time. This is because after reaching the equilibrium point, the process of gas adsorption by nanoparticles stops, and this time is called the end time of the process:

$$\frac{t}{q_t} = \frac{1}{k^2 q_e^2} + \frac{t}{q_e} \tag{6}$$

where q_e is adsorption equilibrium (mmol/gr), q_t is adsorption capacity (mmol/gr), t is time (min), and k^2 is the experimental parameter that varies upon a change in the pressure, and its relationship is obtained by the interpretation of experimental data [1].

9.3 Mass equation

Natural gas can be stored on carbon nanotubes in the following two ways:

- Absorbed gas on the adsorbent.

- Gas storage in the open space of the ship as compressed natural gas (CNG).

After writing the mass balance according to the hypotheses, the following equation was obtained:

$$\frac{dm_g}{dt} = \pm \dot{m_g} - m_s \frac{da}{dt} \tag{7}$$

$$a = M_g \times q_t \tag{8}$$

$$\frac{da}{dt} = M_g \times \frac{dq_t}{dt} \tag{9}$$

$$\frac{da}{dt} = M_g \frac{dq_t}{dt} = M_g \left[\frac{q_t}{t} - \frac{q_t^2}{q_e^t} \right] \tag{10}$$

where $\dot{m}_g$ is inlet (outlet) gas flow (gr/s), m_g is the amount of gas stored in the vessel as gas phase (gr), m_s is loaded mass of nanoparticles in the vessel (gr), a is adsorbed gas relative to adsorbent mass (gr gas/gr adsorbent), and M_g is molecular weight (gr/mol) [1].

9.4 Energy equation

To investigate the thermal behavior of the vessel, the energy equation in one dimension and the radial direction were used based on Eq. (11):

$$r \left(\varepsilon \rho_g C_g + \rho C + \rho_a a C_a \right) \frac{\delta T}{\delta t} + r \rho_g \vartheta C_g \frac{\delta T}{\delta r} = \frac{\delta}{\delta r} \left(r \lambda \frac{\delta T}{\delta r} \right) + \vartheta Q_{st} \rho \frac{\delta a}{\delta t} \tag{11}$$

where C is the specific heat kJ/kg. K, r is radius (m), v is velocity of fluid (m/s), α is the relationship between viscosity and permeability, ε is overall porosity, λ is overall thermal conductivity (W/mK), and ρ is density (kg/m³). Using the Darcy equation, the mass velocity of the fluid inside the porous medium can be obtained. Because the Reynolds range was small during the process, the Darcy equation is used:

$$\vartheta = -\frac{1}{\alpha} \Delta \tag{12}$$

$$\alpha = \frac{150 \mu}{4} \frac{(1 - \varepsilon_b)^2}{\varepsilon_b^3 R_p^2} \tag{13}$$

where $\Delta \rho$ is pressure difference (Pa), ε_b is bed porosity. These laboratory-obtained equations correspond to the experimental results in the main fields for spherical nanoparticles, and their equivalent diameter must be used for nonspherical nanoparticles. Eq. (14) can be used to obtain the equivalent radius of the nanotubes:

$$R_p = \frac{1}{2} \left(\frac{L}{ln \left(\frac{2L}{d} \right)} \right) \tag{14}$$

where R_p is the radius of the particle (m), d is external diameter of nanotubes (nm), and L is nanotube length (nm) [1].

9.5 Initial and boundary conditions

To answer the energy equation, we must first determine the boundary values. For this purpose, the boundary conditions of the system, in the initial network and based on the Eq. (15), was calculated:

$$\frac{\delta T}{\delta r} (r_i, t) = 0 \tag{15}$$

Two thermal resistors named R1 and R2, which show the conductivity and convection resistance, respectively, are used between the end points (vessel wall) and the fluid. The resistors are closed in series, and the resistance of each of them

can be obtained by merging with each other. As **Figure 6** shows, the heat conduction and convection in the wall are balanced, and the thermal equilibrium is applied to the Eq. (16):

$$\lambda_{\text{eff}} \frac{\delta T}{\delta r}(r_o, t) = U(T_{r_o} - T_f) \tag{16}$$

$$U = \frac{1}{R_s} \tag{17}$$

$$R_s = R_1 + R_2 \tag{18}$$

$$R_1 = \frac{r_o \ln\left(\frac{r_w}{r_o}\right)}{\lambda_w} \tag{19}$$

$$R_2 = \frac{1}{h_o} \tag{20}$$

where h_o is convection heat transfer coefficient of surrounding fluid of vessel (w/m.K). r_o is external radius of the vessel (m), Rs is equivalent resistance, r_w is inner radius of vessel (m), T_f is bath temperature of vessel (K), U is the overall heat transfer coefficient (W/m^2.k), λ_{eff} is effective heat transfer conduction coefficient (W/m.K), and λ_w is the thermal conductivity of the vessel's wall (W/m.K) [1].

9.6 Nanotube's properties

The smallest inner diameter of the nanotube has been reported to be 0.4 nm, and the distance between the nanotubes is equal to 0.34 nm. Hence, to obtain the number of the nanotube wall, Eq. (21) is used. As the nanotube diameter increases, the number of wall increases:

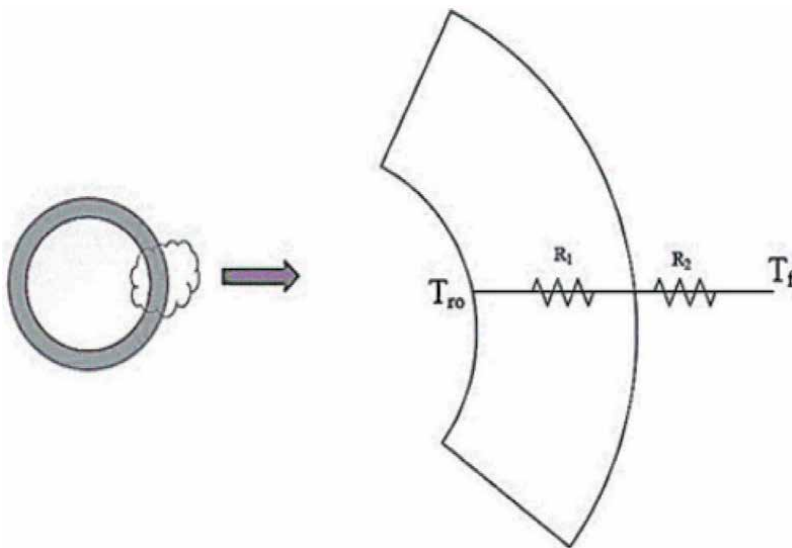$$N_{wall} = \frac{1}{d_d}(d_{ext} - d_{int}) + 1 \tag{21}$$

Figure 6.
Thermal boundary conditions in external environment of vessel [1].

where N_{Wall} is the number of nanotubes wall, d_d is the distance between the walls (nm).

$$\rho = \frac{4000}{1315}\left[\frac{N_{wall}}{d_{ext}} - \frac{2d\sum_{i=0}^{N_{wall}-1}i}{d_{ext}^2}\right] \tag{22}$$

d_{ext} is external diameter of the nanotube (nm), and d_{int} is internal diameter of the nanotube (nm). The weight and density of nanotubes depend on the internal and external diameter of nanotubes and the number of walls.

The properties of methane, natural gas, and carbon nanotubes are given in **Tables 2** and **3**. Nanotubes made of silicon can be called a competitor to carbon nanotubes, because there are many similarities between carbon and silicon. In this experiment, which is performed in a laboratory environment, pure methane gas is used, but on a large and industrial scale, natural gas must be used. By looking at **Table 4**, the natural gas composition used in this experiment can be obtained [1].

10. Influence of different factors on absorption in CNT

10.1 Nanotube's diameter effect on the process

The diameter of the nanotubes with sizes of 5, 10, 15, and 30 nm was considered to investigate the effect of the outer diameter of the nanotubes on the process, and the other parameters listed in **Table 5** were selected. As the diameter of the nanotubes increases, the walls of the nanotubes increase, and thus, the active

Parameter	Unit	Gas type	Value
Conduction heat transfer coefficient	W/(m.K)	Methane	0.035
		Natural gas	0.0335
Specific heat capacity	j/(Kg.K)	Methane	2265
		Natural gas	2340
Dynamic viscosity	Pa.s	Methane	1.5e−5
		Natural gas	1.04e−5
Specific heat ratio	_	Methane	1.32
		Natural gas	1.32
Density	Kg/m^3	Methane	0.656
		Natural gas	0.668–0.717
Molecular weight	gr/mol	Methane	16.04
		Natural gas	19
Critical temperature	°C	Methane	−82.3
		Natural gas	−62.7
Critical pressure	psi	Methane	4.64e+6
		Natural gas	4.564e+6

Table 2.
Natural gas and methane properties [1].

Parameter	Unit	Type	Value
Density	Kg/m^3	C	60–2200
		Si	232.9
Conduction heat transfer coefficient	W/(m.K)	C	12–600
		Si	159
Specific heat capacity	j/(Kg.K)	C	0.75–0.85
		Si	0.7
External diameter	nm	-	4–25
The distance between the nanotubes	nm	-	0.34

Table 3.
Specification of nanotubes [1].

Component	Composition
Methane	95
Ethane	3.2
Propane	0.2
i-Butane	0.03
n-Butane	0.03
i-Pentane	0.01
n-Pentane	0.01
Hexane and heavier	0.01
Nitrogen	1
Carbon dioxide	0.5
Oxygen	0.02
Hydrogen	Nil

Table 4.
Composition of natural gas [1].

surface area of the nanotubes for adsorption increases. As the outer diameter of carbon nanotubes increases, their adsorption capacity increases (**Figure 7**). It has been proven that by doubling the diameter of the nanotube, the absorption of
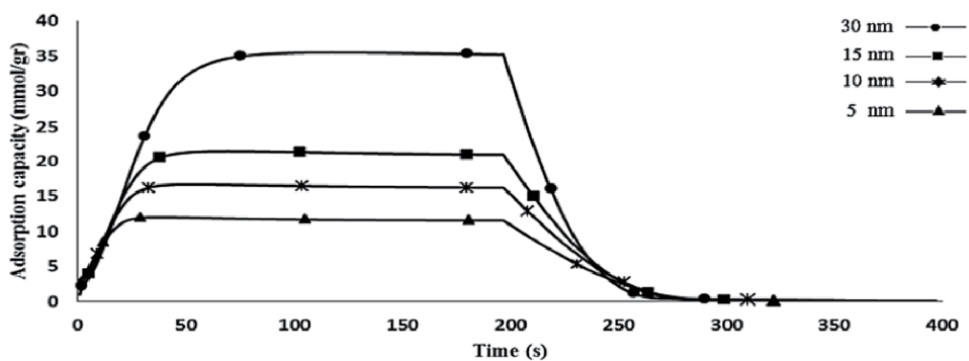

Figure 7.
Adsorption capacity at different diameters of the nanotubes [1].

natural gas in the pipes will increase by 45%. With an increase in the diameter of the nanotube, nanotube walls increase, and due to its density per unit mass, the adsorption capacity increases.

To prove that less porosity causes more gas to be absorbed, the porosity values of 70, 80, 90, and 98 were considered. The other parameters are listed in **Table 5**. Based on this, the mass loaded in the container increases if the porosity decreases, resulting in an increase in the total amount of gas adsorbed in the nanotube. The adsorption capacity of the tubes will not change continuously with changes in porosity (**Figure 8**) [1].

10.2 Loading pressure effect on the process

To evaluate the effect of the applied pressure, pressures of 5, 20, 35, and 50 were applied. The rest of the parameters are listed in **Table 5**. As the applied pressure increases, the amount of gas introduced and the nanotube adsorption capacity increase (**Figure 9**). But increasing pressure has limitations in terms of safety, manufacturing costs, and more. During emptying, the container pressure should be reduced to the ambient pressure. A pressure of 5 Pa was chosen for the ambient pressure. The adsorption capacity tripled when the applied pressure increased from 20 Pa to 35 Pa. This increase in pressure increases the molecular density of the gas in the container space. As the pressure increases, the gas molecules penetrate the inner layers of the adsorbent and the amount of gas absorbed increases [1].

10.3 Surrounding condition effect on the process

To investigate the effect of temperature (water bath temperature) on the process, environmental conditions (water bath temperature) 298 K, 305 K, 320 K, 335 K, and 350 K were considered. The other parameters are based on **Table 5**.

Parameter	First series	Second series	Third series	Fourth series
External diameter (nm)	Changeable	20	20	20
Bed porosity (%)	90	Changeable	90	90
Loading pressure (Pa)	5.2e+6	5.2e+6	Changeable	5.2e+6
Temperature of water bath (K)	310	310	310	Changeable

Table 5.
Input data [1].
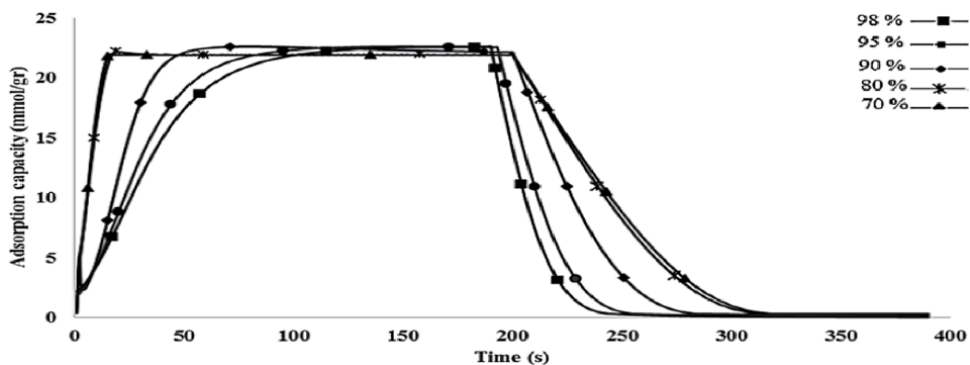

Figure 8.
Adsorption capacity at different porosity [1].
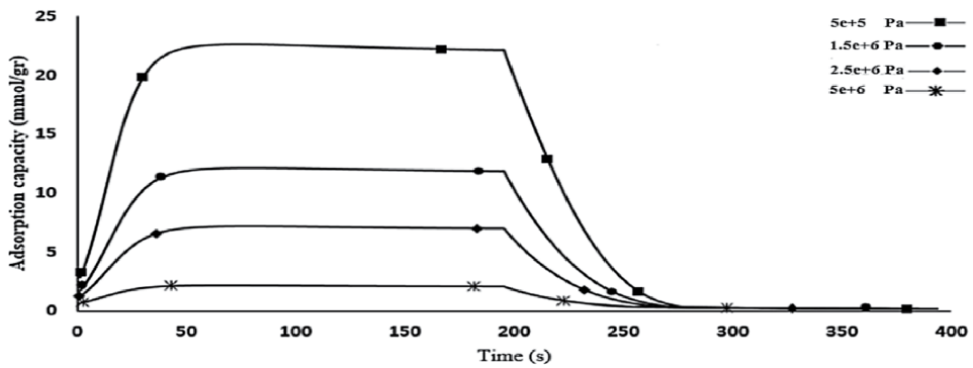
Figure 9.
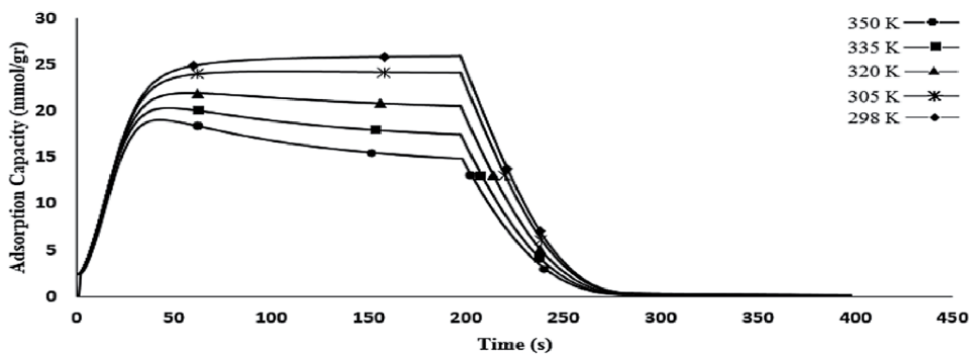*Adsorption capacity at different pressure [1].*

Figure 10.
Adsorption capacity at different temperature [1].

Figure 10 shows that the natural gas adsorption capacity of nanotubes that are exposed to temperature decreases. Because the temperature of the container is low at the beginning of the process, the maximum gas absorption capacity is obtained. Therefore, it is better to keep the temperature low and increase the discharge time to get better results during the charging process. For example, the adsorption capacity at 298 K is 0.4945 g/g. By increasing the temperature to 320, by reducing the adsorption capacity by 22%, 0.3826 g/g is obtained. Optimal conditions for this work include the maximum diameter of the carbon nanotubes and the applied pressure and the minimum amount of porosity (**Table 6**).

Numerical adsorption capacity (gr/gr)	Material	Study type	Adsorption capacity (gr/gr)
0.83	SWCNT	Numerical	0.35
	KOH activated	Experimental	0.1
	BPL	Experimental	0.06
	Pre-oxidized		0.065
	Notpre-oxidized		0.05
	Chemical activation	Experimental	0.09

Table 6.
Comparison of gas adsorption capacity in the presence of different adsorbents [1].

The absorbed gas in the CNG tank is 11.2 grams, which is 25.9 grams using multiwalled nanotubes. By comparing the results, it can be seen that nanotubes have the highest and best percentage of storage and use to absorb and store natural gas in tanks [1].

11. Conclusion

Natural gas is a clean source of energy, but an efficient and economical means of storing and transporting it is a challenge that is a growing research area of interest. CNTs have the potential to store natural gas at low pressures and are an economical and efficient candidate for storing and transporting natural gas. Structural defect in SWCNT improves its methane adsorption capacity. Purification of MWCNT with acids increases its methane adsorption capacity. Increasing pressure increases CNT methane adsorption capacity while increasing temperature decreases CNT methane adsorption capacity. Adsorption capacity and adsorbed gas increase with increasing MWCNT diameter. Increasing the diameter of the nanotube reduces its density. Natural gas is more absorbed in carbon nanotubes than in silicon nanotubes. The porosity of the tanks has a significant effect on the adsorption capacity (gr/gr), but affects the total adsorbed mass of the gas (gr). By reducing the porosity of the tank, the loaded mass of the adsorbent in the container increases, and as a result, natural gas storage becomes more. Adsorption capacity is a function of adsorbent, temperature, and pressure. As the loading pressure increases, the inlet and gas absorption capacity improves. The adsorption capacity of the bed decreases with increasing bed temperature. Optimal conditions are a combination of maximum nanotube diameter, loading pressure, minimum possible porosity, and water bath temperature in the presence of carbon nanotubes.

Author details

Mohsen Askaryan
Independent Researcher, Boroujerd, Iran

*Address all correspondence to: asmohsen10417@gmail.com

IntechOpen

References

[1] Jafari A, Askari S. A novel model for natural gas storage on carbon nanotubes. Applied Nanoscience. 2019;**10**:1115-1129

[2] Naomi A. Ogolo, Feasibility of Natural Gas Storage on Carbon Nanotubes. 2020. pp. 1-9

[3] Chen S-Y, Hui Y, Yang YB. Monte Carlo simulations of adsorption and separation of binary mixtures of CO2. Soft Materials. 2020;**18**:1-13

[4] Mehrabi M, Parvin P, Reyhani A, Mortazavi SZ. Hydrogen storage in multi-walled carbon nanotubes decorated with palladium nanoparticles using laser ablation/chemical reduction methods. Materials Research Express. 2017;**4**:9

[5] Oriňáková R, Orinak A. Recent applications of carbon nanotubes in hydrogen production and storage. Fuel. 2011;**90**:3123-3140

[6] Sandeep Kumara KT. Progress in Energy and Combustion Science. 2017. pp. 1-35

[7] Yang Y-B, Hao Q, Müller-Plathe F, Böhm MC. Monte Carlo Simulations of SO2. Journal of Physical Chemistry. 2020;**124**:5838-5852

[8] Gao Z, Song N, Zhang Y, Schwab Y, He J, Li X. Carbon Nanotubes Derived from Yeast-Fermented. ACS Sustainable Chemical Engineering. 2018;**6**:9

[9] Irajia N, Hojjat M, Aghamiri S, Talaie MR, Molyanyan E. Adsorption of CO2 and SO2 on multi-walled carbon nanotubes: Experimental data and modeling using artificial neural network. Journal of Particle Science and Technology. 2019;**5**:34-42

The Dynamic of Residential Energy Demand Function: Evidence from Natural Gas

Mohamed Jaouad Malzi

Abstract

This analysis uses annual data on residential gas use for 29 Organization for Economic Cooperation and Development nations from 2005 to 2016 to look at per capita energy demand. The effect of price and income on natural gas demand elasticities has been studied in the past, but most research have ignored demographic aspects. The goal of this study is to incorporate these characteristics into natural gas demand modeling. A dynamic panel system dubbed the Generalized Method of Moments (GMM) estimator was used to address the endogeneity issue. The following are the study's main findings: First, the residential sector consumes more natural gas per capita as the population grows. Second, the consumption of per capita residential natural gas in Organization for Economic Cooperation and Development countries is decreasing as the population ages. Finally, as the population density rises, so does per capita gas consumption.

Keywords: dynamic function, energy demand, generalized method of moments

1. Introduction

The OECD[1] countries have encountered many challenges throughout the years, including rapidly aging societies and diminishing fertility rates. The share of the senior population (those over 65 years old) climbed from less than 9% in 1960 to 17% in 2015, and it is anticipated to continue to rise, reaching 28% in 2050.[2]

Furthermore, since 1970, most OECD countries have faced the difficulty of a primarily urban population. In OECD countries, particularly Australia, Korea, Chile, France, and Japan, urbanization is higher, and the trend is anticipated to continue.[3]

Because demographic shifts pose serious distributional issues and are projected to have significant economic effects, OECD nations must take these factors into account.

Indeed, natural gas' adaptability, low price, and lower greenhouse gas emissions from combustion than coal and oil have pushed natural gas demand to rise rapidly, gaining share in all sectors, particularly residential. Residential natural gas usage has

---

[1] Organization for Economic Co-operation and Development.

[2] Health at a Glance 2017.

[3] Trends in Urbanization and Urban Policies in OECD Countries 2010.

risen consistently in OECD countries over time. The amount has increased from around 8 million terajoules (TJ) in 1980 to more than 11 million TJ in 2016. As shown in **Figure 1**, the total has moved from about 8 million terajoules (TJ) in 1980 to more than 11 million TJ in 2016. Moreover, in order to understand the individual trend of per capita residential natural gas consumption considered as the dependent variable, during the period of study (2005–2016), per capita natural gas demand was plotted in a time-series graph for each country in **Figure 2** and note that each country has its own specific trend.

These two figures are useful for econometric reasons since they show the evolution of aggregate and per capita individual demand for natural gas in the residential sector over time.
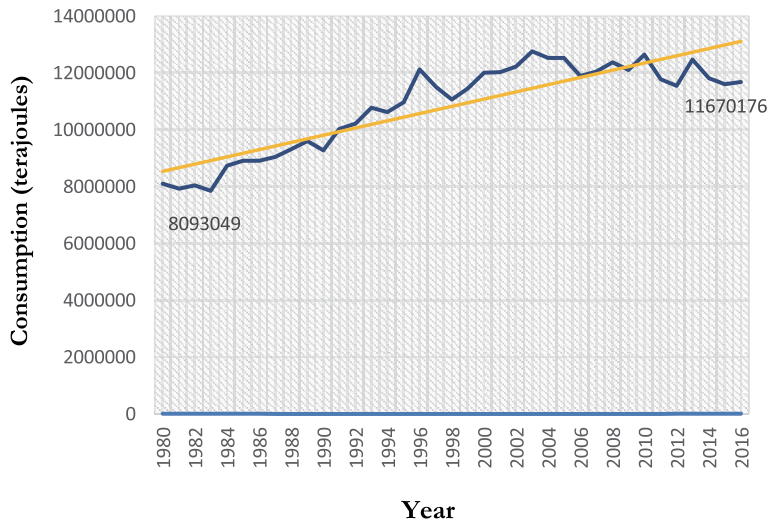

Figure 1.
Evolution of aggregate residential consumption for natural gas in OECD countries (terajoules, 1980–2016). Reference: own elaboration based on IEA data.
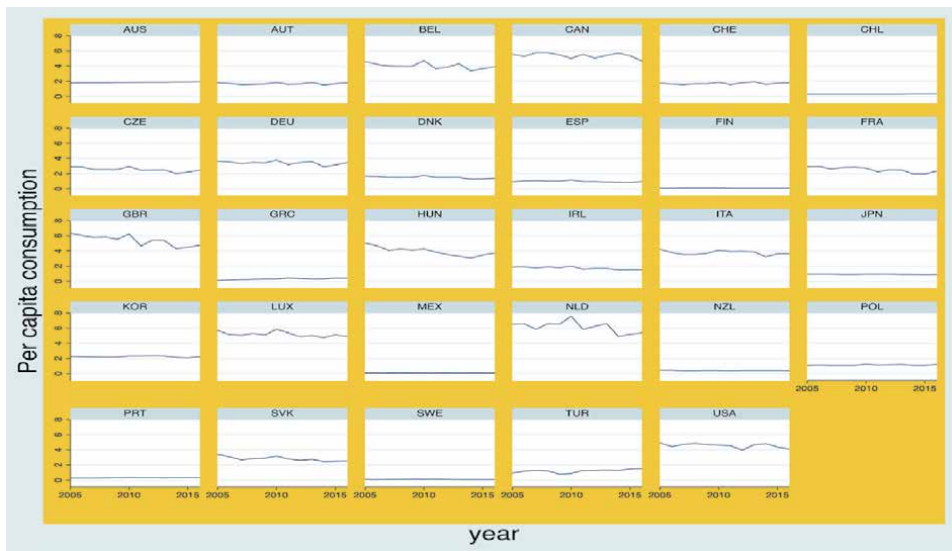

Figure 2.
Evolution of per capita residential consumption for natural gas by country (MWh, 2005–2016). Reference: own elaboration based on IEA data.

In fact, knowing the numerous factors of residential natural gas consumption and thus estimating the demand equation accurately is critical to creating natural gas legislation and corporate strategies for investors in the natural gas residential sector. To estimate household natural gas demand, the literature has concentrated on the effect of price and income. The majority of these research used static or dynamic models, or both, to simulate natural gas consumption behavior.

In previous energy research [1–5], demographic factors such as the elderly, population density, and urbanization have received little attention, despite the fact that they influence household natural gas consumption explicitly or implicitly. Furthermore, with the exception of Gautam et al. [5], the majority of these research are based on data from before 2010, and it is critical to update studies, especially in this economic field where inputs are rapidly changing.

Policymakers need to know not only how natural gas demand will respond to income and price changes in order to make holistic decisions.

The goal of this research is to estimate the dynamics of per capita residential natural gas demand in 29 OECD nations from 2005 to 2016. The rest of the paper is organized as follows. A brief survey of the literature is presented in Section 2. Section 3 gives a description of the data as well as some descriptive statistics. In Section 4, the estimation findings are shown. A brief conclusion is included in the concluding section.

2. Literature review

The impact of population characteristics, particularly age, density, and proportion of urban population, on residential natural gas demand is rare; this could be due to a lack of data. To estimate natural gas demand, most studies focused on price and income elasticities. Several studies, however, have shed light on the impact of population factors on overall household energy usage over the last two decades.

According to several studies, there is a link between household age and space heating energy use. That is, because elderly people are more sensitive to temperature, they consume more energy for space heating than younger people because they spend more time at home. Meanwhile, Chen et al. [6] found that age has a greater impact than wealth in a study of Hangzhou, China, and that there is a negative relationship between occupant age and residential energy usage, particularly for heating and cooling. It was discovered that older housewives are more supportive of economic conduct than younger housewives.

Kronenberg [7] observes in his study on energy consumption and greenhouse gas emissions in Germany that demographic changes, defined by a rise in the number of elderly persons, have a favorable impact on energy demand, particularly for heating.

Liao and Chang [8] used the discrete technique to estimate the space heating and water heating energy demands of senior residents in the United States using data from the 1993 Residential Energy Consumption Survey. They believe that the elderly consumes more natural gas and electricity to heat their homes. However, there is a considerable negative association between water heating energy use and age.

Ota et al. [9] found that the aging of the society has no substantial impact on residential electricity and city gas demand in 47 Japanese prefectures every 5 years between 1990 and 2010. Furthermore, population decline and the rise of nuclear households raise electricity usage while lowering city gas consumption.

Residents who live in densely populated locations (such as Dublin) use less energy for space heating than those who live in less densely populated areas. According to Elnakat et al. [10], a socioeconomic and demographic study on the

residential sector in San Antonio, Bexar County, and Texas, areas with higher population density spend less energy per capita than those with lower population density. Furthermore, Arbabi and Mayfield [11] found that for increasing population densities, falling per capita gas consumption patterns are observed in a study aimed at investigating consumption behavior within the transport and home sectors in England and Wales.

Furthermore, He et al. [12] conclude, based on data from 2001 to 2011, that the greater the urban population, the greater the total natural gas consumption.

Rather than calculating natural gas demand price and income elasticities, as most research has done, the focus of this work is on demographic characteristics, particularly the elderly, population density, and urbanization rate.

3. Empirical framework

3.1 Data

Between 2005 and 2016, annual data for OECD nations was used. The dataset is based on two main sources: the International Energy Agency (IEA) dataset for residential natural gas consumption and residential natural gas and electricity prices, and the World Bank dataset for per capita income, overall population, population density, urban population percentage, aged population, heating and cooling degree days.

Due to a lack of data, five of the 34 current members of the Organization for Economic Cooperation and Development were excluded from the sample. Due to lacking price data or no reported natural gas demand, Estonia, Iceland, Israel, Norway, and Slovenia were omitted from the list. **Figure 3** depicts the study's precise countries. Every year, each country in the sample is observed, ensuring that the data set is balanced. The following are the descriptive data for the remaining 29 members, as shown in **Table 1**.

The elderly, the urban population, and population density are three crucial variables in the model, taking into account the paper's demographic methodology. The mid-year population is divided by the land area in square kilometers to get the density.

Figure 4 shows the evolution of the senior population (over 65 years) and the urbanization rate (the fraction of the population living in cities) in OECD countries. The percentage of the population over 65 years old and the population living in urban regions are both growing over time, as seen in **Figure 4**. These two variables are critical since they account for around 17 and 79% of the total in 2016.

Then, the population density[4] of different OECD countries in 2016 was exposed as the year of reference (the most recent one). **Figure 5** shows that population density varies dramatically across countries and Korea, Japan, Belgium and Netherlands are the densest countries.

The entire population aged 65 or older in the total population at the national level is included in the empirical model, indicating that each country is aging. The urbanization rate is also included to look into the role of the growing rate of people moving from rural to urban areas. Furthermore, the study considers population density when examining the effects of densely populated countries on residential natural gas use. Other control variables are also included in the model. To determine the income level, the study takes into account the total population (POPit),
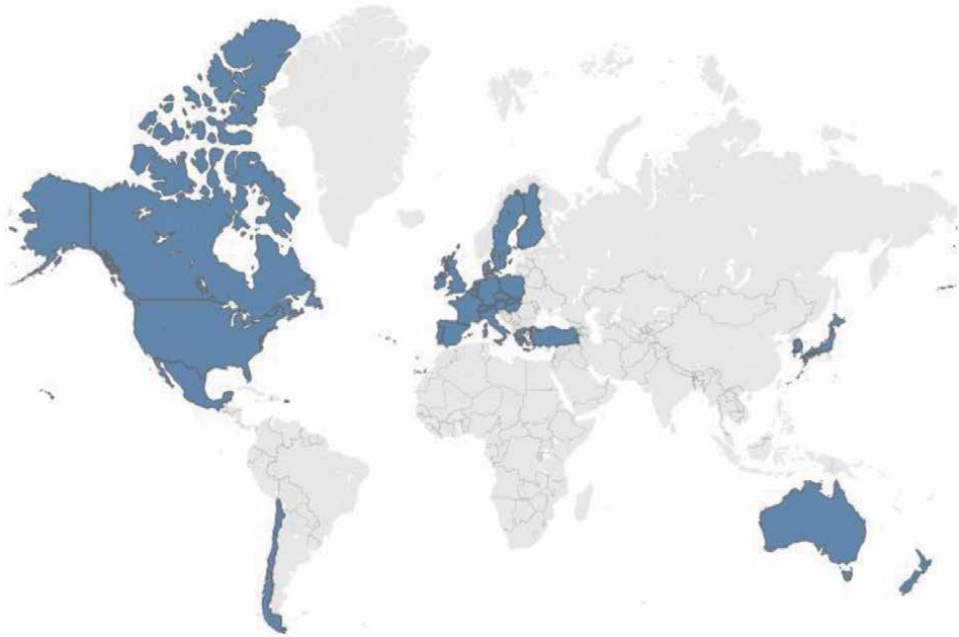
---

[4] Inhabitants/km^2.

Figure 3.
Countries in the study. Reference: own elaboration with tableau public software.

Variable	Label	Mean	Standard deviation	Minimum	Maximum
Per capita residential natural gas consumption, MWh	GT	2.276022	1.835515	0.036086	7.55551
Elderly population (total)	ELD	6,316,611	9,100,802	67,079	4.86e+07
Urban population (% of total population)	URB	77.1913	9.726607	53.468	97.897
Population density (Inhabitants/Km^2)	DEN	139.3273	128.5861	2.654778	525.7048
Population (total)	POP	4.23e+07	6.10e+07	465,158	3.23e+08
Natural gas end-user price (US$ per MWh)	GP	75.96573	31.68349	15	169.6404
Electricity end-user price (US$ per MWh)	EP	201.9823	67.54572	63.73	405.56
Per capita income (current US $)	INC	38234.41	21450.6	7384.258	119225.4
Annual Heating degree Days[a] (baseline: 18°C)	HDD	3078.315	1573.367	128.9046	8929.906
Annual Cooling degree Days[b] (baseline: 18°C)	CDD	252.0716	08.8645	0	1875.273

[a]*Heating degree day (HDD) is a quantitative index reflecting demand for energy to heat buildings or businesses.*
[b]*Cooling degree day (CDD) is a quantitative index reflecting demand for energy to cool buildings or businesses.*

Table 1.
Definition of variables and descriptive statistics. N*T (number of observations × time series) =348.

end-user natural gas price (GPit), and gross domestic product per capita (INCit). In addition, to account for weather effects, the price of electricity (EPit) as the closest replacement, as well as the Heating and Cooling Degree Days (HDDit) and CDDit) were included.
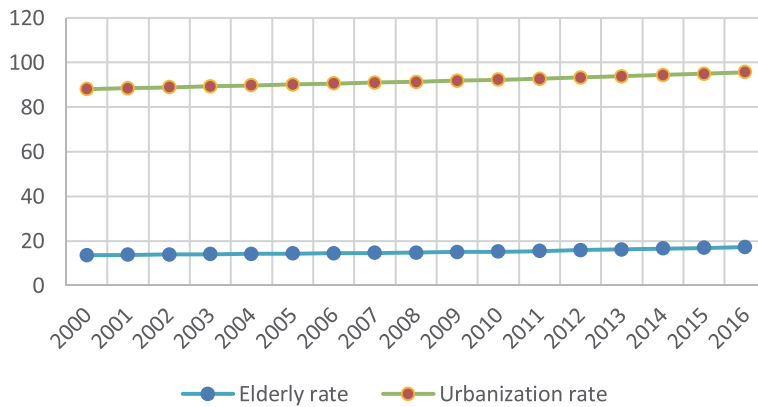
Figure 4.
Elderly and population rate (percentage, 2000–2016). Reference: own elaboration based on World Bank data (with tableau public software).

Figure 5.
Population density (inhabitants/km², 2016). Reference: own elaboration based on World Bank data (with tableau public software).

The correlation matrix was used to show the statistical correlation between the dependent variable and the regressors. **Table 2** shows that per capita natural gas demand is positively correlated with the fraction of the elderly (ELDit) and population density (DENit) (GTit). The matrix also reveals a negative relationship between urbanization rate (URBit) and natural gas consumption. Furthermore, natural gas usage is inversely connected with its own prices (GPit) and cooling degree days (CDDit), but favorably with per capita income (INCit), population (POPit), electricity price (EPit), and heating degree days (HDDit). The correlation matrix, on the other hand, is a basic statistical link between two variables; as a result, a more precise specification is required to investigate the impact of demographic variables on natural gas demand.

3.2 Econometric technique

Household production theory, which considers the consumer as a firm, assumes that households employ inputs (natural gas in this case) to manufacture nonmarket commodities or utility-yielding items. Thus, the demand for welfare services such

	IGT	IELD	IURB	IDEN	IPOP	IGP	IINC	IEP	IHDD	CDD
GT	1.0000									
IELD	0.1264	1.0000								
IURB	-0.0953	0.0758	1.0000							
IDEN	0.3230	0.1224	-0.1979	1.0000						
IPOP	0.0840	0.9737	0.0640	0.0751	1.0000					
IGP	-0.0783	-0.0391	0.0245	0.4051	-0.1324	1.0000				
IINC	0.2804	-0.1861	0.3879	-0.0331	-0.3078	0.2021	1.0000			
IEP	0.1619	-0.1635	-0.0334	0.2615	-0.2900	0.6016	0.4029	1.0000		
IHDD	0.2240	-0.1373	-0.0499	0.1075	-0.2208	0.1814	0.2796	0.0572	1.0000	
CDD	-0.2327	0.2219	0.1113	-0.258	0.2995	-0.3060	-0.2887	-0.1846	-0.8953	1.0000

Table 2.
Correlation matrix.

as space heating, water heating, cooking, and so on is not directly produced from natural gas. Households use natural gas to meet these demands.

The production function of the welfare services S can be written as:

$$S = S(G) \tag{1}$$

Natural gas is denoted by the letter G. The quantity of natural gas acquired determines the output, which is welfare services (S). In fact, welfare services S, as well as total consumption X, are regarded to be an element of the household's utility function. The demographic factors Z and the weather of the household's country, designated W, have an impact on this utility function. As a result,

$$U = U(S(G), X, Z, W) \tag{2}$$

The above utility function is maximized by the household under a budget constraint:

$$Y - P \cdot S - X = 0 \tag{3}$$

Where Y is the household income and P is the price of natural gas. Solving this optimization issue involves demand function for natural gas:

$$G* = G*(P, Y; Z, W) \tag{4}$$

Based on the Eq. (4) and employing a log linear specification, The static model is as follows:

$$\ln GT_{it} = B_0 + B_1 \ln ELD_{it} + B_2 \ln URB_{it} + B_3 \ln DEN_{it} + B_3 sum \ln X_{it} + e_{it} \tag{5}$$

Where GT_{it} is per capita residential natural gas consumption, ELD_{it} is the elderly population, URB_{it} is the urban population, DEN_{it} is the population density in the country I in year t, X_{it} is the sum of the control variables that are likely to influence per capita natural gas consumption, and e_{it} is the error component to account for unobserved factors. The parameters were simply interpreted as demand elasticities after the dependent variable and regressors were transformed into logarithms.

When estimating a static energy demand model using panel data, the endogeneity problem is often addressed by using the fixed or random effects with the Within estimator or GLS [13], respectively, to avoid the heterogeneity bias with a constant term that the OLS may suffer from.

Nerlove [14], on the other hand, claims that economic behavior models are dynamic in nature, and that current behavior is dependent on the state of the system defining it. Furthermore, according to Gutiérrez [15], disregarding the influence of path-dependency can lead to erroneous estimations of the entire variables. The lagged dependent variable was inserted on the right-hand side of the equation to compensate for the intrinsic dynamic feature of the demand function, assuming that natural gas demand in the residential sector is affected by prior levels. As a result, the dynamic version of the natural gas demand model is:

$$\ln GT_{it} = B_0 + B_1 \ln GT_{it-1} + B_1 \ln ELD_{it} + B_2 \ln URB_{it} + B_3 \ln DEN_{it} + B_3 sum \ln X_{it} + e_{it} \tag{6}$$

According to Achen [16], the lagged dependent variable will capture not only the impact of the omitted variables, but also the impact of the variables that have previously been included, with the possibility of modifying or decreasing their impact, sometimes to the point of being inconsequential.

In reality, adding a lagged dependent variable to a static model will result in skewed results because the latter variable may be associated with the error component e_{it}. Thus, the within transformation and GLS will be biased since ($Y_{i,t}^{-1}$-1) is linked with (e_{it}-i.) and its consistency is dependent on T being big, where y is the log natural gas consumption per capita and. -1 are the average lagged log per capita natural gas consumption inside nation i. [13]. To deal with this problem, one can first change the model to remove the country-fixed effects:

$$\Delta \ln GT_{it} = B_0 \, \Delta \ln GT_{it-1} + \Delta \ln ELD_{it} \, B_1 + \Delta \ln URB_{it} \, B_2 + \Delta \ln DEN_{it} \, B_3$$
$$+ \Delta sum \ln X_{it} \, B_4 + \Delta e_{it} \tag{7}$$

Then using $Y_{i,t}^{-2}$ as an instrument for Yi,t-1 [17]. Because it does not use all of the available moment conditions, this instrumental variable estimation approach produces consistent but not necessarily efficient estimates of the model's parameters [18]. Arellano and Bond [19] presented a generalized method of moment (GMM), which entails using the orthogonality criteria that exist between lagged values of Yit and the disturbances e_{it} in Eq to add additional instruments (7). As a result of this discussion, as well as the fact that the dataset had $N = 29$ and $T = 12$, the dynamic demand function was estimated and stated in Eq. (6) using a dynamic system GMM using differenced and lagged variables as instruments for the differenced and level equations, respectively. The GMM system uses the entire set of instruments and puts cross-equation limitations on the coefficients entering the two models (corresponding to the full set of orthogonality conditions for both models). The validity of the orthogonality assumptions in the estimate procedure determines the consistency of the system GMM estimator. Two specification tests are used, as recommended by Arellano and Bond [19, 20]; and Blundell and Bond, [21]. The Arellano-Bond tests (AR1) and (AR2) were used to assess the first and second serial correlation among error terms and the Sargan/Hansen test was used to check the validity of the instruments. These experiments assist us in determining the most appropriate model for national natural gas demand.

4. Empirical results

This section presents the estimated results and their implications on how the demand for natural gas responds to demographic and non-demographic factors in OECD countries. The estimation results for the static model utilizing the fixed effect to adjust for unobserved heterogeneity are shown in **Table 3**. This indicates that the majority of the coefficients are statistically significant and are nearly identical to previous research findings. In terms of the overall picture, per capita residential demand is statistically significant and positively correlated with urbanization rate, electricity prices, heating and cooling degree days, while elderly, population density, and natural gas prices are negatively correlated with per capita natural gas consumption.

However, because static models aren't ideal for observing economic trends over time, a dynamic panel model was employed to estimate energy demand, which may be more accurate than a static model. In addition, using a lagged dependent variable as a regressor to investigate residential natural gas demand violates the rigorous exogeneity constraint in static models; thus, the lagged dependent variable is included in the explanatory variables in the dynamic model in this work. The dynamic estimating model for residential natural gas demand is shown in **Table 4**.

The regression results for the dynamic model generated using the two-step system GMM estimator are shown in **Table 4**. First, the findings suggest that the lagged value of natural gas has a beneficial impact on demand. Furthermore, the

Dependent variable: log residential natural gas consumption per capita	Coefficients
lELD	-0.63^{***} (0.16)
IURB	1.96^{**} (0.68)
IDEN	-0.31^{**} (0.15)
IPOP	0.54 (0.45)
IGP	-0.12^{**} (0.06)
IINC	0.07 (0.09)
IEP	0.2^{**} (0.08)
IHDD	0.38^{***} (0.1)
CDD	0.01^{**} (0.1)
Intercept	-10.76^{*} (6.5)
Sample size	348
R^2 within	0.13
R^2 between	0.06
Overall	0.05

Note: Figures in () are the standard error.
*Significant at the 10% level.
**Significant at the 5% level.
***Significant at the 1% level.

Table 3.
Estimation results: static model—FE.

Dependent variable: log residential natural gas consumption per capita	Two-step system
Lagged lGT	0.1^{*} (0.05)
lELD	-0.61^{**} (0.19)
IURB	1.1^{*} (0.65)
IDEN	-0.16^{*} (0.09)
IPOP	0.82^{**} (0.26)
IGP	-0.21^{***} (0.06)
IINC	0.15 (0.10)
IEP	0.08 (0.10)
IHDD	0.78^{***} (0.11)
CDD	0.01^{***} (0.01)
Intercept	-15.89^{***} (3.01)
Sample size	319
Hansen test	3.96 (0.79)
Arellano-Bond test for AR(1)	-1.62 (0.11)
Arellano-Bond test for AR(2)	-0.71 (0.48)

Note: Figures in () are corrected standard error.
*Significant at the 10% level.
**Significant at the 5% level.
***Significant at the 1% level.

Table 4.
Estimation results: dynamic GMM estimation.

calculated results suggest that the elderly coefficient (ELD_{it}) in the residential natural gas demand dynamic equation is significantly negative. That is, as the population ages, natural gas usage declines. The senior elasticity of per capita natural gas demand is estimated to be -0.6. This appears counterintuitive, given that older people are more sensitive to temperature and consume more natural gas to suit their comfort demands, notably for space and water heating, and they spend more time at home [22]. However, possible explanations for the negative effect of ELD on residential natural gas consumption could be related to the fact that either old people in OECD countries have an economic behavior, or that OECD old people do not spend much time inside the house and prefer to do more activities outside. It could also be due to the fact that older folks prefer electric equipment to gas appliances. Another explanation is that, with the recent ubiquity of electrified houses, a major share of appliances used for daily life at home in OECD countries may be electric appliances. The fact that the estimation revealed a negative influence on residential natural gas demand backs up the previous claims.

Second, in the residential natural gas demand dynamic equation, the urbanization rate (URBit) coefficient is notably positive. The elasticity of per capita natural gas demand in relation to urbanization rate, in other words, is expected to be +1.1. The result appears to be consistent with previous research, as natural gas is widely used in cities and less so in rural areas, where coal and wood are commonly used. Coal, wood, and other conventional fuels are being replaced by cleaner energy sources, particularly natural gas and electricity, as the population of rural areas migrates to cities and towns.

Third, when it comes to the influence of population density (DENit), the study reveals that the DENit coefficient is strongly negative. A decrease in per capita natural gas usage occurs when population density rises. The population density elasticity of per capita natural gas demand is estimated to be around -0.16. Residential natural gas consumption per capita is lower in countries with dense populations. A probable explanation for the finding is that the majority of OECD countries apply energy saving processes and choose to use central heating systems, which provide warm space and water to the entire interior of the building.

Almost all of the control variable estimated coefficients are statistically significant, have the predicted sign, and have appropriate magnitudes. Gas prices (GP_{it}) have a negative impact on per capita natural gas demand, whereas population (POP_{it}), heating degree days (HDD_{it}), and cooling degree days (CDD_{it}) have positive impacts on residential natural gas consumption, indicating that natural gas demand is more sensitive to hot than cold weather.

When it comes to assessing the dynamic model, the AR1 and AR2 tests show that there is no significant autocorrelation in the model, which is a need for the instruments' validity. Furthermore, the Hansen test demonstrates that the null hypothesis, namely, that the over-identifying constraints are valid, is not rejected.

5. Conclusion

Using a static and dynamic model, this study looked at per capita natural gas demand in the residential sector in OECD countries from 2005 to 2016. The goal of this study is to add to the empirical literature on residential natural gas demand research by analyzing the impact of demographic characteristics on natural gas consumption in the OECD environment, specifically urbanization rate, density, and elderly population.

In fact, no previous study in the OECD has employed a comprehensive model to estimate residential natural gas demand. Previous research has frequently focused

on price and income. It is suggested that adding demographic variables will be helpful for policymakers.

A considerable effect of urbanization, density, and elderly population on residential natural gas usage was discovered using a dynamic framework. Due to policy efficiency, rapid urbanization leads to the use of more natural gas per capita, whereas population density leads to the use of less natural gas per capita, especially in buildings. Furthermore, older adults use less natural gas per capita and are more likely to use electric appliances.

Although previous studies have shown that older persons use more energy for heating, these findings appear to be counterintuitive in terms of economic behavior, preference, or the ubiquity of such appliances in OECD buildings.

Author details

Mohamed Jaouad Malzi
Mohammed V University in Rabat, Morocco

*Address all correspondence to: mohamedjaouadmalzi@gmail.com

IntechOpen

References

[1] Alberini A, Gans W, Velez-Lopez D. Residential consumption of gas and electricity in the US: The role of prices and income. Energy Economics. 2011;**33**(5):870-881

[2] Al-Sahlawi MA. The demand for natural gas: A survey of price and income elasticities. The Energy Journal. 1989;**10**(1)

[3] Burke PJ, Yang H. The price and income elasticities of natural gas demand: International evidence. Energy Economics. 2016;**59**:466-474

[4] Dagher L. Natural gas demand at the utility level: An application of dynamic elasticities. Energy Economics. 2012;**34**(4):961-969

[5] Gautam TK, Paudel KP. The demand for natural gas in the northeastern United States. Energy. 2018;**158**:890-898

[6] Chen J, Wang X, Steemers K. A statistical analysis of a residential energy consumption survey study in Hangzhou, China. Energy and Buildings. 2013;**66**:193-202

[7] Kronenberg T. The impact of demographic change on energy use and greenhouse gas emissions in Germany. Ecological Economics. 2009;**68**(10):2637-2645

[8] Liao HC, Chang TF. Space-heating and water-heating energy demands of the aged in the US. Energy Economics. 2002;**24**(3):267-284

[9] Ota T, Kakinaka M, Kotani K. Demographic effects on residential electricity and city gas consumption in the aging society of Japan. Energy Policy. 2018;**115**:503-513

[10] Elnakat A, Gomez JD, Booth N. A zip code study of socioeconomic, demographic, and household gendered

influence on the residential energy sector. Energy Reports. 2016;**2**:21-27

[11] Arbabi H, Mayfield M. Urban and rural—Population and energy consumption dynamics in local authorities within England and Wales. Buildings. 2016;**6**(3):34

[12] He GJ, Xiao RG, Liang S. Prediction and Influencing Factors Analysis of Natural Gas Consumption in China Based on SPSS. Mexico: AMCCE; 2015

[13] Baltagi BH, Baltagi BH, editors. A Companion to Theoretical Econometrics. Oxford: Blackwell; 2001

[14] Nerlove M (2000, June). An essay on the history of panel data econometrics. In Panel Data Conference in Geneva.

[15] Gutiérrez LH. The effect of endogenous regulation on telecommunications expansion and efficiency in Latin America. Journal of Regulatory Economics. 2003;**23**(3):257-286

[16] Achen CH. Why lagged dependent variables can suppress the explanatory power of other independent variables. In Annual Meeting of the Political Methodology Section of the American Political Science Association, UCLA. 2000;**20**(22):07-2000

[17] Anderson TW, Hsiao C. Formulation and estimation of dynamic models using panel data. Journal of Econometrics. 1982;**18**(1):47-82

[18] Ahn SC, Schmidt P. Efficient estimation of models for dynamic panel data. Journal of Econometrics. 1995;**68**(1):5-27

[19] Arellano M, Bond S. Some tests of specification for panel data: Monte Carlo

evidence and an application to employment equations. The Review of Economic Studies. 1991;**58**(2):277-297

[20] Arellano M, Bover O. Another look at the instrumental variable estimation of error-components models. Journal of Econometrics. 1995;**68**(1):29-51

[21] Blundell R, Bond S. Initial conditions and moment restrictions in dynamic panel data models. Journal of Econometrics. 1998;**87**(1):115-143

[22] Yamasaki E, Tominaga N. Evolution of an aging society and effect on residential energy demand. Energy Policy. 1997;**25**(11):903-912

Edited by Maryam Takht Ravanchi

Natural gas as a non-renewable hydrocarbon is used as an energy source for cooking, heating, vehicle fuel, and electricity generation. It is also used as a chemical feedstock in the manufacturing of plastics and organic chemicals. This book brings together new perspectives and future developments in natural gas. Chapters address such topics as adsorbed natural gas, fermentation processes for producing value-added products from natural gas, processes for separating C3+ hydrocarbon from natural gas, natural gas dehydration, and much more.

IntechOpen